Volume 9, Number 4
July–August 2001

ISSN: 0869-5938

STRATIGRAPHY AND GEOLOGICAL CORRELATION

English Translation of *Stratigrafiya. Geologicheskaya Korrelyatsiya*

Editor-in-Chief
Boris S. Sokolov

http://www.maik.ru

Journal of the Fundamental and Applied Aspects of Stratigraphy and the Correlation of Geologic Events and Processes in Time and Space

МАИК "НАУКА/INTERPERIODICA" PUBLISHING

Stratigraphy and Geological Correlation

(Stratigrafiya. Geologicheskaya Korrelyatsiya)

ISSN: 0869-5938

Editor-in-Chief
Boris S. Sokolov
Member of the Russian Academy of Sciences,
Counsellor of the Presidium of the Russian Academy of Sciences (RAS)
Address for correspondence:
Staromonetnyi per. 22, Moscow, 109180 Russia
Phones: 7 (095) 951-2164; Fax: 7 (095) 233-5590.

Deputy Editor-in-Chief
Mikhail A. Semikhatov
Member of the Russian Academy of Sciences
Head of Laboratory, Geological Institute, RAS
E-mail: semikhatov@ginran.msk.su

Assistant Editor
Aleksei B. Herman
Senior Scientist,
Geological Institute, RAS
E-mail: herman@ginran.msk.su

EDITORIAL BOARD

Mikhail A. Akhmet'ev
Dr. Sci. (Geol.–Min.),
Head of Laboratory, Geological Institute, RAS
akhmetev@ginran.msk.su

Aleksandr S. Alekseev
Professor, Dr.Sci. (Geol.–Min.),
Department of Paleontology,
Moscow State University
aaleks@geol.msu.ru

Mikhail N. Alekseev
Dr. Sci. (Geol.–Min.),
Chief Scientist, Geological Institute, RAS
alekseev@ginran.msk.su

Ivan A. Basov
Dr. Sci. (Geol.–Min.), Laboratory Chief,
Institute of the Lithosphere, RAS
basov@ilsan.msk.ru

Michael G. Basset
Professor, National Museum of Wales,
Cardiff, UK

William A. Berggren
Professor, Department of Geology and Geophysics,
Woods Hole Oceanographic Institute, USA

Elena V. Bibikova
Dr. Sci. (Geol.–Min.), Chief Scientist,
Vernadsky Institute of Geochemistry
and Analytical Chemistry, RAS
sergei@bibikov.genebee.msu.su

Nikita A. Bogdanov
Corresponding Member of
RAS, Director, Institute of the Lithosphere, RAS
bogdanov@ilsan.msk.ru

Kiyotaka Chinzei
Professor, Institute of Geology,
University of Tokyo,
Tokyo, Japan

Nikolai M. Chumakov
Dr. Sci. (Geol.–Min.),
Chief Scientist, Geological Institute, RAS
chumakov@ginran.msk.su

Yurii B. Gladenkov
Dr. Sci. (Geol.–Min.),
Head of Laboratory, Geological Institute, RAS
gladenkov@ginran.msk.su

Mikhail A. Fedonkin
Corresponding Member of RAS, Laboratory Chief,
Paleontological Institute, RAS
mfedon@paleo.ru

Dmitrii L. Kaljo
Professor, Institute of Geology, Tallinn, Estonia

Kirilla I. Kuznetsova
Dr. Sci. (Geol.–Min.), Chief Scientist,
Geological Institute, RAS
kuznetsova@ginran.msk.ru

Victor E. Khain
Member of RAS, Chief Scientist,
Institute of the Lithosphere, RAS

Evgenii E. Musatov
Dr. Sci. (Geol.–Min.), Chief of St. Petersburg
Division, Institute of the Lithosphere, RAS
musatov@gocean.spl.su

Lidiya A. Nevesskaya
Dr. Sci. (Biol.), Laboratory Chief,
Institute of Paleontology, RAS
lenin33@paleo.ru

Aleksandr G. Ponomarenko
Dr. Sci. (Biol.), Chief Scientist,
Institute of Paleontology, RAS
vtopor@paleo.ru

Jurgen Remane
Professor, Institute de Géologie,
Université de Neuchâtel, Switzerland

Aleksei Yu. Rozanov
Corresponding Member of RAS,
Director, Institute of Paleontology, RAS
aroza@paleo.ru

Boris A. Sokolov
Corresponding Member of RAS, Professor, Dean,
Faculty of Geology, Moscow State University
mfedon@paleo.ru

Otto Walliser
Professor, Göttingen University, Göttingen,
Germany

Sun Weigo
Professor, Nanjing Institute of Geology
and Paleontology, Academia Sinica, China

Victor A. Zakharov
Dr. Sci. (Geol.–Min.), Head of Laboratory, Institute
of Geology, Geophysics, and Mineralogy, Siberian
Division, RAS, Novosibirsk

Aleksandr I. Zhamoida
Corresponding Member of RAS,
Russian Geological Institute, St. Petersburg

Staff Editor Tamara V. Trishkina

Editor of the English Translation Anatolii Ya. Sharas'kin, Dr. Sci. (Geol.–Min.)

SCOPE

Stratigraphy and Geological Correlation (*Stratigrafiya. Geologicheskaya Korrelyatsiya*) is the only journal in the world designed to provide comprehensive coverage of the fundamental and applied aspects of stratigraphy and the correlation of geological events and processes in time and space. Articles are based on the results of multidisciplinary research and are directed toward researchers, university professors, students, and geologists interested in understanding stratigraphy and the chronological features of the world's geological record.

Stratigraphy and Geological Correlation is abstracted and/or indexed in *Petroleum Abstracts*, *Research Alert*, *SciSearch*, *Current Contents* (*Physical*, *Chemical*, and *Earth Sciences*) and *World Translations Index*.

SUBSCRIPTION OFFICE
INTERPERIODICA
P.O. BOX 1831, BIRMINGHAM, AL 35201-1831 USA
PHONE: (800) 633-4931; (205) 995-1567 (outside US and Canada)
FAX: (205) 995-1588

PUBLISHER
INTERNATIONAL ACADEMIC PUBLISHING
COMPANY "NAUKA/INTERPERIODICA"
PROFSOYUZNAYA UL. 90, MOSCOW, 117997 RUSSIA
PHONE: 7 (095) 336-1600; FAX: 7 (095) 336-0666
E-mail: compmg@maik.ru
Web Site: http://www.maik.ru

SUBSCRIPTION PRICES (2001, Volume 9, 6 issues)
US $1068.00 (North America), $1226.00 (elsewhere). A 5% discount is given on 2-year orders. Subscriptions may be entered at any time. Orders may be placed at agencies or directly. There is a 5% discount to all subscription agencies. Cancellations not allowed except for duplicate payment. Prepayment required. Advance payment required in US$/US bank. MasterCard/Visa accepted. Make checks payable to *Stratigraphy and Geological Correlation* or Interperiodica.

Stratigraphy and Geological Correlation (ISSN: 0869-5938) is published bimonthly for US $1068.00 (North America), outside North America for $1226.00 per year by MAIK "Nauka/Interperiodica", 5724 Hwy. 280 East, Birmingham, Alabama 35242-5724 USA. Periodical postage paid at Birmingham, Alabama, and additional mailing offices. POSTMASTER: Send address changes to *Stratigraphy and Geological Correlation*, P.O. Box 1831, Birmingham, Alabama 35201 USA.

The journal was founded in 1993.

Original Russian Edition Copyright © 2001 by the Russian Academy of Sciences
and Division of Geology, Geophysics, Geochemistry, and Mining Sciences, RAS.
English Translation Copyright © 2001 by MAIK "Nauka/Interperiodica" (Russia).
Printed in the USA by Pleiades Publishing, Inc.

Contents

Vol. 9, No. 4, 2001

Simultaneous English language translation of the journal is available from MAIK "Nauka/Interperiodica" (Russia).
Stratigraphy and Geological Correlation ISSN 0869-5938.

Age of Rocks in the Baikal–Muya Foldbelt
E. Yu. Rytsk, Yu. V. Amelin, N. G. Rizvanova, R. Sh. Krimsky, G. L. Mitrofanov, N. N. Mitrofanova, V. I. Perelyaev, and V. S. Shalaev 315

The Timan–Pechora Paleogeography and Facies in the Kungurian–Ufimian Boundary Period
E. O. Malysheva, G. P. Kanev, and N. A. Koloda 327

Paleogeography and Sedimentation Settings during Permian–Triassic Reorganizations in Biosphere
M. A. Zharkov and N. M. Chumakov 340

Permian–Triassic Biotic Crisis and Foraminifers
E. Ja. Leven and O. A. Korchagin 364

The Lower Oligocene Kurgan Beds of West Siberian and Trans-Uralian Regions
M. A. Akhmet'ev, G. N. Aleksandrova, V. N. Beniamovskii, O.N. Vasil'eva, V. I. Zhelezko†, and N. I. Zaporozhets 373

Palynological Assemblages and Macrofloras from Eocene–Miocene Deposits of the Tatar Strait Coast (Eastern Sikhote Alin)
D. A. Lopatina 387

Late Quaternary Planktonic Foraminifers of the Extreme Northeastern Kuril Basin (Sea of Okhotsk, Station V34-98)
M. P. Chekhovskaya, I. A. Basov, and S. A. Gorbarenko 406

Stratigraphy and Geological Correlation, Vol. 9, No. 4, 2001, pp. 315–326. Translated from Stratigrafiya. Geologicheskaya Korrelyatsiya, Vol. 9, No. 4, 2001, pp. 3–15.
Original Russian Text Copyright © 2001 by Rytsk, Amelin, Rizvanova, Krimsky, Mitrofanov, Mitrofanova, Perelyaev, Shalaev.
English Translation Copyright © 2001 by MAIK "Nauka/Interperiodica" (Russia).

Age of Rocks in the Baikal–Muya Foldbelt

E. Yu. Rytsk*, Yu. V. Amelin, N. G. Rizvanova*, R. Sh. Krimsky*, G. L. Mitrofanov***, N. N. Mitrofanova***, V. I. Perelyaev***, and V. S. Shalaev***

**Institute of Precambrian Geology and Geochronology, Russian Academy of Sciences, nab. Makarova 2, St. Petersburg, 199034 Russia*

***Geochronological Laboratory, Royal Ontario Museum, Queen's Park, Toronto, Ontario, M5S 2C6 Canada*

****East Siberian Research Institute of Geology, Geophysics and Mineral Resources, ul. Dekabr'skikh Sobytii 29, Irkutsk, 664007 Russia*

Received April 18, 1999; in final form, December 14, 1999

Abstract—The presented results of U–Pb zircon dating (those for individual grains included) and Sm–Nd isochron ages for whole-rock samples and mineral fraction characterize magmatic complexes of the Muya segment of the Baikal–Muya foldbelt. New isotopic dates indicate the Late Riphean–Vendian age of volcanogenic–sedimentary and igneous rocks, which have been formed in the Muya segment during the Early Baikalian (from about 1.0 to 0.8 Ga) and Late Baikalian (0.8–0.62 Ga) stages of tectogenesis. The distinguished syntectonic granitoids of the Early Baikalian stage mark a collision event that happened 0.8 Ga ago. The results obtained are used to refine the traditional scheme of Precambrian stratigraphy and magmatism in the Middle Vitim Mountains.

Key words: geochronology, Late Precambrian, granitoids, rhyolites, gabbroids, stratigraphy, magmatism, tectonics.

The problem concerning formation stages of oldest magmatic complexes in the Baikal–Muya foldbelt (BMF) of the Baikal mountainous region is of prime significance for understanding of initial stages of the Paleo-Asian ocean evolution. These complexes are thought to be either the Early Proterozoic (Salop, 1964; Gusev *et al.*, 1992) or Riphean in age (Mitrofanov, 1978, 1981, 1984; Bulgatov, 1983), and the last viewpoint was recently substantiated in biostratigraphic aspect (Stanevich and Perelyaev, 1997). The rocks in question belong to the Muya Group and synonymous intrusive complex originally distinguished by Salop (1964) in the Middle Vitim Mountains. Factual data obtained in the course of recent geological mapping in the region (project "Gosgeolkarta-200") show that the available regional schemes of regional stratigraphy and magmatic evolution should be thoroughly revised that is impossible without reliable geochronological data. In this connection, we carried out the isotopic dating of rock samples from the Muya Group and coeval intrusive complex, and also of the Early (?) Precambrian granites distinguished in the Muya tectonic block. The results presented here are obtained using the Sm–Nd isochron method and U–Pb dating of zircon fractions and individual grains. The results are used to discuss some problems of stratigraphy, magmatism, and tectonic evolution of the BMF.

1. BRIEF GEOLOGICAL CHARACTERISTIC OF THE REGION AND STUDIED OBJECTS

The Baikal–Muya foldbelt that includes the Verkhnyaya Angara and Muya segments extends from the Baikal Lake to middle courses of the Vitim River. Its Muya segment situated in central area of the Middle Vitim Mountains is subdivided into the Karalon–Mamakan and Anamakit–Muya structural zones (Fig. 1A).

1.1. Anamakit–Muya Zone

The zone consists of the Bambui–Olindya and Muya subzones, the last of which includes the Kindikan–Ileir and Kedrovka–Shaman blocks.

Kindikan–Ileir block. In accord with general opinion (Salop, 1964; Dobrzhinetskaya *et al.*, 1983; Kozyreva *et al.*, 1990; *Geologicheskaya karta...*, 1992), both the northern and southern parts of the block are composed of the Lower Precambrian rocks. In the local nomenclature, these are the Dzhaltuk and Kindikan groups of predominant biotite, biotite–amphibole, and carbonate–siliceous crystalline schists intercalated with amphibolite interlayers and eclogite lentils. Intrusive rocks of the block are represented by synmetamorphic gneissoid granites of the Kuanda and Ileir complexes. Gabov *et al.* (1984) demonstrated that eclogites are confined to basal planes of thrust faults that bound tectonic domains of metamorphic rocks. The relatively

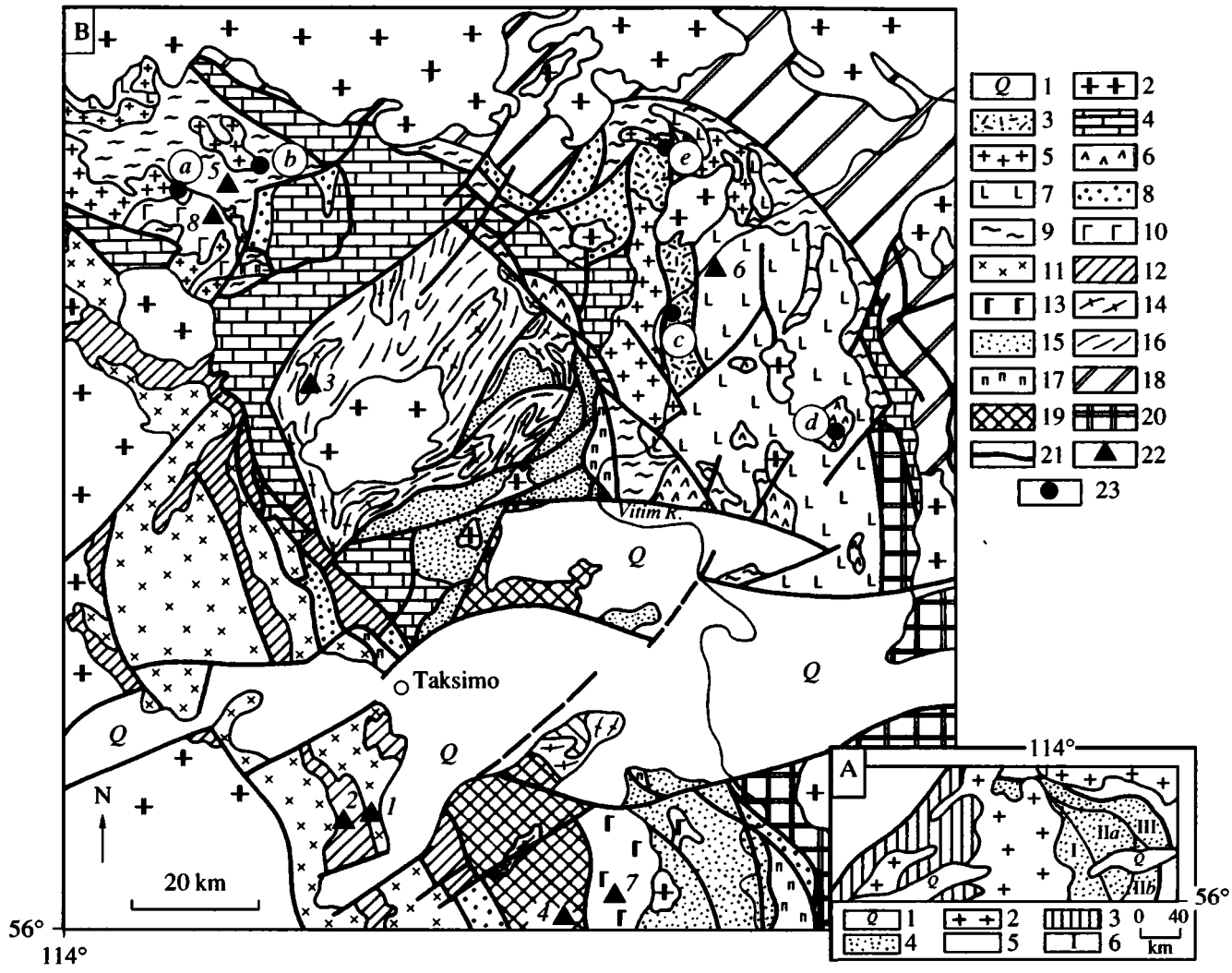

Fig. 1. Geological schemes of the Baikal–Muya foldbelt (A) and its Muya segment (B).

Fig. 1A: (1) Cenozoic rifts; (2) Paleozoic granitoids; (3) Verkhnyaya Angara and (4) Muya segments of the foldbelt; (5) Precambrian rocks; (6) structural–formational zones of the Muya segment; (I) Bambui–Olindya and (II) Muya subzones of the Anamakit–Muya zone with the Kindikan–Ileir (IIa) and Kedrovka–Shaman (IIb) blocks; (III) Karalon–Mamakan zone.

Fig. 1B: (1) Quaternary deposits; (2) Late Paleozoic granitoids; (3) Padra group of the Vendian–Lower Paleozoic; (4) Mamakan Group and (5) granitoid complexes (Lesnoi and others) of the Vendian–Cambrian. (6–10) Upper Riphean–Lower Vendian rocks of the Karalon–Mamakan zone: (6) Zaoblachnyi peridotite–pyroxenite–gabbronorite complex, (7) Tallaya gabbro–diorite–plagiogranite complex; (8) Shumna, Delyun, Tuluya, and other formations of rudaceous deposits, (9) Yakor' and Karalon groups of volcanogenic–sedimentary deposits, (10) Srednii Mamakan peridotite–gabbro complex. (11, 12) Upper Riphean rocks of the Bambui–Olindya subzone: (11) Muya gabbro–diorite–plagiogranite complex and (12) Ust'-Kelyana Group of volcanogenic–sedimentary rocks. (13–15) Upper Riphean rocks of the Muya subzone: (13) Kedrovka complex of layered anorthosite–gabbro intrusions; (14) Ileir complex of synmetamorphic gneissoid granites; (15) Param Group of volcanogenic–sedimentary rocks (Samokut, Bulunda, Ust'-Param, Nadporozhnaya, Bezymyannyi, and Kedrovka formations). (16–20) Riphean and older rocks of the Muya subzone: (16) Dzhaltuk group of carbonate terrigenous rocks; (17) Param ultramafic complex; (18) Riphean Delyun-Uran group; (19) Proterozoic Kindikan Group; (20) Archean Chara Group. Other symbols: (21) faults; (22) sampling sites studied in this work; (23) sites with previously known geochronological data (*a*, granites of the Lesnoi complex; *b*, plagiogranites of the Malyi Yakor' complex; *c*, rhyolites of the Padra Group; *d*, gabbroid rocks of the Zaoblachnyi massif).

young Sm–Nd age of 653 ± 21 Ma was defined for eclogites of the Muya domain (Shatskii *et al.*, 1996).

The Dzhaltuk Group is discordantly overlain (Salop, 1964; Bulgatov, 1983) by volcanogenic–sedimentary rocks of the Param Group, which have experienced the greenschist metamorphism and enclose bimodal volcanic rocks with lentils of tuffaceous conglomerate, quartz–biotite schist, metasandstones and carbonates. Some researchers (Salop, 1964; Dobrzhinetskaya *et al.*, 1983) considered these rocks as representing the lower Muya Subgroup of the Lower Prot-

erozoic, but Mitrofanov (1978) attributed them to the Param Group of the Riphean, considering this subdivision as coeval to the Kelyana succession. Relationships between the Param Group and volcanic rocks of the Kelyana Subgroup of the Muya Group are however debatable, like the significance of hiatus at the base of the former. At the same time, the anorthosite–gabbro intrusions of the Kedrovka complex, which crosscut the Param Group, undoubtedly define its upper age limit. In paleogeodynamic reconstructions (Kozyreva *et al.*, 1990; Gusev *et al.*, 1992), the Param Group is considered as indicator of rifting events in the continental crust. The Precambrian rocks of the region underlie terrigenous–carbonate sediments of the Mamakan Group, which are unmetamorphosed and yield Vendian–Early Cambrian fossils (Salop, 1964).

As one can see, the gneissoid granites of the Kindikan–Ileir block represent the key object that may clarify the tectono-stratigraphic succession of rocks of the Muya subzone, because their emplacement recorded the culmination of regional metamorphism and tectonic dislocations. Similarly significant are layered intrusions of the Kedrovka complex, which are indicators of the post-Param period of tectonic stabilization (Mitrofanov *et al.*, 1981).

In the north of the Kindikan–Ileir block, we studied gneissoid granites of the Sira River basin, where these rocks of the palingenic-metasomatic origin occur as a massif emplaced into biotite–amphibole schists and metasandstones of the Dzhaltuk Group (Site *3* in Fig. 1B). The central part of the massif consists predominantly of gneissoid meso- and leucocratic medium-grained biotite and biotite–amphibole granites grading into banded porphyroblastic biotite granite gneisses of the outer zone. Surrounding rocks experienced feldspathization but are lacking signs characteristic of hornfels facies. In their chemical composition, rocks of the massif correspond to the K–Na granodiorite–subalkaline granite series. For the U–Pb dating, we used samples of porphyroblastic granites gneisses, the mineral lineation of which is conformable to metamorphic banding of surrounding rocks.

In the Kindikan rock succession that is exposed along the Tuluya River in the south of the Kindikan–Ileir block (Site *4* in Fig. 1), we studied the widespread migmatite injections. Rock samples of altered leucocratic plagiogranites have been collected here from vein boudins 2 to 3 m thick.

In order to date the Kedrovka complex, we collected samples of fine-grained gabbronorite from the layered anorthosite–gabbro pluton exposed along the Strelka Creek (collection of V.G. Mitrofanov). These rocks (Site *7* in Fig. 1) have the well-preserved original parageneses of magmatic minerals.

Bambui–Olindya subzone. The elongated tectonic slices of the subzone are intruded by the Hercynian granitoids. In the east, the subzone is bounded by the Kelyana–Irokindya melange enclosing the size-variable exotic blocks of magmatic, volcanogenic, and sedimentary rocks. Konnikov and Tsygankov (1992) suggested that lentils of apoharzburgite serpentinite occurring here represent fragments of the Riphean ophiolite association. The subzone is composed predominantly of Riphean island-arc rocks, which are considered, disregarding data of recent geological survey, as constituents of the "Kelyana subgroup of the Muya Group" and also as rocks of the "Muya complex" (Tsygankov *et al.*, 1998) in contrast to the viewpoint of Salop (1964) who suggested their Early Proterozoic age. Dominant in the island-arc association are gabbro–diorite-plagiogranite–granite intrusions with xenoliths representing the comagmatic basic and acid metavolcanic rocks of the Ust'-Kelyana complex and the synonymous succession of volcanogenic–sedimentary rocks. Despite the inconsiderable metamorphic grade, plagiogranites experienced the intense cataclasis and are transformed into blastomylonites. The apparent rock succession of the Bambui–Olindya subzone is crowned by rudaceous deposits (Tuluya and other formations), which have been accumulated in local grabens and bear pebbles derived from underlying granitoids and volcanic rocks.

Microphytoliths from the Ust'-Kelyana deposits are similar to microfossils of the Middle–Upper Riphean Patom Group (Stanevich and Faizulina, 1992). The preliminary Rb–Sr dates obtained for whole-rock samples from the Muya granitoid complex fall within the time range of 700–800 Ma (Tsygankov *et al.*, 1998). A single confident Sm–Nd date of 835 ± 12 Ma characterizes gabbroids of the Marinka peridotite–troctolite pluton that may belong to the island-arc rock association. Rocks dated in this work are the almost unaltered coarse-grained biotite plagiogranites and Na-metarhyolites of the Ust'-Kelyana complex. Their samples have been collected in the source area of the Krivoi Creek, the left tributary of the Mudirikan River (sites *1* and *2* in Fig. 1B).

1.2. Karalon–Mamakan Zone

The zone comprising the Mamakan and Tallaya blocks is located between the Anamakit–Muya zone of the BMF and the Delyun–Uran zone of the Patom sedimentary basin (Fig. 1B). Predominant in this zone, like in the Bambui–Olindya subzone, are the volcanogenic–sedimentary deposits of the Kelyana Subgroup and intrusive rocks of the Muya complex (Salop, 1964). Stanevich and Perelyaev (1997) recently suggested that the rock succession of the Mamakan block begins with the ophiolite association of metaperidotites, cumulate gabbro, diabase dikes, and pillow-lavas of the suprasubduction origin. The Yakor' Group overlying the ophiolite association consists of island-arc volcanics, volcaniclastic turbidites, sandstones, and silty pelites interrelated via transitional facies. Coarse-grained graywackes of the Yakrya and Paradokan formations crown the rock succession of the block. The diverse biota of the Zhuya Horizon implies the Late Riphean

age of the Yakor' Group (Stanevich and Faizulina, 1992). Granites of the Lesnoi complex, which crosscut gabbro, volcanics, and sedimentary rocks (localities *a* and *b* in Fig. 1), are 556 ± 16 Ma old according to results of U–Pb zircon dating (Sryvtsev *et al.*, 1992). In the Mamakan block, we selected for dating the Srednii Mamakan peridotite–gabbro massif and Na-metarhyoltes, which are presumably coeval to tuffaceous–sedimentary deposits of the Yakor' Group. The analyzed samples of clinopyroxenite, mesocratic gabbro, leucocratic gabbronorite, and gabbro-anorthosite characterize the individual magmatic rhythm of the massif (Site *8* in Fig. 1B). The apple-green metamorphosed porphyries sampled in the Bol'shoi Yakor'–Yakrya–Kaalu watershed (Site *5* in Fig. 1B) represent an extrusive body more than 50 m thick that is intercalated with basaltic andesites of the Yakor' Group.

In the **Tallaya block,** the dismembered ophiolite association is represented by the Param ultramafic massif of unknown age (Gusev *et al.*, 1992). The Karalon Group of volcanogenic–sedimentary rocks overlies here the eroded surface of the Delyun-Uran Group of carbonate–terrigenous rocks (Dobrzhinetskaya *et al.*, 1983). The Karalon Group that is correlated with the Yakor' Group of the Mamakan block by virtue of lithologic similarity and stratigraphic position represent either the island-arc (Stanevich and Faizulina, 1992) or the rifting-related rock association (Fedorovskii, 1985).

A large gabbro–diorite–tonalite massif in central area of the Tallaya block was attributed by Salop (1967) to the Muya intrusive complex. As this massif is close in composition to differentiated intrusions in the Kelyana and Muya river basins, it was considered as a member either of the Early Proterozoic Muya complex (Salop, 1967; Gusev *et al.*, 1992) or the Late Riphean Tallaya complex (legend to map series GK-200). In the Tallaya River basin, plagiogranites and metavolcanics of the Karalon Group are intruded by the peridotite–pyroxenite–gabbro plutons and the Sm–Nd isotopic age of one of them (the Zaoblachnyi pluton, locality *d* in Fig. 1B) is 612 ± 62 Ma (Izokh *et al.*, 1998). The apparent section is crowned by the Upper Riphean rudaceous deposits (the Shumna and Delyun formations) and by the continental volcanic and volcaniclastic rocks of the Padra Group. The Rb–Sr isotopic ages obtained for the latter are discordant and vary from 362 ± 16 and 496 ± 5 Ma (Buldygerov *et al.*, 1995) to 765 ± 50 Ma (Mitrofanov, 1978). Despite the variability, these dates show that the Padra Group cannot be correlated with the Middle Proterozoic Akitkan Group.

Within the block under consideration, we also collected for isotopic analysis the plagiorhyolite and plagiogranite samples. Some time ago, we already tried to date plagiorhyolites of the Karalon Group using the U–Pb zircon method. Unfortunately, we failed to determine the reliable dates because of the deficiency of zircon separates available at that time, in which we detected presence of an inherited component. At present, we can control their geochronological parameters using the Sm–Nd isotopic data. Plagiogranite samples for isotopic dating have been collected in the Tallaya–Kychiga interfluve at the right side of the Vitim River (Site *6* in Fig. 1B).

2. ANALYTICAL PROCEDURE

The decomposition of zircons and extraction of U and Pb for isotopic age determination are preformed using the modified method by Krough (1973). The isotopic dilution method was used to measure the U and Pb concentrations. The total processing blank was 0.1 ng for Pb and 0.005 ng for U, which mean that the laboratory contamination was negligible. Isotopic ratios were measured with the help of Finnigan MAT-261 mass spectrometer, and the analytical uncertainty of measurements corresponded to 0.5% (2σ). Individual zircon grains were analyzed at the Royal Ontario Museum. The applied method was formerly described in detail by Amelin (1998). In our analytical runs, the total blank was 0.5–1 pg for Pb and less than 0.1 pg for U. The decay constants used in calculations correspond to those reported by Steiger and Jager (1977). Analytical data were corrected for the common lead admixture in accord with the model of Stacey and Kramers (1975). Calculations are preformed using computer programs PbDAT (Ludwig, 1991) and ISOPLOT (Ludwig, 1992).

In the Sm–Nd isotopic analysis, the total blank was 0.3 ng for Sm and 0.5 ng for Nd. The Nd isotope compositions were corrected for fractionation relative to the ratio $^{148}Nd/^{144}Nd = 0.241570$. The analytical uncertainty is ±0.3 (2σ) for $^{147}Sm/^{144}Nd$ ratios and ±1% for element concentrations. During the period of experimental runs, the laboratory average of 0.511879 ± 14 ($n = 45$) was determined for the La Jolla $^{143}Nd/^{144}Nd$ standard, and the value of 0.512673 ± 15 ($n = 10$) was obtained for the BCR-1 standard. The uncertainty values correspond to the confidence level of 95%. The $\varepsilon_{Nd}(t)$ parameters are calculated relative to CHUR values $^{147}Sm/^{144}Nd = 0.1967$ and $^{143}Nd/^{144}Nd = 0.512638$. The one-stage (Goldstein and Jacobsen, 1988) and two-stage (Liew and Hoffmann, 1988) model ages TDM are calculated using ratios $^{147}Sm/^{144}Nd = 0.2136$ and $^{143}Nd/^{144}Nd = 0.513151$ in the depleted mantle and $^{147}Sm/^{144}Nd = 0.12$ in the crust.

3. RESULTS

The U–Pb and Sm–Nd data obtained are presented in Tables 1–3 and illustrated in Figs. 2–5.

3.1. U–Pb Systematics

3.1.1. Plagiogranites and Rhyolites of the Bambui–Olindya Subzone

Prismatic zircon crystals from plagiogranite Sample 472 are transparent colorless or light yellow with the

Table 1. U–Pb isotopic characteristics of zircons from granitoids of the Muya segment of the BMF

Fraction size, mm	Weight, mg	U, ppm	Pb, ppm	$^{206}Pb/^{204}Pb^a$	$^{206}Pb/^{207}Pb^a$	$^{206}Pb/^{208}Pb^a$	$^{206}Pb/^{238}Pb^b$	$^{207}Pb/^{235}Pb^b$	t(207/206) Ma	Rho
Gneissoid granite 95-008-2										
<0.06	2.08	477	59	11365	15.036	10.79	0.12496	1.126	785.1 ± 0.97	0.99
>0.06	0.15	541	69	1826	13.696	8.928	0.12688	1.143	784.7 ± 3.1	0.91
>0.08	1.47	458	67	392	9.8167	5.541	0.12669	1.141	784.7 ± 1.7	0.97
>0.1 (transparent)	0.13	413	58	540	10.572	6.192	0.12881	1.213	878.0 ± 22	0.54
Gneissoid granite YuM-2b										
0.06–0.085	0.90	725	87	9334	15.147	10.85	0.12092	1.076	760.4 ± 0.88	0.99
0.085–0.1	0.96	813	99	6670	15.009	10.37	0.12166	1.083	759.5 ± 0.92	0.99
>0.15	0.85	726	89	10400	15.116	10.90	0.12336	1.103	770.0 ± 2.8	0.92
0.1–0.15	0.09	1176	149	1960	13.894	8.757	0.12421	1.109	766.1 ± 3.1	0.93
0.085–0.1 (brown)	0.31	2448	274	4380	14.893	18.98	0.11589	1.022	739.4 ± 0.99	0.99
Sphene	11.58	75	17	190	7.3937	0.752	0.09426	0.762	552.6 ± 5.3	0.81
Plagiogranite 472										
<0.05	0.77	201	27	1767	13.459	4.477	0.1189	1.087	816.0 ± 1.5	0.98
0.05–0.06	0.93	255	34	3340	14.198	4.691	0.1194	1.090	814.2 ± 1.6	0.97
>0.085	1.03	148	20	2130	13.723	4.693	0.1230	1.124	814.9 ± 3.8	0.87
Plagiogranite 90045										
<0.053	1.12	94	11.8	398	10.163	3.439	0.10200	0.8763	684 ± 14	0.53
>0.070	1.87	97	10.6	1476	13.984	5.684	0.10280	0.8773	671 ± 6	0.74
>0.100	2.83	118.6	13.1	2200	14.723	5.621	0.10280	0.8717	656 ± 3	0.92
Plagiogranite 90046-6										
>0.070	1.22	145	18.9	1484	12.186	3.990	0.11280	1.129	1002 ± 2.6	0.93
0.045–0.070	.22	185	22.5	826	12.334	3.804	0.10600	0.9333	737.3 ± 5	0.91

Note: *a*, measured ratios; *b*, recalculated ratios.

Table 2. U–Pb isotopic characteristics of individual zircon grains from acid volcanics of the Yakor' (YaK-12) and Ust'-Kelyana (477/1) groups

Sample	Weight, mg	U, ppm	Pb*, ng	$^{206}Pb/^{204}Pb$	$^{206}Pb/^{238}U$	$^{207}Pb/^{235}U$	$^{207}Pb/^{206}Pb$
YaK-12(z1)	<0.002	206.7	0.5	4589.78	0.17458	1.89491	0.07872
YaK-12(z2)	<0.002	73.7	1.4	593.98	0.10317	0.87025	0.06118
YaK-12(z3)	<0.002	126.4	3.1	941.72	0.14151	1.44119	0.07387
YaK-12(z4)	<0.002	59.3	1.1	450.77	0.10770	0.86286	0.06013
YaK-12(z5)	<0.002	40.5	1.7	428.89	0.10893	0.91230	0.06074
YaK-12(z6)	<0.002	20.9	7.9	285.25	0.10631	0.85675	0.05845
YaK-12(z7)	<0.002	19.1	1.3	355.10	0.10802	0.92612	0.06218
477/1(z1)	<0.002	122.5	0.8	1633.34	0.13602	1.24493	0.06638
477/1(z2)	<0.002	44.6	8.2	285.73	0.13727	1.24211	0.06563
477/1(z3)	<0.002	100.6	7.1	357.06	0.13622	1.25921	0.06704
477/1(z4)	<0.002	56.6	1.3	435.38	0.13627	1.23320	0.06563
477/1(z5)	<0.002	59.9	2.5	354.89	0.13554	1.15725	0.06192

Sample	T(206/238) Ma	2σ	T(207/235) Ma	2σ	T(207/206) Ma	2σ	Discordance, %	Rho
YaK-12(z1)	1037.3	4.1	1079.3	3.1	1165.2	5.4	11.9	0.82
YaK-12(z2)	633.0	3.5	635.7	14.8	645.5	61.9	2	0.52
YaK-12(z3)	853.2	2.7	906.2	7.3	1037.8	21.8	19	0.55
YaK-12(z4)	659.4	4.6	647.9	27.9	608.1	118.1	–8.9	0.61
YaK-12(z5)	666.5	4.1	658.3	29.3	630.1	122.5	–6.1	0.69
YaK-12(z6)	651.3	26.3	628.4	299.4	546.6	1127.2	–20.1	0.73
YaK-12(z7)	661.2	7.2	665.6	50.9	680.4	210.1	3.0	0.68
477/1(z1)	822.1	6.0	821.1	6.0	818.5	14.6	–0.5	0.76
477/1(z2)	829.2	12.4	819.8	114.5	794.6	411.4	–4.6	0.88
477/1(z3)	823.2	5.5	827.6	42.8	839.2	147.1	2.0	0.83
477/1(z4)	823.5	5.5	815.8	28.7	794.7	99.5	–3.9	0.61
477/1(z5)	819.4	7.0	780.7	54.9	671.5	203.9	–23.5	0.78

Note: Common Pb, the blank concentration included, and initial Pb (if present).

elongation coefficient C_e = 1.2–2 and small inclusions of ore phase. Data points characterizing three size fractions of crystals plot along discordia (Fig. 2A) that intersects concordia at two points, the upper of which corresponds to the age value of 812 ± 19 Ma (MSWD = 1.12).

In the rhyolite sample 477/1, zircons are represented by very small colorless euhedral crystals. All five crystals, which have been analyzed, yielded the concordant ages, and the average age value of 823.8 ± 2.1 Ma evidently corresponds to the crystallization time of these zircons (Fig. 2B). Calculations are performed using the computer program by Ludwig (1992).

3.1.2. Synmetamorphic Granites of the Kindikan–Ileir Block

The dominant zircon fraction from gneissoid granites of the Sira River basin (Sample 5008-2) consists of light brown prismatic transparent crystals with C_e = 1.5–2. They show etching marks, microfractures, and scarce inclusions of ore phase. The discordia plotted for three size fractions (Fig. 3A) has upper intercept with concordia that corresponds to 784.2 ± 5.9 Ma (MSWD = 0.0006). Data points for largest colorless grains are significantly displaced from discordia to the right, and this means, according to the general opinion, that crystals contain an older inherited component.

The migmatite injections in the Tuluya River basin (Sample UM-2b) yielded two types of zircon crystals: light brown transparent prismatic grains with C_e = 2–3 that are concentrated in the fine fraction and larger dark brown crystals, which are hazy and corroded to a certain extent. The discordia was plotted for five data points, four of which characterize the fine fraction. Its upper intercept with concordia corresponds to 785.7 ± 9 Ma. The fifth point, the lowermost one in the discordia, exemplifies the dark brown zircon crystals

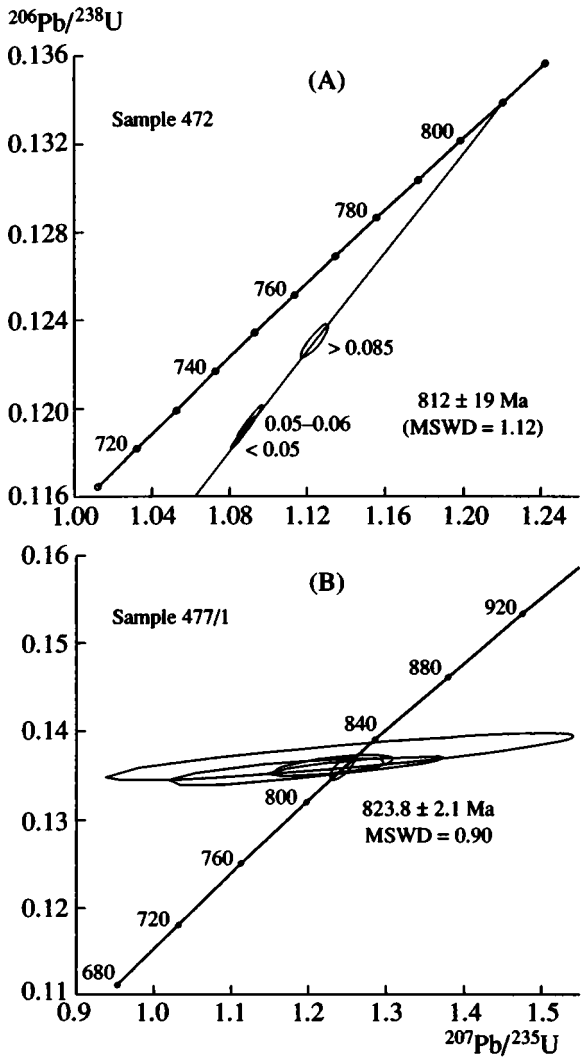

Fig. 2. Concordia diagrams for zircons from plagiogranites (A) and rhyolites (B) of the Bambui–Olindya zone.

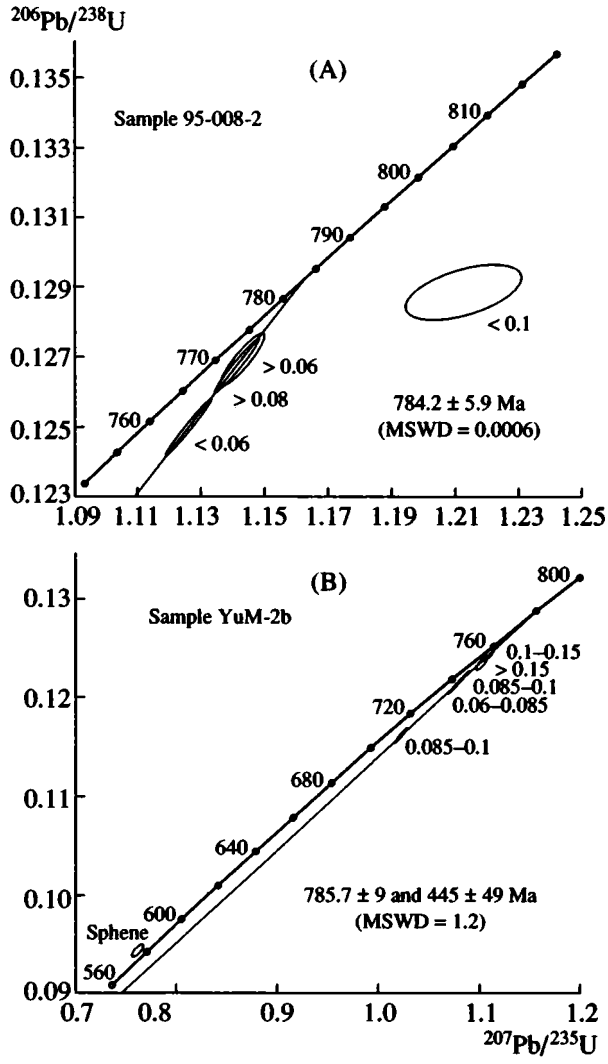

Fig. 3. Concordia diagrams for zircons from synmetamorphic gneissoid granites of the North (A) and South Muya (B) areas of the Kindikan–Ileir block.

enriched in uranium (Fig. 3B). The lower intercept with concordia (449 ± 49 Ma) can be interpreted as the time mark of superimposed processes, e.g., of hypergenesis that most significantly affected the U-rich fraction. On the other hand, this could be a result of superimposed metamorphism, the influence of which is easily detectable by petrographic examination. To check the time of metamorphic event, we analyzed the sphene fraction separated from the same rocks. The tentative time range of 550–580 Ma that was calculated for sphene separates is close to the age of the granitoid Lesnoi complex (Sryvtsev *et al.*, 1992).

3.1.3. Plagiogranites and Rhyolites of the Mamakan and Tallaya Blocks

Zircon crystals from metarhyolite sample YaK-12 are very small, colorless, and euhedral. After preliminary abrasion, we analyzed seven grains, two of which seem to contain the older inherited component (Fig. 4). Four other absolutely similar grains yield the concordant age of 664 ± 3 Ma. The fine zoning observable in these grains allows us to interpret this value as corresponding to the crystallization time. The large elliptical area in the figure corresponds to the grain with very insignificant concentration of radiogenic Pb. The younger age (633 Ma) of another grain may indicate, with due regard for analytical uncertainty, the Pb loss during the recent time.

Zircon crystals from plagiogranites (samples 90045 and 90046) are transparent and prismatic, having C_e = 1.5–2. Some of them are corroded, showing signs of crystal–melt interaction. The discordia that is plotted for five zircon fractions has the lower intercept with concordia at the time mark of 625 ± 14 Ma (Fig. 4).

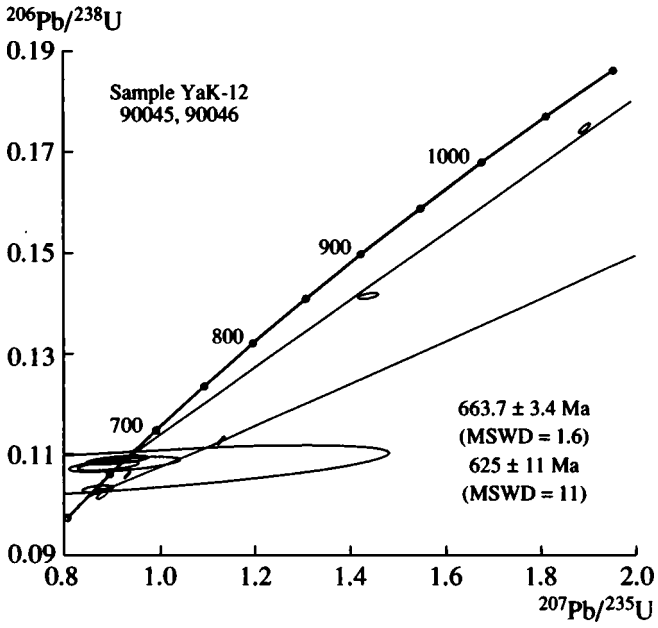

Fig. 4. Concordia diagram for zircons from plagiogranites (shaded ellipses, T = 625 ± 11 Ma) and rhyolites (empty ellipses, T = 663.7 ± 3.4 Ma), the Karalon–Mamakan zone.

Data points are clustered in proximity to the intercept, and this may indicate the old Pb presence in the analyzed zircons. The calculated age value cannot be accepted for the crystallization time, because we have analyzed grains without preliminary abrasion and may expect that the obtained value could be decreased owing to the recent Pb loss. If the last speculation is admissible, the analyzed plagiogranites and metarhyolytes could be close in age.

3.2. Sm–Nd Dates

3.2.1. Kedrovka Gabbro–anorthosite Massif

Two whole-rock samples of mesocratic gabbronorite from the massif, as well as plagioclase and clinopyroxene fractions, were selected for the Sm–Nd isotopic analysis (Table 3). The corresponding data points plot along the isochron that defines the age value of 735 ± 26 Ma and $\varepsilon_{Nd}(T) = -0.8$ (Fig. 5A).

3.2.2. Srednii Mamakan Peridotite–gabbro Massif

In this case, we analyzed whole-rock samples of clinopyroxenite, mesocratic gabbro, leucocratic gabbronorite, and gabbro-anorthosite, all collected from a common magmatic rhythm. In addition, the mineral fractions (Opx, Cpx, and Pl) of leucocratic gabbronorite have been analyzed. The mineral isochron parameters correspond to the age 704 ± 71 Ma and $\varepsilon_{Nd}(T) = 0.7$ (Fig. 5B). Data points of whole-rock samples, that of leucocratic gabbronorite included, also define the linear regression, the age of which is 774 ± 67 Ma and $\varepsilon_{Nd}(T) = 2.8$. Both age values are concordant within the limits of determination errors. It is necessary to stress as well that the Sm–Nd isotopic parameters of rocks from the Srednii Mamakan massif are closer to those of continental layered intrusions than to parameters of gabbroic rocks of ophiolite associations.

3.2.3. Granitoids and Rhyolites

According to Sm–Nd isotopic data obtained (Table 4), the studied granitoids and rhyolites represent two groups of rocks. One includes granitoids and rhyolites of the Anamakit–Muya zone, where their $\varepsilon_{Nd}(T)$ parameter varies from –4.3 to –11, and the respective model

Table 3. Sm–Nd isotopic characteristics of gabbroid rocks from the Muya segment

Sample no.	Rock or mineral	Age, Ma	Sm, ppm	Nd, ppm	$^{147}Sm/^{144}Nd$	$^{143}Nd/^{144}Nd$	±2σ, %	$\varepsilon_{Nd}(T)$
			Kedrovka massif					
462-90	Gabbro, whole rock	735	8.45	30.7	0.1666	0.512448	0.003	–0.88
464-90	Gabbro, whole rock	735	5.32	19.9	0.1618	0.512435	0.003	–0.68
464-90	Pyroxene		18.3	51.9	0.2141	0.512672	0.003	
464-90	Plagioclase		1.27	8.65	0.0892	0.512072	0.003	
			Srednii Mamakan massif					
YaK-259	Pyroxenite, whole rock	750	1.24	3.83	0.1965	0.512776	0.003	+2.7
YaK-259/1	Mesocratic gabbro, whole rock	750	1.39	5.46	0.1547	0.512559	0.003	+2.5
YaK-259/3	Gabbro-anorthosite, whole rock	750	0.475	2.27	0.1269	0.512421	0.008	+2.5
YaK-259/2	Leucocratic gabbronorite, whole rock	750	1.49	5.58	0.1615	0.512609	0.003	+2.8
YaK-259/2	Orthopyroxene		0.317	0.943	0.2041	0.512683	0.010	
YaK-259/2	Clinopyroxene		8.24	26.1	0.1914	0.512668	0.010	
YaK-259/2	Plagioclase		0.281	2.60	0.0656	0.512063	0.010	

ages T(DM1) and T(DM2), which range from 1.8 to 2.4 Ga, indicate that protolith of the rocks corresponded to the Early Proterozoic crust. Rocks of the second group are granitoids and rhyolites of the Karalon–Mamakan zone. These show the high positive $\varepsilon_{Nd}(t)$ parameters +7.1 to +8.2 and the Late Riphean model ages varying from 700 to 750 Ma. The last data indicate that the rocks were related in origin with the juvenile magmas extracted from the mantle reservoir about 750 Ma ago. We should mention as well that the Sm–Nd isotopic characteristics of acid volcanics of the Yakor' and Karalon groups are identical. The $\varepsilon_{Nd}(t)$ = 3.9 and model age of about 1.0 Ga, which are calculated for granites of the Lesnoi complex may indicate a significant contribution of the Late Riphean juvenile component to their composition.

DISCUSSION

The generalized stratigraphic scheme and successive magmatic events in the Muya segments of the BMF, geochronology of which is modified by virtue of new isotopic data, are presented in Table 5. The additional substantiation of stratigraphic nomenclature is a particular task, but we can state even now that the Muya Group in original definition of Salop (1964) has lost the proper stratigraphic meaning. The same can be stated with respect to the Muya intrusive complex. New data clearly show that both subdivisions formerly united the Upper Riphean and Vendian rocks, which originated in the course of two independent stages of Precambrian tectogenesis, one separated from another by the phase of tectonic deformation, metamorphism, and granite emplacement 0.8 Ga ago. With this inference in mind, we think that the traditional term "Muya Group" can be used to designate only the whole succession of stratified Riphean–Vendian rocks of the Muya segment. The Early Vendian gabbro–diorite–plagiogranite intrusions in the Tallaya River basin of the Karalon–Mamakan zone should be defined then as the Tallaya complex of igneous rocks, and the term "Muya complex" could be retained (?) for the Late Riphean intrusions of similar composition in the Muya River basin of the Bambui–Olindya zone.

Considering principal stages of the Muya segment evolution, we should mention that it is impossible unambiguously define their upper age limit. The fact is that conglomerates of the Upper Vendian Mamakan Group, which underlies carbonate deposits bearing the Early Cambrian fossils, enclose pebbles of two-feldspar granites of the Lesnoi complex that is 556 ± 16 Ma old according to results of U–Pb dating. At the same time, granites of this complex experienced the quartz–feldspar metasomatism that was able to disturb the U–Pb system of analyzed zircons, and the obtained age value of 556 ± 16 Ma (Sryvtsev *et al.*, 1992) may denote, as we believe, the time of superimposed thermal event and associated alterations under influence of fluids. As a result, the time range of 0.62–(0.57–0.55?) Ga

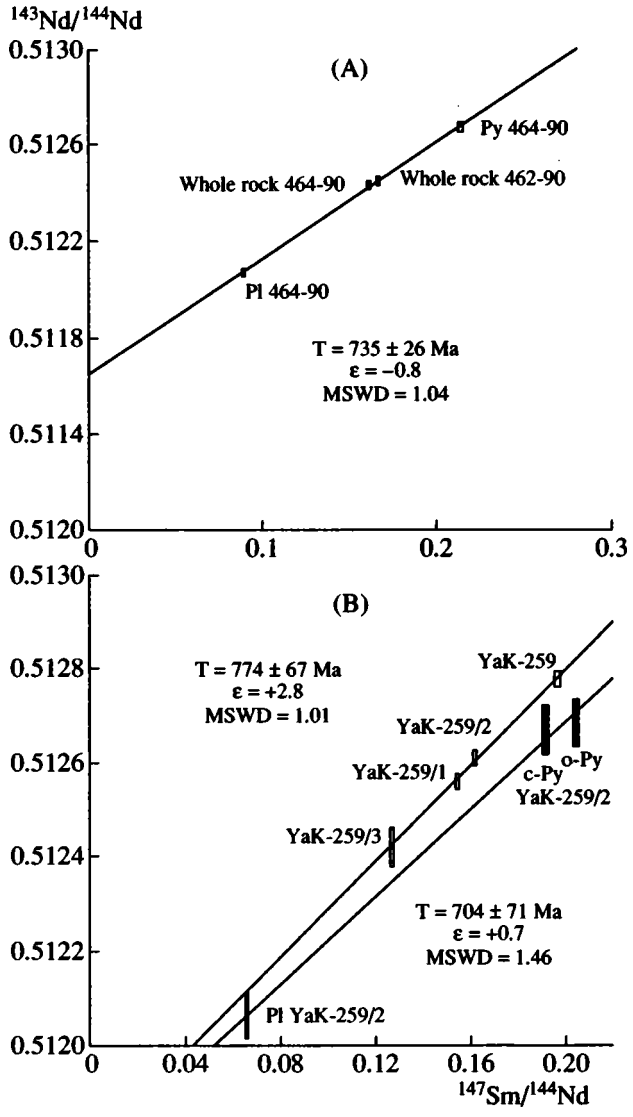

Fig. 5. Sm–Nd isochron diagrams for gabbroid rocks of the Kedrovka (A) and Srednii Mamakan (B) massifs.

can be accepted for the upper age limit of rocks in the Muya segment.

Unfortunately, the lower boundary of the Ust'-Kelyana and Param groups of the Anamakit–Muya zone cannot be dated precisely as well. The age value of 0.8 Ga obtained for synmetamorphic gneissoid granites of the Kindikan–Ileir block calls into question the pre-Riphean age of metamorphic rocks of the Dzhaltuk and Kindikan (?) groups, although the old components recognizable in zircons and the Sm–Nd isotopic data undoubtedly point to the presence of the Early Precambrian crust in the Anamakit–Muya zone. To a first approximation, we can admit that active volcanic and magmatic processes commenced in the Muya segment about 1.0 Ga ago, as this moment corresponds to the Sm–Nd isotopic age of oldest metatholeiites in the Verkhnyaya Angara segment of the BMF (Neymark

Table 4. Sm–Nd isotopic characteristics of whole-rock samples

Sample no.	Rock	Age, Ma	Sm, ppm	Nd, ppm	$^{147}Sm/^{144}Nd$	$^{143}Nd/^{144}Nd$	$\pm 2\sigma$, %	$\varepsilon_{Nd}(T)$	$T_{(DM)1}$, Ma	$T_{(DM)2}$, Ma
477-1	Rhyolite	815	8.75	45.1	0.1176	0.511640	0.002	–11.2	2388	2428
472	Plagiogranite	812	3.52	13.5	0.1580	0.512187	0.003	–4.7	2620	1889
95008-3	Gneissoid granite	785	8.99	52.4	0.1041	0.511854	0.003	–6.1	1806	1979
YuM-2b	Gneissoid granite	785	2.80	12.3	0.1386	0.511885	0.004	–8.8	2549	2200
YaK-12	Rhyolite	665	2.82	12.4	0.1379	0.512800	0.002	+8.2	707	699
95045	Plagiogranite	630	2.08	6.76	0.1863	0.512960	0.003	+7.1	1066	757
YaK-14A	Granite	550	3.08	14.3	0.1302	0.512597	0.004	+3.9	1012	962

Table 5. Stratigraphic units and magmatic complexes of the Muya segment

Age	Anamakit–Muya zone			Karalon–Mamakan zone
	Bambui–Olindya subzone	Muya subzone		
		Kindikan–Ileir block	Kedrovka–Shaman block	
Vendian	Lesnoi complex of two-feldspar granites, 556 ± 16 Ma Tuluya Group		Samodur Group	Lesnoi complex of two-feldspar granites, 556 ± 16 Ma Shumna, Delyun, and Yakrya formations
Vendian–Late Riphean				Zaoblachnyi complex of gabbroid rocks and gabbronorites 612 ± 34 Ma Tallaya gabbro–diorite–plagiogranite complex, 625–670 Ma Yakor' and Karalon groups, 625–670 Ma
Late Riphean			Bambukoi complex of granites and Zhanok Formation, 723 ± 4 Ma Kedrovka anorthosite–gabbro complex, 735 ± 26 Ma	Srednii Mamakan peridotite–gabbro complex, 704–774 Ma
	Ileir complex of gneissoid granites	Ileir complex of gneissoid granites,		
		784 ± 6 Ma	786 ± 9 Ma	
	Muya gabbro-diorite–plagiogranite complex, 812 ± 19 Ma			
	Ust'-Kelyana Group, 824 ± 2 Ma (upper part) (Buroma Formation)	Bezymyannyi Formation		
	Levyi Bambui Formation	Param Group	Kedrovka Group	
Riphean–Early Proterozoic	Vostochnyi Gorbylok Group	Dzhaltuk group Kindikan Group	Shaman group	

et al., 1991). Admitting this, we can suggest that the time ranges of 1.0(?)–0.8 and 0.8–0.62 (0.57–0.55) Ga, which are correlative with well-known Late Baikalian and Early Panafrican events in the global tectonic scale, delimit the principal formation stages of volcanogenic-sedimentary and intrusive rocks in the considered Muya segment.

Leaving aside the problem of ophiolites, which are distinguished in the BMF just tentatively, we can briefly outline the following scenario of the Late Riphean–Vendian geodynamic evolution of the Muya segment.

The first stage corresponded to the accumulation time of volcanogenic–sedimentary Ust'-Kelyana and

Param groups. According to Sm–Nd isotopic data, sediments and acid volcanics of both groups represent, along with granitoids of the Muya complex, the products of reworking of the Early Proterozoic continental crust. The corresponding processes could develop in the course of continental rifting that affected the ancient Siberian continent and was interrupted 0.8 Ga ago by the phase of deformations and metamorphism, when that continent collided with another large block of sialic crust (Rytsk *et al.*, 1998). Another assumption is that they characterize the formation period of ensialic island arcs along the continental margin and the subsequent collision of these structures that triggered processes of granitization.

The formation of layered plutons of the Kedrovka and Srednii Mamakan complexes characterizes the initial period (0.8–0.7 Ga) of the second stage. This could be either the stabilization period of tectonic structures with thick continental crust, or the post-collision events of continental rifting. The volcano-plutonic depressions with the Zhanok complex of trachyrhyolites and Bambukoi complex of two-feldspar granitoids (the U–Pb age of zircons from rhyolites is 735 Ma, personal communication of A.M. Larin and L.A. Neymark) originated during the same period in the south of the Bambui–Olindya zone. As we suspect, this peculiar period of the BMF evolution could be classified with the help of additional data as a new independent stage of tectogenesis.

The Tallaya intrusive complex and volcanogenic–sedimentary deposits of the Yakor' and Karalon groups originated in the Karalon–Mamakan zone during the terminal Late Riphean and Vendian (0.7–0.62 Ga). According to their Nd isotope characteristics, these rocks belong to the newly formed juvenile crust. Lithologic peculiarities, segmented structure, intracratonic position of the Karalon–Mamakan zone, and the fact that zircons from its volcanic rocks contain components inherited from the old continental crust, suggest that this zone represented the backward basin of crustal extension in the vast continental margin of the Paleo-Asian ocean. Tectonic deformations and metamorphism of the terminal Early Vendian time are the consequences of the Late Baikalian collision events responsible for the closure of that basin.

CONCLUSION

The obtained U–Pb and Sm–Nd isotopic data enable the following inferences:

(1) In the Middle Vitim mountainous region, volcanogenic–sedimentary and intrusive rocks of the Muya Group and synonymous intrusive complex are of the Late Riphean–Vendian age and have been formed during the Early Baikalian [1.0(?)–0.8 Ga] and Late Baikalian [0.8–0.62 (0.57–0.55?) Ga] stages of tectogenesis.

(2) As it turned out, the syntectonic granites of the Anamakit–Muya zone are 0.8 Ga old and mark a decisive moment in the tectonic evolution of the Baikal–Muya foldbelt and southeastern Siberia as a whole (Mitrofanov *et al.*, 1984). They are related in origin to the important collision events terminating the Early Baikalian phase of tectogenesis.

(3) In the current state, the Muya segment consists of two parts, where the constituent rocks reveal different isotopic signatures: products of reworking of the pre-Riphean continental crust prevail in one part of the segment, whereas the other one is predominantly composed of rocks genetically related to the depleted mantle reservoir of the Late Riphean time.

ACKNOWLEDGMENTS

We are grateful to A.F. Makeev and B.M. Gorokhovskii for their assistance in analytical procedures, to A.M. Larin for his helpful criticism, and to G.P. Pleskach for graphical drawing. The work was supported by the Russian Foundation for Basic Research, project nos. 95-05-15104 and 98-05-65593.

Reviewer E.V. Bibikova and A.B. Kotov

REFERENCES

Amelin, Yu.V., Geochronology of the Jack Hills Detrital Zircons by Precise U–Pb Isotope Dilution Analysis of Crystal Fragments, *Chem. Geol.*, 1998, vol. 146, pp. 25–38.

Buldygerov, V.V., Sryvtsev, N.A., and Isakov, Yu.A., The Early Paleozoic volcanism in Central Area of the Baikal Mountain Region, *Geol. Geofiz.*, 1995, vol. 36, no. 1, pp. 31–38.

Bulgatov, A.N., *Tektonotip baikalid* (The Tectonic Standard of Baikalides), Novosibirsk: Nauka, 1983.

Dobretzov, N.L., Berzin, N.A., and Buslov, M.M., Opening and Tectonic Evolution of the Paleo-Asian Ocean, *Intern. Geol. Rev.*, 1995, vol. 37, pp. 335–360.

Dobrzhinetskaya, L.F., Korikovskii, S.P., Rile, G.V., *et al.*, The Lower Proterozoic Stratigraphy of the Delyun-Uran and Northern Muya Ridges, in *Stratigrafiya dokembriya regiona Srednei Sibiri* (The Precambrian Stratigraphy of Central Siberia), Leningrad: Nauka, 1983, pp. 103–113.

Fedorovskii, V.S., *Nizhnii proterozoi Baikal'skoi gornoi oblasti* (The Lower Proterozoic of the Baikal Mountain Region), Moscow: Nauka, 1985.

Gabov, N.F., Dobretsov, N.L., and Kushev, V.G., Eclogites and Eclogite-like Rocks in the Northern Baikal Region, in *Petrologiya i mineralogiya bazitov Sibiri* (Petrology and Mineralogy of Basic Rocks from Siberia), Moscow: Nauka, 1984, pp. 36–50.

Geologicheskaya karta Irkutskoi oblasti i sopredel'nykh territorii. Masshtab 1 : 500000 (Geological Map of the Irkutsk Region and Adjacent Areas, Scale 1 : 500000), Moscow: Min. Geol. SSSR, 1982.

Goldstein, S.J. and Jacobsen, S.B., Nd and Sr Isotopic Systematics of River Water Suspended Material: Implications for Crustal Evolution, *Earth Planet. Sci., Lett.*, 1988, vol. 87, pp. 249–265.

Gusev, G.S., Peskov, A.I., and Sokolov, S.K., Paleogeodynamics of the Muya Segment of the Proterozoic Baikal–Vitim Belt, *Geotektonika*, 1992, no. 2, pp. 72–86.

Izokh, A.E., Gibsher, A.S., Zhuravlev, D.Z., and Balykin, P.A., The Sm–Nd Age of Mafic-Ultramafic Massifs in the Eastern Branch of the Baikal–Muya Ophiolite Belt, *Dokl. Ross. Akad. Nauk*, 1998, vol. 360, no. 1, pp. 88–92.

Konnikov, E.G. and Tsygankov, A.A., On the Heterogeneity of the Baikal–Muya Ophiolite Belt, *Dokl. Akad. Nauk SSSR*, 1992, vol. 327, no. 1, pp. 115–120.

Kozyreva, I.V., Konnikov, A.Z., and Travin, L.V., Metamorphic Grades of Lower Precambrian Rocks in the Northern Muya Block and Surrounding Structures (the Middle Vitim Mountains), in *Geologiya i geokhronologiya dokembriya Sibirskoi platformy i ee obramleniya* (Precambrian Geology and Geochronology of the Siberian Platform and Surrounding Structures), Leningrad: Nauka, 1990, pp. 67–88.

Krogh, I.E., A Low Contamination Method for Hydrothermal Decomposition of Zircon and Extraction of U and Pb for Isotopic Age Determinations, *Geochim. Cosmochim. Acta*, 1973, vol. 37, pp. 485–494.

Liew, T.C. and Hoffman, A.W., Precambrian Crustal Components, Plutonic Associations, Plate Environment of the Hercynian Fold Belt of Central Europe: Indications from Nd and Sr Isotopic Study, *Contrib. Mineral. Petrol.*, 1988, vol. 98, pp. 129–138.

Ludwig, K.R., A Computer Program of Processing Pb–U–Th isotope data, *US Geol. Surv. Open File Report*, 1991, no. 88-542.

Ludwig, K.R., A Plotting and Regression Program for Radiogenic Isotopic Data, *US Geol. Surv. Open File Report*, 1992, no. 91-445.

Mitrofanov, G.L., Tectonic Evolution and Stages of the Continental Crust Development in the Northwestern Baikal Region, in *Tektonika i metallogeniya Vostochnoi Sibiri* (Tectonics and Metallogeny of Eastern Siberia), Irkutsk: Irkut. Gos. Univ., 1978, pp. 38–57.

Mitrofanov, G.L., The Baikal Megacomplex in Inner Zones of the Baikal Mountainous Region, in *Tektonika Baikal'skogo (rifeiskogo) megakompleksa Sibiri* [Tectonics of the Baikal (Riphean) Megacomplex in Siberia], Novosibirsk: Inst. Geol. Geofiz., 1981, pp. 73–87.

Mitrofanov, G.L., Levitskii, V.V., and Mitrofanova, N.N., Magmatism and Endogenic Metallogeny as Related to the Basement Blocky Structure in the Kater–Ukolkit and Muya Areas, Western Sector of the Baikal–Amur Railroad, in *Magmatizm i metamorfizm zony BAM i ikh rol' v formirovanii poleznykh iskopaemykh* (Magmatic and Metamorphic Events near the Baikal–Amur Railroad and Their Influence on Regional Metallogeny), Novosibirsk: Nauka, 1983, pp. 73–80.

Mitrofanov, G.L., Nikol'skii, F.V., Taskin, A.P., and Khrenov, P.M., Late Precambrian Foldbelts in the South of East Siberia, in *Geologiya dokembriya, 27 MGK, sektsiya C.05. Doklady* (Proc. 27th Intern. Geol. Congress, Section C.05: Geology of the Precambrian), Moscow: Nauka, 1984, vol. 5, pp. 119–125.

Neymark, L.A., Rytsk, E.Yu., and Gorokhovskii, B.M., Pb Isotope Composition and Genesis of the Pb–Zn Mineralization in the Olokit Zone of the Northern Baikal region, *Geol. Rudn. Mestorozhd.*, 1991, no. 6, pp. 34–49.

Rytsk, E.Yu., Krimsky, R.Sh., Rizvanova, N.G., and Shalaev, V.S., Sedimentary Basins and Rifts of the Late Precambrian in the Baikal Mountainous Region, *Konferentsiya: Osadochnye formatsii dokembriya i ikh rudonosnost'* (Conference: Precambrian Sedimentary Formations and Their Metallogeny), Novosibirsk, 1998, p. 64.

Salop, L.I., *Geologiya Baikal'skoi gornoi oblasti* (Geology of the Baikal Mountainous Region), Moscow: Nedra, 1964, vol. 1, 1967, vol. 2.

Shatskii, V.S., Jagoutz, E., Ryboshlykov, Yu.V., *et al.*, Eclogites of the Northern Muya Block: Indicators of Vendian Collision in the Baikal–Muya Ophiolite Belt, *Dokl. Ross. Akad. Nauk*, 1996, vol. 350, no. 5, pp. 677–680.

Sryvtsev, N.A., Khalilov, V.A., Buldygerov, V.V., and Perelyaev, V.I., Geochronology of Granitoids in the Baikal–Muya Belt, *Geol. Geofiz.*, 1992, no. 9, pp. 72–78.

Stacey, J.S. and Kramers, J.D., Approximation of Terrestrial Lead Isotope Evolution by a Two-Stage Model, *Earth Planet. Sci. Lett.*, 1975, vol. 26, pp. 207–221.

Stanevich, A.M. and Faizulina, Z.Kh., *Mikrofossilii v stratigrafii pozdnego dokembriya Baikalo-Patomskoi gornoi oblasti* (Microfossils in the Upper Precambrian Stratigraphy of the Baikal–Patom Mountainous Region), Moscow: Nedra, 1992.

Stanevich, A.M. and Perelyaev, V.I., To the Upper Precambrian Stratigraphy of the Middle Vitim Mountains, *Geol. Geofiz.*, 1997, vol. 38, no. 10, pp. 1642–1652.

Steiger, R.N. and Jager, E., Convention on the Use of Decay Constants in Geo- and Cosmochronology, *Earth Planet. Sci. Lett.*, 1977, vol. 36, pp. 359–362.

Tsygankov, A.A., Vrublevskaya, T.T., Konnikov, E.G., and Posokhov, V.F., Geochemistry and Petrology of Granitoids from the Muya Intrusive Complex, *Geol. Geofiz.*, 1998, vol. 39, no. 3, pp. 361–374.

Stratigraphy and Geological Correlation, Vol. 9, No. 4, 2001, pp. 327–339. Translated from Stratigrafiya. Geologicheskaya Korrelyatsiya, Vol. 9, No. 4, 2001, pp. 16–28.
Original Russian Text Copyright © 2001 by Malysheva, Kanev, Koloda.
English Translation Copyright © 2001 by MAIK "Nauka/Interperiodica" (Russia).

The Timan–Pechora Paleogeography and Facies in the Kungurian–Ufimian Boundary Period

E. O. Malysheva, G. P. Kanev, and N. A. Koloda

Institute of Geology, Komi Scientific Center, Uralian Division, Russian Academy of Sciences, Pervomaiskaya ul. 54, Syktyvkar, 167610 Russia

Received January 5, 1999, in final form, March 29, 1999

Abstract—The complicatedly intercalated marine and continental Permian beds of the Timan–Pechora region are subdivided using the combination of the litho- and biostratigraphic methods and the sequence stratigraphy technique. Among the distinguished intervals favorable for paleogeographic reconstructions, one across the Kungurian–Ufimian boundary is considered in this work. The well-studied sections that are exposed in the Uralian foredeep and those recovered by boreholes in the Pechora syneclise are chosen to be the reference ones. The regional correlation is based on the established facies changes along the boundaries of and inside the units of the reference sections. Ten facies–paleogeographic zones are recognized in the Timan–Pechora region for the Kungurian–Ufimian boundary period.

Key words: facies, paleogeography, correlation, sequence stratigraphy, fossil biota, Kungurian–Ufimian boundary beds, Timan–Pechora region

INTRODUCTION

Paleogeographic maps represent the most significant result of detailed stratigraphic and facies investigations and are especially useful for mineral prospecting in sedimentary sequences. Paleogeographic reconstructions for periods of contrasting tectonic and sedimentation events always meet difficulties. This especially concerns the periods of transition from marine to continental sedimentation environments, when we usually observe an abrupt decrease in abundance of stratigraphically important biota.

We faced these problems in reconstructing the Late Permian paleogeography of the Timan–Pechora region located in Northeastern Europe between the Urals and Timan (Fig. 1). In this region, the Late Permian time was characterized by active orogeny in the Urals that caused structural transformations and transition from predominantly marine sedimentation to continental one. The regional lithological–facies and paleogeographic maps are necessary in this case, because main commercial coal reserves and significant oil and gas resources are concentrated in the Upper Permian deposits of the region.

BRIEF INVESTIGATION HISTORY

The best studied in the region are the Upper Permian deposits of the Pechora coal basin, the northern part of the Uralian foredeep included. Main contribution to lithological–facies investigations of the coal-bearing deposits in the region was done by geologists from Vorkuta (Ivanov, 1947; Ivanov and Makedonov, 1977; Makedonov, 1958, 1965; Yaroslavtsev, 1962; Khaitser, 1962a, 1962b; Afanas'ev, 1968; Shurekov, 1976; and others). Results of combined lithological–stratigraphic studies of the 1930s–1960s are summarized in some collective monographs (*Geologiya...*, 1965; *Istoriya...*, 1965). Works by Chalyshev (1974), Chalyshev and Varyukhina (1968), Murav'ev (1972), and Murav'ev *et al.* (1975, 1984) represent an important contribution to understanding of Permian lithology not only in the Pechora coal basin, but also in the entire Uralian foredeep. Among the latest publications, we should mention the summarizing monograph of the geologists from Vorkuta and Syktyvkar (*Uglenosnaya...*, 1990) and a number of articles of geologists from Yekaterinburg on the Lower Permian stratigraphy of the Cis-Urals (Chuvashov *et al.*, 1990a, 1990b; Chuvashov, 1997).

The history of lithological–facies investigations in the Pechora syneclise is associated with works by Entsova *et al.*, (1969), Nikonov and Golovan' (1983), Oknova and Kozulina (1984), Lyubina (1984), Vazhenin and Galkina (1984), Malysheva (1985) and Malysheva *et al.* (1993). Despite the different approach and scaling, the listed works characterize sedimentary facies of the Upper Permian, substantiate cyclic development of marine-continental sedimentation, suggest models of the coal-deposition cycle and accumulation of deltaic and alluvial deposits, and include lithological–facies maps for different Permian stages (*Atlas...*, 1972; Murav'ev *et al.*, 1975). Because of significant facies variability even within a stage, these maps are however conventional to some extent and inappropriate

for proper understanding of paleogeographic environments.

Our main purpose was the facies–paleogeographic mapping of the region for particular time intervals of the Permian. The Lower–Upper Permian boundary beds most fully characterized by paleontological remains were chosen as the priority object in the Timan–Pechora region. Our paleogeographic reconstructions are based on the detailed biostratigraphic data interpreted using the sequence stratigraphy approach.

METHODS

Sequence stratigraphy, which involves the bio-, litho-, and seismostratigraphic methods, is used in practice of subdivision and correlation of petroliferous basins since the 1980s. Fundamental in this case is the concept of sedimentary sequences defined as relatively conformable successions of genetically related strata, which are bounded by unconformities or correlative conformable boundaries (Mitchum, 1977). Unconformity is a surface separating younger and older beds, which show signs of being truncated during long subaerial exposure, or eroded sometimes in submarine conditions (Van Wagoner *et al.*, 1988, 1990; *Siliciclastic...*, 1994). Sequences include system tracts distinguishable by their position inside the sequence and by structure of constituent parasequences. The latter are defined as relatively conformable successions of genetically related strata bounded by flooding surfaces. System tracts are associations of relatively synchronous facies or lateral facies successions (Van Wagoner *et al.*, 1990; Posamentier and Vail, 1988). They are of great importance for understanding of facies development. For instance, the lowstand system tract is formed during the period from a sharp fall to the subsequent rise of sea level. Thick fans are the first to be accumulated, and afterward, as the sea level slowly rises, the complex of superimposed stream and coastal facies is formed. Sequence boundaries and flooding surfaces are considered as chronostratigraphic framework for correlation and mapping of sedimentary complexes. Along with signs of subaerial erosion, an important criterion of recognizing sequence boundaries in outcrops, core sections, and well-log diagrams, is a sharp facies displacement evidencing for the basin shoaling. At the sequence boundaries, the facies changes associate with noticeable transformations of the section structure. For these reasons, system tracts seem to be the most favorable objects of paleogeographic mapping.

The detailed analysis of facies lithology was performed using the existing methods (Zhemchuzhnikov *et al.*, 1959; Timofeev, 1969; Ivanov *et al.*, 1977; Visher, 1969; Muromtsev, 1984, and others) and results of studies of modern accumulative forms (Reinek and Singkh, 1981; *Sandstone...*, 1982). We should emphasize the great significance of the facies analysis not only for reconstruction of sedimentation environment but also for stratigraphic correlation. The latter is the primary purpose of the facies analysis proper.

Basic data used in this work are the results of lithological and paleontological investigations of representative borehole sections and outcrops in the Timan–Pechora region (Koloda *et al.*, 1992; Kanev, 1994). We also used the results of identifications of paleontological remains from borehole sections, which have been donated by the Timan–Pechora Scientific Center (Ukhta). The naturally exposed and recovered sections, which represent stratotypes of certain facies zones and are well characterized by palynological and faunal remains, were chosen as the reference ones for genetic interpretation and distinguishing of sequences and system tracts. We paid main attention to the nature of those boundaries between stratigraphic units, which are well defined on the basis of paleontological remains. In particular, we studied eight reference sections of the Kungurian–Ufimian boundary beds (Fig. 1). The regional correlation is established on the base of regular facies changes along the boundaries and inside stratigraphic units of the reference sections. The lithological-facies cross-sections (Fig. 2) characterize the main structural elements and recognizable facies zones. Paleogeography is reconstructed for the initial period of the Ufimian Age that corresponds to the lowstand system tract of the first Ufimian sequence. The corresponding map is ordinarily interpolated from the structural map of a top surface of the Permian carbonates (*Tektonika...*, 1988).

REFERENCE SECTIONS

The Kungurian–Ufimian boundary section **at the Kozhym River** (Fig. 3) is most complete and well-studied in paleontological aspect. It is located in the southern Kos'yu-Rogov depression of the Uralian foredeep. The section characterizes sedimentation in a humid zone, which the Pechora coal basin is referred to. The upper Kungurian (Kozhym) and lower Ufimian (Kozhym Rudnik) formations are described in detail in the collective monograph "Biota of the Early–Late Permian Boundary Time in East European Russia" (1998). The upper part of the Kozhym Formation (Beds 456–448) is a typical cyclic regressive sequence characterized by easily recognizable parasequences of uniform structure. Each parasequence begins with horizontally or indistinctly bedded and frequently bioturbated silty siltstones grading into sandy–silty and sandy deposits. Sandstones grade upward from fine- to medium-grained. They predominantly reveal the cross-bedded textures and bedding planes with fine ripple marks. Terminal beds of the cycles exhibit slightly eroded flooding surfaces frequently associated with residual small clayey pebbles and coquina. These features suggest the coastal-bar environment of sedimentation. Fossil biota includes small foraminifers, ostracodes, brachiopods, bryozoans, crinoids, bivalves, and gastropods (*Putevoditel'...*, 1995; *Biota...*, 1998). According to Koloda, successive miospore spectra indicate the Kun-

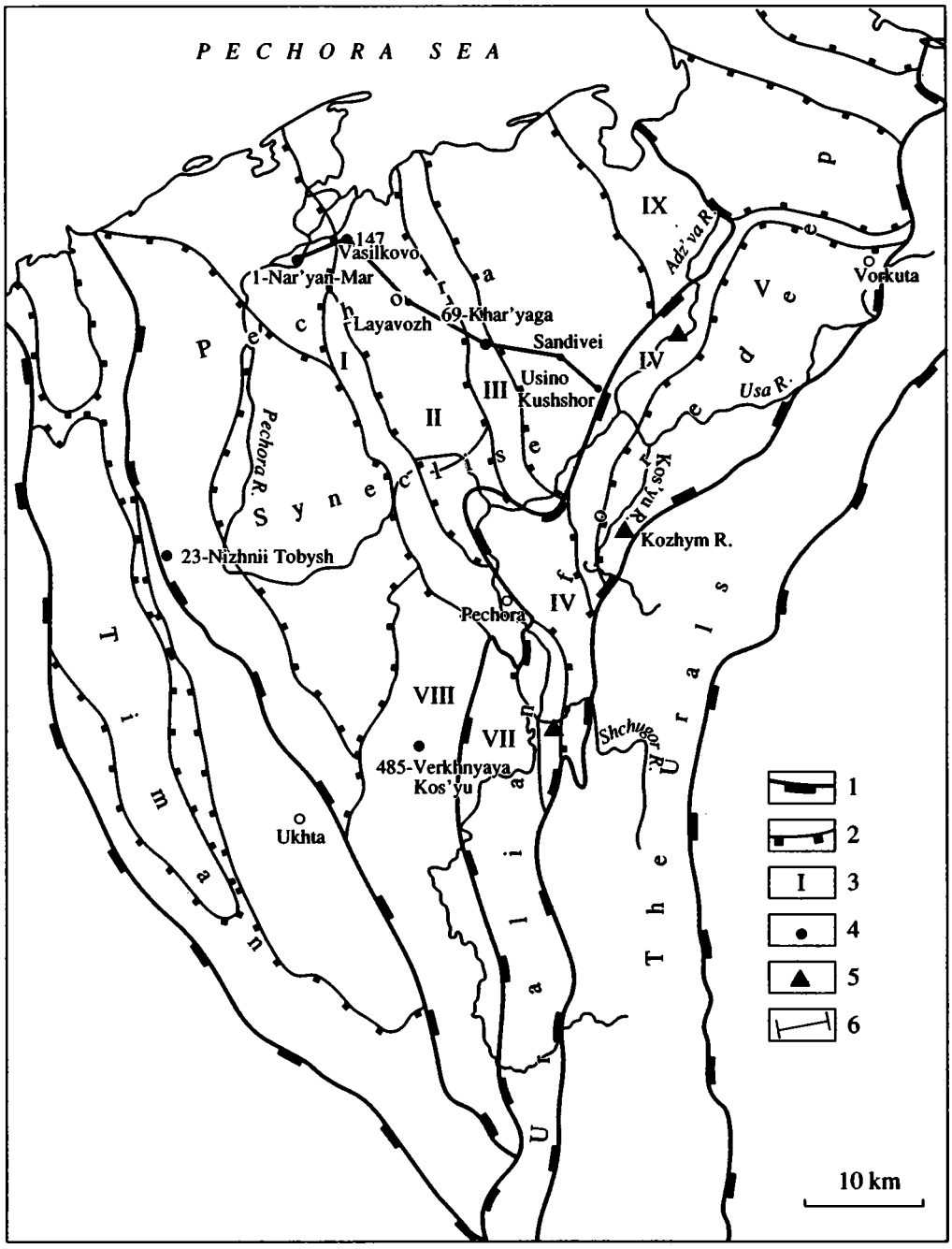

Fig. 1. Generalized structural map of the Timan–Pechora region: (1) boundary between superorder structures; (2) boundary between first-order structures; (3) structure number; (4) reference borehole section; (5) naturally exposed reference section; (6) line of facies profile. The first-order structures by numbers: (I) Pechora-Kozhva swell, (II) Denisovo depression, (III) Kolva swell, (IV) Chernyshev Ridge, (V) Kos'yu-Rogov depression, (VI) Bol'shaya Synya depression, (VII) Verkhnyaya Pechora depression, (VIII) Omra-Luza saddle, and (IX) Varandei-Adz'va zone.

gurian age of the Kozhym Formation. At the base of the Kozhym Rudnik Formation, there is a sandy unit of complex structure (Bed 447) formerly referred to the previous formation (Rotai, 1947). The lower part of the unit (members 447.1–447.7) is represented by blocky fine- and medium-to-fine-grained sandstones displaying first horizontal and then multidirectional cross bedding. This part includes interbeds with fragmented brachiopod and bivalve shells and silty material. In the structure and depositional environment, this part is similar to the underlying deposits described above. The upper part of the unit (members 447.8–447.11) is predominantly composed of inequigranular and medium-grained sandstones showing unidirectional furrow-like

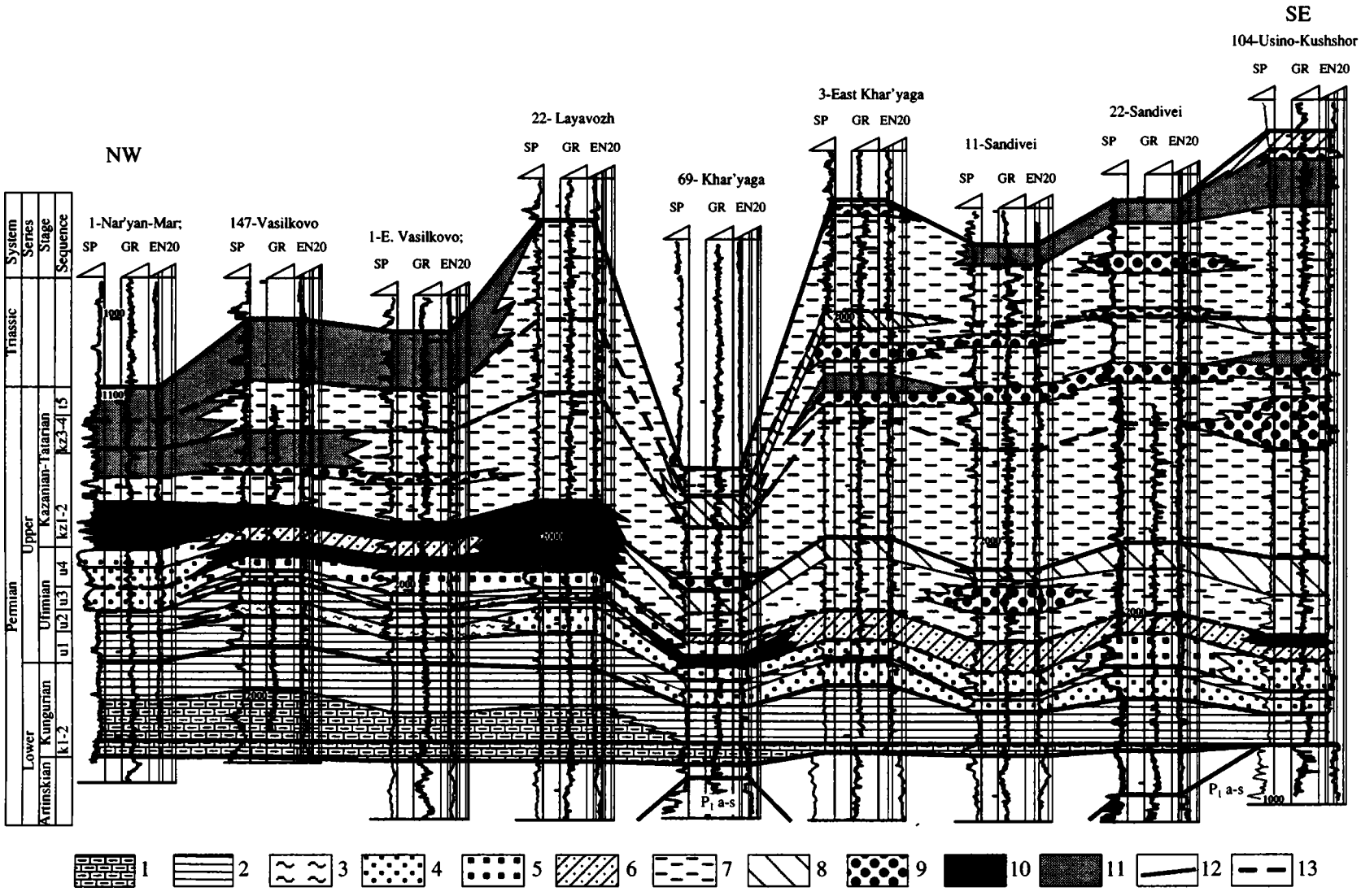

Fig. 2. Facies profile along the line Borehole-1 Nar'yan-Mar–Borehole-104 Usino-Kushshor. Facies: (1) terrigenous–carbonate sediments of the open shelf; (2) terrigenous sediments of the open shelf; (3) sandy–silty sediments of distant bars; (4 and 5) sandy sediments of the lower and upper shoreface, respectively; (6) terrigenous sediments of the intertidal zone; (7) undivided predominantly gray and (8) red continental deposits; (9) sandy to gravel stream-channel deposits; (10) coaliferous deposits of the tidal flat; (11) coaliferous deposits of the lacustrine-alluvial plain; (12) stratigraphic boundaries (coincident with sequence boundaries); (13) sequence boundary.

cross bedding. There are clayey pebble inclusions, carbonaceous detritus, imprints and even fossil stems of plants. The topmost sandstones are brownish in color and show the roots-bioturbation texture. This unit has distinct erosional contact with the underlying deposits, frequently truncated. The sandstones are overlain by succession of carbonaceous siltstones, white clay, and first coal interbed of Permian age (members 446–444). According to lithological peculiarities, members 447.8–444 can be generally attributed to tidal flat deposits, the channel and marshy facies included. Some interbeds show signs of being reworked. The clayey–silty members 443.2–442 containing brachiopods, bryozoans, and marine bivalves were deposited during the rapidly developing transgression. The earliest Ufimian palynological assemblage characterizes the lower Solikamsk Horizon (Beds 447–419). According to palynological data, there was no chronostratigraphically significant hiatus in sedimentation between the Kungurian and Ufimian deposits of this section. However, it can be suggested that the Kungurian–Ufimian boundary coincides with significant structural changes in the section, which originated in response to abrupt shoaling of sedimentary basin and transition from shallow-marine to continental sedimentation. The lower boundary of the first Ufimian sequence should be drawn at the base of the Member 447.8, and members 447.8–444 can be assigned to the lowstand system tract.

The section located at the "lower gates" of *the Shchugor River* (Outcrop 24 of Chalyshev, or Outcrop 3 of Murav'ev; Fig. 3) is chosen as the reference section of Kungurian–Ufimian boundary beds for the southern areas of the Uralian foredeep. In this section, the indicated boundary coincides with the that separating the Kyrtada and Bol'shoi Elmach formations (Murav'ev, 1972). The section is less exposed and less fossiliferous than the Kozhym section. Facies investigation shows that, similarly to the upper Kozhym Formation, the upper part of the Kyrtada Formation was formed under the conditions of cyclically alternating upper shoreface and shelf environments. At the base of the Bol'shoi Elmach Formation, there are sandy oolitic limestones (Bed 29.5) that yield abundant fragmentary shells of brachiopods *Rhynchopora*. The limestones are overlain by poorly exposed predominantly clayey–silty deposits with fine-grained sandstone interbeds (Beds 30–36). Upward, the vaguely cross-bedded and fine-grained sandstones rest on slightly eroded wavy surface. They reveal indistinct imprints of small bivalve shells. The sandstones grade into oolitic limestones (Beds 37 and 38) that underlie the predominantly sandy deposits with gravelstone conglomerate interbeds (Beds 40–42). The structure of sandstone members, along with presence of gravelstone conglomerates and absence of marine fauna widespread below, indicate that the Bol'shoi Elmach Formation was accumulated in a tidal flat with abundant shoals and stream channels. Consequently, the Kyrtada–Bol'shoi Elmach boundary corresponds to the level of structural changes caused by a sudden shoaling of sedimentary basin and can be considered as the sequence boundary. The Kungurian age of the Kyrtada Formation is indicated by enclosed fusulinids, ammonoids, and brachiopods (Chuvashov *et al.*, 1990b; Chuvashov, 1997), and the same age of the Bol'shoi Elmach Formation is inferred on the basis of small foraminifers (the lower part of the section), bivalves, and miospore assemblages occurring in this unit.

In **the Adz'va River** section (the Chernyshev Ridge) located in the junction zone of the Uralian foredeep and the Pechora syneclise, the Kungurian–Ufimian boundary is recognized inside the Adz'va Formation (Fig. 3) (*Skhemy...*, 1994). Here, the boundary less distinct lithological aspect also corresponds to changes in the section structure, which are combined with a significant renewal of the foraminiferal species and genera, and also of marine bivalve and brachiopod assemblages (Sukhov and Igonin, 1990; Kanev, 1994). The lower part of the Adz'va Formation (Beds 1–11) is composed of clayey–silty shelf sediments, and its middle part (Beds 12–17) that yields the earliest Ufimian palynological assemblage consists of the upper shoreface silty–sandy deposits similar to those in the upper parts of the Kozhym and Kyrtada formations. The Kungurian–Ufimian boundary corresponds in this section to the transition from shelf to upper shoreface environments.

Characterizing the Kungurian–Ufimian boundary deposits, we also used data on the most complete borehole sections of the Pechora syneclise, where they are well studied in paleontological aspect (*Reshenie...*, 1990). Sections of **the Khar'yaga, Vasilkovo and Nar'yan-Mar areas** (Fig. 4) are chosen as the reference ones for the northern part of the syneclise. The Kungurian–Ufimian boundary is established here most reliably on the basis of palynological evidence analyzed by Tel'nova (the Khar'yaga area) and Koloda (the Vasilkovo and Nar'yan-Mar areas). The miospore assemblages allowed us as well to reveal contact between the Kungurian and Ufimian deposits in the Vasilkovo section. The contact is recognized inside marine shelf sediments, at the base of a thick sandy stratum that exemplifies, in our opinion, the facies of offshore bars. In the Khar'yaga section, the Kungurian and Ufimian deposits, age of which is proved by paleontological evidence, are separated by a thick sandy stratum that is of typical bar genesis and has been deposited in the lower shoreface zone. In the Nar'yan-Mar section, the boundary is marked by an insignificant increase in abundance of sandy material in the marine shelf deposits. The above data suggest that the Kungurian–Ufimian boundary well substantiated by paleontological materials marks the beginning of intense sand removal to the north of the Pechora syneclise. As for the Uralian foredeep, the boundary corresponds here to the structural changeover in the sections.

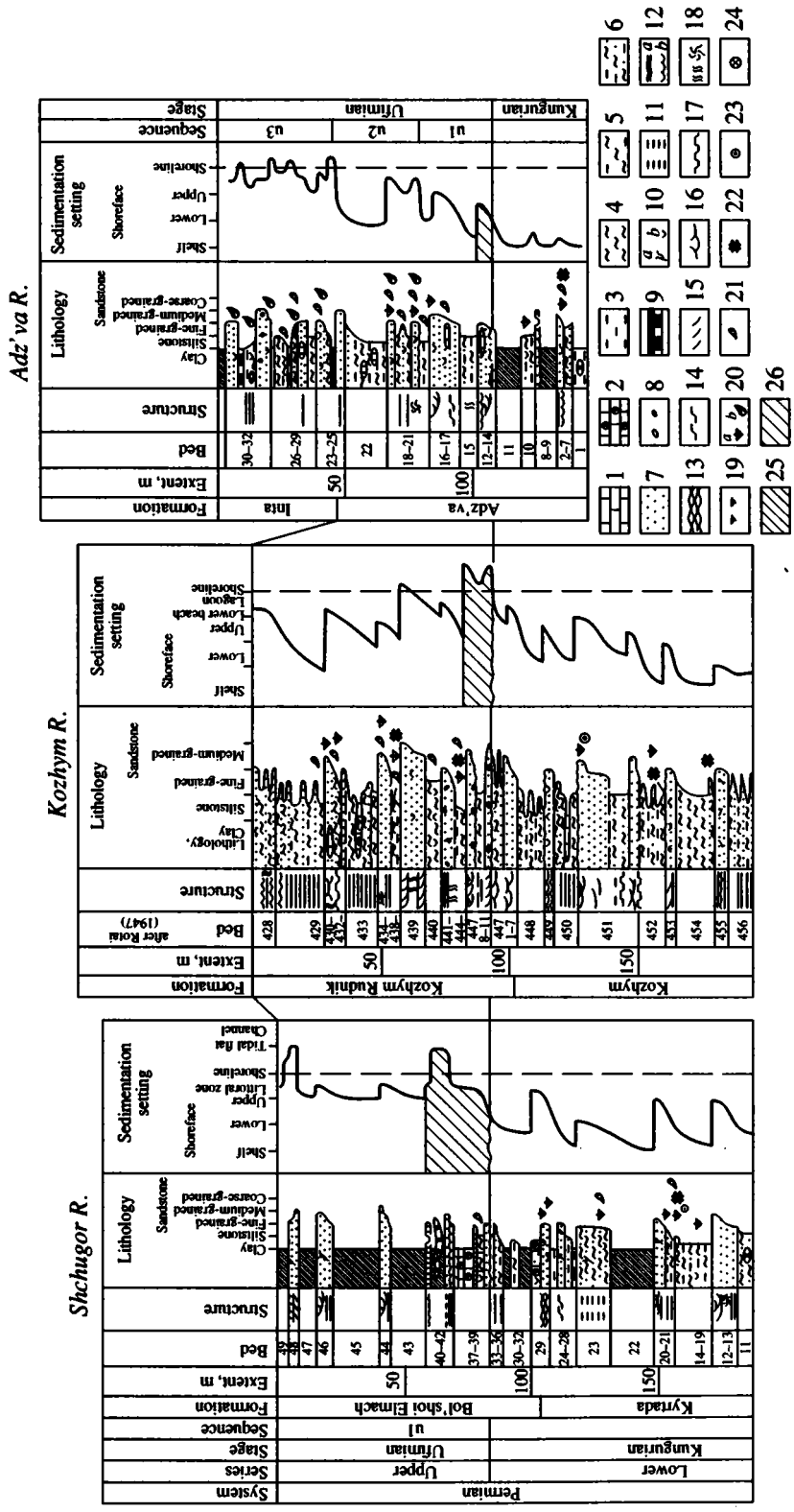

Fig. 3. Reference sections of naturally exposed Kungurian–Ufimian boundary deposits: (1) limestone, (2) oolitic limestone, (3) mudstone and clay, (4) siltstone, (5) alternating clay and siltstone, (6) alternating clay, siltstone, and sandstone, (7) sandstone, (8) pebble and gravel inclusion, (9) coal and coaliferous deposits; (10) remains of flora (*a*) and fauna (*b*). Structural features: (11) massive, (12) sinuous bedding (*a*) and ripple marks on bedding planes (*b*), (13) lenticular bedding, (14) current bedding, (15) unidirectional cross bedding, (16) multidirectional cross bedding, (17) bioturbation, (18) fucoids, (19) signs of pedogenesis. Fauna and other symbols: (20) brachiopods, including *Lingula* (*a*), (21) bivalves, (22) bryozoans, (23) crinoids, (24) foraminifers; (25) unexposed interval; (26) mapped interval.

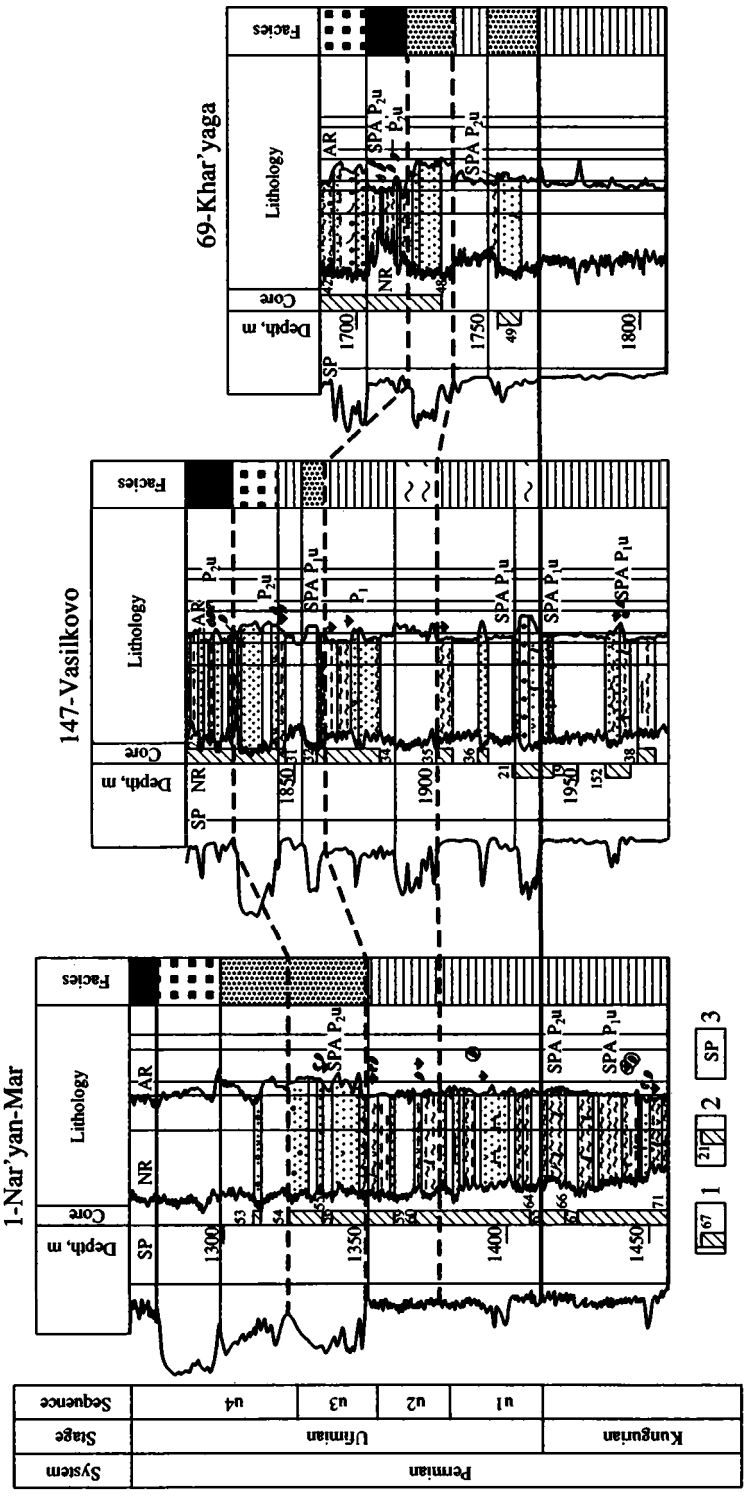

Fig. 4. Reference borehole sections of the Kungurian-Ufimian boundary deposits (the northern Pechora syneclise): (1) sampling interval and its number, Borehole 1-Nar'yan-Mar; (2) ditto for other boreholes; (3) logs of spontaneous polarization (SP), apparent resistance (AR), and natural radioactivity (NR); (SPA) spores-and-pollen assemblage; other symbols as in Figs. 2 and 3.

The Borehole 485 of the Verkhnyaya Kos'yu area was drilled with continuous core sampling by the Ukhta Geological Prospecting Expedition holding the contract with Association "Pechorageofizika." This section was used as a reference one for the southern part of the Pechora syneclise (Fig. 5). It should be noted that terrigenous Permian deposits, particularly the Kungurian–Ufimian boundary beds, are poorly characterized by

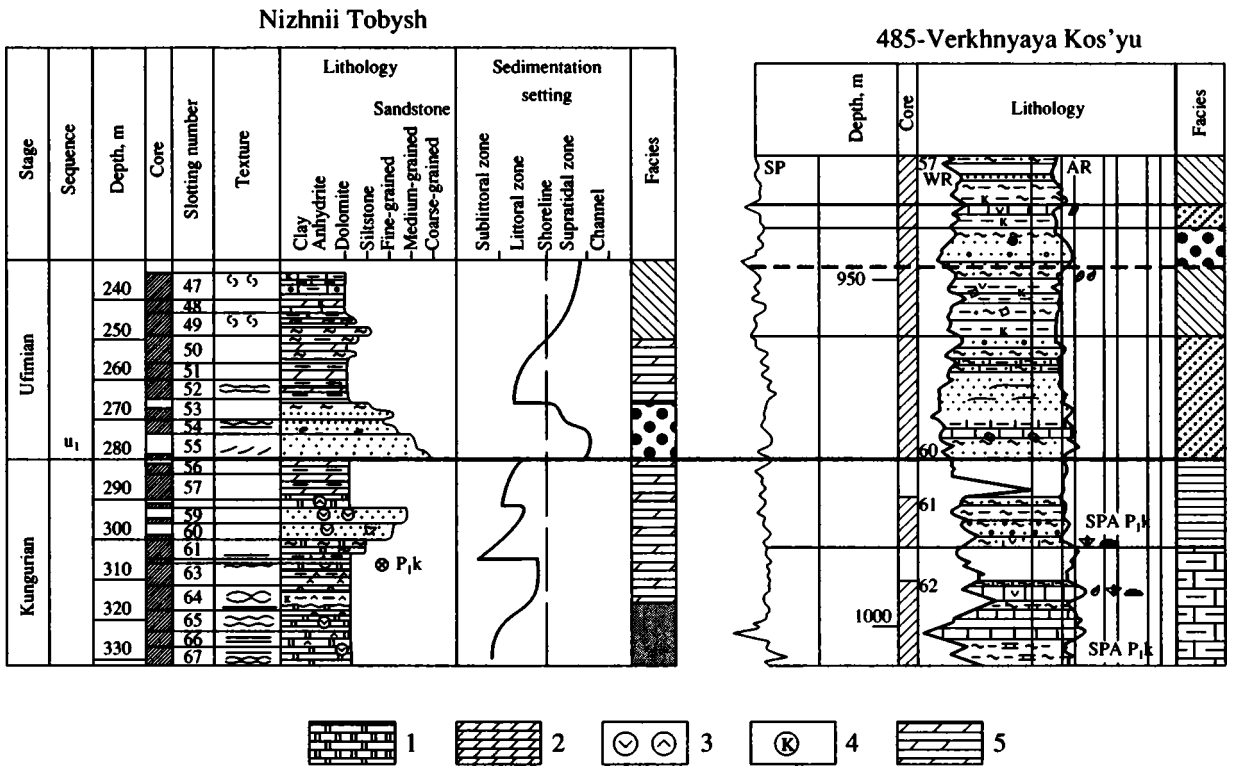

Fig. 5. Reference borehole sections of the Kungurian-Ufimian boundary deposits (the southern Pechora syneclise): (1) dolomite; (2) marl; (3) gypsum and anhydrite; (4) red beds; (5) facies of semiinsulated shelf; other symbols as in Figs. 2–4.

fossils. By comparison with neighboring (e.g., Shchugor) sections, the boundary can be placed here at the level of the oolitic limestone interbed. The underlying limestones and mixed clayey–carbonate and clayey–silty deposits, which include interbeds with marine brachiopods, gastropods, and bivalves, were formed in an open shelf environment. According to Koloda, they yield the Kungurian miospore assemblages. The basal Ufimian sandy member is represented by fine-grained sandstones showing horizontal or oblique bedding. The member includes several clayey–silty interbeds showing fucoids and one interbed of oolitic limestones. Makarova identified the palynological assemblage of Ufimian age from this member. Clayey–silty deposits lying above are colored brown and contain abundant carbonate nodules, presumably of the calcrete type. The described sandy member and overlying deposits were probably formed in the tidal flat with frequent supratidal settings. Thus, in this section, the boundary under discussion marks the moment of a sudden shoaling of sedimentary basin, and thus it can be interpreted as the sequence boundary.

The interesting and peculiar section of **the Borehole 23 of the Nizhnii Tobysh area** (Fig. 5), which was almost completely sampled, characterizes the westernmost part of the Pechora syneclise. Anhydrite–dolomitic deposits, which are referred to the Kungurian Stage on the base of small foraminifers, include here gypsum and anhydrite interbeds, veins, and nodules. The deposits have a sharp erosional contact with the overlying gray- to red-colored terrigenous–carbonate deposits resting on the basal sandy member. The sandstones of obvious channel genesis show gradation from lower coarse-grained to upper medium- to fine-grained varieties, unidirectional cross bedding, and presence of clay balls. These lithological changes observable across the Kungurian–Ufimian boundary indicate once again a quick shoaling of the basin and transition from saline lagoonal to tidal flat settings.

The analyzed lithological features of the Kungurian–Ufimian boundary deposits in the studied borehole and exposed sections show that this boundary marks the regional shoaling event and commencement of an intense sand removal. The level under discussion can also be interpreted as the lower boundary of the first Ufimian sequence that begins with deposits of the maximal regression phase, or of the lowstand system tract. In the sections described above, these deposits characterize facies of marshy tidal flat, intertidal zone, lower shoreface and shelf settings, and facies of the offshore bar. They lie under the relatively deep-water shelf sediments of the distinct transgressive system tract, which are easily recognizable owing to their lithological features and fossil groups, and also logging. Sediments of the highstand system tract corresponding to the initial regression phase are poorly represented in the sections.

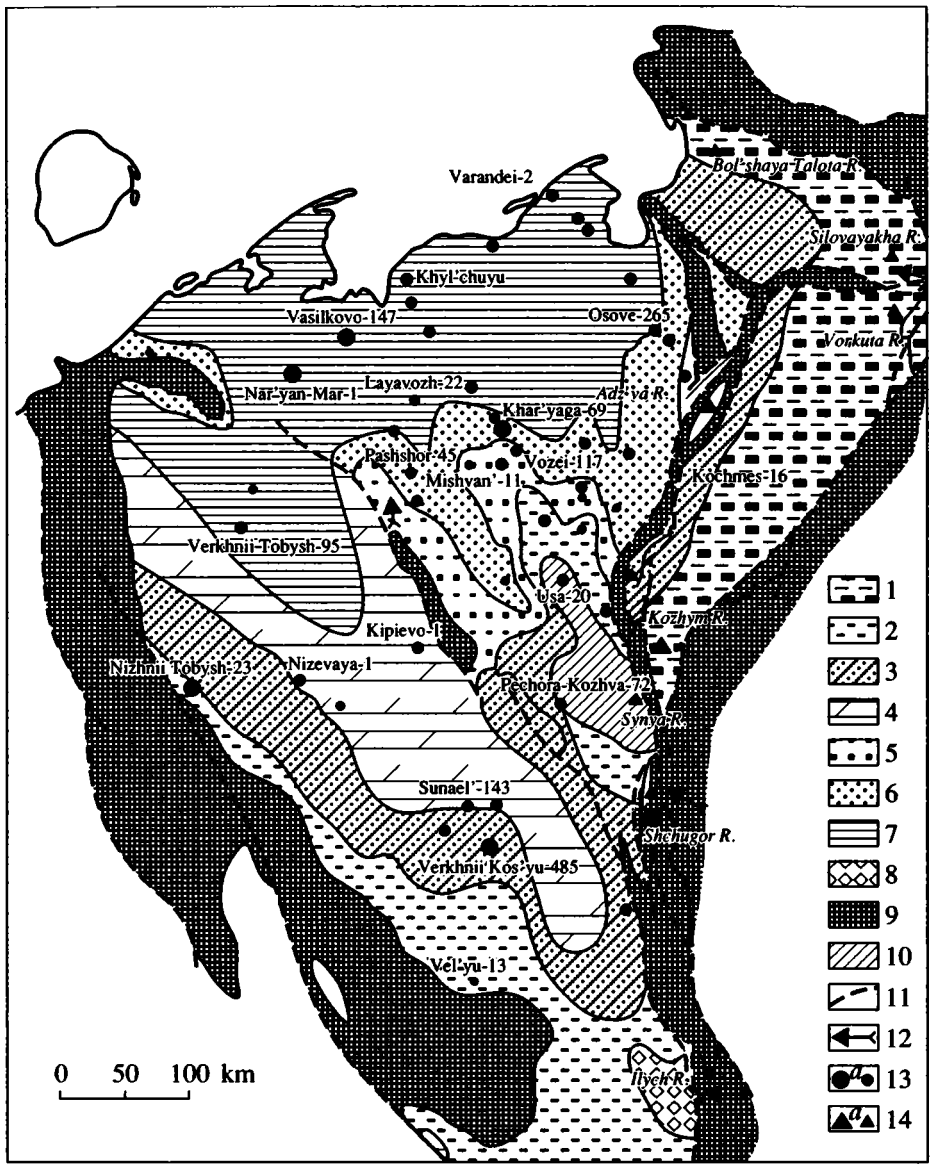

Fig. 6. Paleogeographic map of the Timan–Pechora region for the Kungurian–Ufimian boundary period. Paleogeographic zones: (1) marshy tidal flat; (2) tidal flat; (3) intertidal zone; (4) semiinsulated shelf or fresh-water lagoon; (5) upper shoreface; (6) lower shoreface; (7) open shelf; (8) fan and mountain river channels; (9) zone lacking Upper Permian deposits; (10) zone lacking lower Solikamsk deposits. Other symbols: (11) fault; (12) supply direction of coarse clastic material; (13) borehole (*a*, reference one); (14) outcrop (*a*, reference section).

In most areas of the Pechora basin, the Kungurian–Ufimian boundary is conformable, because we failed to reveal any unconformity of stratigraphic significance. Only section of the Bol'shaya Synya depression is lacking some basal beds of the Ufimian Stage (Murav'ev, 1972; Kanev, 1994; Kanev and Koloda, 1997). In the southern part of the Kolva megaswell, the Ufimian deposits overlie different levels of the Lower Permian and Carbonaceous.

FACIES AND PALEOGEOGRAPHY

The lowstand system tract of the first Ufimian sequence seems to be most favorable for reconstruction of the Timan–Pechora paleogeography during the Kungurian–Ufimian boundary period. This system tract corresponds to the maximum regression phase.

In the facies–paleogeographic map (Fig. 6), the study region is divided into following ten zones:

(1) The marshy tidal flat; its deposits are represented by alternating coaliferous beds, clayey–silty sediments with brackish-water fauna, interbeds with signs of pedogenesis, and channel sandstones. This zone distinguishable due to presence of coal measures is studied in detail in the Kozhym and Vorkuta sections.

(2) The tidal flat; in contrast to the preceding zone, this one is lacking records peat formation, but hosts the continental red deposits, alluvium included. The zone was studied in the borehole sections of the Pechora-Kozhva, Vel'yu and Nizhnii Tobysh areas.

(3) The intertidal zone; its deposits are represented by sandy facies of tidal channels, beach settings (frequent coquina intercalations), and oolitic shoals, as well as by terrigenous–carbonate facies of neritic and supratidal zones. The type sections of this zone are bed successions of the Shchugor River and Borehole 485 of the Verkhnyaya Kos'yu area, which differ in some lithological parameters depending on climatic conditions and distance from the open shelf.

(4) The semiinsulated shelf area or brackish-water lagoon; the zone accumulated mainly the carbonate–terrigenous deposits with scarce faunal remains. Its lithological characteristics are poorly known, because the corresponding interval of the borehole sections studied is represented by scanty core samples.

(5) The upper shoreface zone; typical sediments of the zone are medium-to coarse-grained sandstones with unidirectional cross bedding. Sediments of this type have been penetrated by the Vozei-117 and other boreholes indicated in Fig. 6.

(6) The lower shoreface zone; characteristic deposits are sandstones locally intercalated with siltstone interbeds containing frequent marine fossils. These deposits are bioturbated or characterized by massive structures. They usually associate with the upper shoreface sediments. The Khar'yaga section is most typical of the zone.

(7) The open shelf zone is characterized predominantly by clayey–silty deposits with frequent remains of marine bivalves, brachiopods, bryozoans, and other organisms. The zone includes submarine accumulative sandy and silty–sandy bodies. Most typical sections of the zone are located in the northern and northwestern parts of the region. The corresponding rocks are detected in core sections of the Nar'yan-Mar (Borehole 1), Vasilkovo and Khyl'chuyus areas.

(8) Fans and mountain river channels filled with coarse clastics. The southern fan of the Ilych River area is shown according to data of Murav'ev (1972). The Bol'shoi Patok and Silova sections show regular cyclic occurrence of gravelstone conglomerates throughout the Upper Permian section. According to Khaitser (1962b), who thoroughly studied conglomerates of the Paemboi and Nizhnyaya Vorkuta formations at the Silova River, these rocks are of deltaic genesis.

(9) The zone lacking Upper Permian deposits is outlined as in the structural map of top surfaces of the Lower Permian carbonates (*Tektonika...*, 1988).

(10) The zone lacking the lower Solikamsk deposits is interpreted as the transit area of nondeposition inside the actively developing positive structures, where erosion was of subordinate importance. However, the absence of basal beds of the Ufimian Stage is proved by paleontological data only in the sections of the Bol'shaya Synya River and within the Usa area. The zone is distinguished mainly by means of indirect data on the section structure and lateral facies distribution.

The analyzed distribution of the facies–paleogeographic zones and mineral composition of their deposits (Malysheva *et al.*, 1993) suggest that zones lacking Upper Permian sediments can be interpreted in most cases as past land areas. The main provenance of the clastic material was the orogenic structure of the Paleourals young at that time and located to the east of the region under consideration. The land area of Paleotiman bordering the region in the southwest represented a denudation plain and probably was a transit area for clastic material derived from the Paleourals. The northern Timan was likely an area of marine and coastal-marine sedimentation. Areas of the present-day Pai-Khoi and the central Pechora-Kozhva swell presumably represented an insular land. Carbonate pebbles occurring in the Upper Permian beds and especially frequent in the lower Ufimian deposits of the Shapkino-Yur'yakhin swell may be the erosion products of carbonate substratum of the central Pechora-Kozhva swell. The transportation tracks of coarse polymictic clastic material are distinctly localized in three zones transversely oriented relative to the strike of the Paleourals.

The southern part of the Pechora-Kolva aulacogen was probably a transit area morphologically resembling peninsula, where erosional processes inside some actively developing positive structures were of minor importance. The upper and lower shoreface sandy deposits, which intensely accumulated around this area, can be considered in general as the bar–deltaic complex. As a result, the southwestern part of the basin was semisolated from the open sea. Along with climatic parameters, this situation caused difference in sedimentation in the northeastern and southwestern parts of the Timan–Pechora region. In the northeast, the facies distribution was controlled by transformation of the tidal flat, where peat formation took place, first into the intertidal and shoreface zones, and finally into the open shelf area. In contrast, the southwestern part (adjacent to the Timan) was characterized by isolated sedimentation settings of the tidal flat, where peat formation was untypical, and bar complexes were poorly developed.

CONCLUSIONS

On the basis of lithological and biostratigraphic investigations with the help of the sequence stratigraphy methods, we subdivided the complicatedly intercalated marine and continental Permian deposits, distinguished the section intervals favorable for paleogeographic reconstructions, and depicted the facies–paleogeographic environments in the Timan–Pechora region for the Kungurian–Ufimian boundary period. We arrived at the following conclusions on the early Ufimian sedimentation:

—In the greater part of the study region, a significant stratigraphic hiatus between the Kungurian and Ufimian stages is not recorded;

—The early Ufimian time was characterized by the intense removal of sandy and coarse clastic material and by the basin shoaling until the commencement of continental sedimentation in eastern and southern parts of the Uralian foredeep, where the tidal flat deposits were accumulated;

—The Pechora syneclise represented at that time an area of predominantly marine sedimentation that resulted in accumulation of sediments characteristic of open shelf and distant to coastal bar settings, submarine deltaic facies included;

—Distribution of sandy conglomerates of the stream-channel genesis marks extremities of the continental facies progradation;

—The facies distribution reflects the peculiar restructuring of the Timan–Pechora region during the considered time.

It seems reasonable to focus future investigations on data compilation for a series of facies–paleogeographic maps characterizing maximal regressive and transgressive phases of the basin evolution during the Late Permian epoch and on paleoecological reconstructions on the basis of stratigraphic distribution of fossil biota in the corresponding deposits.

ACKNOWLEDGMENTS

We thank V.I. Bogatskii, Director of the Timan–Pechora Research Center, and P.P. Tarasov, Chief Geologist of AO "Severgeofizika," who donated core samples, stratigraphic catalogues, and seismic materials for this study. We are also grateful to D. Baum who consulted us on sequence stratigraphy methods, A.A. Gudel'man and A. Zhemchugov from AO "Severgeofizika" for collaboration in the field work, and our colleagues V.A. Noskov, D. Poletskii, and Z. Skok for technical assistance. The work was supported by the Russian Foundation for Basic Research, project no. 96-05-65847.

Reviewers A.S. Alekseev and B.I. Chuvashov

REFERENCES

Atlas litologo-paleogeograficheskikh kart paleozoya i mezozoya Severnogo Priural'ya (Atlas of Lithologic-Paleogeographic Maps of the Paleozoic and Mesozoic in the Northern Cis-Urals), Leningrad: Nauka, 1972.

Afanas'ev, B.L., *Paleotektonika i uglenosnost'* (Paleotectonics and Coal Resources), Moscow: Nedra, 1968.

Biota vostoka Evropeiskoi Rossii na rubezhe rannei i pozdnei permi (Biota in the East European Russia across the Early–Late Permian Boundary), Grunt, T.A., Esaulova, N.K., and Kanev, G.P., Eds., Moscow: GEOS, 1998.

Chalyshev, V.I., *Iskopaemye pochvy permskikh uglenosnykh otlozhenii Severo-Vostoka Evropeiskoi chasti SSSR. Syktyvkar* (Fossil Soils in Permian Coal-Bearing Sediments, the Northeastern European Part of the Soviet Union), Komi Fil. Akad. Nauk SSSR, 1974.

Chalyshev, V.I. and Varyukhina, L.M., *Biostratigrafiya permi Severo-Vostoka evropeiskoi chasti SSSR* (Biostratigraphy of the Permian in the Northeastern European Soviet Union), Leningrad: Nauka, 1968.

Chalyshev, V.I., Varyukhina, L.M., and Molin, V.A., *Granitsa permi i triasa v krasnotsvetnykh otlozheniyakh Severnogo Priural'ya* (The Permian–Triassic Boundary in Red Beds of the Northern Cis-Urals), Moscow: Nauka, 1965.

Chuvashov, B.I., Kungurian Stage of the Permian System (Problems of Recognition and Correlation), *Stratigr. Geol. Korrelyatsiya*, 1997, vol. 5, no. 3, pp. 10–28.

Chuvashov, B.I., Mizens, G.A., and Chernykh, V.V., On Correlation between Artinskian–Kungurian Sediments in the Cis-Urals and Pechora River Basin, *Ezhegodnik-1989*, Inst. Geol. Geokhim., Ural. Otd. Akad. Nauk SSSR, 1990b, pp. 7–13.

Chuvashov, B.I., Dyupina, G.V., Mizens, G.A., and Chernykh, V.V., *Opornye razrezy verkhnego karbona i nizhnei permi zapadnogo sklona Urala i Predural'ya* (Upper Carboniferous and Lower Permian Reference Sections in the Cis-Urals and Western Slope of the Urals), Sverdlovsk: Ural. Otd. Akad. Nauk SSSR, 1990a.

Dedeev, V.A., Malyshev, N.A., Yudin, V.V., *et al.*, Platform Cover Tectonics of the Pechora Plate, *Tektonika platformennykh oblastei* (Tectonics of the Platform Regions), Novosibirsk: Nauka, 1988, pp. 137–150.

Entsova, F.I., Konovalova, M.V., Slivkova, R.P., and Tel'nova, V.D., Permian Sediments of the Timan–Pechora Province and their Gas Resources, *Neftegaz. Geol. Geofiz.*, 1969, no. 6, pp. 32–36.

Geologiya mestorozhdenii uglya i goryuchikh slantsev SSSR (Geology of Coal and Combustible Shale Deposits in the Soviet Union), Yaroslavtsev, G.M., Ed., Moscow: Nedra, 1965, vol. 3.

Istoriya uglenakopleniya v Pechorskom basseine (Coal Accumulation History in the Pechora Basin), Makedonov, A.V., Ed., Leningrad: Nauka, 1965.

Ivanov, G.A., On Cyclic Structure of Coal-Bearing Sediments in the Vorkuta Coal Field, *Tr. Inst. Geol. Nauk, Ugol'naya Ser.*, 1947, vol. 90, no. 2, pp. 19–20.

Ivanov, G.A. and Makedonov, A.V., Rhythmical (Cyclic) Sedimentation and Distribution Patterns of Coals and Combustible Shales, *Tsiklichnost' otlozhenii neftegazonosnykh i uglenosnykh basseinov* (Cyclic Sediments in Oil- and Gas-Bearing Basins), Moscow: Nauka, 1977, pp. 38–61.

Kanev, G.P., *Permskie dvustvorchatye mollyuski gryady Chernysheva* (Permian Bivalve Mollusks of the Chernyshev Ridge), Syktyvkar: Komi Nauchn. Tsentr Ural. Otd. Ros. Akad. Nauk, 1994.

Kanev, G.P. and Koloda, N.A., The Detailed Biostratigraphy of Upper Permian Deposits in the Bol'shaya Synya Depression of the Northern Cis-Urals, *Geologiya evropeiskogo severa Rossii* (Geology of the North European Russia), Syktyvkar: Inst. Geol. Komi NTs UrO RAN, 1997, pp. 46–53.

Khaitser, L.L., New Data on the Permian and Triassic Stratigraphy, the Adz'va River, Northern Part of the Chernyshev Ridge, *Byull. Mosk. O–va Ispyt. Prir., Otd. Geol.*, 1962, vol. 37, no. 1, pp. 57–61.

Khaitser, L.L., On Sand and Pebble Facies in Coal-Bearing Strata of the Pechora Basin, *Dokl. Akad. Nauk SSSR*, 1962, vol. 147, no. 4, pp. 912–915.

Koloda, N.A., Molin, V.A., and Fefilova, L.A., *Palynology of the Permian Deposits in Western Russian Arctic*, St. Petersburg–Trondcheim, 1992–1993.

Lyubina, Yu.N., Lithology and Geomorphology of the Northern Timan–Pechora Province in the Late Permian Time, *Usloviya formirovaniya lovushek neantiklinal'nogo tipa na Severe evropeiskoi chasti SSSR* (Formation Conditions of the Non-Anticlinal Traps in the North European part of the Soviet Union), Leningrad: Vses. Nauch.-Issled. Geol.-Razved. Inst., 1984, pp. 52–57.

Makedonov, A.V., Lithology and facies of Permian Coal-Bearing Deposits, *Geologiya mestorozhdenii uglya i goryuchikh slantsev* (Geology of Coal and Combustible Shale Deposits), Moscow: Nedra, 1965, vol. 3, pp. 83–96.

Makedonov, A.V., Lithology and Genesis of Productive Strata in the Pechora Coal Basin, *Trudy geologicheskogo soveshchaniya, posvyashchennogo 25-letiyu geologicheskogo izucheniya Pechorskogo ugol'nogo basseina* (Proc. Geol. Conference Dedicated to the 25th Anniversary of Investigations in the Pechora Coal Basin), Syktyvkar, 1958, pp. 159–196.

Malysheva, E.O., Genesis of Natural Reservoirs in Permian Sediments of the Pechora Petroliferous Basin, *Pechorskii neftegazonosnyi bassein (kriterii perspektivnoi otsenki). Syktyvkar* (Pechora Petroliferous Basin: Evaluation Criteria of Potentials), Inst. Geol., Komi Fil., Akad. Nauk SSSR, 1985, pp. 72–82.

Malysheva, E.O., Larionova, Z.V., Ryabinkina, N.N., and Timonina, N.N., *Prirodnye rezervuary v terrigennykh formatsiyakh Pechorskogo neftegazonosnogo basseina* (Natural Reservoirs in Terrigenous Formations of the Pechora Petroliferous Basin), Syktyvkar: Komi Nauchn. Tsentr Ural. Otd. Ros. Akad. Nauk, 1993.

Mitchum, R.M., Seismic Stratigraphy and Global Changes of Sea Level. Part 1: Glossary of Terms Used in Seismic Stratigraphy, *Seismic Stratigraphy—Applications to Hydrocarbon Exploration*, Tulsa (Oklahoma): AAPG, 1977, Mem. 26, pp. 205–212.

Murav'ev, I.S., *Stratigrafiya i usloviya formirovaniya permskikh otlozhenii Pechorskogo Priural'ya* (Stratigraphy and Formation Conditions of Permian Sediments in the Pechora Area of the Cis-Urals), Kazan: Kazansk. Univ., 1972.

Murav'ev, I.S., Igonin, V.M., Kalashnikov, N.V., *et al.*, New Data on Stratigraphy of the Lower–Upper Permian Boundary Sediments in the Urals and East European Platform, *Dokl. Akad. Nauk SSSR*, 1984, vol. 274, no. 4, pp. 901–903.

Murav'ev, I.S., Konovalova, M.V., Slivkova, R.P., and Ioffe, G.A., The Study State of Permian Sediments in the Timan–Pechora Region and Problems of Further Investigations, *Materialy po regional'noi geologii* (Materials on Regional Geology), Kazan: Kazansk. Univ., 1975, pp. 31–60.

Muromtsev, V.S., *Elektrometricheskaya geologiya peschanykh tel – litologicheskikh lovushek nefti i gaza* (Electrometric Geology of Sand Bodies, the Lithological Traps for Oil and Gas), Leningrad: Nedra, 1984.

Nikonov, N.I. and Golovan', V.S., Oil and Gas Resources of Upper Permian Sandstones in the Central Part of the Kolvin Megaswell, *Geol. Nefti Gaza*, 1983, no. 1, pp. 8–14.

Oknova, N.S. and Kozulina, T.N., Paleogeography and Formation of Terrigenous Reservoirs in the Late Permian Sediments of the Timan–Pechora Province: Implications of Mineralogical Analysis, *Usloviya formirovaniya lovushek neantiklinal'nogo tipa na Severe evropeiskoi chasti SSSR* (Formation Conditions of Non-Anticlinal Traps in the North European Part of the Soviet Union), Leningrad: Vses. Nauch.-Issled. Geol.-Razved. Inst., 1984, pp. 44–51.

Posamentier, H.W. and Vail, P.R., Eustatic Controls on Clastic Deposition II-Sequence and Systems Tract Models, *Sea-Level Changes: An Integrated Approach*, Cheryl K. Wilgus *et al.*, Eds., Tulsa (Oklahoma): Soc. Econ. Paleontol. Mineral., 1988, no. 42, pp. 125–154.

Putevoditel' ekskursii na permskie otlozheniya r. Kozhim, Mezhdunarodnyi simpozium "Problemy evolyutsii permskoi morskoi bioty" (Guidebook for Excursion to Permian Sediments in Kozhim River, Intern. Symp. on Problems of the Permian Marine Biota Evolution), Moscow: Paleontol. Inst. Ross. Akad. Nauk, 1995.

Reineck, H.-E. and Singh, I.B., *Depositional Sedimentary Environments*, Berlin, 1975. Translated under the title *Obstanovki terrigennogo osadkonakopleniya*, Moscow: Nedra, 1981.

Reshenie mezhvedomstvennogo stratigraficheskogo soveshchaniya po srednemu i verkhnemu paleozoyu Russkoi platformy 1988 g. Permskaya sistema (Resolution of Interdepartmental Stratigraphic Conference on the Middle and Upper Paleozoic of the Russian Platform, 1988, Permian System), Leningrad: Vses. Geol. Inst., 1990.

Rotai, A.P., New Data on Coal Resources in the Southern Pechora Basin, *Tr. Inst. Geol. Nauk, Ugol'naya Ser.*, 1947, vol. 90, no. 2, pp. 111–133.

Sandstone Depositional Environments, Scholle, P.A. and Spearing, D., Eds., Tulsa (Oklahoma): AAPG, 1982.

Shurekov, N.A., *Permskie uglenosnye otlozheniya yuga Pechorskogo basseina* (Permian Coal-Bearing Sediments of the Southern Pechora Basin), Kazan: Kazansk. Univ., 1976.

Siliciclastic Sequence Stratigraphy: Recent Developments and Applications, Mem. 58, Weimer, P. and Posamentier, H.W., Eds., Tulsa (Oklahoma): AAPG, 1994.

Skhema stratigrafii permskikh otlozhenii Urala. Ob"yasnitel'naya zapiska k stratigraficheskim skhemam Urala (dokembrii, paleozoi). Prilozheniya: Regional'nye stratigraficheskie skhemy permi Urala, 17 listov (Stratigraphic Scheme of Permian Sediments in the Urals. Explanatory Note to Stratigraphic Schemes of the Urals—Precambrian and Paleozoic. Appendixes: Regional Stratigraphic Schemes of the Permian in the Urals, 17 sheets), Chuvashov, B.I., Sofronitskii, P.A., Molin, V.A., *et al.*, Eds., Yekaterinburg: 1994, pp. 128–152.

Sukhov, E.E. and Igonin, V.M., *K biostratigraficheskoi kharakteristike pogranichnykh otlozhenii nizhnei i verkhnei permi po r. Adz'va (gryada Chernysheva)* (To the Biostratigraphic Characteristic of the Lower–Upper Permian Boundary Sediments, the Adz'va River, Chernyshev Ridge), Available from VINITI, 1990, Kazan, no. 3853-V90.

Timofeev, P.P., *Geologiya i fatsii yurskoi uglenosnoi formatsii yuzhnoi Sibiri* (Geology and Facies of the Jurassic Coal-Bearing Formation of Southern Siberia), Moscow: Nauka, 1969.

Uglenosnaya formatsiya Pechorskogo basseina (Coal-Bearing Formation of the Pechora Basin), Dedeev, V.A., Ed., Leningrad: Nauka, 1990.

Van Wagoner, J.C., Mitchum, R.M., Campion, K.M., and Rahmanian, V.D., Siliciclastic Sequence Stratigraphy in Well Logs, Cores, and Outcrops: Concepts for High Resolution Correlation of Time and Facies, *Methods in Exploration, Series no. 7*, Tulsa (Oklahoma): AAPG, 1990.

Van Wagoner, J.C., Posamentier, H.W., Mitchum, R.M., *et al.*, An Overview of Fundamentals of Sequence Stratigraphy and Key Definitions, *Mem. Soc. Econ. Paleontol. Mineral., Tulsa, Oklahoma*, 1988, no. 42, pp. 39–45.

Vazhenin, G.V. and Galkina, L.V., Formation Conditions of Permian Productive Strata in the Khar'yaga Field of the Kolvin Megaswell, *Geologiya i prognoz neftegazonosnosti Timano-Pechorskoi provintsii* (Geology and Forecast for Oil and Gas Resources in the Timan–Pechora Province), Leningrad: Vses. Nauchno-Issled. Geol.-Razved. Inst., 1984, pp. 66–74.

Visher, G.S., How to Distinguish Barrier Bar and Channel Sands, *World Oil*, 1969, vol. 168, no. 8, pp. 160–113.

Yaroslavtsev, G.M., To Methods of Studying Paleogeographic Conditions of Coal Formation, *Materialy po geologii i poleznym iskopaemym Severo-Vostoka evropeiskoi chasti SSSR. Sb. 2* (Materials on Geology and Minerals of the Northeastern European Part of the Soviet Union, Collection of Works no. 2), Moscow, 1962, pp. 67–73.

Zhemchuzhnikov, Yu.A., Yablokov, V.S., Bogolyubova, L.I., *et al.*, *Stroenie i usloviya nakopleniya osnovnykh uglenosnykh svit ugol'nykh plastov srednego karbona Donetskogo basseina* (The Structure and Accumulation Conditions of the Middle Carboniferous Coal-Bearing Formations and Coal Beds in the Donets Basin), Moscow: Akad. Nauk SSSR, 1959.

Stratigraphy and Geological Correlation, Vol. 9, No. 4, 2001, pp. 340–363. Translated from Stratigrafiya. Geologicheskaya Korrelyatsiya, Vol. 9, No. 4, 2001, pp. 29–54.
Original Russian Text Copyright © 2001 by Zharkov, Chumakov.
English Translation Copyright © 2001 by MAIK "Nauka/Interperiodica" (Russia).

Paleogeography and Sedimentation Settings during Permian–Triassic Reorganizations in Biosphere

M. A. Zharkov and N. M. Chumakov

Geological Institute, Russian Academy of Sciences, Pyzhevskii per. 7, Moscow, 109017 Russia

Received November 30, 1999

Abstract—Origination and growing aridity of Pangea and transition from glacial to ice-free climate led in the Permian–Early Triassic to substantial reorganization in all biosphere subsystems. Lithological–paleogeographic maps drawn for the late Sakmarian–early Artinskian and late Kazanian–early Toarcian periods of the Permian and for the Induan Age of the Early Triassic illustrate main paleogeographic changes that were related to the Pangea uplift, successive regression of epicontinental seas, disappearance of glacial sedimentation areas, progradation of arid and semiarid sedimentation, expansion and multiplication of closed basins, and reduced surficial but enhanced groundwater discharge into shelf seas surrounding Pangea. This distorted the global balance of mineral exchange between land and ocean and reduced the terrigenous influx of nutrients and primary productivity in ocean that could destruct the former feeding chains and represent one of possible factors responsible for mass extinction at the end of the Permian.

Key words: Permian, Triassic, paleogeography, sedimentation settings, Pangea, global mineral exchange, biosphere reorganizations.

1. INTRODUCTION

Permian and Early Triassic climatic changes and reorganizations in biosphere are most remarkable in the Phanerozoic history. They are manifested in transition from the glacial to ice-free climate, in growing aridity of Pangea (Parrish, 1993, 1995), and in mass extinction of marine and terrestrial faunas at the end of the Permian Period (Maxwell, 1989; Raup and Sepkoski, 1986; Erwin, 1995; Alekseev, 1998; Ochev and Shishkin, 1998; Ponomarenko and Sukacheva, 1998; and others). Substantial changes affected all subsystems of biosphere and were accompanied by global changes in Sr, C, and S isotopic ratios (Burke *et al.*, 1982; Baud *et al.*, 1989; Denison and Koepnik, 1995; Erwin, 1995a; Scholle, 1995).

The most intense biosphere reorganizations developed since the second half of the Early Permian until the Induan Age of the Early Triassic. They were preceded by durable paleogeographic and climatic changes, which should significantly influence sedimentation environments and, consequently, habitat conditions of organisms in the Pangea supercontinent and surrounding shelf seas and oceans. The interrelated succession of such changes is, however, insufficiently studied so far.

This work is dedicated to most important paleogeographic features and peculiarities in distribution of sedimentation settings. To define them, we compiled global lithological–paleogeographic maps for three time slices: late Sakmarian–early Artinskian of the Early Permian (Fig. 1), late Kazanian–early Toarcian of the Late Permian (Fig. 2), and Induan Age of the Early Triassic (Fig. 3). Reconstructions prepared for the international project "Pangea" (Scotese and Langford, 1995; Golonka *et al.*, 1994) global topographic schemes for every Permian age (Ziegler *et al.*, 1997, 1998) were used as the cartographic base for these maps. The maps summarize and systematize data published in works presented in the reference list. Difficulties accompanying interregional correlation of Permian deposits are well known. Several slightly different schemes of such correlation were proposed recently. In this work, we used the stratigraphic scheme proposed for the project "Pangea" (Ross *et al.*, 1994). Maps presented here are used to reconstruct most significant paleogeographic and depositional transformations that occurred on the Earth during the Permian and Early Triassic. Owing to known differences in correlation of events, the transformation ages estimated here are conditional to a certain extent, but this does not affect their essence and succession.

2. MAIN FEATURES OF THE PERMIAN–TRIASSIC PALEOGEOGRAPHY

Comparing the lithological–paleogeographic maps, one can see that disposition of global paleogeographic features was almost unchangeable during the considered time period. The Earth retained the longitudinal asymmetry: its oceanic hemisphere was occupied by the Panthalassa, and continental hemisphere congregated the huge Pangea continent, Paleotethys and Neot-

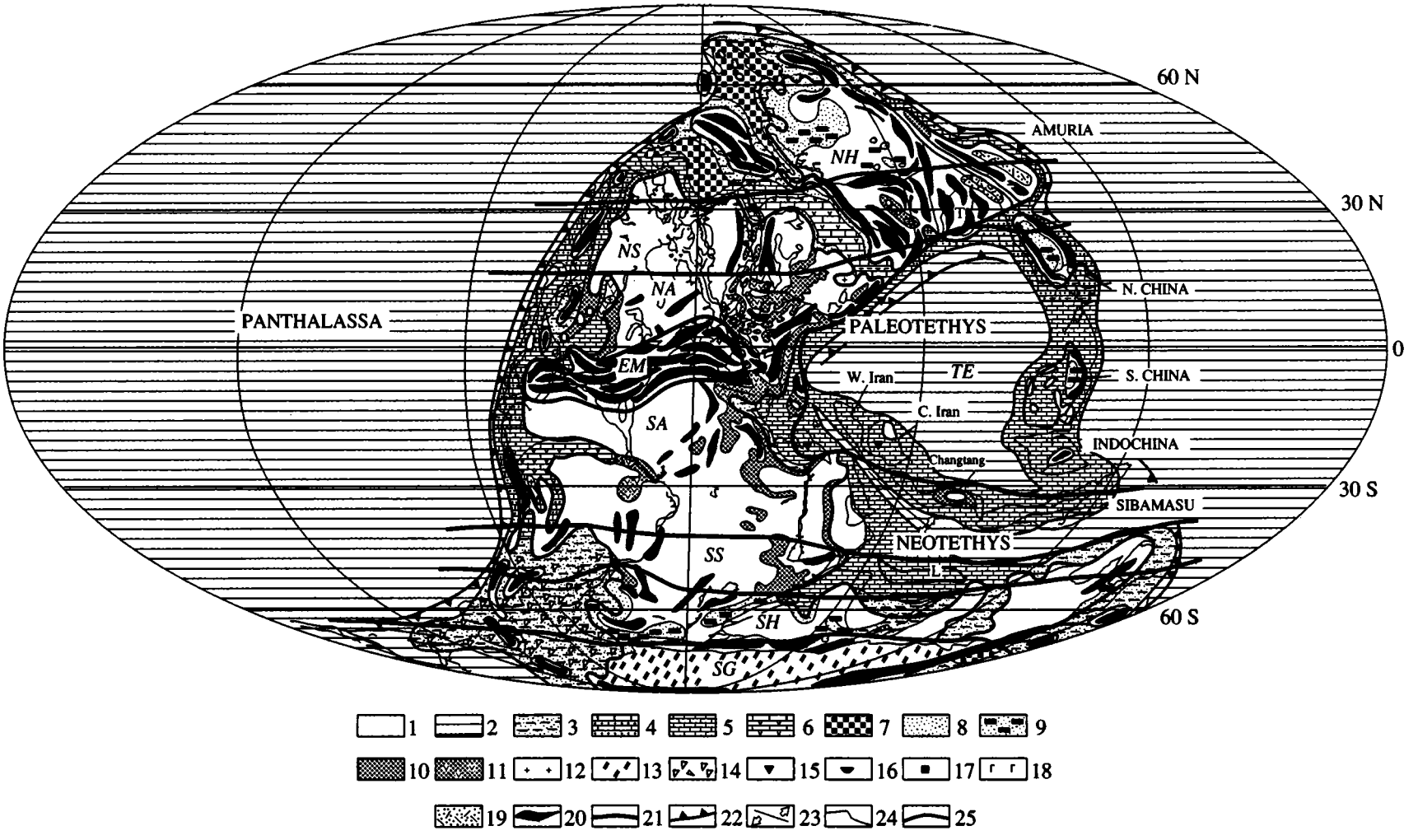

Fig. 1. Lithological–paleogeographic map for the Late Sakmarian–early Artinskian time of the Early Permian: (1) land; (2) oceans; (3) shelf seas with terrigenous sedimentation; (4) shelf seas with terrigenous–carbonate sedimentation; (5) carbonate platforms; (6) evaporite–carbonate platforms; (7) anoxic basins with black shale sedimentation; (8) inland and coastal alluvial and alluvial–lacustrine basins; (9) coal-bearing basins; (10) inland and coastal basins of arid zones that accumulated alluvial, eolian, and lacustrine red beds; (11) inland and coastal basins with alluvial, lacustrine, and sabkha gypsum-bearing red beds; (12) saliferous basins; (13) areas of predominant continental glacial sedimentation; (14) areas of predominant marine glacial sedimentation; (15) laterites, bauxites; (16) kaolin clays, kaolin-bearing sediments; (17) iron ores; (18) terrestrial basalts; (19) volcanogenic–sedimentary deposits; (20) orogenic structures; (21) boundaries of sedimentation–climatic belts; (22) subduction zones; (23) axes of spreading; (24) modern shore line; (25) ancient shore line. Belt types: (EM) equatorial–mountainous; (NA) northern arid, evaporite; (NS) northern semiarid; (NH) northern humid, coal-bearing; (SA) southern arid, evaporite; (SS) southern semiarid; (SH) southern humid, coal-bearing; (SG) southern glacial; (TE) tropical–equatorial coal- and bauxite-bearing; (T) Tarim and (L) Lhasa blocks.

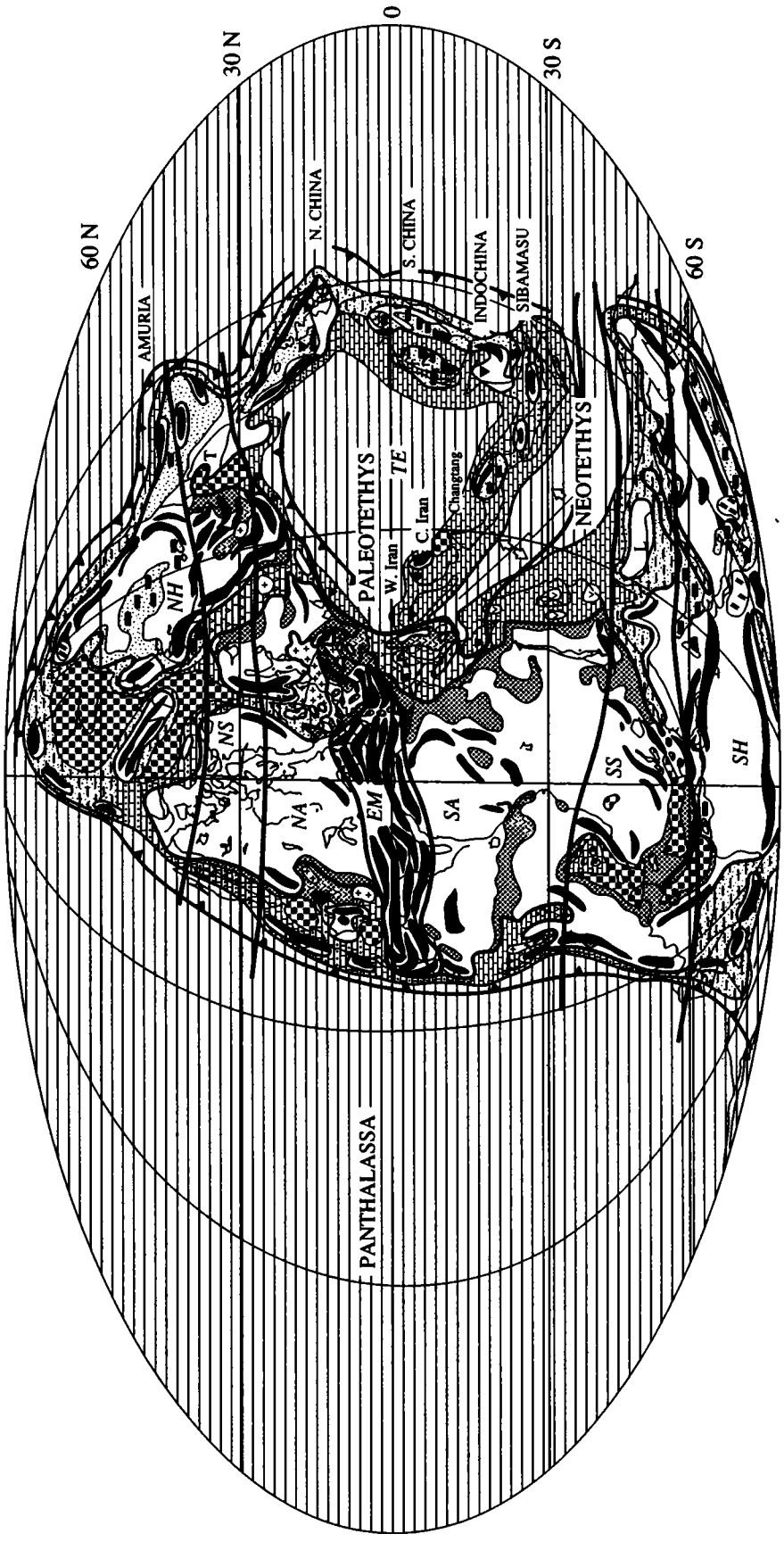

Fig. 2. Lithological–paleogeographic map for the Late Kazanian–early Tatarian time of the Late Permian (symbols as in Fig. 1).

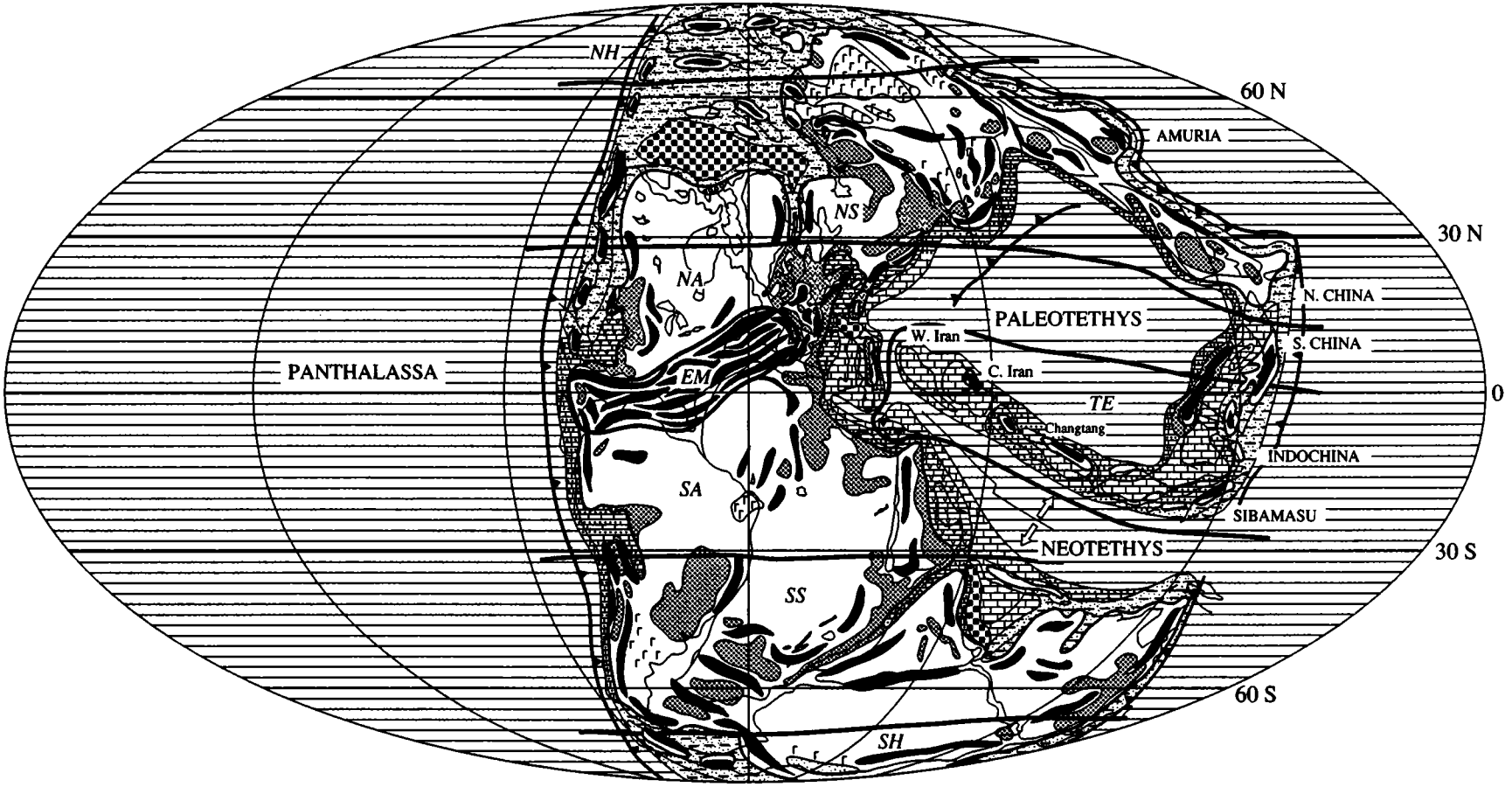

Fig. 3. Lithological–paleogeographic map for the Induan Age of the Early Triassic (symbols as in Fig. 1).

ethys oceans, Cathaysian and Cimmerian systems of microcontinents (Metcalfe, 1994; Golonka *et al.*, 1994; Scotese and Langford, 1995; Ziegler *et al.*, 1997, 1998). The Pangea that amalgamated the Laurasian continents (North America, Baltia, Siberia, and Kazakhstan) and Gondwanan (South America, Africa, Hindustan Peninsula, Australia, and Antarctica) groups of continents extended, as a single supercontinent, from the south pole to 75–85°N crossing all latitudinal belts. The Cathaysian system comprising the North and South Chinese microcontinents extended almost in the longitudinal direction bordering the Paleotethys in the east (Scotese and Langford, 1995). The Cimmerian system separated the Neotethys from the Paleotethys and included microcontinents of Western and Central Iran, North Tibet (Qiangtang), and Burma–Malaysia (Sibamasu) (Scotese and Langford, 1995). The period in question was marked by a slight northward drift of Pangea (by 5–10°) (Scotese and Langford, 1995; Ziegler, 1997, 1998). The most intense northward drift was characteristic of the Cimmerian and Cathaysian systems of microcontinents in connection with the Neotethys extension (Scotese and Langford, 1995; Ziegler *et al.*, 1998).

The principal stability in disposition of main planetary paleogeographic structures suggests that biosphere transformations in the Permian and initial Triassic geological history were probably caused by durable and successive changes in Pangea that slowly transformed its interrelation with surrounding seas and oceans, rather than by rapid and drastic paleotectonic and paleogeographic events. Accordingly, a special attention should be paid to paleogeographic evolution of the supercontinent Pangea and to changes in sedimentation settings within its territory and in adjacent seas.

Main orographic features of Pangea during the late Sakmarian–early Artinskian time were as follows. Its central near-equatorial part was occupied by a tremendous collision system of Central Pangea mountains (Scotese and Langford, 1995; Ziegler *et al.*, 1997), which crossed the supercontinent in the latitudinal direction dividing it into two halves: the northern (Laurasian) and southern (Gondwanan) parts. The inner continental areas of the Laurasian and Gondwanan segments of the supercontinent hosted collision-related mountain systems and belts, remnant Precambrian and Paleozoic mountains, arched uplifts, and plateau-like rises (Ziegler *et al.*, 1997). The collision systems of mountains were located in the Kazakhstan–Angara region of Laurasia. The Byrranga, Urals, and Kyzylkum mountain belts extended along the western and southern margins of the Laurasian part; the Sayan, Altai, and Verkhoyansk systems stretched along its eastern periphery, and the Yenisei–Zaisan mountain system occupied the central part (Ziegler *et al.*, 1997). The remnant and intraplate mountain systems were represented by the Antler, Grenville, and Ancestral mountains, Front Range, and Uncompahgre uplift in North America and by Scandinavian Mountains in western Baltia (Ziegler *et al.*, 1997). Large regions in the Laurasian part of Pangea were occupied by plateau-like rises such as the Baikalian and Patom uplands of the Angaraland and the Oslo highland in Baltia. The inner and remnant mountain systems in the Gondwanan part of Pangea included the Asuncion Mountains located along the western border of the Parana Basin in South America, the Espinhaco mountains in eastern South America, the Mauritania belt and the Ougarta and Iforas mountains in northwestern Africa, the Lomagundi, Muchinga, Makutu, Mikumi, Atacora, Mayombe, Mitumba, and Windhoek mountain belts in the eastern, central, and southern parts of Africa, and the Lachland Highland and the MacDonnel, Flinders, Hamersley and Musgrave ranges in Australia (Ziegler *et al.*, 1997). There were also the Ahaggar and Ennedi plateau-like and arched uplifts in Africa and the Great Plains of Australia. The mountainous structures of the Andean type stretched along the western extremity of South America (Andes), southern margin of Antarctica, and in eastern Australia (New England) (Scotese and Langford, 1995; Ziegler *et al.*, 1997).

It can be assumed that, in their orographic structure, many inner regions of Pangea were probably similar, to a significant extent, to modern drainless uplands, such as the Central African and Botswana plains and plateaus of the Central Iran, Gobi, Central Atlas, or High Plains of North America, West Australian plateau and others. These paleogeographic peculiarities predetermined a wide development of spacious blind drainage areas in both the arid and humid climatic zones.

Simultaneously, the shelf, marginal, and inland seas still occupied spacious areas of Pangea during the late Sakmarian–early Artinskian. In the northern periphery of Pangea, there were the Verkhoyansk–Chukchi, Sverdrup, and Barents marginal seas. The Midcontinent, Midland, Delaware, Williston, and other inland seas extended far inside western North America. They were separated from the western shelf seas by the Uncompahgre, Pedernal, and Diablo uplifts and islands. The large East European inland sea was located almost in the center of the Laurasian half of Pangea. It served as a seaway for the intermittent water exchange between the Paleotethys and Arctic basins. The entire periphery of the Gondwanan part, represented a spacious marginal sea located between South America, South Africa, and Antarctica. The Peru–Bolivian and sub-Andean sea gulfs were located in the west of Gondwana, and the Mozambique–Madagascar and West Australian seas of the same type occupied the eastern areas. These inland seas and gulfs divided the Pangea into several independent land areas of the Kazakhstan–Angaraland region, Laurentia (North America + West Europe), Western Gondwana, and Eastern Gondwana. Worthy of mention are also large marginal seas that were located along the eastern periphery of Pangea and occupied Italy and Dinarides in Europe, northern areas of Africa, almost entire northern half of the Arabian Peninsula, and the northern margin of Hindustan.

The main trend in the paleogeographic evolution of Pangea during the Late Permian–Early Triassic (Induan Age) was controlled by its steady rising. Geological records evidence the gradual sea retreat from inner areas and the reduction of marginal sea areas along the northern and southern peripheries of Pangea. Par example, the East European inland sea completely disappeared in Laurasia by the end of the Permian. Marginal seas located in northwestern and western Angaraland, as well as inland seas of western North America, reduced. Significantly reduced in dimensions were also marginal sea that occupied the southeastern periphery of the Gondwanan part of Pangea. The regression of inner and marginal seas was most likely conditioned by the Pangea uplift rather than by the global sea-level fall, as some researchers assumed (Schopf, 1974; Parrish, 1995; and others). This is evident from the fact that dimensions and positions of shelf zones around Pangea remained almost unchanged. Only marginal seas experienced reducing, whereas inland seas became replaced by basins of internal drainage. Thus, in the second half of the Late Permian and initial Early Triassic, Pangea represented a huge highly uplifted continent, the western, southern, and northeastern margins of which were occupied by mountain systems separating inner zones from shelf seas and oceans. The central part of Pangea hosted plateau-like rises and intraplate mountain belts, between which there were spacious drainless lowlands with meandering rivers and lake systems.

3. PERMIAN AND EARLY TRIASSIC SEDIMENTATION SETTINGS

The presented lithological–paleogeographic maps (Figs. 1–3) demonstrate sufficiently well the spatial distribution of sedimentation settings of the considered time period. They provide an opportunity to outline belts of arid, humid, and glacial settings and to clarify global changes in paleogeography, sedimentation, and climate. Working on the maps, we tend to define spacious and widespread lithological–facies zones of the same type within shelf seas and inland areas. Arid sedimentation settings represent lithological–paleogeographic zones of four types: (1) inland and coastal zones of alluvial, eolian, and lacustrine red beds; (2) inland and coastal zones of alluvial, lacustrine, and sabkha gypsum-bearing red beds; (3) salt-accumulating basins; and (4) evaporite–carbonate platforms. The humid sedimentation settings are divided into two groups: (1) inland and coastal areas of alluvial and alluvial–lacustrine sedimentation; and (2) coal-bearing basins. Areas of glacial sedimentation are subdivided into zones of predominantly terrestrial or marine settings. Zones of terrigenous and terrigenous–carbonate sedimentation, black-shale accumulation (anoxic environments), and carbonate platforms are distinguished among shelf settings. In addition, the most important paleoclimatic indicators, e.g., laterite, bauxite, kaolin, and iron ores deposits are shown in the maps out of scale.

3.1. Arid Sedimentation Settings

Huge dimensions of Pangea and extended mountain systems along its margins, as well as gradual regression of epicontinental seas and global warming owing to deglaciation, resulted eventually in the increased aridity of inland areas in low and middle latitudes and in displacement of semiarid belts toward poles (Robinson, 1973; Parrish *et al.*, 1986; Parrish, 1993, 1995; Barron and Fawcett, 1995). These changes in the spatial distribution of arid and semiarid settings are well seen in the lithological–paleogeographic maps (Figs. 1–3).

Beginning from the initial Sakmarian time of the Early Permian to the Induan Age of the Early Triassic, all central areas of Pangea located north and south of the mountain system of Central Pangea represented settings of arid sedimentation that outline the northern and southern arid belts. The northern arid belt is well distinguishable in the southern Laurasian part owing to the wide development of eolian deposits, terrestrial and coastal sabkhas, evaporite and saliferous basins, intermittently draining river valleys (wadis), deserts with saline playa lakes, alluvial and alluvial–lacustrine red beds (Mckee *et al.*, 1967; Glennie, 1983; Zharkov, 1974; Merzlyakov, 1979; Peterson, 1980; Drong *et al.*, 1982; Ziegler, 1982; Clemmensen and Abrahamsen, 1983; Glennie and Buller, 1983; Mazzullo *et al.*, 1985; Kukhtinov, 1987a, 1987b; Frenzel *et al.*, 1988; Johnson *et al.*, 1988; Sneh, 1988; Afzali *et al.*, 1989; Smith, 1989; Gast, 1991; Kiersnowski *et al.*, 1995; Mazzullo, 1995; Wardlaw *et al.*, 1995). The belt stretched from the western periphery of North America (Midcontinent, Williston, Delaware, and other basin) to central southern areas of Laurasia (East European, Dnieper–Donets, and Central European basins) and farther to southern margins of the Kazakhstan–Angaraland continent (Chu–Sarysu basin). The southern arid belt is also outlined rather confidently in the northern half of the Gondwanan segment of Pangea. The western part of the southern belt hosted the Peru–Bolivian and sub-Andean saliferous basins. In the west and northwest of Argentina, eolian sediments are recorded (Limarino and Spalletti, 1986). In central and eastern inland areas, arid alluvial–lacustrine red beds, evaporites, and desert settings are registered in the Amazon, Parnaiba, Barreirinhas, Gabon, Mali–Nigeria, North Sahara, Murzuq, Kufrah, Abyad, and Mozambique basins (Vysotskii *et al.*, 1973; Blant, 1973; Nairn and Smithwick, 1976; Cahen *et al.*, 1984; Klitzsch, 1990; Kogbe and Burollet, 1990; Lefran and Guirand, 1990; Wycisk, 1990; Baud *et al.*, 1993; Broutin *et al.*, 1995; Tankard *et al.*, 1995; Salem, 1996). The eastern periphery of the southern arid belt was occupied by a wide zone of carbonate–evaporite plateaus, coastal and continental sabkhas, shelf seas, saliferous and evaporite basins of the flooded and in-island types. The zone comprised

salt basins of the North Italy, Dinarides, Mecsek, Moesian, Arabian, and other regions (Murris, 1980; Berberian and King, 1981; Zharkov, 1981; Sharief, 1981, 1983; Cassins *et al.*, 1992; Husseini, 1992; Ustaömer and Robertson, 1993; Alsharhan and Nairn, 1995).

The northern and southern arid belts were divided by the mountain system of Central Pangea. The system was likely characterized by the Himalayan-type morphology and, probably, by the vertical succession of climatic zones from the piedmont deserts to mountainous–steppe and mountainous–meadow settings in the intermediate and upper belts. In intermontane areas of the eastern system margin, which represented basins of internal drainage with branching and meandering rivers and lakes, sedimentation occurred under semiarid conditions (Cassins *et al.*, 1992, 1995; Ori, 1988; Châteauneuf and Farjanel, 1989). Similar semiarid environments could locally exist also along the western periphery of the mountain system.

Beginning from the second half of the Early Permian, spatial distribution of arid belts peculiarly changed. The South Gondwanan arid belt moved to the north. During the late Sakmarian–early Artinskian time, it was located between 10–15° and 40–45°S, whereas in the Induan Age of the Early Triassic, its northern boundary was near equator, and the southern one had position at 30°S. These changes were to a significant extent related to the Pangea drift northward. As for the northern, Laurasian arid belt, it also migrated northward and simultaneously widened to a significant extent owing to migration of its northern boundary toward the pole. In the Late Permian–Early Triassic, the Laurasian arid belt occupied the permanent position between 5–15° and 30°S.

Very important changes in sedimentation patterns occurred in the Early Triassic and likely affected both the northern and southern arid belts. Salt accumulation terminated in all inland and coastal basins of arid belts at that time. Evaporite sedimentation was characteristic either of alluvial and alluvial–lacustrine plains (sedimentation conditions of continental sabkhas, playa lakes, and takyrs) or, less commonly, of pericratonic evaporite–carbonate platforms. Branching river systems and zones of meandering rivers became widespread (McKee, 1954; Kukhtinov, 1987b; Movshovich, 1987; Klitzsch, 1990; Wycisk, 1990). The changes were probably caused by the enhanced monsoon character of the climate with more contrast seasonal and annual alternation of arid and humid periods (Kutzbach and Gallimore, 1989; Parrish, 1995). It can be stated therefore that sedimentation settings in arid belts became slightly more humid in the Early Triassic, when sedimentation environments in them resembled those of semiarid areas. Other important changes that occurred in arid belts of that time are as follows: inland basins of internal drainage that accumulated red beds, alluvial–lacustrine, evaporite, and desert facies became greater and more abundant, particularly in the western part of Pangea, in response to progressive rising of the supercontinent and retreat of inland seas from its central areas.

3.2. Semiarid Sedimentation Settings

The Permian–Early Triassic time was marked by extremely wide development of areas with insufficient seasonal moistening. During short humid seasons, these areas accumulated sediments of widespread meandering rivers, semiarid alluvial fans, deposits of intermittent flows, eolian sand dunes, soil carbonate concretions and calcretes, red beds, and variegated alluvial and alluvial–lacustrine facies. Coeval black shale sedimentation took place in open and closed lakes. Prolonged arid periods were responsible for deposition of continental sabkha-type and saliferous sediments. It is assumed (Parrish, 1995) that moistening patterns of this kind reflect the monsoon influence that strongly weakened in inland areas of Pangea protected from ocean by mountains.

Semiarid settings of Pangea recorded in southern and northern hemispheres outline respectively the southern and northern semiarid belts. The southern semiarid belt of the Late Permian time is detectable with a sufficient confidence in southern areas of Africa and South America. Sediments of alluvial plains, zones of meandering rivers, and flood plains with ordinary and playa lakes are registered in the Karroo, Tanzania, and some other regions (Kreuser *et al.*, 1990; Smith, 1990; Turner; 1990; Yemane and Kelts, 1990). Sedimentary basins accumulated here thick alluvial–lacustrine varicolored sediments of typical semiarid alluvial fans. In the southeastern part of the Karroo Basin, sedimentary sequence includes also soil carbonate calcrete-like concretions and playa-type gypsum-bearing beds (Turner, 1990). In southern Africa and southeastern South America, zones of meandering rivers surrounded large freshwater lakes with black shale sedimentation (Yemane and Kelts, 1990; Yemane, 1993, 1994; Franca *et al.*, 1995). In proximity to large lakes, local climate was moderately humid, with mean annual temperatures of about 10°C and moderate seasonal variations (Yemane, 1993). In other areas of the southern semiarid belt, the monsoon climate was characterized by alternation of arid and humid seasons and by insignificant precipitation (Smith, 1990).

Semiarid settings of the northern belt are rather certainty recognized in the Moscow syneclise and Volga–Urals region, which corresponded to the central part of the Laurasian segment of Pangea at that time. The complex association of alluvial, alluvial–lacustrine, subaqueous evaporite, terrestrial, and coastal sabkha sediments was formed here during the late Kazanian–early Toarcian (Ignat'ev, 1963, 1987; Kuleva, 1980; Strok, 1987; Tverdokhlebov, 1987a; Tverdokhlebov and Shminke, 1990; Lozovskii, 1998a; Lozovskii and Blom, 1998; Lozovskii and Zharkov, 1998). Prevalent were settings of changeable alluvial–lacustrine plains

with seasonal sedimentation cycles, sedimentation breaks, soil and caliche formation, and gypsum accumulation in playas and sabkhas. Periodically widespread were branching river systems and probable zones of meandering rivers farther from the provenance. Features of the humid climate become well manifested by the end of the Permian (Ignat'ev, 1987; Strok, 1987; Tverdokhlebov, 1987a). Another area of the semiarid sedimentation located in the northern belt is recognizable in the southern Chu–Sarysu depression of the Kazakhstan–Angaraland continent. Terrestrial alluvial–lacustrine, floodplain, and sabkha sediments are represented here by red beds, variegated facies, and saliferous sequences with interbeds of the Na-Ca-sulfate composition (glauberite) indicating alternation of warm humid, arid, and cold seasons. Eolian sedimentation probably developed as well. The winter temperatures could vary from –5 to –15°C, whereas summer temperatures could be as high as +20–+30°C (Zherebtsova, 1977). In general, the northern semiarid belt of the early Late Permian time extended in between 25–30°N and 35–40°N.

In the terminal Late Permian–Early Triassic, the semiarid belts gradually widened in both the southern and northern hemispheres mainly owing to migration of high-latitude boundaries toward the relevant poles. The southern boundary of the southern semiarid belt was located in the Early Triassic at about 70–75°S. This belt covered the greater part of Australia, where semiarid settings of alluvial–lacustrine red beds are registered in the Bowen, Maryborough, Springfield, and Tasmania basins (Brown *et al.*, 1970; Veevers, 1984). The northern boundary of the northern semiarid belt was located in the Early Triassic between 65 and 70°N. It covered northern Cisuralian regions of the East European platform, and also southern and central areas of Angaraland. In the Pechora, Korotaikha, Bol'shaya Synya, Kos'yu–Rogovo, Kuznetsk, Gorlovo, Dzhungar basins, and in western areas of the Verkhoyansk basin of the belt, prevalent were alluvial and alluvial–lacustrine settings that accumulated red and varicolored deposits of semiarid sedimentation (Chelyshev, 1972; Dagys *et al.*, 1979; Kalantar, 1987; Neustroeva and Bogomazov, 1987; Lozovskii and Balabanov, 1988).The northern semiarid belt included also the Tarim, North Chinese, and Amuria microcontinents with red beds, fluvial and varicolored freshwater-lacustrine sediments widespread in the Kuqa, North Chinese, Khanka, and other basins (Kotlyar, 1984; Wang Hongzhen, 1985; Durante, 1998; Lozovskii, 1998b).

Thus, semiarid conditions spread in Pangea during the Late Permian–Early Triassic over spacious areas in middle and high latitudes of both hemispheres. The prevalent sedimentation settings allow their belts of their development to be referred to as "semiarid alluvial–lacustrine" ones. The northern semiarid belt of the Early Triassic time occupied areas between 30 and 65–70°N. The southern, comparatively wide semiarid belt stretched between 30 and 70–75°S. As is seen, both belts were located symmetrically relative to equator. By the beginning of the Triassic, sedimentation settings turned out to be more or less uniform over the entire Pangea supercontinent. This is evident from disappearance of cold belts and also from widened belts of semiarid alluvial–lacustrine sedimentation and a slight humidity increase in arid belts.

3.3. Humid Sedimentation Settings

Humid sedimentation settings and corresponding belts are distinguished, with some degree of certainty, only for the Permian time. They are recognizable by distribution patterns of coal-bearing basins and gray-colored alluvial, alluvial–lacustrine, boggy, and floodplain sediments. The available data allow the northern and southern Permian humid belts to be outlined in Pangea (Fig. 1, 2).

In the northern belt, continental and coastal humid settings were widespread in Angaraland and the northern Aral region, where the Tunguska, Kuznetsk, Gorlovo, Pechora, and other coal-bearing basins are known (*Atlas...*, 1968; Chelyshev, 1972; Bogomazov *et al.*, 1984; Meyen and Golubeva, 1984; Yuzvitskii *et al.*, 1984; Gurevich, 1987; Betekhtina *et al.*, 1988; Durante and Mogucheva, 1998). In the late Sakmarian–early Artinskian time, the humid coal-bearing belt covered the entire northern margin of Pangea northward of 30–40°N. In the late Kazanian–early Toarcian time, the belt occupied the same areas of Angaraland and Cis-Urals northward of 40–45°N. Its northern part is known to host glacial marine and seasonal ice sediments (Chumakov, 1994).

The southern humid belt of coal accumulation was located in the late Sakmarian–early Artinskian between 50–55 and 70–75°S. It included the Karroo, Ruhuhu, Luangua, and other basins in southern Africa, the Sokoto Basin in western Madagascar, the Damodar, Jharia, Mahanadi, Satpura. and other basins in the Hindustan, and the Bowen Basin in eastern Australia (Ahmad, 1964; Brown *et al.*, 1970; Kreuser and Semkiwa, 1987; Cook, 1990; Kreuser *et al.*, 1990; Smith, 1990; Turner, 1990; Mishra, 1991; Mitra, 1991; Langford, 1992). In the Late Permian, the belt covered almost the whole area of East Gondwana, including Australia and Antarctica, and was located south of 55–60°S. In Africa, humid environments were preserved only at its southern extremity, where the Jugella Ferry-Vryheid coal-bearing basin was located (Yemane and Kelts, 1990). In Hindustan, the belt included the above-mentioned coal-bearing basins. The entire southeastern part of Australia with Bowen, Denison, Sydney, Tasmania, Marree, and other coal-bearing basins was also a part of the belt (Langford, 1992). Some coal-bearing basins (Sydney, Tasmania, Marree) enclose glacial marine and continental sediments of the Late Permian (Kazanian) age (Caputo and Crowell, 1985; Langford, 1992; Crowell, 1995; Eyles *et al.*, 1998). This suggests

that intermittent glaciers appeared in the southern humid coal-bearing belt.

During the period under consideration, other settings of humid sedimentation existed in the Cathaysian and Cimmerian microcontinents and in marginal coastal areas of Pangea. They outline the equatorial humid zone of coal- and bauxite-bearing deposits. Coal-bearing basins with alluvial, alluvial–lacustrine, alluvial–floodplain, and boggy sediments are known within this zone in the North Chinese, Amuria, Tarim, South Chinese, and Quingtang microcontinents and in the Quidam, Qinling, and Songpan-Ganzi terranes (Kotlyar, 1984; Lee, 1984, 1985a, 1986b; Ulmishek, 1984; Sheng *et al.*, 1985; Wang Hongzhen, 1985; Yang Zunyi *et al.*, 1986; Enos, 1995; Durante, 1998). Bauxite-bearing sequences are registered in the North Chinese, South Chinese, Indochina, and Western Iran microcontinents, as well as in the Caucasian and Pamirs margins of Pangea (Leven, 1984; Enos, 1995).

In the Early Triassic, coal accumulation ceased over the entire territory of Pangea, and in Cathaysian and Cimmerian microcontinents. The humid belts of the Early Triassic time are distinguishable only in circumpolar zones of northern and southern hemispheres, judging from gray-colored rocks prevailing in sequences of the marginal areas of Angaraland and Antarctica (Dagys *et al.*, 1979; Sadovnikov and Orlova, 1997; Retablak, 1999).

Thus, it can be postulated that the Late Permian–Early Triassic history was associated with several important changes in the humid belts. First, settings favorable for coal accumulation disappeared in the Early Triassic everywhere, including the humid belts as well. Second, the semiarid sedimentation gradually replaced the humid one, thus reducing the distribution area of the latter. Third, the humid belts migrated toward the poles. All these changes were apparently related to global warming and growing aridity of the climate.

3.4. Glacial Sedimentation Settings

As was mentioned, most significant biosphere transformations commenced, when Late Paleozoic glaciations degraded in the Sakmarian Age of the Early Permian.

Most researchers believe that the peak of the Early Permian glaciation was in the Asselian–Sakmarian time (Visser, 1996; Crowell, 1995). At that time, glacial sheets covered high and middle latitudes of South America, Africa (southern Arabia and Madagascar included), India, Tibet, and Australia. That glaciation likely affected also the Malacca–Burma terrane. Antarctica was apparently covered by ice completely. The glacial belt was sometimes as wide as 45–50°. In these continents, ice shields and mountainous glaciers left abundant exaration signs (striated glacier bed with all characteristic structures, trough valleys, fjords), basal tillites, fluvioglacial, lacustrine–glacial, and glacial marine sediments. The latter are particularly widespread. The glacial marine sediments, which accumulated under influence of shelf glaciers, snowmelt runoff, and icebergs, were more or less reworked by underwater colluviation. In the late Sakmarian–initial Artinskian, glaciers began to retreat everywhere, and the glacial belt significantly narrowed. Its northern boundary moved close to the Southern Polar Circle (Fig. 1).

The Karroo, Kalahari, and Karasburg basins of South Africa accumulated the thick Early Permian sequence of glacial sediments (the upper part of the Dwyka Group). Along periphery of these basins and on dividing rises, the sequence is composed of terrestrial glacial sediments, whereas in their central and southeastern parts, it is mainly represented by glacial marine deposits. The last signs of ice rafting in South Africa are registered in the lower part of the Prince Albert Formation corresponding to the base of the Ecca Group presumably of Artinskian age.

In Australia, the Early Permian glacial sediments are preserved in many sedimentary basins between Tasmania in the south and Bonaparte Bay in the north, where they are traceable from the western to eastern coasts of the continent. Many researchers believe that Permian glaciations commenced there during the Sakmarian Age and, reducing in dimensions, continued to exist with breaks during the Artinskian, Kungurian, and to Kazanian ages (Crowell and Frakes, 1971), or even till the Ufimian Age (Eyles *et al.*, 1998). Other authors estimated that glaciation in Australia lasted from the Asselian to early Sakmarian, and that no shield glaciation occurred there after this period (Dickins, 1996; Lindsay, 1997).

The most important glaciation centers were located in the western, central, and southern parts of Australia (Lindsay, 1997), and apparently in the Great Artesian Basin (Frakes, 1979). A thick ice sheet covered mountainous areas in the eastern coast of Australia. Structures observed in the glacial beds and tillites indicate that coastal glaciers of southern Australia moved from the southeast, i.e., from Antarctica, to the northwest (Lindsay, 1997; Bourman and Alley, 1999). The ice-rafted material occurring in southeastern Australia could also be delivered mostly from Antarctica (Eyles *et al.*, 1998).

In South America, Lower Permian glacial deposits are recorded in several basins located south of 10°S (modern coordinates). The largest of them is the Parana Basin of southern Brazil. Upper Paleozoic glacial sediments are distinguished here as the Itarare Group, the larger upper part of which is referred to the Lower Permian, although its age is debatable. Some researchers suggest the Asselian–Sakmarian or Asselian–Artinskian age of the group (Franca *et al.*, 1995), but others refer it to uppermost layers to the Kungurian Stage.

Similarly to Lower Permian glacial sequences of other continents, the Itarare Group shows repeated alternation of glacial marine and terrestrial facies that recorded glacial and interglacial sedimentation episodes, respectively. The latter were frequently accompanied by coal accumulation. South America hosted several glaciation centers. Glaciers advanced into the eastern part of the Parana Basin from the southeast, i.e., from South Africa, and into its western areas from the Asuncion arch of South America (Franca *et al.*, 1995). Glaciation in the Sergipe-Alagoas Basin originated from Equatorial Africa.

Signs of Early Permian glaciations are fairly abundant also in Hindustan. Prevalent here are continental glacial sediments preserved in many grabens, but in the northern structures framing the peninsula, they are represented by glacial marine facies. Tillites, boulder conglomerates, and other glacial sediments occur at the base of the Sakmarian–Artinskian Talchir Formation (Chandra, 1992). In many areas, the formation overlies the glacier bed with characteristic signs of ice exaration. All glaciation signs, such as striation in the glacier bed, orientation of elongated rock fragments, and other structural features of tillites indicate, with few exceptions, the glacier advancement from the south and southeast (Ahmad, 1981), i.e., from Antarctica and Australia.

In Antarctica, Upper Paleozoic glacial sediments are widespread in the Transantarctic Mountains; they are also known from areas bordering the Ronne shelf glacier and from some coastal areas of the Atlantic segment of East Antarctica. Continental and marine facies of glacial sediments fill several sedimentary basins here. They are estimated to be the Carboniferous and Early Permian in age (Isbell *et al.*, 1997). The modern ice cover hampers the detailed reconstruction of Late Paleozoic glaciation, but, taking into consideration the fact that glaciers from this continent advanced in the initial Early Permian as far as to the southern Africa, India, and southern Australia, it is clear that the entire East Antarctica was ice-covered at that time. This glaciation could not degrade before the Artinskian, because Antarctic glaciers reached southern areas of Africa (Visser, 1997) and India (Chandra, 1992) during this age. The Antarctic icebergs carried detrital material to southeastern Australia up to the Kungurian Age (Eyles *et al.*, 1998).

Unequivocal indications of Early Permian glaciations have not been discovered in the northern hemisphere so far. There are only single signs of presence of ice-rafted material and glacial to fluvioglacial sediments (Andrianov, 1966; Bobin, 1940), but their genesis is still debatable (Chumakov, 1994).

The late Kazanian–early Tatarian time was marked only by episodic glacial sedimentation in circumpolar humid belts of the southern and northern hemispheres. In the southern circumpolar belt, indications of ice-rafting ("dropstones") are recorded in Kazanian and Tatarian sequences of the Sydney and Tasmania coal-bearing basins, in the Marree Basin, and in the northern Prince Charles Mountains of southeastern Australia (Corwell and Frakes, 1971; Crowell, 1995; Eyles *et al.*, 1998).

In the circumpolar areas of northern hemisphere, glacial and glacial marine sediments of the Late Kazanian–early Tatarian age are established amid marine facies in the Kolyma and Okhotsk massifs (Epshtein, 1973; Chumakov, 1994). They are probably present as well in the Verkhoyansk fold belt (Andrianov, 1966) and Omolon massif (Kashik *et al.*, 1990). Presence of glacial marine sediments indicates existence of land glaciers in some northeastern areas of Pangea during the Late Permian. These glaciers reached sometimes the sea level and formed icebergs and, probably, shelf ice fields (Chumakov, 1994). These geological data are well consistent with paleomagnetic measurements and geodynamic reconstructions, according to which the northern humid, episodically glaciated belt was located north of 60°N (Khramov *et al.*, 1982; Scotese and Langford, 1995; Parfenov *et al.*, 1999) or 70°N (Ziegler *et al.*, 1998).

The Lower Triassic glacial sediments have not been established either in the northern, or in southern circumpolar areas of Pangea. As was noted, circumpolar zones in the Early Triassic were warm and humid in both hemispheres of the Earth.

3.5. Marine Settings of Carbonate and Evaporite–Carbonate Sedimentation

The analysis of spatial distribution of marine sedimentation settings during the Late Permian–Early Triassic reveals a remarkable feature, namely the extremely wide development of carbonate facies in many shelf seas surrounding Pangea and also Cathaysian and Cimmerian microcontinents. They are known as well as in many inland seas of Laurasia and Gondwana that is particularly true of the late Kazanian–early Tatarian time (Fig. 2).

Carbonate accumulation along the western periphery of Pangea occurred almost in all shelf seas located between 45 and 50°N. Largest shallow carbonate platforms of the open ramp shelves and carbonate platforms of fringed shelves in inland seas are outlined in the Peru, Peru–Bolivian, and sub-Andean basins located along the western margin of the Gondwanan segment of Pangea (Franca *et al.*, 1995; Helwig, 1972; Sempere, 1995). The evaporite–carbonate platforms also formed in inland sea basins.

Another large area of carbonate sedimentation in western Pangea corresponded to the western margin of North America. This zone hosted an extended system of interrelated marginal seas, the Chihuahua, Marfa, Pedregosa, Central Arizona, Central Utah, Dry Mountain, Phosphoria, Central Wyoming, and other shallow-shelf basins with fringed platforms (Franzel *et al.*, 1988; Johnson *et al.*, 1988; Mazzullo, 1995; McKee

et al., 1967; Peterzson, 1980; Rascoe, 1988; Ross and Ross, 1995; Wardlaw *et al.*, 1995). In the west, the zone was separated from the open ocean by isolated islands (Antler and others) and by a chain of volcanic island arcs, whereas in the east, it was bounded by mountain systems (Uncompahre, Pedernal, Diablo, and others), which separated the zone from evaporite basins of the Midcontinent. In general, the entire system of carbonate shelf seas, island arcs, and dividing straits represented a transitional area between the open ocean in the west and inland evaporite basins in the east (Zharkov, 1974, 1978, 1981). Several large basins advanced far into the continent, thus representing inland seas that resembled the gulfs connected via narrow straits with basins of the transitional area. One of such seas was the Delaware basin connected by the narrow Hovey Channel with the Marfa and Chiahuahua carbonate-accumulating seas. A peculiar succession of back-reef settings, pisolite carbonate shoals, terrigenous–carbonate tidal to lagoonal evaporite-accumulation zones, and coastal sabkha and lakes was situated around of the Delaware basin. Toward the central part of the basin, there is recorded a transition from massive reefs to the fore-reef slope and, then, to the deep (from 300 to 550 m) inner zone of the basin that accumulated terrigenous–calcareous sediments (Garber and Harris, 1993; Mazzullo, 1995). Later, the deep uncompensated zone accumulated sulfates and salts (Anderson and Dean, 1995; Lowenstein, 1988). All available data suggest that carbonate and evaporite sedimentation in all marginal and inland sea basins along the southwestern periphery of North America took place in warm waters of the arid tropical zone (Anderson and Dean, 1995).

Widespread carbonate sedimentation settings were characteristic of shelf seas adjacent to the northern margin of Pangea (Stemmerik, 1995; Beauchamp *et al.*, 1989; Trettin, 1989; Dixon and Dietrich, 1990; Davies and Nassichuk, 1991; Jensen and Sørensen, 1992; Koyi *et al.*, 1993; Beauchamp, 1995; Brevik *et al.*, 1995; Nassichuk, 1995; Stemmerik and Worsley, 1995). Carbonate platforms of fringed shelves of variable width and length are traceable along the southern slope of the Sverdrup Basin, in the eastern and, probably, western slopes of the Norwegian–Greenland Basin, and in the southeastern Barents Basin. Carbonate platforms of these basins substantially differed from each other. For instance, carbonates of the relatively narrow Sverdrup fringed shelf are characterized by the impoverished biota dominated by the so-called "bryozoan assemblage". These carbonate rocks largely consist of low-Mg calcite and have the elevated glauconite content that points to deposition of shelf carbonates in temperate cold water environments (Beauchamp, 1993, 1995). The carbonate platform sequence of the Barents Sea includes massive brachiopod or bryozoan limestones and cherts with bioturbation signs, which accumulated in shallow, oxygen-rich and moderately cold waters (Stemmerik and Worsley, 1995). To the contrary, shelf carbonate platforms of the Norwegian–Greenland Basin are composed of bryozoan–algal mounds up to 70 m high and about 500 m wide. The mounds are surrounded by shallow oolitic and allogenic carbonates that are replaced in the coastal zone by sabkha, tidal, and lagoonal sediments, i.e., by calcareous marls, algal carbonates, nodular mosaic gypsum, and oolitic grainstones (Stemmerik, 1995). Evaporite–carbonate platforms of this kind formed under warm water conditions in the semiarid climatic zone.

Carbonate sedimentation settings along the eastern periphery of Pangea were particularly widespread. They were typical of all shelf seas located along the Gondwanan and Laurasian margins of Pangea between 45°S and 30°N. This belt of carbonate accumulation that stretched in the SE–NW and SW–NE directions in the southern and northern hemispheres, respectively, was located in the tropical–subtropical zone favorable for carbonate sedimentation and formation of evaporite–carbonate platforms in addition to ordinary carbonate platforms. One of the largest evaporite–carbonate platforms was located in the Arabian Peninsula. It occupied the almost entire northeastern half of the peninsula and stretched over a distance more than 4500 km, being from 1000 to 2500 km wide. This was a pericratonic fringed-shelf platform, where carbonates accumulated in littoral and intratidal settings and sabkhas of supratidal zone represented areas of sallow-water evaporite sedimentation (Murris, 1980; Berberian and King, 1981; Sharief, 1981, 1983; Husseini, 1992; Alsharhan and Nairn, 1995). In the northeast, the platform was bounded by extended reefal buildups fringing the deep-water continental slope (Murris, 1980; Alsharhan and Nairn, 1995). In the northwest, a relatively deep shelf, the site of carbonate–clayey sedimentation, separated the Arabian evaporite–carbonate platform from the Toros'lar carbonate platform that apparently was of the pericratonic ramp type and fringed the oceanic rift trough in the southwest. Farther to the northwest, there was the Tunisian carbonate shelf platform (Lys, 1988). The area northward of the trough was occupied by the spacious evaporite–carbonate platform that extended over areas of the Dolomitic and Carnic Alps, Dravt Ridge, Durmitor Massif, and High Karst zone of the Dinarides (Miljush, 1973; Buggisch *et al.*, 1976; Zharkov, 1981). Paleogeographic reconstructions suggest that the Italo–Dinarides platform contacted in the east the structural succession of land mass, Moesian Salt Basin, and the easternmost evaporite–carbonate platform (Zhukov *et al.*, 1976; Zharkov, 1981).

Within the shelf of the Paleotethys located along the southeastern margin of Laurasia, there was an extended Caucasian carbonate platform composed of various algal, bryozoan, brachiopod, sponge, coral, oolitic, and calcarenite limestones intercalated with abundant reefal buildups formed in the littoral and intratidal zones of the shallow shelf (Miklukho-Maklay and Miklukho-Maklay, 1966; Leven, 1993; Kotlyar *et al.*, 1984; Rostovtsev, 1984). The Caucasian carbonate platform was

probably of the pericratonic fringed type, but it is not inconceivable that it represented several interrelated autonomous pericratonic carbonate platforms. The presumable Afghan–Pamirs pericratonic carbonate platform extended during the Late Permian along the northern shelf margin of the Paleotethys, where biohermal and organogenic–detrital carbonate buildups formed, whereas littoral and intratidal settings accumulated clayey limestones, clayey marls, and oolitic carbonates (Miklukho-Maklay, 1963; Leven, 1984; Dronov and Kafarskii, 1980; Leven *et al.*, 1989).

Another large region of the warm water carbonate sedimentation corresponded to the Cimmerian and Cathaysian microcontinents, large areas of which were, as was noted, occupied by shelf seas. Carbonate platforms were located along the entire southern and northern peripheries of the Cimmerian microcontinents stretching from Western Iran to Sibamasu. In the Cathaysian microcontinents, carbonate sedimentation was widespread along western margins and in some central areas. The territory of western and central Iran was occupied by a spacious carbonate platform, where intratidal and littoral zones of carbonate accumulation surrounded the relatively deep-water central areas of clayey–calcareous and black-shale sedimentation (Alsharhan and Nairn, 1995). In the northeast, the Iran platform likely joined the carbonate platform of the South Afghan median mass and, probably, the Suleiman–Kirtar region of southeastern Afghanistan. The continuous cover of the Upper Permian shelf facies, mainly of littoral and intratidal carbonate sediments, is traceable in the Zuru, Huspasrud, Hilmand, Tirin, Logar, and Argandab zones, as well as in the northwestern part of the Katawaz trough (Dronov and Kafarskii, 1980). Judging from the accepted version of plate reconstruction (Scotese and Langford, 1995), another carbonate platform of western and southern peripheral zones of the Quingtang microcontinent (northern Tibet) was located eastward of the likely integral Iran–South Afghan carbonate platform. In the west and south, it fringed the coastal zone of paralic and continental sedimentation that was located in the northern central area (Enos, 1995). As is assumed, this carbonate platform extended far to the east, over the southern and eastern Sibamasu margins (Hutchison, 1989). In the South Chinese microcontinent, the shallow carbonate platform originated in the extreme north and west of the craton; its eastern margin was occupied by buildups of the barrier reef (Sheng *et al.*, 1985; Enos, 1995). The greater part of the fringed-shelf carbonate platform stretched along the eastern and northeastern margins of the Amuria microcontinent of the Eastern Sikhote-Alin zone (Kotlyar, 1984).

Finally, we should mention here one of the largest inland basins of evaporite–carbonate sedimentation—the East European sea. Carbonate and local intermittent evaporite sedimentation continued in this basin up to the terminal Kazanian Age and, in places, up to the initial Tatarian Age (*Atlas...*, 1969; Zharkov, 1974). All the time, a spacious evaporite–carbonate platform that extended over the North Caspian syneclise, Volga–Urals region, and northern Moscow syneclise developed in the eastern part of the East European craton. Sedimentation in shallow-water shelf settings of the platform occurred under arid and semiarid conditions parallel to subordinate sulfate sedimentation in submarine settings and sabkhas. In addition, there were large saliferous basins in the northern margin of the North Caspian Basin and adjacent areas.

Thus, carbonate and evaporite sedimentation of the Late Permian time prevailed in shelf seas surrounding Pangea and the system of Cathaysian and Cimmerian microcontinents. Particularly widespread in the arid and semiarid climatic belts were warm-water sedimentation settings. All sea basins located around Pangea or in its interiors between 40–45°N and 40–50°S were of this kind. A nearly continuous belt of carbonate and evaporite–carbonate platforms stretched along the western periphery of Pangea within the tropical–subtropical zone. Another belt of evaporite–carbonate and carbonate platforms was even larger and extended along the eastern margin of Pangea from the Arabian Peninsula in the south to the Caucasian region and further to the north across the East European basin almost up to the Barents Sea. The third spacious belt of warm-water carbonate sedimentation united shelf seas of the Cimmerian and Cathaysian microcontinents. It was entirely located in the equatorial–tropical zone. Hiatuses in sedimentation frequent in some areas, karstification, and local bauxite accumulation (Western Iran, South Chinese carton) represent characteristic features of the platforms (Elon, 1995). During the Late Permian, carbonate accumulation occurred also in moderately cold environments. This type of sedimentation is recorded in the northern middle-latitude humid belt, where carbonate platforms developed on shelves of the Sverdrup and Barents basins. Peculiar Upper Permian carbonate sediments (mainly limestones), which were conditionally termed "Bivalvia reefs" (Ganelin, 1997), accumulated in the northern and southern temperate belts. In the north, they are recorded in the Vrangel Island, Omolon and Kolyma massifs, being known as well in southern New Zealand. These limestones bear taxonomically impoverished, but quantitatively abundant faunas, which lack thermophilic reef-builders and other dwellers of warm-water carbonate platforms. Such faunal assemblages reveal prevalence of pelecypods (sometimes very large) and brachiopods (Runnegar, 1984; Ganelin, 1997). In the Lower Permian sequences of Tasmania, similar limestones laterally grade into tillites (Rao, 1981).

The characteristic feature of all Permian shelf carbonate seas was very limited development of terrigenous sedimentation settings along their coastal zones. For instance, terrigenous sediments are registered only along the southwestern (coastal) margin of the Arabian evaporite–carbonate platform, in some local areas adjacent to small uplifts in Zagros, in the southeastern

Toros'lar region, and in the west of Arabian Peninsula (Alsharhan and Nairn, 1995). Narrow sandy shoals and beaches, or sabkha-type supratidal zones relatively small in extension are recognizable around many others carbonate and evaporite–carbonate platforms confined to western and eastern margins of Pangea. As is established in the Capitan shelf of the Delaware Basin, where zone of sabkha facies is up to several dozens kilometers wide (Garber and Harris, 1993; Mazzullo, 1995), even in the case of a wide zone with coastal sabkhas and intermittently drained lakes (playas), terrigenous sedimentation was of minor importance. Prevalent in this case were mosaic gypsum-bearing rocks alternating with dolomites. Along their coast-facing margins, the carbonate platforms of the Cimmerian terranes were bounded by very narrow zones of detrital sediments, as it is well exemplified by the Iran–South Afghan platform. Littoral terrigenous facies were relatively widespread only around the Khamdian Oldland of the South Chinese microcontinent at the beginning of the Tatarian Age (Enos, 1995). Similar, very narrow coastal zones of shelf terrigenous sedimentation are assumed to be the deposition sites of fine-grained sandstones in the fringe carbonate platforms of the Sverdrup and Barents basins (Beauchamp, 1995; Stemmerik and Worsley, 1995). Terrigenous sediments of coastal zones are recorded only along the Uralian margin of the East European Basin (Chuvashov, 1995).

The Early Triassic was marked by a significant reduction of shelf carbonate accumulation, particularly along the northern and western margins of Pangea, where spacious terrigenous shelves appeared. Nevertheless, the principal distribution patterns of carbonate platforms remained unchanged.

Limited development of coastal detrital sediments in most shelf carbonate seas indicates that carbonate and evaporite–carbonate platforms along lowland margins of Pangea and microcontinents of the Cathaysian and Cimmerian systems were located close to desert areas of the arid and semiarid climatic zones, as it is evident from presence of eolian sediments and dunes there. In the humid zones, carbonate platforms were located near boggy coasts with rare meandering rivers. Thus, the carbonate platforms blocked somehow the lowland margins of Pangea, and this indicates that prevalent in this supercontinent were paleogeographic environments of internal, but not external drainage.

3.6. Black Shale Sedimentation Settings

During the late Early Permian and in the Late Permian–Early Triassic, anoxic settings favorable for black shale sedimentation were characteristic of many shelf seas and inland lakes. They are recorded in all climatic belts.

Sufficiently wide development of cold to moderately cold anoxic setting of black shale sedimentation is established for shelf seas of the northern Pangea margin. In the late Sakmarian–early Artinskian and late Kazanian–early Tatarian periods, there was a zone of interrelated black shale basins that extended from the northern margin of Alaska to the eastern coast of the Barents Sea. The zone included the Sverdrup, Wandel, Björnöya, Hammerfest, Nordcap, Northeastern Spitsbergen, and, probably, northern Novaya Zemlya basins (Beauchamp, 1995; Stemmerik and Worsley, 1995). Deep inner areas of these basins were characterized by stagnant anoxic sedimentation environments. In the Sverdrup Basin, accumulation of spongolites occurred first parallel to prograding clinoform filling of deep-water zones and draining of separate areas of fringed carbonate platform that was characterized by successive accumulation of spicule-bearing clayey mud, interbeds and lenses of carbonates and glauconite-bearing sands, and then by predominant deposition of spongolites in the cold-water environments (Beauchamp, 1995). In the Wandel, Björnöya, Hammerfest, Nordcap, and Northeastern Spitsbergen, prevalent at that time was also sedimentation in the deep-water stagnant settings. The indicated basins accumulated siliceous spiculite shales with bioturbation signs in their central deep areas and dark gray clayey mud with thin interbeds of bioclastic carbonates (packstones and wackestones) in shallower shelf areas near adjacent carbonate platforms (Stemmerik and Worsley, 1995).

North of the Sverdrup–Barents zone of black shale sedimentation, there was the large Verkhoyansk–Chukchi basin with anoxic sedimentation environments. Boundaries of the latter can be established very arbitrarily on the basis of isolated and scattered distribution areas of black shales in the Kolyma–Chukchi and Verkhoyansk regions, and in islands of the Arctic Ocean (Epshtein, 1973; Ganelin, 1984a, 1984b, 1984c, 1984d, 1997; Ustritskii, 1984, 1993; Kashik *et al.*, 1990). In the Vrangel Is., the corresponding sequence is composed of laminated to varved micritic limestones emanating H_2S, black shales, and varicolored shales with siliceous–manganese concretions (Ganelin, 1997). In the southern Yana–Kolyma region, prevalent are black massive and laminated rock sequences of shale and siltstone–shale composition, which accumulated under calm stagnant hydrodynamic conditions in inner zones of the past sea basin (Epshtein, 1973). In general, cold-water and moderately cold-water deep settings of black shale sedimentation were characteristic of many basins located along the northern margin of Pangea in the middle-latitude humid and circumpolar, episodically glacial climatic belts.

Warm-water anoxic settings of black shale sedimentation are registered in several sea basins of subtropical and tropical belts. They are presumed for the Phosphoria, Chihuahua, and some other basins in the southwestern periphery of the North American margin of Pangea, where black shale sedimentation continued probably until the Kazanian Age (Sheldon *et al.*, 1967; Ettensohn, 1994; Woods *et al.*, 1991). Along the eastern periphery of Pangea, anoxic conditions were intermit-

tently restored in many areas of the Arabian and Italian–Dinarides evaporite–carbonate platforms (Zharkov, 1981; Alsharhan and Nairn, 1995). In the southeastern Laurasian segment of Pangea and adjacent northwestern margin of the Tarim microcontinent, conditions favorable for black shale sedimentation existed for a long time in the North Tarim Basin (Enos, 1995). Another region with anoxic sedimentation environments corresponded to central and northeastern areas of the Central Iranian microcontinent, where black micritic bituminous limestones, black marls, and shales with cherty lenses and concretions accumulated in relatively deep-water inner areas of the carbonate platform (*Geological...*, 1977; Sharief, 1981, 1983; Husseini, 1992; Alsharhan and Nairn, 1995). It should be noted that all mentioned areas and basins of warm-water black shale sedimentation were confined to shallow shelf zones of seas located either close to evaporite basins or directly within evaporite–carbonate platforms.

Widespread, particularly since the Kazanian Age, became also lacustrine settings of black shale sedimentation. As was mentioned, an extended belt of spacious freshwater lakes stretched along the southern margin of Western Gondwana occupying significant areas of South America and South Africa (Padula, 1969; Yemane and Kelts, 1990; Yemane, 1993, 1994; Franca *et al.*, 1995). A large lake basin with black shale sedimentation presumably existed in the Turgai lowland of the southern Angaraland–Kazakhstan area of Laurasia (*Atlas...*, 1968).

In the Early Triassic, basins with black shale sedimentation were less common. In the northern margin of Pangea, there remained only the Sverdrup–Barents basin and another small basin in the Chukchi Peninsula (Dagys *et al.*, 1979; Trettin, 1989; Wignall and Hallam, 1992; Ettensohn, 1994; Wignall and Twitchett, 1996). The North Italian basin also continued to exist (Wignall and Hallam, 1992; Wignall and Twitchett, 1996). A new basin with black shale sedimentation appeared in the Cis-Himalayas zone of Hindustan (Kapoor and Tokuoka, 1985). In addition, the deep Early Triassic basin with black shale sedimentation extended along continental slopes of the Amuria and North Chinese microcontinents (Isazaki, 1994; Bragin, 2000).

It seems that several types of basins with anoxic black shale sedimentation can de distinguished. The first group includes the deep shelf basins located in marginal seas that surrounded Pangea. The Sverdrup–Barents and Kolyma–Chukchi basins can be referred to this type. Basins of the second group, such as the Cis-Himalayas and Central Iranian basins of black shale sedimentation, were situated in inner, deeper zones of carbonate platforms. Anoxic basins of the third type occupied an intermediate position between the saliferous and evaporite basins, on the one hand, and the shelf zones of carbonate accumulation, on the other. This type can be exemplified by the Phosphoria, Chihuahua, North Italian, North Tarim, and some other basins. Finally, inland lake basins with black shale sedimentation represent the fourth type.

It is noteworthy that many basins with black shale sedimentation were located close to zones of evaporite accumulation and to coeval or earlier saliferous basins of the Permian time. As is known (Zharkov *et al.*, 1979), deep areas of evaporite basins accumulate large amounts of highly concentrated brines, which later can enter the shelf zones and intermediate basins with groundwater runoff. The subsurface migration of heavy salty brines into subsided areas of shelves or deep basins of marginal seas resulted in water stratification and created stagnant conditions favorable for accumulation of sediments with the elevated content of organic matter. These conditions could stimulate formation of anoxic environments in the Sverdrup, Barents, Phosphoria, Chihuahua, North Italian, North Tarim, East European, Central European, Arabian, and other basins. The Kolyma–Chukchi, Barents, and Sverdrup basins were also characterized by the intermittent thermal stratification of water mass. Spatial distribution patterns of most basins with black shale sedimentation indicate that influx of oxygen-free waters from ocean was hardly responsible for appearance of stagnant environments in shelf and marginal seas, as is assumed by some researchers (Hallam, 1994; Wignall and Hallam, 1992, 1996; Knoll *et al.*, 1996; Wignall and Twitchet, 1996). The available data suggest that most basins with black shale sedimentation formed likely owing to either the influx of highly concentrated brines from evaporite basins that have been located along the Pangea margin, or to the groundwater runoff from the supercontinent. In general, it can be assumed that the groundwater runoff from Pangea during the entire period of its high stand in the Late Permian–Early Triassic could significantly influence surrounding shelf seas.

3.7. Marine Settings of Terrigenous Sedimentation

The remarkable feature of the Permian time is a relatively limited distribution of seas with terrigenous sedimentation around Pangea and also around Cimmerian and Cathaysian microcontinents. More or less significant shallow-water and, particularly, deep-water terrigenous sedimentation commenced only in some sea basins during the Kazanian Age of the Late Permian. It was usually confined either to circumpolar regions of the northern and southern hemispheres, or to eastern margins of Pangea and Cathaysian microcontinents.

The spacious region of marine terrigenous sedimentation extended over the North Alaskan, Yukon, Novaya Zemlya, Verkhoyansk–Okhotsk, and Kolyma–Omolon provinces in the northern Pangea margin (Ganelin, 1984a, 1984b, 1984c; Ustritskii, 1984, 1993; Chernyak, 1984; Kashik *et al.*, 1990; Beauchamp, 1995; Povysheva and Ustritskii, 1996; Sadovnikov and Orlova, 1997). The North Alaskan shallow-water terrigenous shelf was a deposition area of glauconite sandstones,

limy argillites, and clayey limestones, which accumulated in coastal and inner shelf zones, sometimes under storm-wave influence (Beauchamp, 1995). The Novaya Zemlya terrigenous shelf of the Kazanian–Tatarian time accumulated an intricately alternating sequence of sandstones, siltstones, and argillites mainly in tidal and, probably, in proximal–distal zones of inner and outer shelves, where hydrodynamics was highly active. Coastal marine sediments of the Verkhoyansk region are frequently represented by sandstones. They likely accumulated in the intertidal zone under influence of tidal currents and storm waves. The terrigenous shelf of the Kolyma–Omolon region was characterized apparently by shallow-water tidal and wave hydrodynamics that is evident from alternation of glauconite sandstone, siliceous–clayey glauconite limestone, and coquina layers. As a rule, shallow terrigenous shelves of the North Alaskan, Yukon, Taimyr, and Kolyma–Omolon regions were relatively narrow in the Late Permian time and fringed deep inner zones of marginal sea basins with stagnant anoxic environments.

One more large region with shallow-water terrigenous shelf sedimentation is outlined in the northeastern periphery of Pangea along the Mongolian margin of Panthalassa (Shipulina, 1959; Zonenshain *et al.*, 1990). A thick sandstone–shale sequence of this region likely accumulated in the inner and outer shelf zones and, probably, on the continental slope in the course of turbidite sedimentation.

Two other regions with terrigenous marine sedimentation were confined to active continental margins. One of them was located in southeastern areas of the South Chinese microcontinent, and the second one corresponded to the New Zealand margin of the Gondwanan segment of Pangea. As is inferred (Hsü *et al.*, 1990), the South Chinese region represented during the Late Permian a deep piedmont trough that accumulated terrigenous turbidites and molasses, being situated along the northern margin of the Hunan microcontinent; the latter separated from the Yangtze platform by the opening Nanpanjiang ocean. It is assumed that the Late Permian rising and erosion of the Hunan active margin and adjacent island arcs gave rise to accumulation of flyschoid deposits and conglomerates in the deep-water trough. The narrow and shallow terrigenous shelf is also outlined along the southern passive margin of the Hunan microcontinent that faced the Gunanhai ocean.[1] The New Zealand region was characterized by accumulation of thick terrigenous, mainly green- or gray-colored sandy–clayey sediments. They accumulated on shallow shelves and in deep troughs along island arcs (Brown *et al.*, 1970; Steven and Speden, 1978; Veevers, 1984).

Relatively narrow terrigenous shelves are assumed to have been existed also along the western periphery of Pangea. An extended system of subduction-related orogenic structures and volcanic island arcs is outlined here. It stretched from the western margins of Canada and the United States (Nicola, Huntington, Hallavah, Klamath and other island arcs) to southern margins of South America and western Antarctica (the Andean subduction zone, Patagonia island arc, and others). These arcs could have shallow terrigenous shelves (Scotese and Langford, 1995). Nevertheless, no deep troughs with the thick Upper Permian turbidite sequence are established there.

It should be noted again that the terrigenous sea shelves of the Late Permian time were significantly smaller in dimensions and less widespread than shelf settings of carbonate sedimentation. This proportion remains valid in general for the Early Triassic time despite the larger dimensions of shelf areas with terrigenous sedimentation of that time, particularly in the northern and western margins of Pangea.

4. MAIN TRENDS IN EVOLUTION OF SEDIMENTATION–CLIMATIC ZONING

The analyzed spatial distribution of latitudinal belts with arid, semiarid, humid, and glacial sedimentation shows that the period from the late Sakmarian Age of the Early Permian to the Indian Age of the Early Triassic was marked by gradual widening of the arid and semiarid belts and by contrast lowering in the global sedimentation–climatic zoning.

The latitudinal asymmetry of climatic and sedimentation zones was most significant in the late Sakmarian–early Artinskian time. One glacial belt comprised at that time all circumpolar areas of the southern hemisphere located south of 60–75°S. The northern and southern coal-bearing belts were asymmetrically located relative to equator. The southern humid belt was comparatively narrow and stretched between 50–55 and 60–75°S. Some its areas experienced intermittent glaciations. The northern humid coal-bearing belt, unlike the southern one, was sufficiently wide, covering all Pangea regions located north of 30–40°N. Distinctly asymmetrical was location of semiarid and arid belts. These belts extended almost up to 50–55°S in the southern hemisphere and up to 30–40°N in the northern hemisphere.

In the late Kazanian–early Tatarian period, sedimentation belts of Pangea were more symmetrical in the southern and northern hemispheres. The equatorial mountainous belt retained its central position. Regions located to the south and north of it were occupied by arid and semiarid belts. Middle and high latitudes in both hemispheres corresponded to humid coal-bearing belts; small glaciation centers appeared episodically in their circumpolar areas. Simultaneously, some asymmetry in position of sedimentation–climatic belts continued to exist. For instance, the arid and semiarid belts were of different width and had different positions rel-

[1] In our lithological–paleogeographic maps based on geodynamic reconstructions by Scotese and Langford (1995), the Hunan microcontinent, as well as the Nanpanjiang and Hunanhai oceans are not indicated.

ative to equator. The arid belt of the southern hemisphere extended almost up to 35–40°S, whereas in the northern hemisphere, its counterpart was limited by latitude of 30°S. The southern semiarid belt, which was located between 35–40 and 50–60°S, was substantially wider and closer to the pole. The northern semiarid belt stretched between 30 and 40°N. A similar migration toward the pole is also registered for the southern humid coal-bearing belt. The asymmetric location of belts could be a consequence of the asymmetrical position of continental blocks and seas in circumpolar zones of the Earth relative to equator. A large continental block of East Pangea was located in southern high latitudes, whereas the land areas in northern circumpolar zone were much lesser and surrounded by seas. In the late Kazanian–early Tatarian time, the asymmetry was even more pronounced, because the large regions of the Laurasian segment of Pangea were still occupied by spacious inland and shelf seas.

The terminal Permian and initial Early Triassic were periods of less contrast latitudinal sedimentation zoning in Pangea, where the almost ideal symmetry relative to equator characterized positions of belts with arid, semiarid, and humid sedimentation. The belts of arid evaporite sedimentation were located between 30°S and 30°N. The semiarid alluvial–lacustrine belts extended between 30 and 65–70°N in the northern hemisphere and between 30 and 75°S in the southern hemisphere. The circumpolar zones of both hemispheres corresponded to the humid sedimentation belts. Prevalent in Pangea became settings of arid and semiarid sedimentation. As a result, basins of internal drainage with prevalent arid evaporite and semiarid alluvial–lacustrine sedimentation multiplied and became larger in the inner areas of Pangea by the end of the Permian.

5. GLOBAL EXCHANGE OF MATTER BETWEEN LAND AND OCEANS DURING PERMIAN–TRIASSIC BIOSPHERE TRANSFORMATIONS

Data discussed in previous sections indicate that most important paleogeographic changes of the Late Permian–Early Triassic time were the degradation of glacial belts and the gradual uplift of Pangea responsible for regression of inner and marginal seas. These events resulted in global warming, widened belts of arid and semiarid sedimentation settings, and increased areas and number of basins of internal drainage. Simultaneously, settings of humid sedimentation became less widespread that caused the gradual reduction of surficial runoff and displacement of terrigenous deposition centers from marginal to inner areas of Pangea.

In this connection, we should point to a significant disproportion between intensities of terrigenous sedimentation in terrestrial and marine settings, and also between volumes of carbonate and terrigenous sediments accumulated in the Late Permian. Even approximate estimates indicate that the intensity of continental terrigenous sedimentation in the second half of the Late Permian was about an order higher than that of marine terrigenous sedimentation. Simultaneously, the intensity of accumulation of carbonate sediments was 1.5–2 times higher than that of marine terrigenous deposits. In the Cretaceous, for instance, the proportion was opposite, and the carbonate/terrigenous sediment ratio was approximately 1 : 2 (Ronov, 1980). During the Pliocene, the volume of accumulated marine carbonates was 15 times lesser than that of marine terrigenous sediments (Ronov, 1980).

Nowadays, the intensity of biogenic carbonate sedimentation in shelf seas is also many times lesser than that of marine terrigenous sedimentation (Garrels and Mackenzee, 1974; Lisitsyn, 1974). All these proportions unambiguously indicate that the global exchange of matter between land and shelf seas of the Late Permian time was principally different. The unbalanced mineral exchange between the supercontinent and oceans was probably counterbalanced by the increased groundwater runoff into shelf zones of oceans.

The groundwater runoff volume can be estimated approximately in the following way. The current proportion between intensity of terrigenous marine and continental sedimentation is evidently close to the Pliocene one and could be about 1 : 2 (Ronov, 1980). As was mentioned, terrigenous sedimentation in the Late Permian marine settings was almost by an order less intense than in continental ones (proportion 1 : 10), i.e., 5 times slower than now. The present-day influx of different chemical components into oceans is approximately 237×10^{14} g/year; about 210×10^{14} g/year (88.6%) is contribution of the surface runoff, and only 4.3×10^{14} g/year (1.8%) characterize the groundwater runoff (Garrels and Mackenzee, 1974), i.e., the proportion is now about 50 : 1. In the terminal Permian, the contribution of groundwater runoff could be several times greater that now. As was shown for the Caspian and Aral seas, the groundwater runoff in modern arid and semiarid zones can be as great as 25–27% of the total continental runoff (Zektser *et al.*, 1984). Taking these assessments into consideration, one can assume that the groundwater runoff at the end of the Permian, when semiarid and arid settings prevailed in Pangea, could be at least by an order higher than the modern one. These approximate calculations provide only general idea about the groundwater runoff rate in the Late Permian. Nevertheless, they imply that the groundwater runoff from Pangea supercontinent into shelf seas was quite significant in the Late Permian.

The gradual reduction of the surface influx and increasing significance of the groundwater runoff should change substantially the global exchange of matter between Pangea and oceans. First of all, the total continental runoff should be of different chemical composition. The available data (Shvartsev, 1979; Meybeck, 1979; Savenko and Zakharova, 1997; Savenko, in press) indicate that it should be characterized by signif-

icantly higher Na, Mg, Ca, Cl, SO_4, and HCO_3 concentrations, but by the decreased P content. The influx of large volumes of anoxic underground Cl–Mg and Cl–Ca brines depleted in phosphorus and originated from arid and semiarid areas could significantly affect biota of shelf seas.

6. CONCLUSION

1. Paleogeographic evolution of Pangea and changes in sedimentation settings during the period from the late Sakmarian (Early Permian) to Induan (Early Triassic) ages progressed very slowly and depended on the general uplift of supercontinent, regression of inner and marginal seas, formation of marginal and inland collision orogenic belts, crustal arching, and plateau-like highlands, and plains. As a result, the drainless basins became widespread in Pangea. The surface runoff into surrounding shelf seas and oceans gradually decreased, while the inland basins of internal drainage became more widespread.

2. The Permian-Early Triassic global warming resulted in degradation of the glacial belt, widened arid and semiarid sedimentation zones, reduced humid areas, and decreased contrast of the sedimentation–climatic zoning.

3. At the beginning of the Early Triassic, salt accumulation and coal formation terminated throughout the entire Pangea supercontinent. This was likely caused by the greater influence of monsoons in low and middle latitudes of Pangea (Parrish, 1995) and also by the widening of semiarid sedimentation belts.

4. The Late Permian–Early Triassic time was characterized by extremely wide development of carbonate and evaporite–carbonate platforms. The platforms extended between 40–45°N and 40–50°S along the western and eastern margins of Pangea and around the Cimmerian and Cathaysian microcontinents. Conditions favorable for carbonate sedimentation in both the warm and moderately cold marine settings were controlled by the limited influx of detrital material from land into surrounding shelf seas, and this indicates that internal, but not external drainage prevailed on the supercontinent.

5. In the Late Permian, shelf seas with terrigenous sedimentation were of very restricted distribution. They were localized, as a rule, either along the northern and southern margins of Pangea in the middle and high latitude zones of the humid belts, or along the eastern periphery of the Cathaysian microcontinents in the tropical–equatorial humid belt. The insignificant development of terrigenous shelf sedimentation around Pangea additionally proves a minor significance of river runoff from the supercontinent.

6. In contrast, anoxic basins with black shale accumulation were very characteristic of the Permian–Early Triassic period. Three types of these basins are distinguishable: (1) deep-water shelf basins; (2) inner zones of carbonate and evaporite–carbonate platforms; and (3) inland lacustrine basins. Many shelf basins with black shale sedimentation were located near the coeval or older areas of evaporite accumulation, which gave rise to influx of heavy brines into shelf zones. As a consequence, stratification saline water mass resulted in appearance of stagnant environments favorable for accumulation of sediments with the elevated content of organic matter. Sufficiently wide development of such anoxic shelf basins around Pangea indicates that the underground brine flows played a significant role in the mineral exchange between the supercontinent and surrounding shelf seas.

7. The way for the Permian–Triassic biotic crisis was probably paved by the growing aridity of the postglaciation Late Permian climate that substantially reduced the river discharge from Pangea and significantly increased the groundwater runoff. This drastically distorted the balance of mineral exchange between land and oceans and could cause the crisis because of reduction of primary production in oceans and total biomass of continental biota. The unavoidable results are the sharply decreased influx of nutrients from Pangea, the general biomass reduction, extinction of phytoplankton (Zezina, 1991), and subsequent destruction of the entire food chain in oceans.

ACKNOWLEDGMENTS

We are grateful to M.A. Semikhatov, E.Ja. Leven, and V.G. Ganelin for discussion of relevant problems and for their valuable comments and recommendations used to improve the manuscript. The work was supported by the Russian Foundation for Basic Research, project nos. 99-05-65004 and 99-05-64077.

Reviewers A.S. Alekseev and E.Ja. Leven

REFERENCES

Afzali, H., Badia, D., Baroz, F., *et al.*, Synthése géologique des bassins Permiens Français. *Mem. BRGM*, 1989, no. 128.

Ahmad, F., The Permian Basin of Peninsular India, *Report of the Twenty-Second Session Int. Geol. Congr. India*, New Delhi, 1964, part 9, pp. 123–138.

Ahmad, H., Late Palaeozoic Talchir Tillites of Peninsular India, *Earth's Pre-Pleistocene Glacial Record*, Hambrey, M.J. and Harland, J., Eds., Cambridge: Cambridge Univ., 1981, pp. 326–330.

Alekseev, A.S., Mass Extinction in the Phanerozoic, *Doctoral (Geol. –Mineral.) Dissertation*, Moscow State Univ., Moscow, 1998, p. 76.

Alsharhan, A.S. and Nairn, A.E.M., Stratigraphy and Sedimentology of the Permian in the Arabian Basin and Adjacent Areas: a Critical Review, *The Permian of Northern Pangea*, Scholle, P.A., Peryt, T.M., and Ulmer-Scholle, D.S., Eds., Berlin: Springer, 1995, vol. 2, pp. 187–214.

Anderson, R.Y. and Dean, W.E., Filling the Delaware Basin: Hydrologic and Climatic Controls on the Upper Permian

Castile Formation Varved Evaporite, *The Permian of Northern Pangea*, Scholle, P.A., Peryt, T.M., Ulmer-Scholle, D.S., Eds., Berlin: Springer, 1995, vol. 2, pp. 61–78.

Andrianov, V.N., *Verkhnepaleozoiskie otlozheniya Zapadnogo Verkhoyan'ya* (Upper Paleozoic Sediments of the Western Verkhoyansk Region), Moscow: Nauka, 1966.

Atlas litologo-paleogeograficheskikh kart SSSR (Atlas of Lithologic-Paleogeographic Maps of the Soviet Union), Moscow, 1968, vol. 2.

Atlas of the Paleogeography of China, Wang Hongzhen, Ed., Beijing: Cartograph. Publ. House, 1985.

Bardossy, G., Carboniferous to Jurassic Bauxite Deposits as Paleoclimatic and Paleogeographic Indicators, *Pangea: Global Environments and Resources*, Embry, A.F., Beauchamp, B., and Glass, D.J., Eds., *Mem. Can. Soc. Petrol. Geol.*, 1994, no. 17, pp. 283–293.

Barron, E.J. and Fawcett, P.J., The Climate of Pangea: a Review of Climate Model Simulations of the Permian, *The Permian of Northern Pangea*, Scholle, P.A., Peryt, T.M., and Ulmer-Scholle, D.S., Eds., Berlin: Springer, 1995, vol. 1, pp. 37–52.

Baud, A., Magaritz, M., and Holser, W.T., Permian-Triassic of the Tethys: Carbon Isotope Studies, *Geol. Rundsch.*, 1989, vol. 78, pp. 649–677.

Baud, A., Marcoux, J., Guirand, R., Ricou, L.-E., and Gaetani, M., Late Murgabian (266 to 264 Ma), *Atlas Tethys Paleoenvironmental Maps. Explanatory Notes*, Paris: Gauthier-Villars, 1993.

Beauchamp, B., Harrison, J.C., and Henderson, C.M., Upper Paleozoic Stratigraphy and Basin Analysis of the Sverdrup Basin, Canadian Arctic Archipelago: Current Res., Part G, *Pap. Geol. Surv. Can.*, 1989, no. 89-1G, pp. 105–124.

Beauchamp, B., Permian History of Arctic North America, *The Permian of Northern Pangea*, Scholle, P.A., Peryt, T.M., and Ulmer-Scholle, D.S., Eds., Berlin: Springer, 1995, vol. 2, pp. 3–22.

Beauchamp, B., Tropical versus Temperate Permian Carbonates in the Sverdrup Basin, Canadian Arctic, *Carboniferous to Jurassic Pangea. Core Workshop, Guidebook*, Karvonen, R., Haan, J.D., Keenon, J., *et al.*, Eds., Calgary (Alberta, Canada): MCARA, 1993, pp. 109–130.

Berberian, M. and King, G.C.P., Towards a Paleogeography and Tectonic Evolution of Iran, *J. Can. Earth. Sci.*, 1981, vol. 18, pp. 210–265.

Betekhtina, O.A., Gorelova, S.G., Dryagina, L.L., *et al.*, *Verkhnii paleozoi Angaridy* (Upper Paleozoic of the Angaraland), Novosibirsk: Nauka, 1988.

Blant, G., Structure t Paleogeographic du Litoral meridionalé et oriental de L'Afrique, *Sedimentary Basins of the African Coasts: Southern and Coasts*, Blant, G., Ed., Paris: Assoc. Afr. Geol. Surv.,1973, vol. 2, pp. 193–231.

Bobin, E.S., Yudoma–Allakh-Yun' Watershed, *Tr. Tresta "Zolotorazvedka" Inst. NIGRIZoloto*, 1940, vol. 13, pp. 31–53.

Bogomazov, V.M., *Pozdnepaleozoiskie ozera Uralo-Mongol'skogo podvizhnogo poyasa* (Late Paleozoic Lakes of the Ural–Mongolia Mobil Belt), Martinson, G.G. and Neustroeva, I.Yu., Eds., Leningrad: Nauka, 1987, pp. 96–114.

Bogomazov, V.M., Makedonov, A.V., and Gorskii, V.P., The Pechora Province, *Osnovhye cherty stratigrafii permskoi sistemy SSSR* (Basic features of Permian Stratigraphy in the USSR), Kotlyar, G.V. and Stepanov, D.L., Eds., Leningrad: Nedra, 1984, pp. 87–98.

Bourman, R.P. and Alley, N., Permian Glaciated Bedrock Surfaces and Associated Sediments on Kangaroo Island, South Australia: Implications for Local Gondwanan Icemass Dynamics, *Australian J. Earth Sci.*, 1999, vol. 45, no. 4, pp. 523–531.

Bragin, N.Yu., The Permian–Triassic Crisis in the Biosphere as Manifested in the Paleo-Pacific Deep-Water Sequences, *Stratigr. Geol. Korrelyatsiya*, 2000, vol. 8, no. 3, pp. 25–36.

Brown, D., Campbell, K., and Crook, K., *The Geological Evolution of Australia and New Zealand*, London: 1968. Translated under the title *Geologicheskoe razvitie Avstralii i Novoi Zelandii*, Moscow: Mir, 1970.

Breivik, A.J., Gudlaugsson, S.T., and Faleide, J.I., Ottar Basin, SW Barents Sea: a Major Upper Palaeozoic Rift Basin Containing Large Volumes of Deeply Buried Salt, *Basin Res.*, 1995, vol. 7, no. 4, pp. 299–312.

Broutin, J., Roger, J., Platel, J.P., *et al.*, The Permian Pangea. Phytogeographic Implications of New Paleontological Discoveries in Oman (Arabian Peninsula), *C. R. Acad. Sci. Paris, Ser. IIa*, 1995, vol. 321, pp. 1069–1086.

Buggisch, W., Fluger, E., Leitz, F., and Tietz, G.-F., Die Fazielle und palaogeographische Entwicklung im Perm der Karnischen Alpen und in den Raudgebieten, *Geol. Rundsch.*, 1976, vol. 65, H. 2, pp. 649–690.

Burke, W.H., Denison, R.E., Hetherington, E.A., *et al.*, Variation of Seawater $^{87}Sr/^{86}Sr$ Throughout Phanerozoic Time, *Geology*, 1982, vol. 10, pp. 516–519.

Cahen, L., Snelling, N.J., Delhal, J., and Vail, J.R., *The Geochronology and Evolution of Africa*, Oxford: Clarendon, 1984.

Caputo, M.V. and Crowell, J.C., Migration of Glacial Centers across Gondwana during Paleozoic Era, *Bull. Geol. Soc. Am.*, 1985, vol. 96, pp. 1020–1036.

Cassins, G., Toutin-Morin, N., and Virgili, C., A General Outline of the Permian Continental Basins in Southwestern Europe, *The Permian of Northern Pangea*, Scholle, P.A., Peryt, T.M., and Ulmer-Scholle, D.S., Eds., Berlin: Springer, 1995, vol. 2, pp. 137–157.

Cassins, G., Toutin-Morin, N., and Virgili, C., Permian and Triassic Events in the Continental Domains of Mediterranean Europe, *Permo-Triassic Events in the Eastern Tethys*, Sweet, W.C., Yang, Z.Y., Dickins, J.M., and Yin, H.J., Eds., Cambridge: Cambridge Univ., 1992, pp. 60–77.

Chandra, S., Changing Patterns of the Permian Gondwana Vegetation, *Palaeobotanist*, 1992, vol. 40, pp. 73–100.

Châteauneuf, J.J. and Farjanel, G., Syntèse géologique des bassins permiens français, *Bull. Rech. Geol. Min. (Orléans)*, 1989, Mem. 128.

Chelyshev, V.I., *Litologo-paleogeograficheskie karty kazanskogo, tatarskogo i indskogo vekov* (Lithologic-Paleogeographic Maps of the Kazanian, Tatarian, and Induan Ages), Chermnykh, V.A., Ed., Leningrad: Nauka, 1972.

Chernyak, G.E., The Novaya Zemlya Province, *Osnovnye cherty stratigrafii permskoi sistemy SSSR* (Basic Features of Permian Stratigraphy in the USSR), Kotlyar, G.V. and Stepanov, D.L., Eds., Leningrad: Nedra, 1984, pp. 98–105.

Chumakov, N.M., *The Problems of Old Glaciations (Pre-Pleistocene Glaciogeology in the USSR)*, USA: Harwood, 1992.

Chumakov, N.M., Evidence of Late Permian Glaciation in the Kolyma River Basin: A Repercussion of the Gondwana

Glaciation in Northeast Asia?, *Stratigr. Geol. Korrelyatsiya*, 1994, vol. 2, no. 5, pp. 130–150.

Chuvashov, B.I., Permian Deposits of the Ural and Preduralje, *The Permian of Northern Pangea*, Scholle, P.A., Peryt, T.M., and Ulmer-Scholle, D.S., Eds., Berlin: Springer, 1995, vol. 2, pp. 158–183.

Clemensen, L.B. and Abrahamsen, K., Aeolian Stratification and Facies Association in Desert Sediments, Arran Basin (Permian) Scotland, *Sedimentology*, 1983, vol. 30, pp. 311–339.

Cook, P.I., *Australia: Evolution of a Continent*, Canberra: Australian Govern. Publ. Serv., 1990.

Crowell, J.C. and Frakes, L.A., Late Paleozoic Glaciation, IV. Australia, *Bull. Geol. Soc. Am.*, 1971, vol. 82, pp. 2515–2540.

Crowell, J.C., The Ending of the Late Paleozoic Ice Age during the Permian Period, *The Permian of Northern Pangea*, Scholle, P.A., Peryt, T.M., and Ulmer-Scholle, D.S., Eds., Berlin: Springer, 1995, vol. 1, pp. 62–74.

Dagys, A.S., Arkhipov, Yu.V., and Bychkov, Yu.M., *Stratigrafiya triasovoi sistemy severo-vostoka Azii* (Stratigraphy of the Triassic System in Northeastern Asia), Moscow: Nauka, 1979.

Davies, G.R. and Nassichuk, W.W., Carboniferous and Permian History of the Sverdrup Basin, Arctic Islands, *Geology of the Innuitian Orogen and Arctic Platform of Canada and Greenland*, Trettin, H.P., Ed., *Bull. Geol. Surv. Canada*, 1991, vol. 3, pp. 343–368.

Denison, R.E. and Koepnick, R.B., Variation in $^{87}Sr/^{86}Sr$ of Permian Sea-Water: An Overview, *The Permian of Northern Pangea*, Scholle, P.A., Peryt, T.M., and Ulmer-Scholle, D.S., Eds., Berlin: Springer, 1995, vol. 1, pp. 124–132.

Dickins, J.M., Problems of a Late Palaeozoic Glaciation in Australia and Subsequent Climate in the Permian, *Palaeogeogr. Palaeoclimatol. Palaeoecol.*, 1996, vol. 125, pp. 185–197.

Dixon, J. and Dietrich, J.R., Canadian Beaufort Sea and Adjacent Land Areas, *The Geology of North America, vol. 50: the Arctic Ocean Region*, Boulder: Geol. Soc. Am., 1990, pp. 239–256.

Drong, H.-J., Plein, E., Sonnemann, D., *et al.*, Der Schneverdingen—Sondstein des Rotliegendeneine aolische Sedimentfulling alter Grabenstructuren, *Z. Deutsch. Geol. Ges.*, 1982, vol. 133, pp. 699–725.

Dronov, V.I. and Kafarskii, A.Kh., *Permskaya sistema* (Permian System), Dronov, V.I., Ed., Moscow: Nedra, 1980, pp. 112–132.

Durante, M.V., Characteristic Sections of the Continental Permian–Triassic Boundary Sediments in Eurasia: North China, *Granitsa permi i triassa v kontinental'nykh seriyakh Vostochnoi Evropy* (The Permian–Triassic Boundary in Continental Sequences of Eastern Europe), Lozovskii, V.R. and Esaulova, N.K., Eds., Moscow: GEOS, 1998, pp. 175–183.

Durante, M.V. and Mogucheva, N.K., Characteristic Sections of the Continental Permian–Triassic Boundary Sediments in Eurasia: the Kuznetsk Basin), *Granitsa permi I triassa v kontinental'nykh seriyakh Vostochnoi Evropy* (The Permian–Triassic Boundary in Continental Sequences of Eastern Europe), Lozovskii, V.R. and Esaulova, N.K., Eds., Moscow: GEOS, 1998, pp. 162–171.

Enos, P., The Permian of China, *The Permian of Northern Pangea*, Scholle, P.A., Peryt, T.M., and Ulmer-Scholle, D.S., Eds., Berlin: Springer, 1995, vol. 2, pp. 225–256.

Epshtein, O.G., Lithology and Formation Conditions of Upper Permian Glacial-Marine Sediments in the Southern Yana–Kolyma Folded Region, *Cand. Sci. (Geol.–Min.) Dissertation*, Central Geol. Expedition, Magadan, 1973.

Erwin, D.H., The End-Permian Mass Extinction, *The Permian of Northern Pangea*, Scholle, P.A., Peryt, T.M., and Ulmer-Scholle, D.S., Eds., Berlin: Springer, 1995, vol. 1, pp. 20–34.

Ettensohn, F.R., Marine, Organic-Rich, Dark-Shale Deposition on North American Parts of Pangea, Carboniferous to Jurassic: Effects of Supercontinent Organization, *Pangea: Global Environments and Resources*, Embry, A.F., Beauchamp, B., and Glass, D.J., Eds., *Mem. Can. Soc. Petrol. Geol.*, 1994, no. 17, pp. 743–762.

Eyles, C.H., Eyles, N., and Gostin, V.A., Facies and Allostratigraphy of High-Latitude Glacially Influenced Marine Strata of the Early Permian Southern Sydney Basin, *Sedimentol.*, 1998, vol. 45, no. 1, pp. 121–161.

Frakes, L.A., *Climates Throughout Geologic Time*, Amsterdam: Elsevier, 1979.

França, A.B., Milani, E.J., Schneider, R.L., *et al.*, Phanerozoic Correlation in Southern South America, *Petroleum Basin of South America*, Tankard, A.J., Suares, R.S., and Welsink, H.J., Eds., *AAPG Mem.*, 1995, vol. 62, pp. 129–161.

Frenzel, H.N., Bloomer, R.R., Cline, R.B., *et al.*, The Permian Basin Region *Sedimentary Cover of North American Craton, U. S. The Geology of North America*, Sloss, L.L., Ed., Boulder (Co): Geol. Soc. Am., 1988, vol. D-2, pp. 261–306.

Ganelin, V.G., The Taimyr–Kolyma Subregion, *Osnovnye cherty stratigrafii permskoi sistemy SSSR* (Basic Features of Permian Stratigraphy in the USSR), Kotlyar, G.V. and Stepanov, D.L., Eds., Leningrad: Nedra, 1984a, pp. 111–123.

Ganelin, V.G., The Verkhoyansk–Okhotsk Province, *Osnovnye cherty stratigrafii permskoi sistemy SSSR* (Basic Features of Permian Stratigraphy in the USSR), Kotlyar, G.V. and Stepanov, D.L., Eds., Leningrad: Nedra, 1984b, pp. 130–137.

Ganelin, V.G., The Kolyma–Omolon Province, *Osnovnye cherty stratigrafii permskoi sistemy SSSR* (Basic Features of Permian Stratigraphy in the USSR), Kotlyar, G.V. and Stepanov, D.L., Eds., Leningrad: Nedra, 1984c, pp. 137–142.

Ganelin, V.G., Novosibirsk–Vrangel Province, *Osnovnye cherty stratigrafii permskoi sistemy SSSR* (Basic Features of Permian Stratigraphy in the USSR), Kotlyar, G.V. and Stepanov, D.L., Eds., Leningrad: Nedra, 1984d, pp. 142–152.

Ganelin, V.G., Boreal Benthonic Biota of the Late Paleozoic World Ocean, *Stratigr. Geol. Korrelyatsiya*, 1997, vol. 5, no. 3, pp. 29–42.

Garber, R.A. and Harris, P.M., Geology of the Upper Permian Capitan Shelf Margin-A Study from a Continuous Core in the Northern Delaware Basin, *Carboniferous to Jurassic Pangea. Core Workshop—Guidebook*, Karvonen, R., Haan, J.D., Keenon, J., *et al.*, Eds., Calgary (Alberta, Canada): MCARA, 1993, pp. 5–72.

Garrels, R. and Mackenzie, F., *Evolution of Sedimentary Rocks*, New York: Norton, 1971. Translated under the title *Evolyutsiya osadochnykh porod*, Moscow: Mir, 1974.

Gast, R.E., The Perennial Rotliegend Saline Lake in NW Germany, *Geol. Jahrb. A*, 1991, vol. 119, pp. 25–59.

Geological Map of Iran. Sheet no 2, North-Central Iran. M. 1 : 1000000, Teheran: National Iranian Oil Co., 1977.

Geologicheskoe stroenie Mongol'skoi Narodnoi Respubliki (Geology of the Mongolian People's Republic), Shipulin, F.K., Ed., Leningrad: Gostoptekhizdat, 1959.

Geologiya i poleznye iskopaemye Afriki (Geology and Minerals of Africa), Vysotskii, I.V., Kats, Ya.G., Leonov, G.P., *et al.*, Eds., Moscow: Nedra, 1973.

Glennie, K.W., Lower Permian Rotliegend Desert Sedimentation in the North Sea, *Eolian Sediments and Processes. Dev. Sediment, vol. 38*, Brookfield, M.W. and Ahlbrandt, T.S., Eds., Amsterdam: Elsevier, 1983, pp. 521–541.

Glennie, K.W. and Buller, A.T., The Permian Weissliegend of N. W. Europe: the Partial Deformation of Aeolian Dune Sand Caused by the Zechstein Transgression, *Sediment. Geol.*, 1983, vol. 35, pp. 43–81.

Golonka, J., Ross, M.I., and Scotese, C.R., Phanerozoic Paleogeographic and Paleoclimatic Modeling Maps, *Pangea: Global Environments and Resources*, Embry, A.F., Beauchamp, B., and Glass, D.J., Eds., *Mem. Can. Soc. Petrol. Geol.*, 1994, no. 17, pp. 1–48.

Gurevich, A.B., *Pozdnepaleozoiskie ozernye vodoemy territorii Tungusskogo basseina* (Late Paleozoic Lakes in the Tunguska Basin), Martinson, G.G. and Neustroeva, I.Yu., Eds., Leningrad: Nauka, 1987, pp. 114–127.

Hallam, A., The Earliest Triassic as an Anoxic Event, and Its Relationship to the End-Paleozoic Mass Extinction, *Pangea: Global Environments and Resources*, Embry, A.F., Beauchamp, B., and Glass, D.J., Eds., *Mem. Can. Soc. Petrol. Geol.*, 1994, no. 17, pp. 797–804.

Helwig, J., Stratigraphy, Sedimentation, Paleogeography and Paleoclimates of Carboniferous ("Gondwana") and Permian of Bolivia, *AAPG Bull.*, 1972, vol. 56, pp. 1008–1033.

Hsü, K.J., Jiliang Li, Haihong, C., *et al.*, Tectonics of South China: Key to Understanding West Pacific Geology, *Tectonophysics*, 1990, vol. 183, pp. 9–39.

Husseini, M.I., Upper Paleozoic Tectono-Sedimentary Evolution of the Arabian and Adjoining Plates, *J. Geol. Soc. London*, 1992, vol. 149, pp. 419–429.

Hutchison, C.S., *Geological Evolution of the South-East Asia*, Oxford: Clarendon, 1989.

Ignat'ev, V.I., *Tatarskii yarus tsentral'nykh i vostochnykh oblastei Russkoi platformy* (Tatarian Stage in Central Regions of the Russian Platform), Kazan: Kazansk. Univ., 1963, part 2.

Ignat'ev, V.I., *Pozdnepermskie ozera Volgo-Ural'skoi anteklizy* (Late Permian Lakes of the Volga–Urals Anteclise), Martinson, G.G. and Neustroeva, I.Yu., Eds., Leningrad: Nauka, 1987, pp. 140–148.

Isbell, J.L., Seegers, G.M., and Gelhar, G.A., Upper Paleozoic Glacial and Postglacial Deposits, Central Transantarctic Mountains, Antarctica, *Late Glacial and Postglacial Environmental Changes: Quaternary, Carboniferous-Permian and Proterozoic*, Martini, P., Ed., Oxford, Oxford Univ., 1997, pp. 230–242.

Isozaki, Y., Superanoxia Across the Permo–Triassic Boundary: Record in Accreted Deep-Sea Pelagic Chert in Japan, *Pangea: Global Environments and Resources*, Embry, A.F., Beauchamp, B., and Glass, D.J., Eds., *Mem. Can. Soc. Petrol. Geol.*, 1994, no. 17, pp. 805–812.

Jensen, L.N. and Sørensen, K., Tectonic Framework and Halokinesis of the Nordkapp Basin, *Structural and Tectonic Modeling and Its Application to Petroleum Geology*, Larsen, R.M., Brekke, H., Larsen, B.T., and Talleraas, E., Eds., *Spec. Publ. Norw. Petrol. Soc.*, 1992, no. 1, pp. 109–120.

Johnson, K.S., Amsden, T.W., Denison, R.E., *et al.*, Southern Midcontinent Region, *Sedimentary Cover of North American Craton, US, The Geology of North America*, Sloss, L.L., Ed., Boulder (Co): Geol. Soc. Am., 1988, vol. D-2, pp. 307–359.

Kalantar, I.Z., *Triasovye ozera na territorii severa Predural'skogo progiba i Pecherskoi sineklizy* (Triassic Lakes in the Northern Part of the Uralian Foredeep and Pechora Syneclise), Martinson, G.G. and Neustroeva, I.Yu., Eds., Leningrad: Nauka, 1987, pp. 221–235.

Kapoor, H.M. and Tokuoka, T., Sedimentary Facies of the Permian and Triassic of the Himalayas, *The Tethys. Her Paleogeography and Paleobiogeography from Paleozoic to Mesozoic*, Nakazawa, K. and Dickins, J.M., Eds., Tokyo: Tokai Univ., 1985, pp. 23–58.

Kashik, D.S., Ganelin, V.G., Karavaeva, N.I., *et al.*, *Opornyi razrez permi Omolonskogo massiva* (Reference Sequence of the Permian in the Omolon Massif), Leningrad: Nauka, 1990.

Khramov, A.N., Goncharova, G.I., Komissarova, R.A., Pisarevskii, V.V., and Gurevich, E.M., *Paleomagnitologiya* (Paleomagnetology), Leningrad: Nedra, 1982.

Kiersnowski, H., Paul, J., Peryt, T.M., and Smith, D.B., Facies, Paleogeography and Sedimentary History of the Southern Permian Basin in Europe, *The Permian of Northern Pangea*, Scholle, P.A., Peryt, T.M., and Ulmer-Scholle, D.S., Eds., Berlin: Springer, 1995, vol. 2, pp. 119–136.

Klitzsch, E., Paleogeographical Development and Correlation of the Continental Strata (former Nubian Sandstone) in Northeast Africa, *J. African Earth Sci.*, 1990, vol. 10, no. 1/2, pp. 199–213.

Knoll, A.H., Bambach, R.K., Canfield, D.E., and Grotzinger, J.P., Comparative Earth History and Late Permian Mass Extinction, *Science*, 1996, vol. 273, pp. 452–457.

Kogbe, C.A. and Burolett, P.F., A Review of Continental Sediments in Africa, *J. African Earth Sci.*, 1990, vol. 10, no. 1/2, pp. 1–25.

Kotlyar, G.V., The Far East Province, *Osnovhye cherty stratigrafii permskoi sistemy SSSR* (Basic features of Permian Stratigraphy in the USSR), Kotlyar, G.V. and Stepanov, D.L., Eds., Leningrad: Nedra, 1984, pp. 195–205.

Kotlyar, G.V., Kropacheva, G.S., Rostovtsev, K.O., and Chediya, I.O., The Transcaucasian Province, *Osnovnye cherty stratigrafii permskoi sistemy SSSR* (Basic Features of Permian Stratigraphy in the USSR), Kotlyar, G.V. and Stepanov, D.L., Eds., Leningrad: Nedra, 1984, pp. 160–174.

Koyi, H., Talbot, C.J., and Torudbakken, B.O., Salt Diapirs of the Southwest Nordkapp Basin: Analogue Modeling, *Tectonophysics*, 1993, vol. 228, pp. 167–187.

Kreuser, T. and Semkiwa, P.M., Geometry and Depositional History of a Karroo (Permian) Coal Basin (Mchuchuma-Ketewaka) in SW-Tanzania, *N. Jahrb. Geol. Palaontol.*, 1987, no. 2, pp. 69–98.

Kreuser, T., Wopfner, H., Kaaya, C.Z., *et al.*, Depositional Evolution of Permo–Triassic Karroo Basins in Tanzania with Reference to Their Economic Potential, *J. African Earth Sci.*, 1990, vol. 10, no. 1/2, pp. 151–167.

Kukhtinov, D.A., *Pozdnepermskie ozera Aralo-Kaspiiskogo regiona* (Late Permian Lakes of the Aral-Caspian Region), Martinson, G.G. and Neustroeva, I.Yu., Eds., Leningrad: Nauka, 1987, pp. 157–161.

Kukhtinov, D.A., *Triasovye ozera Aralo-Kaspiiskogo regiona* (Triassic Lakes of Aral-Caspian Region), Martinson, G.G. and Neustroeva, I.Yu., Eds., Leningrad: Nauka, 1987, pp. 242–245.

Kuleva, G.V., *Verkhnekazanskie i tatarskie kontinental'nye otlozheniya yugo-vostoka Russkoi platformy* (Upper Kazanian and Tatarian Continental Sediments in Southeastern Russia), Saratov: Sarat. Gos. Univ., 1980.

Kutzbach, J.E. and Gallimore, R.G., Pangean Climates: Megamonsoons of the Megacontinent, *J. Geophys. Res.*, 1989, vol. 94 D. 3, pp. 3341–3357.

Langford, R.P., Permian Coal and Palaeogeography of Gondwava, *BMR Record 1991/95, Paleogeography, Canberra*, 1992, vol. 39.

Lee, K.Y., Geology of the Chaidamu Basin, Qinghai Province, Northwest China, *US Geol. Surv. Open-File. Rep.*, 1984, no. 84–413.

Lee, K.Y., Geology of the Petroleum and Coal Deposits in the Junggar (Zhungaer) Basin, Xinjiang Uygur Zizhiqu, Northwest China, *US Geol. Surv. Open-File. Rep.*, 1985a, no. 85–230.

Lee, K.Y., Geology of the Tarim Basin with Special Emphasis on Petroleum Deposits, Xinjiang Uygur Zizhiqu, Northwest China, *US Geol. Surv. Open-File. Rep.*, 1985b, no. 85–616.

Lee, K.Y., Geology of the Petroleum and Coal Deposits in North China Basin, Eastern China, *US Geol. Surv. Open-File. Rep.*, 1986a, no. 86–154.

Lee, K.Y., Petroleum Geology of the Songliao Basin, Northeast China, *US Geol. Surv. Open-File. Rep.*, 1986b, no. 86–502.

Lefran, J.Ph. and Guirand, R., The Continental Intercalaire of Northwestern Sahara and Its Equivalents in the Neighboring Regions, *J. African Earth Sci.*, 1990, vol. 10, no. 1/2, pp. 27–77.

Leven, E.Ja., The Central Asia Province, *Osnovnye cherty stratigrafii permskoi sistemy SSSR* (Basic Features of Permian Stratigraphy in the USSR), Kotlyar, G.V. and Stepanov, D.L., Eds., Leningrad: Nedra, 1984, pp. 174–195.

Leven, E.Ja., Dmitriev, V.Yu., and Novikov, V.P., *Ob"yasnitel'naya zapiska k regional'noi stratigraficheskoi skheme permskikh otlozhenii Srednei Azii (Pamirskii subregion)* (Explanatory Note to the Regional Stratigraphic Scheme of Permian Deposits in Central Asia, the Pamirs Subregion), Dushanbe: Donish, 1989.

Leven, E.Ja., Main Events of the Permian History of the Tethys and Fusulinids, *Stratigr. Geol. Korrelyatsiya*, 1993, vol. 1, no. 1, pp. 59–75.

Limarino, C.O. and Spalletti, L.A., Eolian Permian Deposits in West and Northwest Argentina, *Sediment. Geol.*, 1986, vol. 49, pp. 109–127.

Lindsay, J.F., Permian Postglacial Environments of the Australian Plate, *Late Glacial and Postglacial Environmental Changes*, Martini, I.P., Ed., New York: Oxford Univ. Press, 1997, pp. 213–229.

Lisitsyn, A.P., *Osadkoobrazovanie v okeanakh* (Sedimentation in Oceans), Moscow: Nauka, 1974.

Lowenstein, T.K., Origin of Depositional Cycles in a Permian "Saline Giant": the Saledo (McNutt Zone) Evaporites of New Mexico and Texas, *Bull. Geol. Soc. Am.*, 1988, vol. 100, pp. 592–608.

Lozovskii, V.R., Characteristic Sections of the Continental Permian–Triassic Boundary Sediments in Eurasia: the Dzhimusar Basin, *Granitsa permi i triassa v kontinental'nykh seriyakh Vostochnoi Evropy* (The Permian–Triassic Boundary in Continental Sequences of Eastern Europe), Lozovskii, V.R. and Esaulova, N.K., Eds., Moscow: GEOS, 1998, pp. 171–175.

Lozovskii, V.R., Characteristic Sections of the Continental Permian–Triassic Boundary Sediments in Eurasia, *Granitsa permi i triassa v kontinental'nykh seriyakh Vostochnoi Evropy* (The Permian–Triassic Boundary in Continental Sequences of Eastern Europe), Lozovskii, V.R. and Esaulova, N.K., Eds., Moscow: GEOS, 1998, pp. 139–145.

Lozovskii, V.R. and Balabanov, Yu.P., Characteristic Sections of the Continental Permian–Triassic Boundary Sediments in Eurasia: the Timan-Pechora Plate, *Granitsa permi i triassa v kontinental'nykh seriyakh Vostochnoi Evropy* (The Permian–Triassic Boundary in Continental Sequences of Eastern Europe), Lozovskii, V.R. and Esaulova, N.K., Eds., Moscow: GEOS, 1998, pp. 145–162.

Lozovskii, V.R. and Blom, G.I., Reference Sections of the Continental Permian–Triassic Boundary Sediments in Eastern Europe. Vetluga River Basin, *Granitsa permi i triassa v kontinental'nykh seriyakh Vostochnoi Evropy* (The Permian–Triassic Boundary in Continental Sequences of Eastern Europe), Lozovskii, V.R. and Esaulova, N.K., Eds., Moscow: GEOS, 1998, pp. 7–13.

Lozovskii, V.R. and Zharkov, I.Ya., Reference Sections of the Continental Permian–Triassic Boundary Sediments in Eastern Europe: the Volga River Basin, *Granitsa permi i triassa v kontinental'nykh seriyakh Vostochnoi Evropy* (The Permian–Triassic Boundary in Continental Sequences of Eastern Europe), Lozovskii, V.R. and Esaulova, N.K., Eds., Moscow: GEOS, 1998, pp. 13–19.

Lys, M., Carboniferous and Permian Marine Deposits in Southern Tunisia–Micropaleontology (foraminifera) and Paleobiogeography, *Bull. Central. Explor.-Prod. Elf.-Aquitaine*, 1988, vol. 12, no. 2, pp. 601–659.

Mader, D., *Evolution of Palaeoecology and Palaeoenvironment of Permian and Triassic Fluvial Basin in Europe*, vol. 1: *Western and Eastern Europe*, vol. 2: *Southeastern Europe and Index*, Stuttgart: Gustav Fischer, 1992.

Martin, H., The Late Palaeozoic Dwyka Group of the South Kalahari Basin in Namibia and Botswana and the Subglacial Valleys of the Kaokoveld in Namibia, *Earth's Pre-Pleistocene Glacial Record*, Humbrey, M.J. and Harland, J., Eds., Cambridge: Cambridge Univ., 1981, pp. 61–66.

Maxwell, W.D., The End Permian Mass Extinction, *Mass Extinctions: Processes and Evidence*, Donovan, S.K., Ed., London: Belkhaven, 1989, pp. 152–173.

Mazzullo, S.J., Mazzullo, J., and Harris, P.M., Significance of Eolian Quartzose Sheet Sands on Emergent Carbonate Shelves; Permian of West Texas–New Mexico, *AAPG Bull.*, 1985, vol. 69, p. 284.

Mazzullo, S.J., Permian Stratigraphy and Facies, Permian Basin (Texas–New Mexico) and Adjoining Areas in the Midcontinent United States, *The Permian of Northern Pangea*, Scholle, P.A., Peryt, T.M., and Ulmer-Scholle, D.S., Eds., Berlin: Springer, 1995, vol. 2, pp. 41–60.

McKee, E.D., Stratigraphy and History of the Moenkopi Formation of Triassic Age, *Mem. Geol. Surv. Am.*, 1954, vol. 61, pp. 12–21.

McKee, E.D., Oriel, S.S., Sheldon, R.P., *et al.*, Paleotectonic Investigations of the Permian System in the United States, *US Geol. Surv. Prof. Paper*, 1967, no. 515.

Meyen, S.V. and Golubeva, I.I., The Central Siberian Province, *Osnovnye cherty stratigrafii permskoi sistemy SSSR* (Basic Features of Permian Stratigraphy in the USSR), Kotl-

yar, G.V. and Stepanov, D.L., Eds., Leningrad: Nedra, 1984, pp. 222–226.

Menning, M., A Numerical Time Scale for the Permian and Triassic Periods An Integrated Time Analysis, *The Permian of Northern Pangea*, Scholle, P.A., Peryt, T.M., and Ulmer-Scholle, D.E., Eds., Berlin: Springer, 1995, vol. 1, pp. 77–97.

Merzlyakov, G.A., *Permskie solenosnye basseiny Evrazii* (Permian Saliferous Basins of Eurasia), Novosibirsk: Nauka, 1979.

Metcalfe, I., Late Palaeozoic and Mesozoic Palaeogeography of Eastern Pangea and Tethys, *Pangea: Global Environments and Resources. Canadian Soc. Petrol. Geol. Mem. 17*, Embry, A.F., Beauchamp, B., and Glass, D.J., Eds., Calgary, 1994, pp. 97–111.

Meybeck, M., Concentration des eau fluviales en elements majeurs et apports en solution aux oceans, *Rev. Geol. Dynam. et Geogr. Phys.*, 1979, vol. 21, no. 3, pp. 215–246.

Miklukho-Maklai, A.D. and Miklukho-Maklai, K.V., The Crimea-Caucasus Alpine Fold Region, *Stratigrafiya SSSR. Permskaya sistema* (Stratigraphy of the USSR: Permian System), Likharev, B.K., Ed., Moscow: Nedra, 1966, pp. 391–402.

Miklukho-Maklai, A.D., *Verkhnii paleozoi Srednei Azii* (Upper Paleozoic of Central Asia), Leningrad: Len. Gos. Univ., 1963.

Miljush, P., Geological–Tectonic Structure and Evolution of Outer Dinarides and Adriatic Area, *AAPG Bull.*, 1973, vol. 57, no. 5, pp. 913–929.

Mirovoi vodnyi balans i vodnye resursy Zemli (World Water Balance and Water Resources of the Earth), Leningrad: Gidrometeoizdat, 1974.

Mishra, H.K., A Comparison of the Petrology of Some Permian Coals of India with Those of Western Australia, *Proc. Gondwana Seven*, Ulbrich H. and Rocha Campos, A.C., Eds., Sao-Paulo: Inst. Geociencias-USP, 1991, pp. 261–271.

Mitra, N.D., The Sedimentary History of Lower Gondwana Coal Basin of Peninsular India, *Proc. Gondwana Seven*, Ulbrich, H., Rocha Campos, A.C., Eds., Sao-Paulo: Inst. Geociencias-USP, 1991, pp. 271–288.

Movshovich, E.V., *Triasovye ozera yuga evropeiskoi chasti SSSR* (Triassic Lakes of the South European Soviet Union), Martinson, G.G. and Neustroeva, I.Yu., Eds., Leningrad: Nauka, 1987, pp. 213–221.

Murris, R.J., Middle East: Stratigraphic Evolution and Oil Habitat, *AAPG Bull.*, 1980, vol. 64, pp. 597–618.

Nairn, A.E.M. and Smithwick, M.E., Permian Paleogeography and climatology, *The Continental Permian in Central, West and South Europe*, Falke, H., Ed., Boston: Reidel, 1976, pp. 283–312.

Nassichuk, W.W., Permian Ammonoids in the Arctic Region of the World, *The Permian of Northern Pangea*, Scholle, P.A., Peryt, T.M., and Ulmer-Scholle, D.S., Eds., Berlin: Springer, 1995, vol. 1, pp. 210–235.

Neustroeva, I.Yu. and Bogomazov, V.M., *Triasovye ozera Kuznetskogo basseina* (Triassic Lakes of the Kuznetsk Basin), Martinson, G.G. and Neustroeva, I.Yu., Eds., Leningrad: Nauka, 1987, pp. 245–249.

Ochev, V.G. and Shishkin, M.A., Changes in Continental Biota across the Paleozoic–Mesozoic Boundary in Eastern Europe: Communities of Terrestrial Vertebrates, *Granitsa permi i triassa v kontinental'nykh seriyakh Vostochnoi Evropy* (The Permian–Triassic Boundary in continental Sequences of Eastern Europe), Lozovskii, V.R. and Esaulova, N.K., Eds., Moscow: GEOS, 1998, pp. 59–74.

Ori, G.G., The Nature of the Permian Rivers in Southern Alps, *Mem. Soc. Geol. Ital.*, 1988, vol. 34, pp. 155–160.

Padula, V.T., Oil Shale of Permian Irati Formation, Brazil, *AAPG Bull.*, 1969, vol. 53, no. 3, pp. 591–602.

Parfenov, L.M., Nokleberg, U.J., Monger, D.U., *et al.*, Formation of Terrain Collage in Orogenic Belts Framing the North Pacific, *Geol. Geofiz.*, 1999, no. 11, pp. 1563–1574.

Parrish, J.T., Climate of the Supercontinent Pangea, *J. Geol.*, 1993, vol. 101, pp. 215–233.

Parrish, J.T., Geologic Evidence of Permian Climate, *The Permian of Northern Pangea*, Scholle, P.A., Peryt, T.M., and Ulmer-Scholle, D.S., Eds., Berlin: Springer, 1995, vol. 1, pp. 53–61.

Parrish, J.M., Parrish, J.T., and Ziegler, A.M., Permian–Triassic Paleogeography and Paleoclimatology and Implications for the Rapsid Distributions, *The Ecology and Biology of Mamma-Like Reptiles*, Hotton, N.H., Maclean, P.D., *et al.*, Eds., Washington: Smithsonian Press, 1986, pp. 109–132.

Peterson, J.A., Permian Paleogeography and Sedimentary Provinces, West Central United States, *Symposium: Paleozoic Paleogeography of West-Central United States, Rocky Mountain Sect. Soc. Econ. Paleontol. Mineral.*, Fouch, T.D. and Magathan, E.R., Eds., 1980, vol. 1, pp. 271–292.

Petroleum Basin of South America. AAPG, Mem. 62, Tankard, A.J., Suares, R., and Welsink, H.J., Eds., 1995.

Ponomarenko, A.G. and Sukacheva, I.D., Changes in Continental Biota across the Paleozoic–Mesozoic Boundary in Western Europe: Insects, *Granitsa permi i triassa v kontinental'nykh seriyakh Vostochnoi Evropy* (The Permian–Triassic Boundary in Continental Sequences of Eastern Europe), Lozovskii, V.R. and Esaulova, N.K., Eds., Moscow: GEOS, 1998, pp. 96–106.

Povysheva, L.G. and Ustritskii, V.I., Permian Deposits of the Novaya Zemlya Islands, *Stratigr. Geol. Korrelyatsiya*, 1996, vol. 4, no. 5, pp. 25–34.

Rao, C.P., Criteria for Recognition of Cold-Water Carbonate Sedimentation: Berriedale Limestone (Lower Permian) Tasmania, Australia, *J. Sediment. Petrol.*, 1981, vol. 51, pp. 491–506.

Rascoe, B., Permian System in Western Midcontinent, *Permian Rocks of the Midcontinent*, Morgan, W.A., Babcock, J.A., Eds., *Spec. Publ. Midcontinent Sect. Soc. Econ. Paleontol. Mineral.*, 1988, vol. 1, pp. 3–12.

Raup, D.M. and Sepkoski, J.J., Jr., Periodicity of Extinctions of Families and Genera, *Science*, 1986, vol. 231, pp. 833–836.

Retallack, G.J. and Krull, E.S., Landscape Ecological Shift at the Permian-Triassic Boundary in Antarctica, *Australian J. Earth's Sci.*, 1999, vol. 46, pp. 785–812.

Robinson, P.L., Palaeoclimatology and Continental Drift, *Implications of Continental Drift to the Earth Scienes*, Tarling, D.H., and Runcorn, S.K., Eds., New York: Academic, 1973, vol. 1, pp. 449–476.

Ronov, A.B., *Osadochnaya obolochka Zemli (kolichestvennye zakonomernosti stroeniya, sostava i evolyutsii)* (The Earth's Sedimentary Cover: Quantitative Parameters of Structure, Composition, and Evolution), Moscow: Nauka, 1980.

Ross, C.A. and Ross, J.R.P., Permian Sequence Stratigraphy, *The Permian of Northern Pangea*, Scholle, P.A., Peryt, T.M.,

and Ulmer-Scholle, D.S., Eds., Berlin: Springer, 1995, vol. 1, pp. 98–123.

Ross, C.A., Baud, A., and Menning, M., A Time Scale for Project Pangea, *Pangea: Global Environments and Resources*, Embry, A.F., Beauchamp, B., and Glass, D.J., Eds., *Mem. Can. Soc. Petrol. Geol.*, 1994, no. 17, pp. 81–83.

Rostovtsev, K.O., The Crimea–Caucasus Province, *Osnovnye cherty stratigrafii permskoi sistemy SSSR* (Basic Features of Permian Stratigraphy in the USSR), Kotlyar, G.V. and Stepanov, D.L., Eds., Leningrad: Nedra, 1984, pp. 157–160.

Runnegar, B., The Permian of Gondwana, *Reports to 27th Int. Geol. Congr.*, Stratigraphy, Section S.01, Moscow: Nauka, 1984, vol. 1, pp. 147–158.

Sadovnikov, G.N. and Orlova, E.F., On the Permian–Triassic Boundary Sediments in Northern and Eastern Margins of the Siberian Platform, *Stratigr. Geol. Korrelyatsiya*, 1997, no. 1, pp. 14–20.

Salem, M.J., *The Geology of Sirt Basin*, Amsterdam: Elsevier, 1996, vols. 1–3.

Savenko, V.S. and Zakharova, E.A., Main Regularities of Phosphorus Behavior in the River Discharge, *Vodnye Resursy*, 1997, vol. 24, no. 2, pp. 159–168.

Savenko, V.S., Water Migration Coefficients of Chemical Elements in the Hypergenesis Zone, *Litol. Polezn. Iskop.* (in press).

Scholle, P.A., Carbon and Sulfur Isotope Stratigraphy of the Permian and Adjacent Intervals, *The Permian of Northern Pangea*, Scholle, P.A., Peryt, T.M., and Ulmer-Scholle, D.S., Eds., Berlin: Springer, 1995, vol. 1, pp. 133–149.

Schopf, T.J.M., Permo-Triassic Extinctions: Relation to Sea-Floor Spreading, *J. Geol.*, 1974, vol. 82, pp. 129–143.

Scotese, C.R. and Langford, R.P., Pangea and Paleogeography of the Permian, *The Permian of Northern Pangea*, Scholle, P.A., Peryt, T.M., and Ulmer-Scholle, D.S., Eds., Berlin: Springer, 1995, vol. 1, pp. 3–19.

Sempere, T., Phanerozoic Evolution of Bolivia and Adjacent Regions, *Petroleum Basin of South America*, Tankard, A.J., Suares, R., and Welsink, H.J., Eds., *Mem. AAPG*, 1995, no. 62, pp. 96–128.

Sepkoski, J.J., Jr., A Compendium of Fossil Marine Families, *Mus. Contrib. Biol. Geol., Milwaukeo Publ.*, 1982, vol. 51, pp. 1–125.

Sepkoski, J.J., Jr., Periodicity in Extinction and the Problem of Catastrophysm in the History of Life, *J. Geol. Soc.* (London), 1989, vol. 146, pp. 7–19.

Sharief, F.A., Lithofacies Distribution of Permo-Triassic Rocks in the Middle East, *J. Petrol. Geol.*, 1981, no. 4, pp. 299–310.

Sharief, F.A., Permian and Triassic Geologic History and Tectonics of the Middle East, *J. Petrol. Geol.*, 1983, no. 6, pp. 95–102.

Sheldon, R.P., Cressman, E.R., Cheney, T.M., and McKelvey, V.E., Middle Rocky Mountains and Northeastern Great Basin, *Paleotectonic Investigation of the Permian System in the United States*, McKee, E.D., Oriel, S.S., *et al.*, Eds., *US Geol. Surv. Prof. Pap.*, 1967, no. 515, pp. 157–170.

Sheng Jin-Zhang, Rui Lin, and Chen Chu-Zhen. Permian and Triassic Sedimentary Facies and Paleogeography of South China, *The Tethys. Her Paleogeography and Paleobiogeography from Paleozoic to Mesozoic*, Nakazawa, K. and Dickins, J.M., Eds., Tokyo: Tokai Univ., 1985, pp. 59–81.

Shvartsev, S.L., *Geokhimiya podzemnykh vod Gipergeneza* (Hydrogeochemistry of the Hypergenesis Zone), Moscow: Nedra, 1978.

Smith, D.B., The Late Permian Palaeogeography of North-East England, *Proc. York. Geol. Soc.*, 1989, vol. 47, pp. 285–312.

Smith, R.M.H., A Review of Stratigraphy and Sedimentary Environments of the Karroo Basin of South Africa, *J. African Earth Sci.*, 1990, vol. 10, no. 1/2, pp. 117–137.

Sneh, A., Permian Dune Patterns in Northwestern Europe Challenged, *J. Sed. Petrol.*, 1988, vol. 58, pp. 44–51.

Stemmerik, L., Permian History of the Norwegian-Greenland Sea Area, *The Permian of Northern Pangea*, Scholle, P.A., Peryt, T.M., and Ulmer-Scholle, D.S., Eds., Berlin: Springer, 1995, vol. 2, pp. 98–118.

Stemmerik, L. and Worsley, D., Permian History of the Barents Shelf Area, *The Permian of Northern Pangea*, Scholle, P.A., Peryt, T.M., and Ulmer-Scholle, D.S., Eds., Berlin: Springer, 1995, vol. 2, pp. 81–97.

Stevens, S.M., Was Development of Brackish Ocean a Factor in Permian Extinctions?, *Geology*, 1997, vol. 88, pp. 133–138.

Stevens, G.R. and Speden, I.G., New Zealand, *The Phanerozoic Geology of the World*, vol. 2: *The Mesozoic*, Amsterdam: Elsevier, 1978, pp. 251–328.

Strok, N.I., *Pozdnepermskie ozera Moskovskoi sineklizy* (Late Permian Lakes of the Moscow Syneclise), Martinson, G.G. and Neustroeva, I.Yu., Eds., Leningrad: Nauka, 1987, pp. 128–139.

Trettin, H.P., Arctic Islands. The Geology of North America - an Overview, *The Geology of North America*, Bally, A.W., and Palmer, A.R., Eds., Boulder: Geol. Soc. Am., 1989, vol. A, pp. 349–370.

Turner, B.R., Continental Sediments in South Africa, *J. Afr. Earth Sci.*, 1990, vol. 10, no. 1/2, pp. 139–149.

Tverdokhlebov, V.P., *Pozdnepermskie ozerno-allyuvial'nye landshafty Yuzhnogo Predural'ya* (Late Permian Lacustrine-Alluvial Landscapes of the Southern Cis-Urals), Martinson, G.G. and Neustroeva, I.Yu., Eds., Leningrad: Nauka, 1987a, pp. 149–157.

Tverdokhlebov, V.P., *Triasovye ozera Yuzhnogo Predural'ya* (Triassic Lakes of the Southern Cis-Urals), Martinson, G.G. and Neustroeva, I.Yu., Eds., Leningrad: Nauka, 1987b, pp. 235–242.

Tverdokhlebov, V.P. and Shminke, L.N., Eolian Formations of the Tatarian Stage, the Vyatka River Basin, *Dokl. Akad. Nauk SSSR*, 1990, vol. 315, no. 4, pp. 934–936.

Ulmishek, G., *Geology and Petroleum Resources of Basin of Western China*, Argonne National Laboratories, ANL/ES 146, 1984.

Ustämer, T. and Robertson, A.H.F., Late Palaeozoic–Early Mesozoic Marginal Basins Along the Active Southern Continental Margin of Eurasia: Evidence From the Central Pontides (Turkey) and Adjacent Region, *Geol. J.*, 1993, vol. 28, nos. 3–4, pp. 219–238.

Ustritskii, V.I., The Taimyr–Khatanga Province, *Osnovnye cherty stratigrafii permskoi sistemy SSSR* (Basic Features of Permian Stratigraphy in the USSR), Kotlyar, G.V. and Stepanov, D.L., Eds., Leningrad: Nedra, 1984, pp. 123–130.

Ustritskii, V.I., The Paleozoic Boreal Biogeographic Region, *Stratigr. Geol. Korrelyatsiya*, 1993, vol. 1, no. 2, pp. 67–78.

Veevers, J.J., *Phanerozoic Earth History of Australia*, Oxford: Clarendon, 1984.

Veevers, J.J. and Powell, C.M.A., Late Paleozoic Glacial Episodes in Gondwanaland Reflected in Transgressive–Regressive Depositional Sequences in Euramerica, *Bull. Geol. Soc. Am.*, 1987, vol. 98, pp. 475–487.

Visser, J.N.J., Controls on Early Permian Shelf Deglaciation in the Karroo Basin of South Africa, *Palaeogeogr. Palaeoclimatol. Palaeoecol.*, 1996, vol. 125, pp. 129–139.

Wardlaw, B.R., Snyder, W.S., Sphinosa, C., and Gallegos, D.M., Permian of the Western United States, *The Permian of Northern Pangea*, Scholle, P.A., Peryt, T.M., and Ulmer-Scholle, D.S., Eds., Berlin: Springer, 1995, vol. 2, pp. 23–40.

Wignall, P.B. and Hallam, A., Anoxia as a Cause of the Permian/Triassic Mass Extinction: Facies Evidence for Northern Italy and the Western United States, *Palaeogeogr. Palaeoclimatol. Palaeoecol.*, 1992, no. 93, pp. 21–46.

Wignall, P.B. and Hallam, A., Facies Change at the End-Permian Mass Extinction in S.E. Sichuan, China, *Palaios*, 1996, vol. 11, pp. 587–596.

Wignall, P.B. and Twitchett, R.J., Oceanic Anoxia and the End Permian Mass Extinction, *Science*, 1996, vol. 272, pp. 1155–1158.

Woods, R.D., Salvador, A., and Miles, A.E., Pre-Triassic. The Gulf of Mexico Basin, *The Geology of North America*, Salvador, A., Ed., Boulder: Geol. Soc. Am., 1991, pp. 109–129.

Wycisk, P., Aspects of Cratonal Sedimentation: Facies Distribution of Fluvial and Shallow Marine Sequences in NW Sudan, SW Egypt Since Silurian Time, *J. African Earth Sci.*, 1990, no. 1/2, pp. 215–228.

Yang Zunyi, Cheng Yuqi, and Wang Hongzhen, *The Geology of China*, London: Oxford Univ. Press, 1986.

Yemane, K. and Kelts, K., A Short Review of Paleoenvironments for Lower Beaufort (Upper Permian) Karroo Sequences from Southern to Central Africa: a Major Gondwana Lacustrine Episode, *J. African Earth Sci.*, 1990, vol. 10, no. 1/2, pp. 169–185.

Yemane, K., Contribution of Late Permian Palaeogeography in Maintaining a Temperate Climate in Gondwana, *Nature* (London), 1993, vol. 362, no. 6407, pp. 51–54.

Yemane, K., Palynoflora and Kerogen Constituents of an Upper Permian Gondwana Deposits, Northern Malawi: Implication for Paleoclimate and Source-Rock Potential, *Pangea: Global Environments and Resources*, Embry, A.F., Beauchamp, B., and Glass, D.J., Eds., *Mem. Can. Soc. Petrol. Geol.*, 1994, no. 17, pp. 449–468.

Yuzvitskii, A.Z., Gorelova, S.G., and Betekhtina, O.A., The Altai–Sayan Province, *Osnovnye cherty stratigrafii permskoi sistemy SSSR* (Basic Features of Permian Stratigraphy in the USSR), Kotlyar, G.V. and Stepanov, D.L., Eds., Leningrad: Nedra, 1984, pp. 208–222.

Zektser, I.S., Dzhamalov, R.G., and Meskheteli, A.V., *Podzemnyi vodoobmen sushi i morya* (Subsurface Water Exchange between the Continent and the Sea), Leningrad: Gidrometeoizdat, 1984.

Zezina, O.N., On Significance of Temperatures and Nutrition Conditions in Historical Evolution of Marine Biota, *Vazhneishie bioticheskie sobytiya v istorii Zemli* (Most Important Events in the Earth's History), Tallinn: Akad. Nauk Estonskoi SSR, 1991, pp. 41–47.

Zharkov, M.A., *Paleozoiskie solenosnye formatsii mira* (Paleozoic Saliferous Formations of the World), Moscow: Nedra, 1974.

Zharkov, M.A., *Istoriya paleozoiskogo solenakopleniya* (History of Paleozoic Salt Accumulation), Novosibirsk: Nauka, 1978.

Zharkov, M.A., *History of Paleozoic Salt Accumulation*, Berlin: Springer, 1981.

Zharkov, M.A., Zharkova, T.M., and Merzljakov, G.A., Die Volumenverhaltnisse halogener Gesteine in paläzoishen Salinarbecken und des Problem des Stoffbestandsentwicklung der Meerwassers, *Z. Geol. Wiss.* (Berlin), 1979, vol. 7, pp. 827–841.

Zherebtsova, I.K., To the Problem of the Continental Halogenesis, *Problemy solenakopleniya* (Problems of Salt Accumulation), Yanshin, A.L. and Zharkov, M.A., Eds., Novosibirsk: Nauka, 1977, pp. 124–128.

Zhukov, F.I., Vozar, I.I., and Yanev, S.N., *Permskie osadochno-vulkanogennye formatsii i rudnye mestorozhdeniya Karpato-Balkanskoi oblasti* (Permian Volcano-Sedimentary Formations and Ore Deposits in the Carpathian–Balkan Region), Kiev: Nauk. Dumka, 1976.

Ziegler, P.A., *Geological Atlas of Western and Central Europe*, Amsterdam: Elsevier, 1982.

Ziegler, A.M., Hulver, M.L., and Rowley, D.B., Permian World Topography and Climate, *Late Glacial and Postglacial Environmental Changes (Quaternary, Carboniferous–Permian and Proterozoic)*, Martini, P., Ed., Oxford Univ. Press, 1997, pp. 111–146.

Ziegler, A.M., Gibbs, M.T., and Hulver, M.Z., A Mini-Atlas of Oceanic Water Masses in the Permian Period, *Proc. Roy. Soc. of Victoria, Australia*, 1998, vol. 110, no. 1/2, pp. 323–343.

Zonenshain, L.P., Kuzmin, M.I., and Natapov, L.M., *Geology, of the USSR: A Plate-Tectonic Synthesis*, Am. Geophys. Union, Geodyn. Ser., 1990, vol. 21.

Stratigraphy and Geological Correlation, Vol. 9, No. 4, 2001, pp. 364–372. Translated from Stratigrafiya. Geologicheskaya Korrelyatsiya, Vol. 9, No. 4, 2001, pp. 55–64.
Original Russian Text Copyright © 2001 by Leven, Korchagin.
English Translation Copyright © 2001 by MAIK "Nauka/Interperiodica" (Russia).

Permian–Triassic Biotic Crisis and Foraminifers

E. Ja. Leven and O. A. Korchagin

Geological Institute, Russian Academy of Sciences, Pyzhevskii per. 7, Moscow, 109017 Russia

Received December 20, 1998; in final form, December 5, 1999

Abstract—Two phases can be distinguished in development of foraminifers during the Late Permian crisis. The first phase was marked by extinction of 40% of total foraminiferal genera. The crisis affected particularly fusulinids, which lost 76% of genera and 70% of families. At the end of the Permian, all foraminifers became extinct. Moreover, fusulinids die off completely, whereas some smaller foraminifers (Lazarus-taxa) appear again in the *I. isarcica* conodont zone. At the beginning, they were represented by archaic Paleozoic forms. The renewal of assemblages owing to development of Mesozoic forms commenced at the end of the Induan Age and significantly accelerated in the Anisian Age.

Key words: Permian, Triassic, foraminifers, crisis.

INTRODUCTION

Biotic changes at the Paleozoic–Mesozoic boundary attracted attention of researchers for a long period, and different aspects of the problem were discussed in many papers. In most publications, authors share the views of Schindewolf (1954) who believed that these changes were catastrophic. However, other researchers argued that the Late Paleozoic extinction was gradual (Ruzhentsev and Sarycheva, 1965; Reitlinger, 1965; and others). This work represents an attempt to solve the problem tracing dynamics in development of foraminiferal assemblages in the terminal Permian–initial Triassic. Although many researchers paid a sufficient attention to foraminifers when they considered biotic changes during this period of the geological history, most publications are dedicated to individual problems being restricted to the analysis of their distribution in particular sections. To the contrary, summarizing works were too generalized to notice all important regularities.

This paper presents the results of generalization of all available published data on foraminifers from the Upper Permian and Lower Triassic Tethyan sequences and of original materials from sequences of the Transcaucasia, Pamirs, and Afghanistan. Distribution of foraminifers through the indicated stratigraphic interval was analyzed, using, where possible, their zonal scales, and foraminifers proper were considered at the genus and family levels, although changes at the species level were also analyzed. The taxonomic revision was beyond the scope of this work, and published lists of foraminiferal species are used therefore without any corrections. Revision of lists would, probably, slightly change the estimated numbers of extinct and newly appeared genera at certain historical boundaries, but this could hardly affect the essence of conclusions. As for higher-rank taxons, their classification follows that in the recently published reference books on Paleozoic foraminifers (*Spravochnik...*, 1993, 1996).

The trustworthiness of inferences concerning the problems under consideration depends, to a large extent, on stratification resolution attained in the examined sections and on accuracy in determination of stratigraphic position of foraminiferal assemblages. Unfortunately, a number of sections, which would comply with these requirements and which we consider as reference sections, is limited, and this compels us to analyze other sections rich in foraminifers, but poorly characterized by conodonts and ammonoids. Correlation of such sections with the reference ones is often ambiguous. Nevertheless, stratigraphic levels we are interested in, such as the Middle–Upper Permian and Permian–Triassic boundaries, are sufficiently distinct in them, and we believe that changes in fossil foraminiferal assemblages across these boundaries are close to the true ones.

STRATIGRAPHY OF THE PERMIAN–TRIASSIC BOUNDARY SEQUENCES

Before going to an essence of the considered problem, we should define a stratigraphic scheme, which will serve as the basis for our interpretations. This is necessary because there is no unified view on the position and definition criteria of the Permian–Triassic boundary. In addition, existing opinions on stage subdivisions and biozonation of boundary strata and on their correlation are also controversial. Relationships between zonations based on different faunal groups, such as fusulinids, conodonts, and ammonoids, are not always interpreted unambiguously.

Inasmuch as thorough consideration of all these problems is beyond the scope of our work, we will just outline and specify variants of our decision.

The Permian–Triassic boundary is accepted to correspond to the base of the *Hindeodus parvus* Zone in line with latest recommendations of the International Working Group on the Permian–Triassic boundary (Yin, 1997). This boundary is of a highest correlation potential, which makes it preferable. However, it is not an event-based boundary. Main events, which are believed to mark the Paleozoic–Mesozoic boundary (regression, facies changes, mass extinctions, geochemical anomalies, and others) occurred slightly earlier and were not synchronous (Wang, 1997).

In line with recommendations of the International Subcommission on the Permian System (SCPS) approved by the International Geological Congress in Beijing in 1997 (Jin *et al.*, 1997), we accept the three-member division of the Permian System, according to which the Lopingian Series is divided into the Wuchiapingian and Changhsingian stages. As for the middle, Guadalupian Series, the SCPS variant of its subdivision into the Roadian, Wordian, and Capitanian stages is unambiguously appropriate only for the North American sequences. Inasmuch as all sections we would like to consider here are located within the Tethyan realm, we prefer to operate thus far with the Kubergandian, Murgabian, and Midian stages of the Mediterranean scale (Leven, 1980, 1981) for the middle series, the more so as the upper boundary of the Midian Stage coincides with the Guadalupian–Lopingian boundary recommended by the SCPS.

Having no universally accepted zonal subdivisions for stages of the upper Permian Series, we take for the basis the conodont zonation proposed by Jin *et al.* (1997). In addition, we refer to cephalopod zones defined in the Transcaucasian and South China sections (Ruzhentsev and Sarycheva, 1965, Yin *et al.*, 1996). To correlate the Permian–Triassic boundary sequences, we use the conodont zones established in the Meishan section of South China (Zhang *et al.*, 1996; Yin *et al.*, 1996). It should be noted however that opinions about paleontological substantiation of these units and their age interpretation are controversial (Mei, 1996). The zonal scheme proposed by Matsuda (1985) was accepted for the Triassic.

Different viewpoints on classification of conodonts and relatively limited number of sections, where their stratigraphic successions are continuous, restrict the correlation accuracy even in case of reference sections. Only several levels can be traced, more or less certainly, in most reference and some supplementary sections. Among these is the boundary between Midian and Wuchiapingian stages placed at the base of the conodont *C. postbitteri* Zone. In the Transcaucasian region, this level corresponds to the base of the Chankhchi or *Codonofusiella–Reichelina* Beds (Reitlinger, 1965; Kotlyar *et al.*, 1989). In the Abadeh section, the considered level coincides with the lower boundary of Bed 5 (*Iranian–Japanese...*, 1981), and in sections of South China, it corresponds to the boundary separating the Maokou and Loping groups (Jin *et al.*, 1994). The next level is the lower boundary of the conodont *C. leveni* Zone, which is defined at the base of the Akhura Formation of the Transcaucasian region (Kozur *et al.*, 1978), in the upper part of Bed 6 of the Abadeh section (*Iranian–Japanese...*, 1981), and inside the Wuchiaping Formation of South China (Jin *et al.*, 1994). Well traceable is also the Wuchiapingian–Changhsingian boundary or the base of the conodont *C. subcarinata* Zone recognizable in Transcaucasian and South China sections (Kozur *et al.*, 1978); Jin *et al.*, 1994). The high correlation potential is characteristic of lower boundaries of the *H. parvus* and *I. isarcica* conodont zones distinguished in section of the Transcaucasian region, Central Iran, Southern Alps, Kashmir, South China, and Tibet (Kozur, 1980; Kozur *et al.*, 1995). As for easily correlative levels in higher parts of the Lower Triassic succession, which yield foraminifers (usually assemblages of the *Meandrospira pusilla* Zone), these are *Parachirognathus turnishies* (=*Neospathodus waageni*) and *Neospathodus triangularis–Neospathodus homeri* conodont zones established in the Guchevo section of Inner Dinarides (Sudar, 1986). It is thought that stratigraphic position of the *Meandrospira pusilla* and *Meandrospira cheni* foraminiferal zones in the biostratigraphic scheme of Balkan Mts. is substantiated by finds of the ammonoid species *Tirolites* sp. (Salaj *et al.*, 1988).

FORAMINIFERS FROM THE PERMIAN–TRASSIC BOUNDARY LAYERS IN BEST-STUDIED AND WELL-DATED SECTIONS

In our opinion, the Dzulfa section of the Transcaucasian region (Leven, 1975, Kozur *et al.*, 1978; Kotlyar *et al.*, 1989; Zakharov, 1988), Abadeh section of Central Iran (*Iranian–Japanese...*, 1981, and Meishan section of South China (Yin *et al.*, 1996) are most important among the well-dated Permian–Triassic boundary successions. Owing to occurrence of conodonts and ammonoids, the Permian part of these sections is subdivided into easily correlative zones. We regard data on these sections as reference ones for solving problems of stratigraphic ranges of Permian foraminifers. Supplementary materials are from sections of the Salt Range (*Pakistan–Japanese...*, 1985; Wardlaw and Pogue, 1995), Alps (Broglio-Loriga *et al.*, 1986; Buggish and Noe, 1986), Taurus (Lys and Marcoux, 1978; Zaninetti and Dager, 1978; Zaninetti *et al.*, 1981; Altiner, 1981, 1984; Köyüglu and Altiner, 1989), northern Caucasus (K. Miklukho-Maclay, 1954; Kotlyar *et al.*, 1983, 1989), southeastern Pamirs (Leven, 1967; Kotlyar *et al.*, 1983, 1989), and Primor'e (Burago *et al.*, 1974; Sosnina and Nikitina, 1977; Kotlyar *et al.*, 1983, 1989; Vuks and Chediya, 1986). These materials were used with the accuracy required for their correlation with reference successions. When possible, data on other

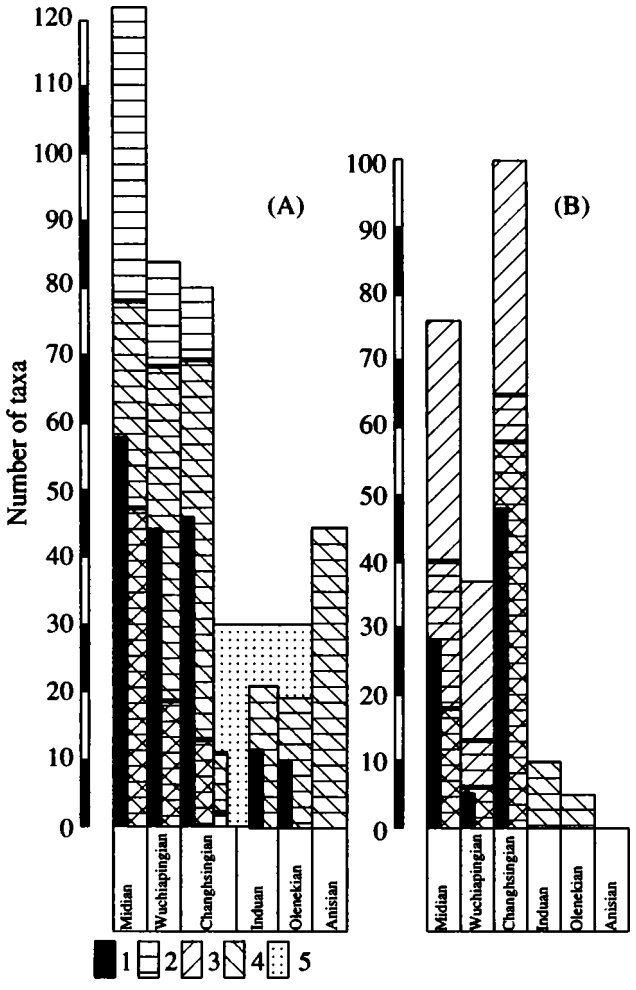

Changes of the Permian–Triassic boundary time in abundance of foraminiferal taxa by the end of each age (A) and percentage of extinct taxa by this moment (B): (1) families; (2) all foraminifers; (3) fusulinids; (4) smaller foraminifers; (5) genera of smaller foraminifers that became extinct at the Permian–Triassic boundary and appeared again (Lazarus-taxa).

Tethyan and North American sections were also considered.

Because of the rare occurrence of Triassic (particularly Lower Triassic) foraminifers, it is difficult to characterize adequately the taxonomic composition and stratigraphic distribution of their assemblages considering only the above-mentioned sections. Therefore, some other sections, where stratigraphic position of foraminiferal assemblages is sufficiently well substantiated, were involved into the analysis. Such sections are known in the following areas: Kuh-e-Ali-Bashi in northwestern Iran (Baud *et al.*, 1974), central and eastern Alborz localities (Brönnimann *et al.*, 1972a, 1972b; Stampfli *et al.*, 1976), Tabas (Brönnimann *et al.*, 1973), eastern Taurus (Dagger and Zaninetti, 1976; Altiner and Zaninetti, 1981), Inner Dinarides (Sudar, 1986), Southern Alps (Jenny-Deshuesses, 1991), Carpathians (Salaj and Borza, 1983), South China (He, 1988; Zhang *et al.*, 1989), northern Caucasus and Ciscaucasia (Efimova, 1974). Generalized data on foraminifers from some of the mentioned sections can be found in the monograph by Zaninetti (1976).

It is reasonable to consider distribution of fusulinid and smaller foraminifer assemblages separately.

Fusulinids. Beginning from the Middle Carboniferous to the terminal Middle Permian, fusulinids were one of the most abundant and diverse groups of benthic organisms populating warm seas. In the Permian, their peak diversity and specialization were in the Midian Age, probably in response to the world-wide transgression (Leven, 1993). The number of families and genera amounted to 20 and 46, respectively, at that time. Prevalent were representatives of orders Schwagerinida and Neoschwagerinida.

By the end of the Midian Age, both these orders became extinct. Significant changes occurred also in the order Schubertellina. For instance, the previously abundant family Yanchienidae completely disappeared, whereas the family Paleofusulinidae experienced essential renewal owing to appearance of its new genera *Ogbinella, Paradunbarula, Pseudodunbarula,* and *Paleofusulina* appeared. They all appeared immediately after extinction of last schwagerinids and neoschwagerinids in the lower part of the Wuchiapingian Stage of South China and in the correlative Chankhchi beds of the Transcaucasian region. Until recently, it was believed that the genus *Paleofusulina* appeared later. A few years ago however, it was found in the lower zone of the Wuchiapingian Stage of China (Zhu, 1996). Two new genera of the Boultoniidae family (*Gallowaiinella, Tewoella*), which were previously considered as occurring in the Changhsingian Stage, also appeared at this level. Nothing substantial happened at this level in the relatively scarce orders Ozawainellida and Staffellida.

The above distribution patterns characterizing the reference sections are also typical of many Tethyan successions, although synchronism of events that are recorded at the Midian–Wuchiapingian boundary cannot be always reliably proved. In addition, we do not exclude that some of typical Midian genera characteristic of the *Lepidolina kumaensis* Zone continue to occur in the Wuchiapingian Stage (Toriyama, 1973). No clear evidence is available so far.

Quantitative changes in fusulinid assemblages at the Midian–Wuchiapingian boundary can be exemplified by the following facts (Figure). Of 20 families and 46 genera of Midian fusulinids, 14 families (70%) and 35 genera (76%) became extinct at this level. Seven of 11 remained genera pass into the Changhsingian Stage. The Wuchiapingian Age was marked by appearance of 8 genera, 5 of which continued to exist in the Changhsingian Age. In fact, the Changhsingian Age was a time of gradual extinction of earlier genera. The only genus *Parananlingella* is unknown from older layers,

but it is not inconceivable that even this genus appeared in the Wuchiapingian Age.

In total, 5 families and 13 genera are registered in the Changhsingian Stage. By the beginning of the Triassic, all of them disappeared. This happened slightly prior to the first occurrence of *Hindeodus parvus*, and this event is believed to mark the Permian–Triassic boundary. In the Meishan section, that is recommended to represent the stratotype boundary succession, last fusulinids are recorded in Bed 20 of the scheme by Zhao *et al.* (1981), which is correlative to Beds 23 and 24 of the scheme by Yin *et al.* (1996). A slightly higher level of last fusulinid occurrence is established in the succession of the Dolomitic Alps where the basal part (1.5–2.0 m) of the Tesero Horizon of the Werfen Formation contains *Nankinella* and *Staffella* forms (Broglio-Loriga *et al.*, 1986). Passini (1984) mentioned also a find of *Paleofusulina* specimens in this section, although the validity of their stratigraphic position is doubtful. Conodont species *Hindeodus latidentatus* ancestral to *H. parvus* is also registered at the considered level. In the Meishan section, this species appears in white clays of Bed 25 (Kozur, 1995; Yin *et al.*, 1996) lacking fusulinids.

According to dynamics of changes in fusulinid assemblages during the period from the Midian to the Changhsingian Age, the two crises in fusulinid evolution are usually recognized (Jin, 1993; Stanley and Yang, 1994). The first one most distinct occurred at the Midian–Wuchiapingian boundary time, when 76% of fusulinid genera, 70% of their families, and all representatives of the Schwagerinida and Neoschwagerinida orders became extinct. The second crisis terminated with the complete disappearance of fusulinids at the end of the Changhsingian Age. Beside the appearance of several genera in the Wuchiapingian Age and one genus in the Changhsingian Age, nothing else significant happened with composition of fusulinid assemblages between these two crises. In fact, there was a belief that the Changhsingian transgression resulted in a significant renewal of foraminiferal assemblages, namely in appearance and flourish of the *Paleofusulina* genus in association with close *Nanlingella* and *Parananligella* genera, and one more genus *Gallowainella*. However, three of these genera were found in the Wuchiapingian Stage, as is mentioned above, and the idea of the Changhsingian renewal lost its validity. In addition, the increased abundance and diversity of Changhsingian fusulinids is recorded only in South China and Indochina sections. In all other Tethyan regions, this event is undetectable.

Smaller foraminifers. Similarly to fusulinids, the peak diversity of smaller foraminifers was in the Midian Age. We know 38 families and 78 genera of that age. Dominant were representatives of orders Nodosariida and Cornuspirida. According to G.P. Pronina who studied in detail foraminifers from Transcaucasian sections, species of the first order prevail in the lower part of the stage and representatives of the second order in its upper part (Kotlyar *et al.*, 1989). In her opinion, these distribution patterns are also characteristic of all sections outside the Transcaucasian region (Pronina, 1995). Most common amid nodosariids are representatives of genera *Pachyphloia, Geinitzina, Pseudolangella*, and some others. Families Hemigordiidae and Hemigordiopsidae are most abundant and characteristic representatives of cornuspirids. Sufficiently diverse is the order Palaeotextulariida, particularly its families Palaeotextulariidae (genera *Palaeotextularia, Climacammina, Cribrogenerina*), Biserimminidae (genus *Globivalvulina*), and Dagmaritidae (genus *Dagmarita*). Characteristic, though supplementary, are genera *Sphairionia* (family Lagenidae), *Abadehella* and *Neoendothyra* (families Valvulinellidae and Endothyranopsidae, respectively).

In contrast to fusulinid case, the Guadalupian–Lopingian boundary in successions of smaller foraminifers is less distinct, marked mostly by changes in dominant taxons. Many Midian genera passed into the Wuchiapingian Stage, and their total number in that stage of reference sections is as high as 48. When the data on smaller foraminifers from the Pamirs, Salt Range, Taurus, and Alps are taken into consideration in addition to those from reference sections, the total number of their Wuchiapingian genera would be close to 68, i.e., they became by 14% less diverse than Midian genera (76% in the fusulinids case). Moreover, only several genera can be considered extinct at the end of the Midian Age. These are genera *Shanita, Sphairionia*, and others characteristic of the Midian Stage. The Wuchiapingian Age was probably marked by an appearance of several new genera, among which *Louisettita, Paradagmarita, Pseudocolaniella*, and *Colaniella* can be mentioned. In general, the main difference between the Midian and Wuchiapingian foraminiferal assemblages is that the dominant taxons changed, since the abundance and diversity of genera belonging to families Hemidordiidae, Hemigordiopsidae, and Baisalidae (order Cornuspirida) decreased, and the leading role of nodosariids was restored to be high until the end of the Permian.

We should emphasize that the above characteristic of foraminiferal assemblages of the Wuchiapingian Stage is averaged. It varies in concrete sections depending on facies enclosing the assemblages. This is also true for the outlined differences between foraminiferal assemblages of the Midian and Wuchiapingian stages. For instance, the depositional settings in many Tethyan areas considerably changed at the beginning of the Wuchiapingian Age, before which there was a regression and short-term break in sedimentation. Shallow-water carbonate facies favorable for benthos development were replaced by pelagic clayey and pelitomorphic limy facies. Correspondingly, abundance of planktonic and nektonic organisms increased in contrast to benthic forms, and this impoverished foraminiferal assemblages, which mostly consisted of benthic forms at that time. This is best manifested in South China sec-

tions, where differences between the Midian and Wuchiapingian foraminiferal assemblages are rather substantial. In Transcaucasian sections, the facies change is confined to the base of the *C. leveni* Zone that is slightly above the base of the Wuchiapingian Stage. Beginning from this level, foraminiferal assemblages are highly impoverished, which was noted earlier by Reitlinger (1965) and Pronina (Kotlyar *et al.*, 1983). Simultaneously, the Midian–Wuchiapingian boundary indistinct in lithological aspect is marked only by a change of some dominant taxons. It is noteworthy that schwagerinids and neoschwagerinids become extinct precisely at this boundary. Even lesser changes are observed in foraminiferal assemblages from the Taurus sections where facies did not change at least until the end of the Wuchiapingian Age.

Similarly to fusulinids, the Wuchiapingian and Changhsingian assemblages of smaller foraminifer are just slightly different in composition and diversity. Prevalent in them are nodosariids, and almost all genera known from the Wuchiapingian Stage continue to occur in overlying beds. The only genus *Meandrospira* (family Meandrospiridae), very characteristic of foraminiferal assemblages from the upper part of the Induan Stage and existing now, appeared at that time. The total number of genera discovered in reference sections is 49 (48 genera occur in the Wuchiapingian Stage). When data on other sections (North Caucasus, Pamirs, Primor'e, Taurus, Southern Alps) are taken into consideration, the number of genera increases to 69 (68 Wuchiapingian genera therewith).

Keeping in mind the problem we deal with, it is interesting to reconstruct dynamics of changes in foraminiferal assemblages throughout the entire Changhsingian Age. In every particular section, their diversity depends on rock facies and significantly varies up to the complete disappearance of foraminifers. The Meishan section more or less uniform in lithology shows the gradual increase of foraminiferal diversity from 6 genera and 9 species at the base of the stage to 20 genera and 52 species at its top (Zhao *et al.*, 1981). The diversity increases also in the Transcaucasia and Southern Alps, where this is related, however, to the lack of favorable facies in the lower part of the stage.

In all studied sections, foraminifers completely disappear near the Permian–Triassic boundary, but this event was diachronous. Leaving aside those sections where the Permian–Triassic boundary cannot be confidently recognized because of probable hiatuses or data deficiency (North Caucasus, Primor'e, Taurus, Central Iran, Salt Range, and some others), we can establish precisely the level of foraminifer extinction only in three regions: the Transcaucasia, South China (Meishan), and Southern Alps.

In the Transcaucasian region, foraminifers are recorded in the *Paratirolites kittli* Zone, where they are represented by 19 genera and 37 species (Pronina, 1989). The overlying layers are completely barren of foraminifers. In the Meishan section, foraminifers occur in the uppermost part of the *Pleuronodoceras–Rotodiscoceras* Zone, where 20 foraminiferal genera and 52 species are registered near the top of the Changshing Limestones (Zhao *et al.*). As was mentioned, the uppermost layers of the Bellerophon Formation in Southern Alps correspond to the same zone. These layers enclose 33 genera and 43 species of smaller foraminifers (Broglio-Loriga *et al.*, 1986; Buggish and Noe, 1986).

The diversity of foraminiferal assemblage in overlaying strata of both the Meishan and South Alpine sections is sharply reduced. In the first locality, single representatives of nine genera belonging to seven families are registered in white clays of Bed 25, i.e., several centimeters below the Permian–Triassic boundary (Yin *et al.*, 1996; Zhao *et al.*, 1981). These several centimeters of the section (Beds 26, 27a, and 27b) are barren of foraminifers like the basal layers of the Triassic. In Southern Alps, the basal part of the Tesero Horizon of oolitic limestone is correlative with Bed 25 of the Meishan section, as it yields *H. latidentatus*, the conodont species ancestral to *H. parvus* (Broglio-Loriga *et al.*, 1986). Similarly to Bed 25, these layers also yield occasional smaller foraminifers of 20 species belonging to 12 genera (Broglio-Loriga *et al.*, 1986; Buggish and Noe, 1986). The upper part of the horizon is barren of foraminifers like the basal part of the overlying Masin Formation below the *H. parvus* Beds.

Foraminifers are unknown so far in the basal Triassic *H. parvus* Zone of either studied sections. They appear again in the *I. isarcica* Zone (Himalayas, northwestern Iran, Eastern Taurus). Their finds are scarce and represented by archaic primitive genera belonging to families Ammodiscidae and Earlnadiidae. Occasionally occurring are the Nodosariidae, Ichthyolariidae, and Cornuspiridae forms whose first representatives appeared in the Permian. In total, 11 genera and slightly more species are discovered at this level in different localities (Altiner *et al.*, 1980; Altiner, 1981; Altiner and Zaninetti, 1981; Kapoor, 1996). The foraminifer-bearing *Otoceras–Ophiceras* Beds from the base of the Kumoan section in Himalayas are probably coeval with the *I. isarcica* Zone (Kristan-Tollman, 1984). If this is true, the foraminiferal list from this zone should include 20 genera.

In the uppermost layers of the Induan Stage and in basal layers of the Olenekian Stage, foraminifers are significantly more abundant. Like in underlying deposits, these boundary interval yields the foraminiferal assemblage dominated by Paleozoic genera belonging mainly to the Ammodiscidae and Nodosariidae families. They are accompanied by first representatives of Mesozoic foraminiferal genera *Arenovidalina, Rectoglomospira, Lenticulina, Gaudryina*, and *Triadodiscus* belonging to four families, one of which (Involutinidae) is newly-appeared (Efimova, 1974; Gazdzicki, 1974; Sudar, 1986; Salaj *et al.*, 1988). Single representatives

of the *Meandrospira* genus registered in the uppermost Permian also appeared approximately at the same level. Slightly higher in the sections (*Parachirognathus turnishies* and *Neospathodus triangularis–N. homeri* conodont zones), they are more frequent and characterize the *M. pusilla* Zone traceable from the Alps in the west to South China in the east. The average diversity remains the same as in the earlier assemblage (18–20 genera), but the number of Mesozoic genera slightly increases. The substantial renewal of foraminiferal assemblages begins from the Anisian Age (the conodont *Neogondolella regale* Zone), being remarkable in its middle part (the conodont *Paragondolella bulgarica* Zone and ammonoid *Balatonites* Beds), where over 10 new genera and 5 families appear almost simultaneously. The total number of genera amounts here to 45 (Gaetani *et al.*, 1970; Efimova, 1974; Gazdzicki, 1974, 1983; Salaj *et al.*, 1983; Sudar, 1986). Thus, since that time, elements of Mesozoic assemblages become dominant.

Summing up the data on development of smaller foraminifers during the Late Permian–Early Triassic, we can state the following:

(1) The maximum diversity of foraminiferal assemblages was characteristic of the terminal Midian Age, when representatives of the Cornuspirida order were prevalent.

(2) At the Midian–Wuchiapingian boundary, the Nodosariida order becomes dominant. The generic and species composition of foraminiferal assemblages becomes impoverished, but less noticeably than that of fusulinids.

(3) Similarly to fusulinids, foraminiferal assemblages did not substantially change during the Wuchiapingian and Changhsingian ages and retained the same generic composition.

(4) The diversity of foraminiferal assemblages became sharply reduced at the base of the *H. latidentatus* Zone or slightly earlier, simultaneously with the sharp and universal facies change.

(5) The Permian–Triassic boundary layers are barren of foraminifers, and all the sections are characterized by this foraminifer-free interval. They appear again in the *I. isarcica* Zone being represented by scarce, mainly archaic forms known since the Paleozoic (Lazarus-taxa). Near the Permian–Triassic boundary, 40 genera (58%) and 17 families (43%) become extinct. This boundary is crossed by 29 genera, 20 of which are recorded in the Induan Stage, whereas other genera appear higher in the section.

(6) New foraminiferal genera and families typical of the Mesozoic time appear in the uppermost layers of the Induan Stage and become prevalent in assemblages only in the Anisian Stage.

CONCLUSIONS

The analysis of considered materials clearly indicates that the Permian–Triassic boundary marks a crisis in development of foraminifers, as well as in evolution of other sea dwellers of that time. The available data suggest that the terminal Permian extinction marks the crisis peak, first distinct signs of which are seen as early as at the Guadalupian–Lopingian boundary time. Correspondingly, two phases, *initial* and *terminal*, can be distinguished in the Late Permian foraminiferal crisis. The first of them decreased diversity of smaller foraminifers and resulted in extinction of schwagerinids and neoschwagerinids. The next one was responsible for complete disappearance of all fusulinids and smaller foraminifers, but the latter, dissimilarly to fusulinids, recovered after a short-term period. A similar conclusion is inferable from distribution patterns of many other fossil groups (Jin *et al.*, 1994; Stanley and Yang, 1994).

When trying to understand causes of the Permian extinction, one should pay attention to the fact that both the initial and terminal phases of the crisis were preceded by the extensive Midian and Changhsingian transgressions. This fact was noted first by Kauffman (1986), when he analyzed peculiarities of Late Cretaceous extinction. He considered it important, believing that extensive transgressions are responsible for rising and leveling of water temperature and increase diversity of stenothermal organisms. As a result, the system appears to be "prepared for the death" that happens by sudden environmental changes. This conclusion is also true for the first phase of the Late Permian extinction. Indeed, foraminifers are most diverse in the Midian sediments. The Midian–Wuchiapingian boundary is marked by sharp environmental changes. In the Lopingian, environments substantially differed from those of the preceding transgression period. The post-Midian regression resulted in expansion of land areas and in appearance of more or less isolated basins, which accumulated mainly clayey and micritic limy sediments. The extremely low admixture of the terrigenous component in the sediments indicates peneplanation of land topography, which, in turn, suggests a calm tectonic regime that prevailed uniformly after the epoch of active Hercynian orogeny. Such a rapid paleogeographic transformation should influence the climate, chemistry of seawater, and other environmental factors, which undoubtedly also changed, although the type and degree of these changes are to be clarified. The unique character of the considered time in the geological history is also evident from a rapid decrease of oxygen content in the atmosphere, which dropped, by the beginning of the Triassic, down to the value lowest for the entire Phanerozoic history (Budyko *et al.*, 1985). This was probably responsible for the onset of anoxic conditions in the World Ocean (Isozaki, 1997). All this was sufficient for destabilization and destruction of ecosystems that formed during the Midian transgres-

sion. Only groups of organisms highly resistant to the ecological stress continued to exist. Smaller foraminifers represented such a relatively eurybiontic group. To the contrary, fusulinids, particularly the larger and highly specialized schwagerinids and neoschwagerinids, became mostly extinct.

Thus, the initiation of the Late Permian extinction was most likely caused by many factors, most important of which was probably the post-Midian regression that triggered all subsequent environmental reorganizations.

This is less apparent when only the terminal phase of extinction coinciding with the Permian–Triassic boundary is considered. This boundary is marked, in addition to paleontological data, by the absolute minimum of the organic carbon content in sediments (Baud *et al.*, 1989). As compared with the post-Midian event, the terminal Permian extinction is much more prominent. Fusulinids become completely extinct. Smaller foraminifers also disappear, although for a short-term period. Recovering, they are initially scarce and dwarfish. Their diversity was more or less restored only in the Middle Triassic. Of interest is the fact that similar distribution patterns are characteristic of radiolarians—an absolutely different group of microorganisms with planktonic way of living in contrast to Paleozoic benthic foraminifers (Kukawa, 1996; Isozaki, 1997). The fact that disappearance of foraminifers and radiolarians was concurrent to the global ceasing of coal accumulation owing to extinction of turf-forming plants (Retallack *et al.*, 1996) means that the terminal Permian crisis was universal and affected both the marine and terrestrial biota. Such a conclusion suggests that factors responsible for this crisis were also more universal than local transgressions and regressions with all their consequences, and their impact was manifested all over the planet (Jin *et al.*, 1994; Hallam, 1994). Inasmuch as biotic reorganizations at the Permian–Triassic boundary happened suddenly, in a catastrophic manner, geological events responsible for destructive effects in the entire biosphere should be equally tremendous. Most probable of them was a catastrophic greenhouse effect related to the outburst of volcanic activity or to an extraordinary meteorite impact (Budyko, 1980; Budyko *et al.*, 1986; Alvarez *et al.*, 1982; Renne and Basu, 1991; Renne *et al.*, 1995; Campbell *et al.*, 1992; Kozur, 1994). The destructive effect of possible catastrophe could be aggravated by the stress state of biota in response to the post-Midian extinction and oxygen deficiency.

Reviewers G.V. Kotlyar and K.I. Kuznetsova

REFERENCES

Altiner, D., Recherches stratigraphiques et micropaleontologiques dans le Taurus Oriental au NW de Pinarbashi (Turquie), Thése no. 2005, Université de Geneve, 1981.

Altiner, D., Upper Permian Foraminiferal Biostratigraphy in Some Localities of the Taurus Belt. Geology of the Taurus Belt, *Intern. Symp. September 26-29, 1983, Ankara, Turkey*, Tekeli, O. and Güncoglu, C., Eds., Ankara: MTA, 1984, pp. 255–268.

Altiner, D., Baud, A., Guex, J., and Stampfli, G., La limite Permien-Trias dans quelques localities du Mouen-Orient: recherches stratigraphiques et micropaleontologiques, *Riv. Ital. Paleont.*, 1980, vol. 85, nos. 3–4, pp. 683–714.

Altiner, D. and Zaninetti, L., Le Trias dans la region de Pinarbasi, Taurus oriental, Turquie: unites litologiques, micropaleontologie, mileux de depot, *Riv. Ital. Paleont.*, 1981, vol. 86, no. 4, pp. 705–760.

Alvarez, L.W., Alvarez, W., Asaro, F., and Michel, H., Current Status of the Impact Theory for the Terminal Cretaceous Extinction, *Spec. Pap. Geol. Soc. Am.*, 1982, vol. 190, pp. 305–315.

Baud, A., Brönnimann, P., and Zaninetti, L., Sur la présence de *Meandrospira pusilla* (Ho) (Foraminifére) dans le Trias inférieur de Kuh-e-Ali Bashi, Julfa, N-W Iran, *Paléont. Zeitschrift*, 1974, vol. 48, no. 3/4, pp. 205–213.

Baud, A., Magaritz, M., and Holser, W. T., Permian-Triassic of the Tethys: Carbon Isotope Studies, *Geol. Rundschau*, 1989, vol. 78, no. 2, pp. 649–677.

Broglio-Loriga, C., Neri, C., Pasini, M., and Posenato, R., Marine Fossil Assemblages from Upper Permian to Lowermost Triassic in the Western Dolomites (Italy), *Mem. Soc. Geol. Ital.*, 1986, vol. 34, pp. 5–44.

Brönnimann, P., Zaninetti, L., and Bozorgnia, F., Triassic (Scythian) smaller Foraminifera from the Elika Formation of the central Albourz, northern Iran, and from the Siusi Formation of the Dolomites, Northern Italy, *Mitt. Ges. Geol. Bergbaustud.*, 1972a, vol. 21, pp. 861–884.

Brönnimann, P., Zaninetti, L., Bozorgnia, F., and Huber, H., *Ammodiscus* and *Ptychocladiis* (Foraminifera) from the Triassic Elika Formation, Nessa-Hassakdar Section, Central Albourz, Iran, *Riv. Ital. Paleont. Strat.*, 1972b, vol. 78, no. 1, pp. 1–28.

Brönnimann, P., Zaninetti, L., Moshtaghian, A., and Huber, H., Foraminifera from the Sorkh Shale formation of the Tabas Area, Eastern-Central Iran, *Riv. Ital. Paleont.*, 1973, vol. 79, no. 1, pp. 1–32.

Budyko, M.I., *Klimat v proshlom i budushchem* (Climate of the Past and Future), Leningrad: Gidrometeoizdat, 1980.

Budyko, M.I., Golitsyn, G.S., and Izrael', Yu.A., *Global'nye klimaticheskie katastrofy* (Global Climatic Catastrophes), Leningrad: Gidrometeoizdat, 1986.

Budyko, M.I., Ronov, A.B., and Yanshin, A.L., *Istoriya atmosphery* (The History of Atmosphere), Leningrad: Gidrometeoizdat, 1985.

Buggisch, W. and Noé, S., Upper Permian and Permian–Triassic Boundary of the Carnia (Bellerophon Formation, Tesero Horizon, Northern Italy), *Mem. Soc. Geol. Ital.*, 1986, vol. 34, pp. 91–106.

Burago, V.I., Kiseleva, A.V., Kotlyar, G.V., *et al.*, Paleontological Characteristic of Permian Sequences in Southern Primor'e, *Paleozoi Dal'nego Vostoka* (The Paleozoic of the Far East), Khabarovsk: DVNTS AN SSSR, 1974, pp. 214–235.

Campbell, I.H., Czamanske, G.K., Fedorenko, V.A., *et al.*, Synchronism of the Siberian Traps and the Permian-Triassic boundary, *Science*, 1992, vol. 258, pp. 1760–1763.

Dagger, Z. and Zaninetti, L., Sur quelques Foraminiferes du Trias inferieur Taurus oriental, Turque, *C. R. Seances, SPHN Geneve, NS.*, 1976, vol. 10, nos. 2–3, pp. 133–137.

Efimova, N.A., Triassic Foraminifers from Northwestern Caucasus and Ciscaucasia, *Vopr. Mikropaleontol.*, 1974, vyp. 17, pp. 54–83.

Gaetani, M. and Gorza, M., The Anisian (Middle Triassic) Carbonate Bank of Camorelli (Lombardy, Southern Alps), *Facies*, 1989, vol. 21, pp. 41–56.

Gaetani, M., Premoli Silva, I., and Zanin Buri, C., Calcare di Dosso dei Morti, *Studi illustr. Carta geol. Italia. Formaz. geol.*, 1970, Fasc. 4, pp. 21–32.

Gazdzicki, A., Rhaetian Microfacies, Stratigraphy and Facial Development in the Tatra Mountains, *Acta Geol. Polon.*, 1974, vol. 24, no. 1, pp. 17–96.

Gazdzicki, A., Foraminifers and Biostratigraphy of the Upper Triassic and Lower Jurassic of the Slovakian and Polish Carpathians, *Paleontol. Polon.*, 1983, no. 44, pp. 109–169.

Hallam, A., The Earliest Triassic as an Anoxic Event, and Its Relationship to the End-Paleozoic Mass Extinction, *Pangea: Global Environments and Resources. Can. Soc. Petrol. Geol.*, 1994, mem. 17, pp. 785–795.

He, Y., Early and Middle Triassic Foraminifera from Jiangsu and Anhui Provinces China, *Acta Micropal. Sinica*, 1988, vol. 5, no. 1, pp. 85–92.

Iranian–Japanese Research Group, *The Permian and the Lower Triassic Systems in Abadeh Region, Central Iran*, 1981, vol. 47, no. 2, pp. 1–133.

Isozaki, Y., Permo-Triassic Boundary Superanoxia and Stratified Superocean: Records from Lost Deep Sea, *Science*, 1997, vol. 276, pp. 235–238.

Jenny-Deshusses, C., The Permian-Triassic of the Gartenkofel-1 Core (Carnic Alps, Austria): Foraminifera and Algae of Core and the Outcrop Section, *Abb. Geol. B.-A.*, 1991, vol. 45, pp. 99–108.

Jin, Y., The Pre-Lopingian Benthos Crisis, *Compte Rendu XII ICCP. Buenos Aires*, 1993, no. 2, pp. 269–278.

Jin, Y., Global Chronostratigraphic Scheme for the Permian System, *Permophiles*, 1996, no. 28, pp. 4–9.

Jin, Y., Wardlaw, B.R., Glenister, B.F., and Kotlyar, G.V., Permian Chronostratigraphic Subdivisions, *Episodes*, 1997, vol. 20, no. 1, pp. 11–15.

Jin, Y., Zhu, Z., and Mei, S., The Maokouan-Lopingian Boundary Sequences in South China, *Paleoworld*, 1994, no. 4, pp. 138–152.

Kakuwa, Y., Permian–Triassic Mass Extinction Event Recorded in Bedded Chert Sequence in Southwest Japan, *Palaeogeogr., Palaeoclimatol., Palaeoecol.*, 1996, vol. 121, pp. 35–51.

Kapoor, H.M., The Guryul Ravine Section, Candidate of the Global Stratotype Section and Point of the Permo-Triassic Boundary, *The Paleozoic-Mesozoic Boundary-Candidates of the Global Stratotype Section and Point (GSSP) of the Permian-Triassic boundary*, Yin, H., Ed., 1996, pp. 99–110.

Kauffman, E.J., Structure of Extinctions of Cretaceous Marine Biotas, *Catastrophes and Earth History*, Berggren, W.A. and Van Couvering, J.A., Eds., Princeton Univ. Press, 1984.

Kotlyar, G.V., Zakharov, Yu.D., Kochirkevich, B.V., Kropacheva, G.S., Rostovtsev, K.O., Chediya, I.O., Vuks, G.P., and Guseva, E.A., *Pozdnepermskii etap evolyutsii organicgeskogo mira. Dzhul'finskii i dorashamskii yarusy SSSR* (Late Permian Stage of Organic World Evolution: The Dzhulfian and Dorashamian Stages of the USSR), Leningrad: Nauka, 1983.

Kotlyar, G.V., Zakharov, Yu.D., Kropacheva, G.S., Pronina, G.P., Chediya, I.O., and Burago, V.N., *Pozdnepermskii etap evolyutsii organicheskogo mira. Midiiskii yarus SSSR* (Late Permian Stage of Organic World Evolution: The Midian Stage of the USSR), Leningrad: Nauka, 1989.

Köylüoglu, M. and Altiner, D., Micropaleontologie (Foraminiferes et biostratigraphie du Permien Superieur de la region d' Hakkari (SE Turquie), *Revue de Paléobiologie*, 1989, vol. 8, no. 2, pp. 467–503.

Kozur, H.W., The Main Events in the Upper Permian and Triassic Conodont Evolution and Its Bearing to the Upper Permian and Triassic Stratigraphy, *Riv. Ital. Paleont. Strat.*, 1980, vol. 85, nos. 3–4, pp. 741–766.

Kozur, H.W., The Permian-Triassic Boundary and Possible Causes of Faunal Change Near the P/T Boundary, *Permophiles*, 1994, no. 24, pp. 51–54.

Kozur, H.W., Permian Conodont Zonation and Its Importance for the Permian Stratigraphic Standard Scale, *Geol. Paléont. Mitt. Innsbruck*, 1995, vol. 20, pp. 165–205.

Kozur, H., Leven, E.Ja., Lozovskii, V.R., and Pyatakova, M.V., Subdivision of the Permian–Triassic Boundary Layers in the Transcaucasian Region Based on Conodonts, *Byul. Mosk. O–va Ispyt. Prir., Otd. Geol.*, 1978, vol. 53, no. 3, pp. 15–24.

Kozur, H.W., Wang, Cheng-Yuan, and Zakharov, Yu.D., The Importance *Hindeodus parvus* (Conodonta) for the Definition of the Permian-Triassic Boundary and Evaluation of the Proposed Section for a Global Stratotype Section and Point (GSSP) for the Base of the Triassic, *Geologia*, 1994/1995, vols. 37/38, pp. 173–213.

Kristan-Tollmann, E., Trias-Foraminiferen von Kumaun im Himalaya, *Mitt. Sterr. Geol. Ges.*, 1984, vol. 77, pp. 263–329.

Leven, E.Ja., *Stratigrafiya i fuzulinidy permskikh otlozhenii Pamira* (Permian Stratigraphy and Fusulinids of Pamirs), Moscow: Nauka, 1967.

Leven, E.Ja., Permian Stratigraphy of the Transcaucasian Region, *Sov. Geol.*, 1975, no. 1, pp. 96–110.

Leven, E.Ja., *Ob'yasnitel'naya zapiska k stratigraficheskoi shkale permskikh otlozhenii oblasti Tetis* (Explanatory Notes to the Permian Stratigraphic Scale of the Tethys), Leningrad: VSEGEI, 1980.

Leven, E.Ja., Permian-Tethys Stage Scale and Correlation of Sections of the Mediterranean-Alpine Folded Belt, *IGCP Newsletter*, 1981, vol. 3, no. 5, pp. 100–112.

Leven, E.Ja., Main Events in Permian History of the Tethys and Fusulinids, *Stratigr. Geol. Korrelaytsiya*, 1993, vol. 1, no. 1, pp. 59–75.

Lys, M. and Marcoux, J., Les niveaux du Permien superieur des Nappes d'Antalya (Taurides occidentales, Turquie), *C. R. Acad. Sc.*, 1978, vol. 286, pp. 1417–1420.

Matsuda, T., Late Permian to Early Triassic Conodont Paleobiogeography in the "Tethys Realm", in *The Tethys*, Tokai University Press, 1985, pp. 157–170.

Mei, S., Restudy of Conodonts from the Permian-Triassic Boundary Beds at Selong and Meishan and the Natural Permian-Triassic Boundary, *Continental Memorial Volume of Prof. Sun Yunzhu: Paleontology and Stratigraphy*, Wang, H. and Wang, X., Eds., China University of Geosciences Press, 1996, pp. 141–148.

Miklukho-Maclay, K.V., *Foraminifery verkhnepermskikh otlozhenii Severnogo Kavkaza* (Upper Permian Foraminifers of the North Caucasus), Moscow: Gosgeoltekhizdat, 1954.

Pakistan-Japanese Research Group. Permian and Triassic Systems in the Salt Range, Pakistan, *The Tethys*, Tokai University Press, 1985, pp. 219–317.

Pasini, M., Biostratigrafia con i Foraminiferi del limite Formazione a Bellerophon/Formazione di Werfen fra Recoaro e la Val Badia (Alpi Meridionali), *Riv. Ital. Paleontol. Strat.*, 1984, vol. 90, no. 4, pp. 481–510.

Pronina, G.P., Foraminifers of the *Paratirolites kittli* Zone of the Upper Permian Dorashamian Stage of the Transcaucasian Region, *Ezheg. Vses. Paleontol. o-va*, 1989, vol. 32, pp. 30–41.

Pronina, G.P., Upper Permian Small Foraminifers Zonal Standard in the Tethyan Realm, in *Abstracts of XIII Intern. Congress on Carboniferous-Permian*, Krakow, 1995, p. 118.

Reitlinger, E.A., Foraminiferal Evolution during the Late Permian–Early Triassic in the Transcaucasian Region, *Vopr. Mikropaleontol.*, 1965, vyp. 9, pp. 45–70.

Renne, P.R. and Basu, A.R., Rapid Eruption of the Siberian Traps Flood Basalts at the Permo-Triassic Boundary, *Science*, 1991, vol. 253, pp. 176–179.

Renne, P.R., Zhang, Z., Richards, M.A., Black, M.T., and Basu, A.R., Synchrony and Causal Relations between Permian-Triassic Boundary Crises and Siberian Flood Volcanism, *Science*, 1995, vol. 269, pp. 1413–1416.

Retallack, G.J., Veevers, J.J., and Morante, J., Global Coal Gap between Permian-Triassic Extinction and Middle Triassic Recovery of Peat-forming Plants, *Bull. Geol. Soc. Amer.*, 1996, vol. 108, no. 2, pp. 195–207.

Ruzhentsev, V.E. and Sarycheva, T.G., *Razvitie i smena morskikh organizmov na rubezhe paleozoya i mezozoya* (Development and Change of Marine Organisms across the Paleozoic–Mesozoic Boundary), Moscow: Nauka, 1965.

Salaj, J., Borza, K., and Samuel, O., *Triassic Foraminifers of the West Carpathians, Geol. Ustav. Dioniza Stura*, Bratislava, 1983.

Salaj, J., Trifonova, E., Gheorghian, D., and Coroneou, V., The Triassic Foraminifera Microbiostratigraphy of the Carpatian-Balkan and Hellenic Realm, *Mineralia slov.*, 1988, vol. 20, no. 5, pp. 387–415.

Schindewolf, O.H., Über die Faunenwende vom Paläozoikum zum Mezozoikum, *Z. Deutsch. Geol. Ges.*, 1954, vol. 105, no. 2, pp. 153–182.

Sosnina, M.I. and Nikitina, A., Upper Permian Smaller Foraminifers of the Southern Primor'e Region, *Iskopaemaya flora i fauna Dal'nego Vostoka i voprosy stratigrafii fanerozoya* (Fossil Fauna and Flora of the Far East and Problems of Phanerozoic Stratigraphy), Vladivostok: DVNTS AN SSSR, 1977, pp. 27–52.

Spravochnik po sistematike melkikh foraminifer paleozoya (The Reference Book for Classification of Paleozoic Smaller Foraminifers), Moscow: Nauka, 1993.

Spravochnik po sistematike foraminifer paleozoya (The Reference Book for Classification of Paleozoic Foraminifers), Moscow: Nauka, 1996.

Stamfli, G., Zaninetti, L., Brönnimann, P., Jenny-Deshusses, C., and Stampfli-Vuille, B., Trias de l'Elbourz oriental, Iran. Stratigraphie, Sédimentologie, Micropaléontologie, *Riv. Ital. Paleont. Strat.*, 1976, vol. 82, no. 3, pp. 467–500.

Stanley, S.M. and Yang, X., A Double Mass Extinction at the End of the Paleozoic Era, *Science*, 1994, vol. 266, pp. 1340–1344.

Sudar, M., Microfossil i biostratigrafija triajasa unutrashn'ikh dinarida jygoslavije ezmezhu Gucheva i L'yulishn'e, *Geol. Anal. Balkan., Poluostr.*, 1986, vol. 50, pp. 151–394.

Toriyama, R., Upper Permian Fusulinian Zones, The Permian and Triassic System and Their Mutual Boundary, *Can. Soc. Petrol. Geol.*, 1973, mem. 2, pp. 498–512.

Vuks, G.P. and Chediya, I.O., Foraminifers from the Lyudyanzino Formation of the Neizvestnaya Bay (Southern Primor'e), *Korrelyatsiya permo–triasovykh otlozhenii vostoka SSSR* (Correlation of Permian–Triassic Sequences of the Eastern USSR), Vladivostok: DVNTS AN SSSR, 1986, pp. 82–106.

Wang, C.Y., Conodont Evolutionary Lineage and Zonation for the Latest Permian and the Earliest Triassic, *Permophiles*, 1997, no. 29, p. 37.

Wardlaw, B.R. and Pogue, K.R., The Permian of Pakistan, *The Permian of Northern Pangea. 2*, Berlin, 1995, pp. 215–224.

Yin, H., Permian-Triassic Boundary Working Group Newsletter? (3 September, 1996), *Permophiles*, 1997, no. 30, pp. 27–28.

Yin, H., Wu, S., and Ding, M., The Meishan Section, Candidate of the Global Stratotype Section and Point of Permian-Triassic Boundary, *The Paleozoic-Mesozoic Boundary-Candidates of the Global Stratotype Section and Point (GSSP) of the Permian-Triassic Boundary*, China University of Geosciences Press, 1996, pp. 31–48.

Yin, H., Zhang, K., Wu, S., and Peng, Y., Global Correlation and Definition of the Permian-Triassic Boundary, in *The Paleozoic-Mesozoic Boundary-Candidates of the Global Stratotype Section and Point (GSSP) of the Permian-Triassic Boundary*, China University of Geosciences Press, 1996, pp. 3–28.

Zakharov, Yu.D., Type and Hypotype of the Permian-Triassic Boundary, *Mem. Sos. Geol. Ital.*, 1988, vol. 34, pp. 277–289.

Zaninetti, L., Les Foraminiferes du Trias, *Riv Ital. Paleontol.*, 1976, vol. 82, no. 1.

Zaninetti, L., Altiner, D., and Çatal, E., Foraminiféres et biostratigraphie dans le Permien supérieur du Taurus oriental, Turquie, *Notes Lab. Pal. Univ. Genéve*, 1981, vol. 7, no. 1, pp. 1–37.

Zaninetti, L. and Dager, Z., Biostratigraphie integree et paleoecologie du Trias de la peninsule de Koçaeli (Turquie), *Eclog. Geol. Helv.*, 1978, vol. 71, no. 1, pp. 85–104.

Zhang, K., Ding, M., Lai, X., and Liu, J., Conodont Sequences of the Permian-Triassic Boundary Strata at Meishan Section, South China, *The Paleozoic-Mesozoic Boundary Candidates of Global Stratotype Section and Point (GSSP) of the Permian-Triassic Boundary*, China University of Geosciences Press, 1996, pp. 57–64.

Zhang, G., Zhu, J., Chou, F., Wang, G., and Zheng, J., Study of the Early and Middle Triassic Lower Jangtze Dsea Basin, *Acta Geol. Sinica*, 1989, vol. 63, no. 2, pp. 134–147.

Zhao, J.K., Sheng, J.C., Yao, Z.O., *et al.*, The Changxinian and Permian-Triassic Boundary of South China, *Bull. Nanjing Inst. Geol. and Paleontol. Acad. Sinica*, 1981, no. 2. pp. 1–95.

Zhu, Z.L., Discovery of Palaeofusulina Fauna in the Lower Part of the Heshan Formation (Early Wuchiapingian) in Laibin, Guangxi, China, *Permophiles*, 1996, no. 28, p. 15.

Stratigraphy and Geological Correlation, Vol. 9, No. 4, 2001, pp. 373–386. Translated from Stratigrafiya. Geologicheskaya Korrelyatsiya, Vol. 9, No. 4, 2001, pp. 65–79.
Original Russian Text Copyright © 2001 by Akhmet'ev, Aleksandrova, Beniamovskii, Vasil'eva, Zhelezko, Zaporozhets.
English Translation Copyright © 2001 by MAIK "Nauka/Interperiodica" (Russia).

The Lower Oligocene Kurgan Beds of West Siberian and Trans-Uralian Regions

M. A. Akhmet'ev*, G. N. Aleksandrova*, V. N. Beniamovskii*, O. N. Vasil'eva, V. I. Zhelezko**†, and N. I. Zaporozhets***

* *Geological Institute, Russian Academy of Sciences, Pyzhevskii per. 7, Moscow, 109017 Russia*
** *Institute of Geology and Geochemistry, Uralian Division of Russian Academy of Sciences, Pochtovyi per. 7, Yekaterinburg, 620151 Russia*

Received December 24, 1999

Abstract—Stratigraphic position and distribution of the lower Oligocene Kurgan Beds in southern West Siberia are considered. Their age is substantiated by the data on malacofauna, ichthyofauna, dinocysts, spores, and pollen. Two scenarios of their formation are probable. According to the first one, the Kurgan Beds were accumulated during the retreat of already brackish Tavda sea from the West Siberian plate in the Eocene–Oligocene boundary time. The second scenario, which seems more probable, especially for the southern areas of the West Siberian plate, supposes the repeated sea ingression from the western Turan plate via the Turgai depression in the early Oligocene (Ashcheairyk) time. Similarly to the sea expansion into the Middle Volga and Cis-Uralian areas along the older river system in the Akchagylian time (Pliocene), the Kurgan sea spread from the south to the north for more than 1000 km along the erosional Turgai depression and former Tobol valley with its tributaries. To the north and east of the town of Kurgan, seawaters penetrated into the Omsk syncline and negative landforms behind the Middle Urals. An extensive deposition of brown iron ores in the Turgai depression (the Lisakovsk basin with estimated reserves of two billion tons) is related to the Kurgan sea ingression. The iron ores were formed at the "geochemical barriers" in the mouths of rivers flowing into the sea strait. A high percentage of small pollen grains of *Quercus graciformis* and other thermophilic plants in the Kurgan Beds is likely a consequence of both the warm seawater ingression to the north and partial reworking of underlying Tavda sediments, where that pollen is dominant component of palynological spectra.

Key words: upper Eocene, lower Oligocene, Kurgan Beds, Tavda and Chegan formations, sea ingression, malacofauna, dinocysts, spores and pollen, Turgai depression, West Siberian plate.

INTRODUCTION

The West Siberian Kurgan Beds enclosing the Oligocene marine malacofauna of the Ashcheairyk type became again an object of intense study in view of elaboration of the Paleogene stratigraphic scheme for West Siberia. They are spread over the northern Turgai depression and its continuation, extending into the West Siberian plate up to the latitude of the town of Kurgan (Korobkov, 1966). A comprehensive analysis of these beds offers a chance to reconstruct the early Oligocene geological and paleogeographic events, which took place after the sea had completely retreated from the Turgai and West Siberia in the Chegan–Tavda time. In addition, the expected results can elucidate the transition from marine sedimentation to continental one complicated by the repeated sea invasion.

As an independent local unit, the Kurgan Beds were originally recognized by Panova (1970) who ranked them as a sequence. However, because of their insignificant thickness (usually not more than few meters), they were later ranked as beds (*Stratigraficheskii...*, 1982). The beds are distinguishable owing to their palynological assemblage that is transitional, connecting the upper marine horizons of the Tavda Beds with abundant pollen of thermophilic plants (*Quercus gracilis, Q. graciliformis, Nyssa crassa*, and others) and the lower Oligocene Atlym and Kurtamysh formations, in which pollen of conifers and moderately thermophilic plants prevails. General composition and dominants of the assemblage gradually change across the Kurgan Beds. Molluscan fauna identified in the beds by Korobkov, allowed Panova to argue for their marine origin and conformable, hiatus-free relationships with the underlying Chegan clays and overlying Atlym sands. When describing the Kurgan Beds for the first time, Panova (1970, p. 127) noted that they "are composed of green silty clay with interbeds and lenses of micaceous–quartz sands and ferruginous sandstones". She insisted on the northward distribution of the Kurgan Beds into the Turgai depression up to the lower coarse of the Ob' River (Martynov *et al.*, 1988). Her conclusion was based on the palynological assemblage of a "mixed type" and on occurrence of *Cyprina* forms at the Aleshkiny Yurty site (Nikolaev, 1947a, 1947b). However, her

† Deceased.

conclusion should be regarded with precaution, because Nikolaev's data suggest that above molluscan forms were found in association with radiolarians, sponge spicules, and selachian remains, and thus they could be derived from the older Paleogene clays of marine origin. Nikolaev did not reported about mollusks from the overlying strata attributed to the Aleshkiny Yurty Formation (*Stratigraficheskii...*, 1982) that was supposed to be grading upward into the Lagernyi Sad Formation bearing the late Oligocene flora and widespread near the Tomsk.

It should be mentioned that Dobrutskaya (1961), Drozhashchikh (1970), Kovalevskaya (1961), and other specialists also reported about mixed palynological assemblages in transitional beds between the Tavda (Chegan) Formation and continental Oligocene deposits of West Siberia and the Trans-Uralian region. The former two authors referred these beds to the Atlym Formation, whereas Kovalevskaya considered them analogs of the Chegan clays. Zakharov (1968) who studied the beds in central and western areas of the West Siberian plate regarded them as the Konolevo Member coeval to the Aleshkiny Yurty Formation (*Stratigraficheskii...*, 1982, p. 29). Depositional environments of the member were greatly variable in the lateral and vertical directions. Facies of meandering rivers grade into lacustrine ones. The largest lakes left after the sea retreat occupied the relief lows. The palynological assemblages of predominantly gray lacustrine sediments intercalated with rewashed green clays of the Tavda (Chegan) Formation do not seem to be identical in age with those of the Kurgan Beds, because the basal Oligocene strata are rich in reworked spores, pollen, and organic-walled phytoplankton derived from the underlying upper Eocene clays. Before the complete revision of materials from central and northern areas of West Siberia, the opinion that the terminal beds of the upper Eocene Tavda Formation are similar in age to the Kurgan Beds has rights to exist. If the so-called "transitional beds" in central areas could be really formed by the retreating Tavda sea, the Kurgan Beds in the type area clearly accumulated during the subsequent northward sea transgression from the Turgai depression to West Siberia. They accumulated in incision valleys of the destructed and partly weathered Tavda sea floor. Similar valleys incised into upper Eocene marine sediments and filled with basal Oligocene beds are also well known outside West Siberia, in the northern periphery of the regressed epicontinental sea (the Pasekovo valley of the Voronezh syneclise, incisions in the Chegan clays of the Aral area, where they are filled with cross-bedded silts of the lower Oligocene Kutan-Bulak Formation, and so on). The Kurgan molluscan assemblage has no species in common with the Tavda–Chegan assemblages. The compositional similarity between different-aged palynological assemblages from northern and southern areas of West Siberia can be reasoned in two ways: (1) there was distinct latitudinal zoning of vegetation cover by the time of late Eocene progressive cooling; (2) one may expect the mass redeposition of palynomorphs from underlying deposits. The latter chance is quite probable in our opinion.

In the early 1980s, the geological mapping of 1 : 200000 scale performed under the leadership of Yu.N. Gorbachev increased our knowledge on distribution of the Kurgan Beds in southern West Siberia. Gray but not green (Tavda) ferruginous sands with mollusks were discovered in several southern localities of the Kurgan area (Nizhnyaya Alabuga and Yurgamysh river valleys to the east of the Nizhnee Settlement and other sites). These sands were also recovered by drilling at the Miass River to the south of the Kargapol'e Settlement.

The Oligocene sea ingression expanded as well into the Omsk depression to the east of the Kurgan, as it is evident from drilling results near the Achair Settlement at the Irtysh River, 30 km to the southeast of Omsk (Borehole 011-BP). In the core samples from transitional beds between the Tavda and overlying Isil'kul' Formation (the age analog of the Kurtamysh and Atlym formations) and one meter above them, Kul'kova and Zaporozhets found diverse green algae, prasinophytes, and a dinocyst assemblage characteristic of the *Phthanoperidinium amoenum* Zone. The assemblage is similar in composition to that of the basal Oligocene beds of the Northern Caucasus, Ergeni, and Ustyurt localities. The corresponding interval of the lower part of the Maikop Group exposed at the Belaya River of the Northern Caucasus corresponds to the nannoplankton *Eriksonia subdisticha* Zone NP21 (Andreeva-Grigorovich, 1991; Zaporozhets, 1999). It is significant that the sandy-clayey member that terminates the section of the Tavda Formation near the town of Kurgan is missing from the section of Borehole 011-BP. The Kurgan Beds rest immediately on dark, greenish gray Tavda clays, which contain the abundant dinocysts characteristic of the upper Eocene *Charlesdowniea clathrata angulosa* Zone marking the peak of the late Tavda transgression.

The most abundant malacofauna confined to ferruginous sandstones was found in quarries near the eastern Kurgan suburbs and in outcrops at the Tobol River and its tributary Utyak River. In the geological survey report, a gradual transition from the Tavda Formation to the Kurgan Beds is suggested most likely in accord with tradition. The beds were regarded as sediments of the terminal phase of the Tavda sea regression from West Siberia that completely ceased in the early Oligocene time. The stratigraphic scheme for the Urals and Trans-Uralian region includes the Kurgan Beds as the lowermost Oligocene local unit of the East Urals and West Turgai subregions and assumes its conformable contact with the Tavda (Chegan) Formation. Only Korobkov (1966) considered the Kurgan Beds as basal marine facies of the Oligocene continental deposits

overlying the erosional surface of the Tavda Formation. We fully share his opinion.

In addition to the mentioned molluscan occurrences, there are some others in the Kurgan and northern Turgai areas (the Abagan River, Lake Kushmurun, Dem'yanovka, Leninskoe, Varvarovka and other localities, Fig. 1). Mollusks collected here by L.E. Pikus, U.N. Maderni, P.F. Li, L.A. Panova, L.V. Mironova, N.K. Ovechkina, and other specialists were identified by Korobkov (1966). These data show that the molluscan occurrences are confined to the meridional belt of the Kurgan Beds distribution that stretches for the distance of about 300 km from the Turgai depression into West Siberia.

In the 1990s, when the new Paleogene stratigraphic scheme for the Urals was under elaboration, specialists from the Institute of Geology and Geochemistry of the Uralian Division of the Russian Academy of Sciences studied the upper beds of the Tavda Formation in the Kurgan area (Vasil'eva *et al.*, 1994). From the Tavda clays exposed in three quarries of the eastern Kurgan area, Vasil'eva macerated the late Eocene dinocyst assemblage of the *Charlesdowniea clathrata angulosa* Zone (D12). Two different-aged selachian assemblages detected here are similar, in the Zhelezko's opinion, to the late Eocene assemblages of Mangyshlak. The ferruginous sandstones, which we attribute to the Kurgan Beds, yielded casts of mollusks exemplifying genera *Arctica, Callista*, and *Cardiopsis* (identifications of G.Kh. Salibaev). The researchers inferred the Eocene age of their host deposits and cautiously referred the Kurgan Beds to the upper Eocene–(?) lower Oligocene.

Some time later, Zhelezko sent a sample of ferruginous sandstone bearing casts of pelecypods and gastropods to the Paleontological Institute of Russian Academy of Sciences. Among them, O.V. Amitrov and S.V. Popov identified some species of genera *Arctica* and *Scalaspira* characteristic of the lower Oligocene Ashcheairyk Formation on the northern Ustyurt, and Zaporozhets distinguished spores, pollen and dinocysts. The phytoplankton group includes *Phthanoperidinium amoenum*, the zonal species of the lower Oligocene zone D13 unknown from the Eocene deposits. The spore–pollen spectrum consists of equally abundant gymnosperm pollen (mostly Taxodiaceae) and partly reworked pollen of flowering plants (predominantly Fagaceae). The associated highly diverse pollen exemplifies other thermophilic plants, such as *Nyssa, Hamamelis, Anacardia*, and others, as well as *Boehlensipollis hohli* characteristic of the Rupelian deposits of Europe and similar to the modern *Elaegnus*. Thus, these data supported the Oligocene age of the Kurgan Beds, as it was suggested by Korobkov and Panova.

The different age interpretations of malacofauna from ferruginous sandstones of the Kurgan Beds are intriguing, and the comprehensive descriptions of their section showing transition to the Chegan (Tavda) Formation have never been published. Bearing this in mind, Aleksandrova, Akhmet'ev, and Beniamovskii (Geological Institute of Russian Academy of Sciences) together with Vasil'eva and Zhelezko (Institute of Geology and Geochemistry) studied again the Kurgan quarries and collected palynoflora and fossil mollusks from the ferruginous sandstones. The mollusks were identified by Amitrov and Popov, spore–pollen and phytoplankton assemblages from the Tavda clays, Kurgan Beds, and overlying Kurtamysh (Atlym) Formation were studied by Vasil'eva and Zaporozhets, and Zhelezko analyzed selachian remains from the Chegan Formation.

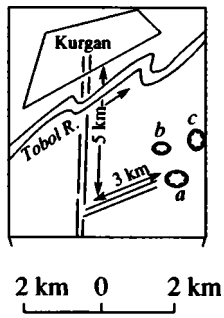

Fig. 1. Location of the Casting Yard 2 (*a*), Brick Yard 1 (*b*), and Chelnokovskii (*c*) quarries exhibiting the upper Tavda Formation and the Kurgan Beds.

THE KURGAN BEDS OF THE TYPE AREA

The Kurgan Beds are exposed near the old bridge in the eastern part of the Kurgan outskirts and near another bridge across the Utyak River. They were studied as well in three quarries (Brick Yard 1, Casting Yard 2, and Chelnokovskii sites in Fig. 1).

The southeastern wall and floor of the Casting Yard quarry exhibits the dark, bluish gray bed of Tavda clays 2.2 m thick. The clays grade upward into dark ash-gray and loose clayey sands with clay interbeds (up to 2 m thick). The upper part of the Tavda Formation represented by the same sand member with clay interbeds is exposed in the same quarry, 100 m to the north. The member is eroded, oxidized, and overlain by Quaternary deposits. An outcrop of the weathering crust above the Tavda Formation (1 m thick) is observable in the northern quarry wall. The Kurgan Beds, with their basal thin horizon of gravel–pebbly composition, rest on the erosional surface of this formation. Above the basal interbed, they include the greenish gray clay bed (0.7 m), the eroded surface of which is overlain by ferruginous sand (0.3 m) grading upward into white cross-bedded sand (1 m). The topmost member of Tertiary deposits is composed of frequently alternating clay and sand laminae presumably attributable to the Kurtamysh Formation. Above, there are Quaternary deposits (about 1.5 m) including three horizons of buried soils. The section is barren of mollusks.

According to Vasil'eva, clays of the Tavda Formation contain the late Eocene dinocyst assemblage of the *Charlesdowniea clathrata angulosa* Zone. In the gravel–pebbly intercalation, Zhelezko earlier found some teeth of the lamnoid sharks *Jaekelotodus trigonalis* (Jaekel) stage *kacharensis*, *Striatolamia sibirica* Zhelezko, *Borealotodus borealis* Zhelezko, and *Araloselachus turgaensis* Zhelezko stage *turgaensis*.

More abundant selachian remains were found in the Brick Yard quarry (Vasil'eva *et al.*, 1994; Zhelezko and Kozlov, 1999), where the rock sequence is of the following structure. The basal dark turquoise clay (0.4 m) of the lower Tavda Subformation is overlain by bright green clay (2 m) of the upper Tavda Subformation with intercalations of glauconite–quartz sand. The clays enclose an interbed of inequigranular quartz sand (0.7 m) with the topmost lens rich in pebbles and large phosphorite nodules yielding plentiful shark teeth. This could be the largest locality of Priabonian elasmobranchian teeth in the northern hemisphere, as it yielded many thousands of specimens. The assemblage of pelagic shark remains is the same as in the Casting Yard quarry. Teeth of *Notorhynchus* sp. and *Galeorhinus* sp., as well as small teeth of odontapsidids and skates, were also found here. The tooth remains characterize species of two biological types: (1) large predators with well-developed tearing and cutting teeth (*Jaekelotodus, Striatolamia, Borealotodus, Clerolamna, Tobolamna*, and *Notorhynchus* sp.) and (2) skates with crushing teeth (*Miliobatus*) and smaller lamnoid and carcharinid sharks that inhabited shallow-water areas. The upper part (5 m) of the Tavda Formation consists of greenish gray foliated clays with sand and silt interbeds. The clays are overlain by Quaternary deposits.

The facies-independent sharks–cosmopolites of seas and oceans are of great value for stratigraphic subdivision of sections and their interregional correlation. These sharks are represented by the genera *Notorhynus, Jaekelton, Borealotodus, Striatolamia*, and *Araloselachus*. Specimens from the Trans-Uralian region, West Siberia, Central Asia, and Kazakhstan allowed understanding the evolution of dentitions of *Jaekelotodus, Striatolamia*, and *Araloselachus* (Glikman, 1964; Zhelezko, 1994; Zhelezko and Kozlov, 1999). The following phyletic lines were established in ascending stratigraphic succession of the Eocene: *Jaekelotodus trigonalis* stages *minor–medius–jaekeli* (Bartonian)–*trigonalis–kacharensis* (Priabonian); *Striatolamia macrota* stages *prima–usakensis–evolutus* (Bartonian)–*Striatolamia macrota* stage *rossica–Striatolamia sibirica* (Priabonian); and *Araloselachus turgaensis* stages *barsukensis* (late Ypresian through Lutetian)–*belinski* (Bartonian)–*turgaensis* (Priabonian)–*Araloselachus aralensis* (Rupelian).

The Tavda selachian assemblage found in the Kurgan quarries characterizes the *Otodus sokolovi sokolovi* Zone (E15) (the middle Priabonian zone according to the Eurasian Paleogene zonation based on elasmobranchii) and includes the leading zonal forms: *Jaekelotodus trigonalis* stage *kacharensis*, *Striatolamia sibirica*, and *Araloselachus turgaensis* stage *turgaensis*. Similar selachian assemblages are known from the Chegan Formation of the southern Turgai and northern Aral areas. *Jaekelotodus trigonalis* stage *kacharensis* was recorded in the Adaevo Formation of Mangyshlak and in the Obukhovka Formation of the Ukraine. In the western Turan plate, teeth characteristic of the selachian *Otodus sokolovi sokolovi* Zone (E15) are known from beds containing planktonic foraminifers of the upper part of the *Globigerapsis tropicalis* Zone, the upper part of NP19/20 Zone, and the lower part of NP21 Zone.

We studied mollusk-bearing samples collected by researchers of the Kurgan Geological Prospecting Party from the ferruginous sandstones overlying the Tavda Formation in the Casting Yard quarry. The collection was supplemented by our own samples from the neighboring Chelnokovskii quarry. Amitrov, Goncharova, and Popov identified *Arctica kasachstanica* (Alexeev), *Gari* sp., *Glossus* (*Glossus*) cf. *subtransversus* Merklin, *Glossus* sp., *Scalaspira* cf. *villana* (Philippi), and *Cyrtodaria angusta parva* Speyer characteristic of the lower Oligocene Ashcheairyk Formation of the northern Ustyurt. Korobkov earlier reported that *Aquilofusus marchicus* Tembr. occurs along with *Arctica, Cyrtodaria*, and *Glossus* forms in sandstones of the Kurgan area. Skate remains (the family Miliobatidae) and *Odontaspis* sp. found by Zhelezko and phytoplankton described by Vasil'eva and Zaporozhets proved the marine genesis of the mollusk-bearing sandstones of the Chelnokovskii quarry. The early Oligocene organic-walled phytoplankton from mollusk-bearing ferruginous sandstones of the Brick Yard quarry (Sample 1a in the table) is characterized below.

The most significant results were obtained in the Chelnokovskii quarry, the south-southeastern wall of which exhibits the unconformable occurrence of the Kurgan Beds above the Tavda clays. The erosional surface of the Tavda Formation is complicated by a groove (Figs. 2 and 3) filled with cross-bedded light yellowish gray well-sorted fine-grained sands (1.2 m thick). The sands are overlain by ferruginous sandstones (0.3 m thick) that armor the quarry scarp. The sandstones contain coquina lenses (up to 0.1 m thick), in which shells of *Arctica kasachstanica* (Alexeev) constitute 80%. Above the sandstones, there is a member of light-colored sands intercalated with gray clays. The member is laterally variable. Its apparent thickness is more than 2 m. The member is exposed in the upper scarp of the quarry. The sandy-clayey Tavda deposits, which experienced weathering and erosion prior to the sand accumulation, are about 3 m thick. Downward they grade into horizontally bedded undisturbed bluish gray-green viscous clays lacking signs of chemical or mechanical destruction. These are typical Tavda clays in autochthonous occurrence. The western side of the erosional groove demonstrates the onlap relations between the

Phytoplankton distribution in the Chelnokovskii quarry section

Taxon	Sample number					
	1	127	133	128	1a	129
Dinocysts						
Heteraulacacysta campanula	+	+	+		+	
Horologinella sp.		+			+	
Charlesdowniea clathrata angulosa		+	+			
Corrudinium incompositum		+				
Impagidinium dispertitum		+				
I. cf. *multiplexum*		+				
Tectatodinium sp.		+				
Wetzeliella irtyshensis		+				
Palaeocystodinium golzowense		+				
Deflandrea sp.		+	+		+	+
Areosphaeridium diktyoplokus		+	+			
Leptodinium sp.		+				
Microdinium sp.		+				
Phthanoperidinium amoenum				+	+	+
Lejeunecysta sp.				+		
Hystrichosphaeropsis sp.						+
Batiacasphaera sp.			+			+
Glaphyrocysta undulata						+
Membranophoridium aspinatum						+
Impagidinium sp.						+
Adnatosphaeridium sp.						+
Spiniferites sp.			+			+
Homotryblium abbreviatum						+
Operculodinium sp.					+	+
Apteodinium sp.						+
Caligodinium sp.			+			+
Pentadinium sp.						+
Systematophora sp.						+
Charlesdowniea fasciata			+			
Thalassiphora kurganica			+			
Phthanoperidinium stockmanii			+		+	
Ph. eocenicum			+			
Ph. geminatum			+			
Wilsonidium sp.			+			
Spiniferites ramosus			+			
Heteralaucacysta leptalea			+			
Kallosphaeridium sp.			+			
Homotryblium oceanicum			+			
Glaphyrocysta semitecta			+			
G. exuberans			+			
Glaphyrocysta sp.			+			
Adnatosphaeridium multispinosum			+			
Dapsilidinium sp.			+			

Table. (Contd.)

Taxon	Sample number					
	1	127	133	128	1a	129
Rottnestia sp.			+			
Samlandia sp.			+			
?*Areoligera* sp.			+			
Cribroperidinium sp.			+			
Lentinia serrata			+			
Lentinia sp.			+			
Chytroeisphaeridia sp.			+			
Rhombodinium (?) *pentagonum*			+			
Paralecaniella indentata					+	
Homotryblium abbreviatum					+	
Apteodinium maculatum					+	
Adnatosphaeridium robustum					+	
Cordosphaeridium sp.					+	
Hystrichostrogylon sp.					+	
Acritarchs and prasinophytes						
Crassosphaera sp.	+	+	+	+	+	+
Paucilobimorpha triradiata	+		+		+	
Tytthodiscus sp.	+	+		+		
Botryococcus sp.	+			+		
Leiosphaeridia sp.	+	+				
Cymatiosphaera sp.	+					
Paucilobimorpha cf. *spinosa*		+		+		
Paucilobimorpha sp.		+				
Schizocysta sp.		+	+			+
Cymatiosphaera radiata				+		
Veryhachium sp.				+	+	
Ptanospermella sp.			+			+
Paucilobimorpha granulifera					+	
Micrhystridium sp.					+	
Pediastrum sp.		+				

Note: Sample 1a was taken from the Brickworks-1 quarry. Samples 1, 127, and 128 were studied by Vasil'eva, and samples 133, 128, 1a, and 129, by Zaporozhets.

sandy member and the Tavda clays, which become sandy upward. The flaggy ferruginous sandstones with mollusks lie immediately on the erosional surface of sandy clay varieties. A series of palynological samples were collected from the section. The sampling sites are shown in Fig. 3. Results of microflora analysis by Vasil'eva (Samples nos. 1, 127, 128) and Zaporozhets (Samples 133, 128, 129) are presented in the table.

The table shows that the Tavda Formation is characterized by a diverse phytoplankton assemblage consisting of over 40 dinocyst species and 10 species of prasinophytes and acritarchs. The occurrence of characteristic taxa, such as *Areosphaeridium diktyoplokus* and *Wetzeliella irtyshensis* in association with *Charlesdowniea clathrata angulosa*, the index-species of the upper Eocene Zone D12 of the West European and Crimean–Caucasian scales, confirms the Eocene age of the upper beds of the formation. Sample 128 from the basal sands of the Kurgan Beds yielded an impoverished phytoplankton assemblage consisting mostly of prasinophytes and acritarchs. We do not exclude that these sands partly accumulated before the sea ingression and could be of alluvial and coastal-marine origin. The phytoplankton assemblage includes *Phthanoperidinium amoenum*, the index-species of the succeeding D13 Zone of the same scales, which indicates the early

Fig. 2. The contact between the Kurgan Beds and Tavda Formation, the exposure in the Chelnokovskii quarry. The onlap relations between the molluscan-bearing ferruginous sandstones and topmost beds of the Tavda Formation can be distinctly observed.

Oligocene age of the sands incised into the Chegan clays. The additional sample 1a taken by Zhelezko from the mollusk-bearing ferruginous sandstones of the Brick Yard quarry yielded a more diverse phytoplankton assemblage. The species *Paralecaniella indentata, Phthanoperidinium stockmani*, and *Ph. amoenum*, as well as acritarchs and prasinophytes represent more than 80% of the assemblage. Among taxa known from the lower Oligocene marine deposits of the Turan plate, the assemblage yielded *Homotryblium abbreviatum, Apteodinium maculatum, Adnatosphaeridium robustum, Heteraulacacysta campanula, Deflandrea* sp., *Horologinella* sp., and *Hystrichostrogylon* sp. Reworked fragments of *Wetzeliella, Samlandia, Areosphaeridium*, and *Cordosphaeridium* forms were also found. Sample 129 from the clay lying above the lens of ferruginous sandstones and below the Kurtamysh continental sands yielded the assemblage of nearly 20 phytoplankton species, some of which are inherited from the underlying Tavda Formation. Taxa occurring most likely *in situ Membranophoridium asxpinatum, Phthanoperidinium amoenum*, and others (the table). Another characteristic feature of their assemblage is abundance (more than 10 specimens) of the type species *Ph. amoenum.*

Spore–pollen spectra of all studied samples (1, 127, and 133) from the Tavda Formation are identical and generally typical of its upper horizons in West Siberia. The assemblage contains single spores of *Osmunda, Gleichenia*, and *Lycopodium*. Pollen of angiosperms noticeably prevails. Scanty pollen of conifers is dominated by that of Taxodiaceae. Among pollen of flowering plants, that of Fagaceae (*Quercus gracilis, Q. graciliformis, Q. conferta*) prevails. It is associated with triporate and tricolpoporate pollen of formal taxa, as well as with pollen of *Nyssa crassa, Rhus, Araliaceopollenites*, Palmae, Hamamelidaceae, and others. Pollen of Betulaceae, Juglandaceae, and deciduous Fagaceae represents not more than 5%. In Sample 128 from the basal part of the Kurgan Beds, pollen of flowering plants also dominates over that of conifers, though it is partly redeposited from the Tavda Formation. The major part of the spectrum corresponds to pollen of oaks (*Quercus gracilis, Q. graciliformis*, and *Q. conferta*) and other thermophilic plants. Essentially different spore–pollen spectra characterize the middle and upper parts of the Kurgan Beds. Sample 1a yielded not less than 50 pollen taxa with approximately equal proportions of conifers and flowering plant species. Panova previously mentioned this ratio as a characteristic feature of the Kurgan Beds. The pollen of Taxodiaceae dominates over that of Pinaceae. Small pollen of oaks is still present, although in a lesser amount. There are single pollen grains of *Keteleeria, Castanopsis, Pterocarya, Engelhardtia, Juglans* (including *J. siebodianiformis*), *Alnus, Hamamelis scotica, Liquidambar, Fothergilla gracilis, Ilex, Rhus, Nyssa, Myrica, Comptonia, Tilia, Ulmus, Loranthus* cf. *L. elegans, Sabal*, and *Fraxinus. Boehlensipollis hohlii* characteristic of West European Oligocene beds also occurs. Abundance of spores is less than 1%. In Sample 129, abundance of Pinaceae pollen is over 70%. Pollen of flowering plants is dominated by that of Fagaceae, the small oak pollen (*Quercus gracilis* and *Q. graciliformis*) included. Species characteristic of the Oligocene deposits in Kazakhstan and South Siberia, such as *Picea, Abies, Keteleeria, Tsuga, Salix, Ulmus, Pterocarya, Juglans* (includ-

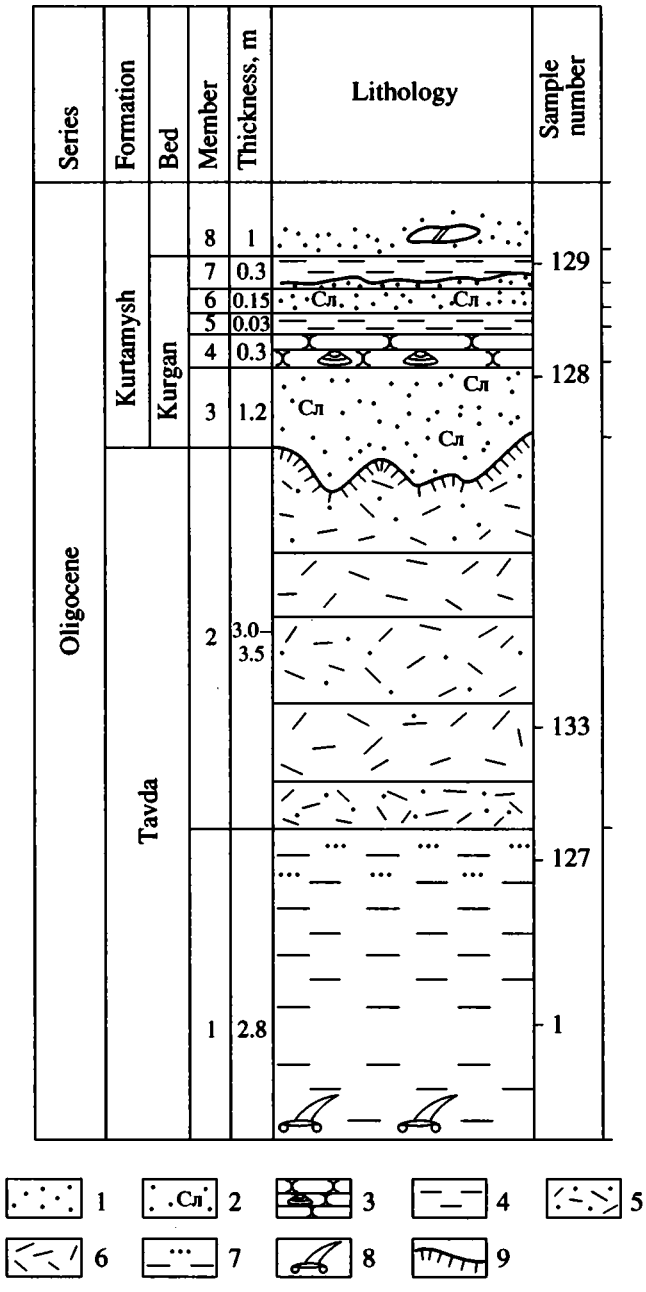

Fig. 3. Section of the upper Tavda Formation and Kurgan Beds in the Chelnokovskii quarry, southeastern outskirts of the town of Kurgan: (1) light gray fine-grained sand; (2) light yellowish gray cross-bedded and fine-grained micaceous sand; (3) limonitized sandstone with coquina lenses; (4) dark bluish to gray-green thick-bedded viscous clay; (5) gray sandy silt; (6) gray silt; (7) light gray clay with sand lenses; (8) shark teeth occurrence; (9) unconformable boundary between the Tavda Formation and Kurgan Beds.

ing *J. sieboldianiformis* and *J. sibirica*), *Carya, Liquidambar, Acer*, and others, are also present.

Summarizing investigation results on the Kurgan quarries, we arrive at the following conclusions:

(1) The Tavda Formation is composed everywhere of two members (subformations in the interpretation of Zhelezko and Vasil'eva). The lower one (apparent thickness is 3 m) is represented by dark greenish lilac-gray fat and soft clays. The upper member (up to 2 m thick) consists of dark gray sandy clays or clayey sands. This one frequently is deeply eroded, being preserved only in some places.

(2) The spore–pollen spectra of the basal sands of the Kurgan Beds are difficult to differentiate from those of the underlying clays of the Chegan Formation (effect of reworking?).

(3) The incisions into the eroded and weathered surface of the Tavda Formation are filled with cross and obliquely bedded sands grading into the flaggy limonitized sandstones with the molluscan fauna of the "Ashcheairyk" type. The overlying thin beds of gray clays and sands represent marine facies of the Kurgan Beds. Resting on their erosional surface, locally without observable hiatus, are lacustrine–alluvial deposits of the Kurtamysh Formation overlain by Quaternary sediments.

(4) Assemblages of mollusks, organic-walled phytoplankton, and fossil ichthyofauna, in combination with the geological observations, suggest the repeated Oligocene sea ingression into southern West Siberian plate, which followed immediately the late Eocene regression of the Tavda sea.

DISCUSSIONS

The Kurgan sea basin of southern West Siberia cannot be considered as residual after the Tavda sea retreat, because there was a break in marine sedimentation that resulted in erosion of some Tavda (Chegan) deposits, in weathering of elevated land areas, and in appearance of the early Oligocene incisions. In this connection, we should find out the ways of northeastward migrations of the early Oligocene marine malacofauna and microplankton, because the Ashcheairyk sea basin of the northern Ustyurt and Aral regions was bounded in the east by the meridional Zhaksybutash-Kulanda uplift zone (Yanshin, 1953; Bronevoi and Kiryukhin, 1968).

It is unlikely that the Ashcheairyk malacofauna, many taxa of which were found at the corresponding level in Kazakhstan and in Rupelian deposits around the North Sea in West Europe, could penetrate into West Siberia via the Arctic basin. The northern way is incompatible with this fauna absence in Oligocene deposits of northern West Siberia and with the Oligocene history of the Arctic basin (*Atlas...*, 1992). The arguments of Podobina (1997), who suggested that the Tavda benthic foraminifers of West Siberia show affinity with their Oligocene assemblages of the North Canadian Arctic shelf, are unconvincing. The Tavda fauna was proved to be similar to that characterizing the Rishtan, Isfara, Khanabad and Sumsar deposits of the Fergana and Tajik depressions of Central Asia (Ushakova and Gurari, 1959; Lipman *et al.*, 1960; Kisel'man, 1978; publications by Podobina of the 1980–1990s).

Now there are no doubts about the Eocene, but not Oligocene, age of the Central Asia marine biota of mollusks, foraminifers, radiolarians, nannoplankton, and organic-walled phytoplankton typical of the Khanabad and greater part of the Sumsar regional stages (Davidson *et al.*, 1982; Salibaev, 1987; Oleinik, 1979; Muzylev and Salibaev, 1988; Muzylev *et al.*, 1996; and others).

Thus, the southern or southwestern connection of the early Oligocene West Siberian and Turan sea basins was the only possible. Analysis of the materials presented suggests that the biota migrated via the same way the Chegan-Tavda sea retreated southeastward from Siberia and the Turgai in the late Eocene.

The occurrence of the Ashcheairyk malacofauna in the meridional zone contiguous to the northern axial part of the Turgai depression was discussed in the introduction. Let us consider now the materials on the central and southern Turgai areas and the northeastern Aral region.

Distribution of malacofauna should be discussed first. According to Korobkov (1966), Ovechkin and Mironova found the Ashcheairyk-type fauna at the Kunduzda River flowing into the Ubagan River to the south of the Kirovskoe valley opened into the Turgai depression. T. Akopov (personal communication) who carried out the geological mapping of the western Turgai reported on the occurrence of the ferruginous sandstones with the Ashcheairyk-type malacofauna at the Shat-Irgiz River upstream off its confluence with the Irgiz River. Vyalov, Alekseev, Merklin, and Korobkov discovered this type fauna in the post-Chegan sands of the Zhaksy Klych outlier located to the northeast of the Sea of Aral. Vyalov (1964) positioned the Zhaksy Klych member at the base of the Ashcheairyk Formation. Amitrov and Popov noted similarity between the Zhaksy Klych and Ashcheairyk molluscan assemblages studying them in the collection of Merklin and personal finds. As shown in Fig. 4, three molluscan localities mentioned above are on the way of the retreating Chegan sea.

In the same area, 50 km to the west of the town of Kustanai, there is the Kachar quarry, where the Chegan clays are overlain by fine-laminated dark green clays (7 m thick), in which Vasil'eva distinguished a dinocyst assemblage with the early Oligocene zonal species *Phthanoperidinium amoenum*.

The sea ingression advanced far to the north along the Turgai depression in the Ashcheairyk time just like another transgression of the Akchagylian (Pliocene) time developed from the Eastern Paratethys along the Volga and Kama paleovalleys. In addition to biostratigraphic evidences, this inference is supported by other data of geomorphology, lithology, geochemistry, and hydrogeochemistry.

Let us begin with *geomorphological* data. As early as in the 1960s, the prospect drilling results were used to map isohypses of the Chegan beds surface. The mapping revealed the early Oligocene sublatitudinal incisions formed before the Oligocene continental deposition. The incisions represent large sublatitudinal buried valleys of the post-Chegan time, which were opened to the Turgai depression both from the west (the Lisakovsk and Shieli valleys) and from the east (the Kirovskoe valley). The valleys happened to be suitable for intense deposition of limonite ores of the Lisakovsk and neighboring basins. The recent contours of the Turgai depression are inherited from the Oligocene time.

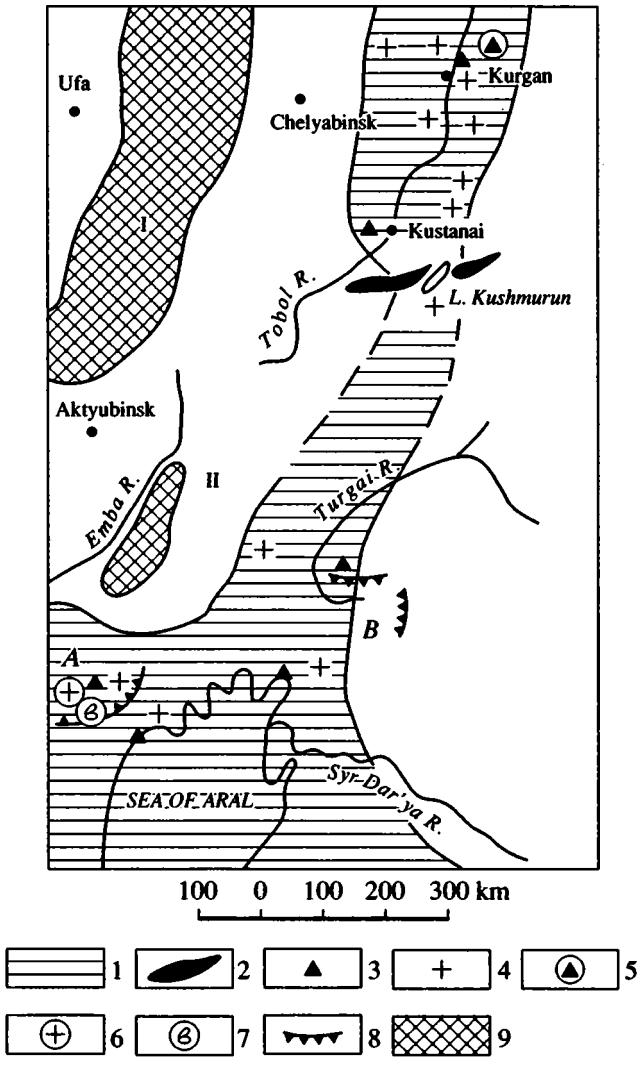

Fig. 4. The mid-early Oligocene Ashcheairyk sea ingression into the southern West Siberian plate: (1) supposed ingressive sea arm; (2) Lisakovsk-type deposits of brown iron ores in the Turgai depression; (3) section of the Kurgan Beds and coeval deposits bearing the early Oligocene dinocyst assemblage; (4) occurrence of the Ashcheairyk-type malacofauna in the Kurgan Beds; (5) occurrence of ichthyofauna in the Kurgan Beds; (6–7) the Ashcheairyk Formation stratotype section, from where the characteristic lower Oligocene assemblages of dinocysts (6) and mollusks (7) are described; (8) lower Oligocene key sections of the Northern Ustyurt (*A*) and Chelkar-Nura (*B*) scarps; (9) the Urals (I) and Mugodzhary uplift (II).

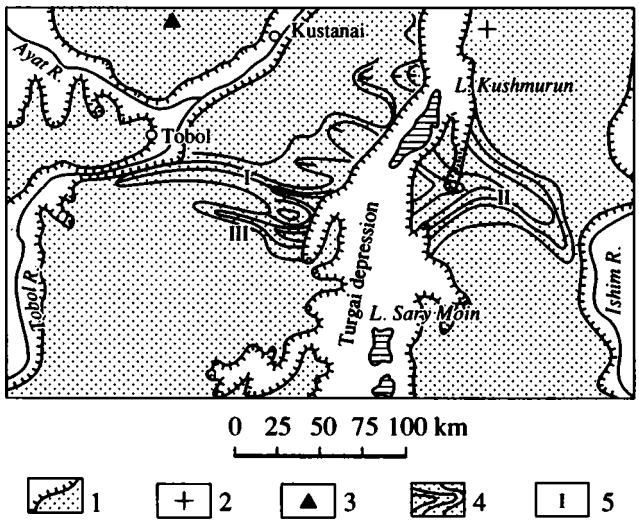

Fig. 5. Schematic geological map of an area of the Lisakovsk iron-ore basin (the Turgai depression): (1) contact between the Oligocene deposits (dotted) and upper Eocene Chegan Formation (blank); (2) malacofauna occurrence in the Kurgan Beds; (3) section that yielded the lower Oligocene dinocyst assemblage; (4) buried valley with the Chegan clays hosting the Oligocene iron-ore deposits; bergstrichs show dipping of the iron-ore base; (5) buried incision valleys of the early Oligocene time in the Tavda sea floor (I) Lisakovsk, (II) Kirovskoe, (III) Shieli.

In the northeastern Turgai depression, the Chegan clays underlying the Oligocene deposits (Nikitin, 1967) have an uneven surface situated 240 to 168 m above the sea level. The buried Lisakovsk and Kirovskoe valleys extend for nearly 150 and 110 km, respectively. The elevation of the Chegan Formation surface changes from 195 to 140 m throughout the Lisakovsk valley and from 190 to 113 m throughout the Kirovskoe valley (Fig. 5). It is remarkable (Nikitin, 1967) that in the pre-Oligocene relief depressions, the iron ore deposition was preceded by accumulation of finely alternating gray clays, sands, and silts, which contain the spore–pollen assemblage characteristic of the Kurgan Beds and associated megafossils of both Mesophytic moderately thermophilic and subtropical flora (subtropical taxa were identified by Boitsova and Vasil'eva in basal Oligocene beds of the Shieli valley, see Boitsova *et al.*, 1961). Nikitin (1967) supposed that a large residual sea basin of the early Oligocene time existed in the central Turgai depression after the Chegan sea retreat. The basin extended to the Lake Sary-Moin in the north and the Zhilanchik River basin in the east; its western boundary coincided with the meridian connecting the Alasor Settlement and the upper course of the Teke River.

The *lithological–geochemical* indicators of the early Oligocene sea basin in the northern Turgai are directly related to deposition of the Lisakovsk-type iron ores. A long discussion on their origin between Formozova (1959, 1969), on the one hand, and Krotov (1937 and others), Sigov (1969), Mikhailov (1960), and Bronevoi (1969), on the other, ended in favor of the latter viewpoint based on the conclusions of Strakhov (1947, pp. 134–135). As Strakhov concluded, "...goethite–chamosite–siderite ores... represent sediments of gulfs, bays, limans, and uppermost shelf area", i.e., typical coastal-marine sediments. Formozova also admitted such a genesis of some iron ore deposits in the Aral region. The inferable existence of the early Oligocene sea basin may be a decisive argument to finish the discussion. Mikhailov (1960) reported the occurrence of the Oligocene iron ore deposit of the Lisakovsk type in the Irgiz River basin, within the area of the supposed sea ingression from the Aral region to the Turgai. When sampling the Lisakovsk deposits in the 1950s, he observed their persistent cross bedding directed SW 220–240° and explained this as the backwater effect in the Lisakovsk valley mouth in response to transgression in the "terminal" basin. Such a basin was most likely the sea arm in the axial zone of the Turgai depression.

In the opinion of Sigov (1956, 1969), the provenance of iron regenerated in the Lisakovsk-type ore deposits was the Chegan Formation, where iron concentration is 6–8% in average. Sigov distinguished two types of the Lisakovsk ore deposits, considering the basal massive oolitic ores of siderite-leptochlorite composition, which are concentrated in the eastern flank of the Lisakovsk ore basin, as deposits of lagoonal or estuary settings (Toporkov, 1958; Sigov, 1969). The same deposits are known in the Kirovskoe ore basin on the opposite side of the Turgai depression axis.

Hydrogeological and hydrochemical data are of special importance for defining the nature of basin, which collected the past river discharge of the northern Turgai region. The lower Oligocene deposits include a separate water-bearing horizon (Ivanov and Gorlach, 1967). In places of the surface water penetration, the ground waters are of hydrocarbonate composition. These are confined to the "opened" valley-like depressions above the waterproof horizon. Weakly saline and brackish waters with mineral concentration of 3–10 to 15 g/l and higher are characteristic of structures with a minor infiltration influence (the Kustanai depression, the Boshchakul depression of the Ishim slope, and others). In these structures with stagnant hydrodynamic regime and insignificant water exchange, the chloride–sodium, sometimes sulfate–chloride–calcium–manganese–sodium composition of ground waters reflects most likely their past connections with original marine settings.

The presumable early Oligocene sea ingression from the Turan plate into West Siberia makes it interesting to analyze the evolution of the Ashcheairyk sea proper and to determine the time of its maximal transgressive phase. The materials were obtained by studying the stratotype section of the Ashcheairyk Formation of the northern Ustyurt (Akhmet'ev and Zaporozhets,

1992). Using the ratio between dinocysts and prasinophytes, the "facultative desalting organisms" such as *Micrhystridium, Pediastrum*, spores of water ferns *Hydropteris indutus* and *Azolla*, and calculating the maximal "marine condition index" (the ratio of phytoplankton specimens to the total amount of palynomorphs), researchers mentioned above revealed at least three phases of freshening and salination during the short-term transgressions of the Ashcheairyk time. The maximum transgression was at the accumulation time of basal beds in the "*Cyprina*" member, where one level yields abundant *Arctica* shells. Like "eggshell" chains, these shells encircle the slopes outlining the upper part of the Ashcheairyk Formation. The transgression peak corresponds to the level above the first occurrence of *Wetzeliella gochtii* in the zone NP22 of southern Russia concurrent to that of Belgium and northern Germany (Kothe, 1990; Andreeva-Grigorovich, 1991; Zaporozhets, 1998, 1999). *Phthanoperidinium amoenum* still occurs at this level in both the Ustyurt and West European sections (the zone D14a). Noteworthy is the first occurrence level of *Cyprina* coinciding with that of limonite and hydrogoethite concretions in the Ashcheairyk stratotype section. It should be also stressed that the palynological assemblage of the Ashcheairyk Formation is dominated by pollen of gymnosperms and deciduous angiosperms. Pollen of Fagaceae and evergreen plants is of minor importance, probably because the Eocene Chegan clays have been covered by younger Oligocene sediments by that time, and pollen has been sheltered from reworking.

A similar conclusion about the maximal phase of the Ashcheairyk transgression in the Aral and northern Ustyurt regions was obtained by Voznesenskii (1978, pp. 65 and 67) who analyzed sedimentological and lithological peculiarities of these regions. According to his data, the transgression peak corresponded to the beginning of Mesocycle II, when the sea basin spread to the north along the Chelkar trough and eastward of it to form two large bays in the southern parts of the Tuguz and Chukus synclines.

Zaporozhets obtained very interesting, unexpected results analyzing palynology of the Kutanbulak Formation in the Aral region (the Perovskii Bay site of the Altyn-Chokusu Range to the north of the Saksaul'skaya railway station) and of the Urkimbai and Chelkar-Nura formations in the southern Turgai region (sections of the Chelkar-Nura and easterly Dongustau and Atambas scarps). The mentioned formations used to be considered as continental in origin, but many samples of their rocks yielded dinocysts, prasinophytes, and acritarchs. Along with taxa redeposited from the Chegan Formation into the Oligocene beds, there are abundant palynomorphs buried *in situ*. Akhmet'ev and Amitrov sampled the upper beds of the Urkimbai Formation of the Chelkar-Nura scarp to the east of the continental Oligocene section with the well known burial of *Indricotherium* fauna. In their samples, Zaporozhets identified Oligocene dinocysts, the zonal species *Wetzeliella symmetrica* and *W. gochtii* included, in association with abundant reworked Eocene forms of the Chegan Formation.

The organic-walled phytoplankton from this section of the Chegan Formation is exceptionally diverse, represented by nearly 100 species of dinocysts and prasinophytes. More than 70 of their species were found in the upper beds of the formation (3 m below the top), which are devoid of marly–siderite concretions. Especially abundant and diverse are forms of genera *Deflandrea, Cordosphaeridium, Phthanoperidinium*, and species of the *Wetzeliella* group. Genera *Phelodinium, Microdinium, Glaphyrocysta*, and *Areosphaeridium diktyoplokus* group are less diverse. Spores and pollen constitute about a half of the palynological assemblage. In contrast to the assemblage from the Chegan Formation type section of the Ustyurt, pollen of conifers (*Pinus*) dominates. Pollen of Fagaceae, that of *Quercus graciliformis, Q. gracilis*, and *Q. conferta* included, is prevailing in the spectrum of flowering plants. The assemblage also contains pollen of deciduous broad-leaved thermophilic taxa *Liquidambar, Hamamelis, Rhus, Fothergilla*, Moraceae, *Platanus*, and others; pollen of Juglandaceae is accessory, and pollen of Betulaceae has not been detected.

The early Oligocene sea expanded not only into West Siberia, but also into the inner depressions of Kazakhstan, as is suggested by Sotnikova (1996). At that time, the sea reached the Betpak-Dala and western areas of the Chu River valley in the east advancing either from Central Asia, or from the Ustyurt and Aral regions around the Greater Karatau in the north. The Ustemir Formation of greenish gray middle Eocene clays is overlain here without observable unconformity by the gray clayey member of the lower Oligocene. Earlier, both clay units were attributed to an undivided sequence. The diverse dinocyst assemblage indicates however that the upper clay member corresponds to the dinocyst *Phthanoperidinium amoenum* Zone (D13) of Western Europe. The spore–pollen assemblage of the member consists of taxa mostly characteristic of temperate warm zone and is associated with minor subtropical elements. Abundance of Taxodiaceae pollen and taxonomic composition of flowering plants makes the assemblage correlative with those from the early Oligocene *Carya spackmania–Tilia grandireticulata–Juglans sieboldianiformis* Zone of the Aral and Turgai regions and *Carya spackmania–Carpinus perfectus* Zone of West Siberia. Comparing the Kurgan and Ashcheairyk sea transgressions, we can suggest two equally probable scenarios by virtue of data presented above.

(a) The Kurgan transgression coincided with the most extensive transgression responsible for accumulation of the *Cyprina* beds in the Ustyurt. Arguments in favor of this suggestion are the close similarity of molluscan assemblages in both regions and presence of *Bohlensipollis hohli* and *Phthanoperidinium amoenum*

in phytoplankton assemblages. However, the Kurgan and *Cyprina* beds yield different spore–pollen spectra. Spectra of the Kurgan Beds show a high content of small pollen of evergreen oaks, thus resembling those of the Tavda Formation. In spectra at the corresponding level of the Ashcheairyk Formation, dominant taxa of flowering plants are represented by Juglandaceae and Betulaceae, and diversity of other thermophilic families is comparatively low.

(b) The Kurgan transgression could be concurrent to one of the preceding short-term transgressions of the early Oligocene, which were responsible for accumulation of basal beds of the Ashcheairyk Formation. This variant is in agreement with the results of the spore–pollen and phytoplankton analyses but contradicts the molluscan data (the basal Ashcheairyk beds contain abundant *Nortia* and other small shelly fossils, but they are virtually devoid of *Arctica* and associated forms characteristic of the Kurgan Beds). It is also probable that the sea reached West Siberia from the Turan plate during the early Oligocene transgression peak.

Both versions are equally probable until appearance of new arguments in favor of one of them.

CONCLUSIONS

(1) It is unlikely that the Kurgan Beds (*sensu stricto*) distinguished by Panova in southern West Siberia represent deposits of the regressing Tavda basin. They accumulated most likely during the early Oligocene sea ingression from the western Turan plate that advanced along the Turgai seaway inherited from the early Paleogene history of the region.

(2) The early Oligocene age of the Kurgan Beds is indicated by their malacofauna, by the organic-walled phytoplankton that includes *Phthanoperidinium amoenum*, the index-species of the early Oligocene zone D13, and by associated pollen taxon *Boehlensipolis hohlii* unknown in the pre-Oligocene deposits.

(3) The marine genesis of the Kurgan Beds is proved by occurrence of mollusks characteristic of sea basins with normal or slightly lowered salinity, and by associated dinocysts and ichthyofauna.

(4) The Kurgan Beds unconformably overlie the erosional surface of the Tavda Formation.

(5) The early Oligocene sea ingression advanced from the Aral area along the Turgai depression and Tobol River paleovalley up to the latitude of the town of Kurgan (Fig. 4). Most likely, the warm water ingression to the north resulted in climatic warming and gave rise to distinctly seasonal character of the climate in the second half of the early Oligocene. From that time, the Eurasian arid belt expanded to reach its maximum in the terminal early Oligocene.

(6) The Lisakovsk-type iron ore deposits were formed in the geochemical barrier zone of paleorivers flowing in the arm of transgressing sea.

ACKNOWLEDGMENTS

We thank O.V. Amitrov, I.A. Goncharova, and S.P. Popov from the Paleontological Institute of Russian Academy of Sciences, who identified the malacofauna of the Kurgan Beds. Geologists of the Kurgan Geological Prospecting Party kindly offered the possibility to study the geological survey reports of the 1960–1980s and results of drilling in the southern Kurgan areas. The work was supported by the Russian Foundation of Basic Research, projects nos. 98-05-64944, 99-05-65174, 00-05-64917, 00-15-98490, and 98-05-79001.

Reviewer S.V. Popov

REFERENCES

Akhmet'ev, M.A. and Zaporozhets, N.I., Late Eocene–Oligocene Pollen, Spores, Plant Megafossils, and Phytoplankton from Stratotypes of the Chegan and Ashcheairyk Formations (Northern Ustyurt, Kazakhstan), *Byull. Msk. O–va Ispyt. Prir., Otd. Geol.*, 1992, vol. 67, issue 3, pp. 96–105.

Andreeva-Grigorovich, A.S., Paleogene Phytoplankton Zonation of the Southern USSR as Indicated by Dinocysts and Phytoplankton, *Abstract of Doctor. Sci. (Geol.–Min.) Dissertation*, Kiev: Inst. Geol. Nauk, Akad. Nauk Ukr. SSR, 1991.

Atlas paleogeograficheskikh kart shel'fov Evrazii v mezozoe i kainozoe (Palaeogeographic Atlas of the Shelf Regions of Eurasia for the Mesozoic and Cenozoic), Alekseev, M.N., Ed., Llandudno: The Robertson Group, 1991.

Boitsova, E.P., Vasil'ev, I.V., and Ovechkin, N.K., The Oligocene Boundaries and Scope in the Turgai Depression and Adjacent Regions (by Paleobotanical Data), *Materialy Vses. Geol. Inst., Nov. Ser.*, 1961, issue 43, pp. 45–52.

Bronevoi, V.A., On Conditions of the Northern Aral Iron Ore Formation, *Litol. Polezn. Iskop.*, 1969, no. 2, pp. 101–113.

Bronevoi, V.A. and Kiryukhin, A.G., The Middle Oligocene of the Northern Aral and Northern Ustyurt Areas, *Izv. Akad. Nauk SSSR, Ser. Geol.*, 1968, no. 1, pp. 120–127.

Davidzon, R.M., Kreidenkov, G.P., and Salibaev, G.Kh., *Stratigrafiya paleogenovykh otlozhenii Tadzhikskoi depressii i sopredel'nykh territorii* (Paleogene Stratigraphy of the Tajik Depression and Adjacent Regions), Dushanbe: Donish, 1982.

Dobrutskaya, N.A., Continental Tertiary Stratigraphy of the Lower Ob' River Area, in *Resheniya i trudy Mezhvedomstvennogo soveshchaniya po dorabotke i utochneniyu stratigraficheskikh skhem Zapadno-Sibirskoi nizmennosti* (Resolutions and Reports of the Interdepartmental Conference on Modification of Stratigraphic Scheme for the West Siberian Lowland), Novosibirsk: Gostoptekhizdat, 1961, pp. 19–21.

Drozhashchikh, N.B., Paleogene Spore–Pollen Assemblages from the Western Part of the West Siberian Lowland, in *Resheniya i trudy Mezhvedomstvennogo soveshchaniya po dorabotke i utochneniyu unifitsirovannoi i korrelyatsionnoi stratigraficheskikh skhem Zapadno-Sibirskoi nizmennosti* (Resolutions and Reports of the Interdepartmental Conference on Modification of the Unified and Correlation Stratigraphic Schemes for the West Siberian Lowland), Part 2,

Tyumen': Zap. Sib. Nauchn.-Issled. Geol. Neft. Inst., 1970, pp. 231–244.

Formozova, L.N., Iron Ores of the Northern Cis-Urals Region, *Tr. Geol. Inst. Akad. Nauk SSSR*, 1959, issue 29.

Formozova, L.N., A Letter to the Editorial Board, *Litol. Polezn. Iskop.*, 1969, no. 2, p. 133.

Glikman, L.S., *Akuly paleogena i ikh stratigraficheskoe znachenie* (Paleogene Sharks and Their Stratigraphic Significance), Moscow: Nauka, 1964.

Ivanov, V.A. and Gorlach, V.F., Hydrogeology of the Northern Turgai Depression, in *Geologiya Turgaiskogo progiba i Priaral'ya* (Geology of the Turgai Depression and the Aral Region), Leningrad: Nedra, 1967, pp. 180–202.

Kisel'man, E.N., Paleogene Foraminiferal Assemblages of West Siberia, in *Paleogen i neogen Sibiri* (The Paleogene and Neogene of Siberia), Novosibirsk: Nauka, 1978, pp. 41–51.

Korobkov, A.I., On Occurrence of the Rupelian Marine Sequences in the Northern Turgai Depression and Southern West Siberia, *Dokl. Akad. Nauk SSSR*, 1966, vol. 171, no. 3, pp. 677–678.

Kothe, A., Paleogene Dinoflagellates from North West Germany, *Geol. Jahrb.*, 1990, Reiche A, vol. 118.

Kovalevskaya, I.G., The Paleogene and Neogene Stratigraphy of the Southern Part of the West Siberian Lowland and the Turgai, in *Resheniya i trudy Mezhvedomstvennogo soveshchaniya po dorabotke i utochneniyu stratigraficheskikh skhem Zapadno-Sibirskoi nizmennosti* (Resolutions and Reports of the Interdepartmental Conference on Modification of Stratigraphic Schemes for the West Siberian Lowland), Novosibirsk: Gostoptekhizdat, 1961, pp. 33–35.

Krotov, V.P., Classification, Nomenclature and Features of Exogenic Deposits, *Trudy konferentsii po genezisu rud zheleza, margantsa i alyuminiya* (Proc. Conf. on Iron, Manganese and Aluminum Ore Genesis), Moscow: Akad. Nauk SSSR, 1937, pp. 67–82.

Lipman, P.Kh., Burtman, E.S., and Khokhlova, I.A., Paleogene Stratigraphy and Fauna of the West Siberian Lowland, *Tr. Vses. Geol. Inst., Nov. Ser.*, 1960, vol. 28.

Martynov, V.A., Panova, L.A., and Nikitin, V.P., Principal Rearrangement of the West Siberian Nature at the Eocene–Oligocene Boundary, in *Geologiya i poleznye iskopaemye yuga Zapadnoi Sibiri* (Geology and Mineral Deposits of the Southern West Siberia), Novosibirsk: Nauka, 1988, pp. 147–155.

Mikhailov, B.M., *Litologiya mezozoiskikh i kainozoiskikh otlozhenii Turgaiskogo burougol'nogo basseina* (Lithology of the Mesozoic and Cenozoic Deposits of the Turgai Brown Coal Basin), Leningrad: Gostoptekhizdat, 1959.

Muzylev, N.G. and Salibaev, G.Kh., Age of Some Paleocene and Eocene Tajik Horizons Based on Nannoplankton Data, *Izv. Akad. Nauk Tajik SSR, Otd. Fiz.-Math., Khim., Geol. Nauk*, 1988, no. 3, pp. 91–93.

Muzylev, N.G., Rasulov, U.M., Khokhlova, I.E., and Kushakov, A.R., The Upper Eocene of the Fergana Depression and Adjacent Regions, *Stratigr. Geol. Korrelyatsiya*, 1996, vol. 4, no. 2, pp. 38–45.

Nikitin, P.A., Cretaceous and Paleogene Stratigraphy of the Northwestern Part of the Turgai Depression, in *Geologiya Turgaiskogo progiba i priaral'ya* (Geology of the Turgai Depression and the Aral Region), Leningrad: Nedra, 1967, pp. 25–32.

Nikolaev, V.A., Miocene Stratigraphy of the West Siberia Lowland, *Dokl. Akad. Nauk SSSR, Nov. Ser.*, 1947a, vol. 58, no. 1, pp. 101–103.

Nikolaev, V.A., Stratigraphic Position of the Tomsk Flora, the Lagernyi Sad Site, *Dokl. Akad. Nauk SSSR, Nov. Ser.*, 1947b, vol. 58, no. 4, pp. 639–640.

Oleinik, E.M., Late Eocene and Oligocene Microphytoplankton of the Southern Tajik Depression and the Gissar Ridge (Taxonomic Composition, Ecology, and Stratigraphic Significance), *Abstract of Cand. Sci. (Geol.-Min.) Dissertation*, Tashkent: Tashkent Univ., 1979.

Panova, L.A., Paleogene Spore and Pollen Assemblages from the Southern and Central Parts of the West Siberian Lowland, in *Resheniya i trudy Mezhvedomstvennogo soveshchaniya po dorabotke i utochneniyu unifitsirivannoi i korrelyatsionnoi stratigraficheskikh skhem Zapadno-Sibirskoi nizmennosti* (Resolutions and Reports of the Interdepartmental Conference on Modification of the Unified and Correlation Stratigraphic Schemes for the West Siberian Lowland), Part 2, Tyumen': Zap. Sib. Nauchn.-Issled. Geol. Neft. Inst., 1970, pp. 121–132.

Podobina, V.M., Geodynamics and Changes in Microfauna Assemblages across the Paleogene Epoch Boundaries in West Siberia and the Arctic Basin, in *Voprosy geologii i paleontologii Sibiri* (Problems of Siberian Geology and Paleontology), Tomsk: Tomsk Univ., 1997, pp. 66–70.

Salibaev, G.Kh., Late Eocene Bivalve-Based Stratigraphy and Paleogeography of the Eastern Central Asia, *Abstract of Doctor. Sci. (Geol.-Min.) Dissertation*, Moscow: Moscow Inst. of Geol. Prospecting, 1987.

Sigov, A.P., Genesis of the Tertiary Oolitic Iron Ores in the Trans-Uralian Region, *Tr. Gorn. Geol. Inst., Ural. Fil. Akad. Nauk SSSR*, 1956, issue 24, pp. 19–35.

Sigov, A.P., *Metallogeniya mezozoya i kainozoya Urala* (The Mesozoic and Cenozoic Metallogeny of the Urals), Moscow: Nedra, 1969.

Sotnikova, M.A., Marine Oligocene of the Betpak-Dala, Southern Kazakhstan, in *Palinologiya v biostratigrafii, paleoekologii i paleogeografii* (Palynology as Applied to Biostratigraphy, Paleoecology, and Paleogeography), Moscow: Inst. Geol. Razved. Goryuch. Iskop., 1996, p. 132.

Stratigraficheskii slovar' SSSR. Paleogen, neogen, chetvertichnaya sistema (Stratigraphic Glossary of the USSR: Paleogene, Neogene, and Quaternary System), Leningrad: Nedra, 1982.

Strakhov, N.M., *Zheleznorudnye fatsii i ikh analogi v istorii Zemli* (Iron Ore Facies and Their Analogues in the Earth History), Moscow: Akad. Nauk SSSR, 1947, pp. 97–125.

Toporkov, D.D., *Geologicheskie osobennosti, tipy i resursy zheleznykh ryd Turgaiskogo progiba* (Geological Peculiarities, Types and Reserves of Iron Ores in the Turgai Depression), Alma-Ata: Akad. Nauk Kaz. SSR, 1958, pp. 17–29.

Ushakova, M.V. and Gurari, F.G., The Tertiary Stratigraphy of the Ob'-Irtysh Interfluve, in *Materialy o paleontologii i stratigrafii Zapadnoi Sibiri* (Materials on the Paleontology and Stratigraphy of West Siberia), issue 1, Novosibirsk: Zap. Sib. Nauchn.-Issled. Geol. Nef. Inst., 1959, pp. 48–54.

Vasil'eva, O.N., Zhelezko, V.I., and Papulov, G.N., Paleogene Biostratigraphy of Marine Deposits in the Kurgan Area Based on Dinocysts and Sharks, in *Novye dannye po stratigrafii verkhnego paleozoya–nizhnego kainozoya Urala* (New Data on the Upper Paleozoic–Lower Cenozoic Stratigraphy

of the Urals), Yekaterinburg: Inst. Geol. Geokhim., Ural. Otd. Ross. Akad. Nauk, 1994, pp. 139–151.

Voznesenskii, A.I., *Sedimentogenez i litogenez oligotsenovykh otlozhenii Priaral'ya* (The Oligocene Sedimentogenesis and Lithogenesis in the Aral Region), Moscow: Nauka, 1978.

Vyalov, O.S., Oligocene and Lower Miocene Deposits in the Ustyurt and Aral Regions as Equivalents of the Maikop Group, in *Maikopskie otlozheniya i ikh vozrastnye analogi na Ukraine i v Srednei Azii* (The Maikop Deposits and Their Age Equivalents in Ukraine and Central Asia), Kiev: Naukova Dumka, 1964, pp. 144–187.

Yanshin, A.L., *Geologiya Severnogo Priaral'ya* (Geology of the Northern Aral region), Moscow: Mosk. O–vo Ispyt. Prir., 1953.

Zakharov, Yu.F., The Oligocene Konolevo Member in West Siberia, in *Materialy po stratigrafii mezozoiskikh i kainozoiskikh otlozhenii Zapadnoi Sibiri* (Materials on the Mesozoic and Cenozoic Stratigraphy of West Siberia), Moscow: Nedra, 1968, p. 161.

Zaporozhets, N.I., New Data on Eocene and Oligocene Phytostratigraphy of Severnye Ergeni (the South of the Russian Platform), *Stratigr. Geol. Korrelyatsiya*, 1998, vol. 6, no. 3, pp. 56–73.

Zaporozhets, N.I., Palynostratigraphy and Dinocysts Zonation of the Middle Eocene–Lower Miocene Deposits at the Belaya River (Northern Caucasus), *Stratigr. Geol. Korrelyatsiya*, 1999, vol. 7, no. 2, pp. 61–78.

Zhelezko, V.I., Sharks of the Family Jaekelotodontidae from the European and Central Asia Paleobiogeographic Realms, *Byull. Mosk. O–va Ispyt. Prir., Otd. Geol.*, 1994, vol. 69, issue 5, pp. 47–62.

Zhelezko, V.I. and Kozlov, V.A., *Elasmobrankhii i biostratigrafiya paleogena Zaural'ya i Srednei Azii* (Paleogene Stratigraphy and Elasmobranchia of the Trans-Ural and Central Asia Regions), Yekaterinburg: Inst. Geol. Geokhim. Ural. Otd. Ross. Akad. Nauk, 1999.

Stratigraphy and Geological Correlation, Vol. 9, No. 4, 2001, pp. 387–405. Translated from Stratigrafiya. Geologicheskaya Korrelyatsiya, Vol. 9, No. 4, 2001, pp. 80–98.
Original Russian Text Copyright © 2001 by Lopatina.
English Translation Copyright © 2001 by MAIK "Nauka/Interperiodica" (Russia).

Palynological Assemblages and Macrofloras from Eocene–Miocene Deposits of the Tatar Strait Coast (Eastern Sikhote Alin)

D. A. Lopatina

Institute of the Lithosphere of Marginal Seas, Russian Academy of Sciences, Staromonetnyi per. 22, Moscow, 109180 Russia

Received November 22, 1999; in final form, May 16, 2000

Abstract—Palynological characteristics of Eocene–Miocene deposits of the Tatar Strait coast between the Son'e and Dembi bays (eastern Sikhote Alin) are presented. The study spore-and-pollen assemblages and plant imprints show that flora-bearing deposits near the Son'e and Bui bays are comparable in age: they are of the late Eocene around the Son'e Bay and of the late Eocene–early Oligocene near the Bui Bay. Flora-bearing deposits of the Dembi Bay yield macroflora of the second half of the early Miocene and microflora of the late Oligocene–middle Miocene. When compared, the spore-and-pollen and fossil plant assemblages from corresponding units show their similarity at the generic level. Genera of anemophilous plants are common for micro- and macrofloral assemblages. Remains of entomophilous plants are less abundant in spore-and-pollen assemblages than among plant imprints. Judging from the composition of floral assemblages, they characterize vegetation of a moderately warm and humid climate.

Key words: Eocene, Oligocene, Miocene, eastern Sikhote Alin, correlation, spore-and-pollen assemblage, vegetation, climate.

INTRODUCTION

Paleobotanical methods of studying macroflora (remains of leaves, fruits, and seeds) and palynological assemblages (spores and pollen) are of prime importance for subdivision and correlation of Cenozoic continental deposits in the Far East. The advantage of palynological method is determined by the mass occurrence of spores and pollen preserved in sedimentary sequences of different genesis that is favorable for direct correlation between marine and continental deposits.

The convergence of results can be checked by the study of microphytofossils macerated from samples that simultaneously bear remains of macroflora in particular sections. The complementary macro- and microfloral paleobotanical analysis is useful for acquiring combined paleofloristic data of practical significance for the age determination and correlation, and for regional climatic and phytogeographic reconstructions.

The combination of two traditional paleobotanical methods is not an innovation. Such an approach was applied by Akhmet'ev (1973) who studied Miocene deposits of the Botchi River in the Far East, by V.P. Nikitin, I.A. Il'inskaya and A.F. Fradkina who investigated Miocene deposits of the Mt. Mamontovaya section at the Aldan River (*Miotsen...*, 1977), and by some others. In this work, I studied spores and pollen macerated from samples with plant imprints, which have been collected from the Eocene–Miocene deposits of the Tatar Strait coast between the Son'e and Dembi bays (eastern Sikhote Alin). The data obtained were compared with the results of earlier macrofloral studies of the same section (Akhmet'ev, 1973, 1974, 1988; Akhmet'ev and Vikulin, 1995; Akhmet'ev and Manchester, 2000).

INVESTIGATION HISTORY

The analyzed section is exposed along the distance of 12 km along the Tatar Strait coast between the Son'e and Dembi bays not far away from the Settlement of Nelma (Fig. 1). North of the Son'e Bay, the basal tuff conglomerate and andesite tuff beds of the section rest on Upper Cretaceous dacite tuffs. The sequence is overlapped by a series of basaltic flows with scoriaceous crusts and agglomerates. In the area between the Bui and Son'e bays, the lower part of the section is up to 250–300 m thick in total. South of the Bui Bay, the monocline is complicated by the basement inlier composed of the early Paleogene granodiorites of the Bui massif. Further northward, near the Dembi Bay, there exposed a packet of tuffaceous–sedimentary rocks with lava flows. The total thickness of the middle part of the section in the Bui Bay–Okno Cape area approximates 400 m (Fig. 2). The upper part of the section, about 400 m thick, is ruptured and partially overlapped by more acid clastic lavas and flows of trachyandesite and hornblende dacite. The rocks extend northwards to the

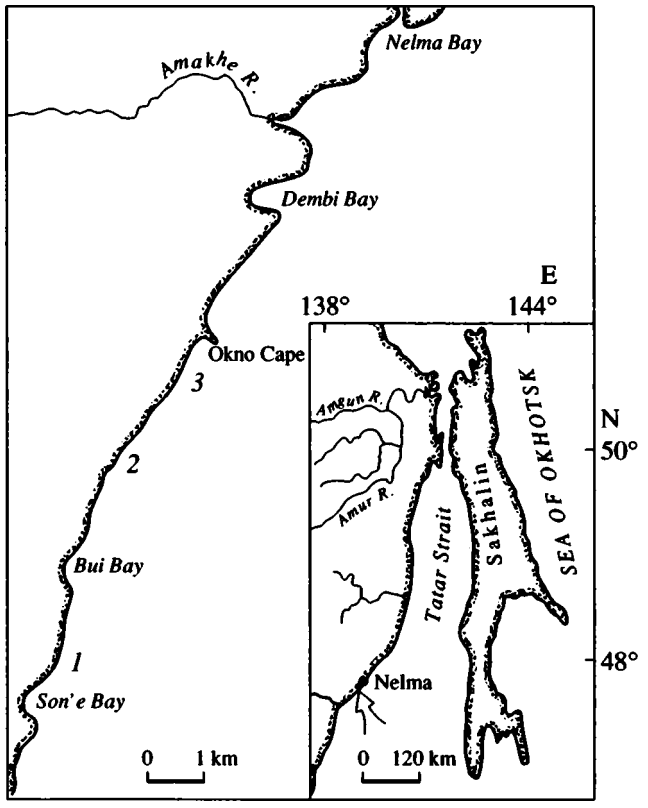

Fig. 1. Son'e Bay (1), Bui Bay (2), and Dembi Bay (3) flora localities in the Tatar Strait coast.

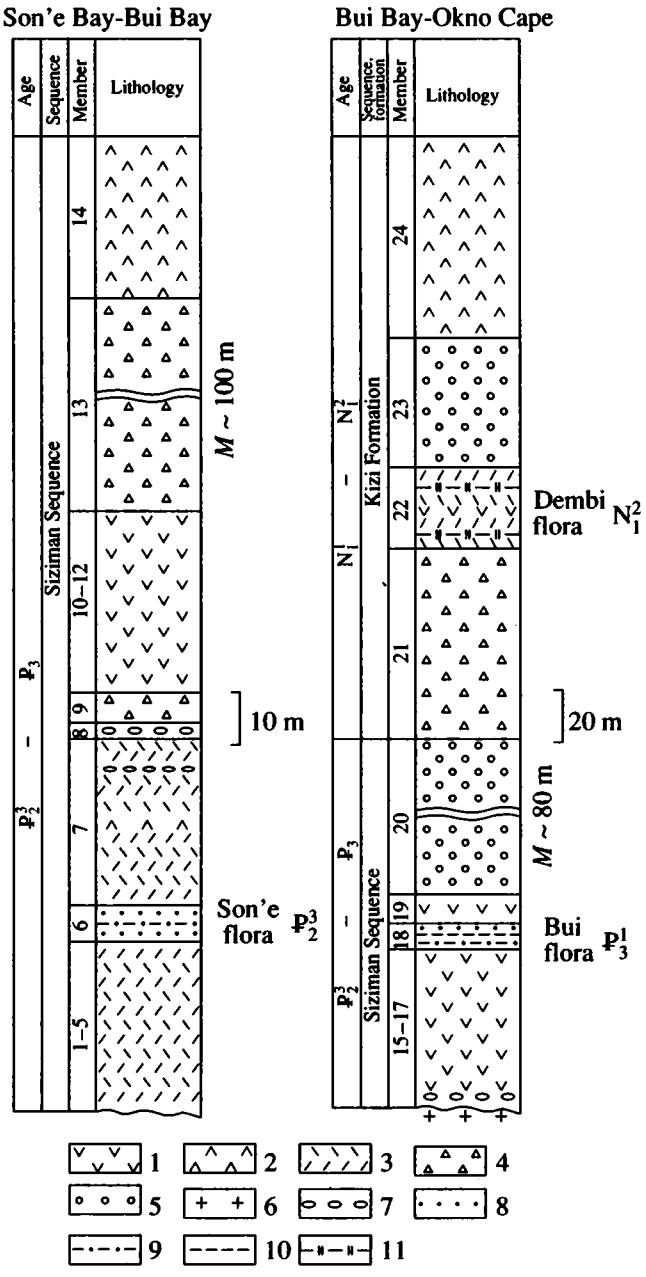

Fig. 2. Lithostratigraphic section of Eocene–Miocene deposits in the Tatar Strait coast between the Son'e Bay and Okno Cape (section description and member numbers after Akhmet'ev, 1988): (1) basalt; (2) andesite-basalt; (3) tuff; (4) clastic lava; (5) lava clasts; (6) granite; (7) conglomerate; (8) sandstone; (9) siltstone; (10) mudstone; (11) diatomite.

Amakhe Bay, where they are overlapped by plateau basalt of the Sovgavan' Formation.

Plant remains were collected in three localities: in the 4-m-thick member of alternating tuff sandstone and tuff siltstone at the lower part of the section near the Son'e Bay (Son'e Bay flora); in the 9-m-thick member of dark-colored sandstone alternating with tuff siltstone and tuff mudstone lenses that is exposed 1.5 km north of the Bui Bay (Bui Bay flora); and in the 30-m-thick member of alternating tuff, tuffite, diatomite beds, and pillowed basaltic flows, the site 3.5 km south of Dembi Bay (Dembi Bay flora).

Akhmet'ev (1988) came up with a proposal for accepting the section Son'e–Dembi as a lectostratotype of the Kizi Group. The Kizi Formation of intermediate to basic effusive rocks, their tuffs, and tuffaceous–sedimentary rocks was distinguished by Plakhotnik (1962) in the course of geological survey in the eastern Sikhote Alin. Volcanogenic deposits of the formation are exposed within a wide strip along the eastern slope of Sikhote Alin that extends from the Amur River mouth in the north to the latitude of the Settlement of Velikaya Kema in the south. According to Akhmet'ev, the Kizi Formation should be disposed to the group rank because of a considerable thickness of its volcanogenic and volcano-sedimentary deposits, which exceeds 1000 m in the key section and has been accumulated during a long period from the late Eocene to the early Miocene. The Son'e–Dembi section is selected for a lectostratotype of the Kizi Group first by virtue of three macroflora assemblages found in volcano-sedimentary members characterizing it. Second, the section belongs to a single volcano-tectonic structure being exposed in its southern flank, where volcanic rocks show a gentle monoclinal folding. Nonetheless, the proposal to rank

the Kizi Formation as a group has not been authorized. In accord with the most recent regional stratigraphic scheme of Paleogene and Neogene deposits of the southern part of the continental Far East, which was approved by the Interdepartmental Stratigraphic Commission (ISC) in 1991, volcanogenic-sedimentary deposits of members 1–21 of the section are attributed to the Siziman Sequence and those of members 22–24 to the Kizi Formation.

Plant imprints from the section were studied by M.I. Borsuk (see in Plakhotnik, 1962). Plant remains were collected from diatomite interlayers at the Dembi Bay locality, and their investigation resulted in referring the Kizi Formation deposits to the middle Miocene. The Miocene age of diatomites was confirmed by the diatom analysis carried out by L.A. Struve (Plakhotnik, 1962).

On the basis of plant imprints from other sections of the Kizi Formation (the section of the Toni Lake area, lower reaches of the Listvennaya and Kema rivers), Klimova (Oleinikov and Klimova, 1977; Rybalko *et al.*, 1980; Klimova, 1983) inferred the early Miocene age of these deposits.

Akhmet'ev studied in detail floral remains from the Son'e, Bui and Dembi localities and determined on these grounds that the deposits from the section under consideration span the range of the upper Eocene to the upper half of the lower Miocene (Akhmet'ev, 1988; Akhmet'ev and Vikulin, 1995).

The Son'e Bay flora is characterized by the prevalence of gymnosperm plants, dominant among which are Taxodiaceae *Cryptomeria, Metasequoia*, and others. Representatives of the *Thuja* and *Pinus* genera are numerous. Angiosperms are represented by two groups. The first one consists of genera typical of the early Paleogene, such as *Trochodendroides, Platanus, Alangium*, and *Viburnum*. The second group includes taxons characteristic of the late Paleogene and Miocene floras, among which genera *Fagus, Quercus, Alnus, Cercidiphyllum*, and *Acer* are dominant. The Son'e Bay flora correlative with floras occurring in the upper part of the Paleogene coal-bearing series of Sakhalin [*Alnus onorica, Acer ezoana, Platanus aceroides, Trochodendroides arcticum* (=*Cocculus ezoanum*) and others]. It is dated back to the late Eocene (Akhmet'ev, 1988).

Gymnosperms (*Pinus, Tsuga*, and dominant *Thuja*) of the Bui Bay flora are poorly represented. Among angiosperms, there are found species *Alnus keferstainii, Carpinus subcordata, Palaeocarpinus sikhotealinensis, Craigia bronni, Quercus pseudocastanea, Acer ezoana, Cercidiphyllum crenatum, Macaranga peltata, Tilia* sp., and others. The maximum abundant among imprints are *Tilia* and *Macaranga* genera. The Bui Bay flora occupies an intermediate stratigraphic position between the Son'e and Dembi floras. Compositionally, it is similar to late Paleogene floras which are devoid of early Paleogene relics (*Trochodendroides, "Acer" arcticum*). The Bui Bay flora is comparable with floras of the northern Kyushu and central Honshu, which were referred by T. Tanai first to the early Miocene and afterward to the Oligocene; these floras show presence of Paleogene species and rare thermophilic elements. The Bui Bay flora is dated back to the early Oligocene (Akhmet'ev, 1988; Akhmet'ev and Vikulin, 1995). Its late Eocene age is not improbable, because it includes, according to the most recent data, such genera as *Platanus, Palaeocarpinus*, and *Macaranga* characteristic of the Paleocene and Eocene floras (Akhme'ev and Manchester, 2000).

Conifers represent 18% in the Dembi Bay macroflora. *Metasequoia* is dominant taxon, *Taxodium* and *Glyptostrobus* are less abundant, and other genera were encountered as single components. The most abundant among angiosperms are divided-leaf oaks (up to 35–40%) and *Fagopsis*. Species *Ostrya oregoniana, Carpinus subcordata, Carpinus* sp., *Fagus palaeocrenata, Castanea miomollissima, Ulmus longifolia*, and others are also present. Deciduous arboreal forms dominate. The Dembi Bay flora is the youngest among floras of the Kizi Formation. In addition to forms listed above, it includes some taxons characteristic of the Daidzima-type flora of the Honshu green-tuff belt. These are *Comptonia naumanni, Engelhardtia koreanica*, and *Astronium ninae*. Floras of the Daidzima type were found in the Rettikhovskaya and Kraskinskaya depressions of the Primor'e, as well as in the Sikhote Alin volcanic belt. They exemplify plants of the climatic optimum of the second half of the early Miocene (Akhmet'ev and Vikulin, 1995).

Spores and pollen from flora-bearing deposits of all the three bays were studied by V.F. Morozova (see in Akhmet'ev, 1973; 1974), those from the Bui Bay deposits by N.I. Zaporozhets (see in Akhmet'ev and Manchester, 2000). In samples from the Son'e Bay complex, pollen of angiosperms *Myrica, Juglans, Carya, Betula, Carpinus*, and *Quercus* dominates, whereas the *Pinus* genus and Taxodiaceae family are abundant among gymnosperms. This assemblage is compositionally similar to that from the Lower Due deposits of Sakhalin. Angiosperm families Juglandaceae, Fagaceae, Betulaceae, and Ulmaceae dominate in palynological spectra of samples from the Bui Bay deposits. Their assemblage resembles that from lower horizons of the Birofeld Formation of the Central Amur Depression. Palynological spectra from the Dembi Bay deposits are characterized by prevalence of gymnosperms, dominant among which are genera *Pinus* (up to 60%) and *Picea* (up to 30%). Fagaceae and Juglandacea forms prevail among angiosperms. By virtue of palynoflora and with due regard to data on plant imprints, the Son'e Bay flora is dated back to the middle–late Eocene, that of the Bui Bay to the late Eocene–early Oligocene, and the Dembi Bay flora to the second half of the Oligocene (Akhmet'ev, 1973, 1974; Akhmet'ev and Manchester, 2000).

Investigation of fossil spores and pollen from samples with plant imprints is necessary for refining the age of deposits under consideration, and for their detailed correlation with sections in adjacent territories. The comparative analysis of spore-and-pollen assemblages and macrofloras is of methodological significance, as it elucidates the results reproducibility of macrofloral and palynological methods.

MATERIALS AND METHODS

Spores and pollen were macerated from samples with plant imprints that have been collected by Akhmet'ev and are stored at the Geological Institute, Russian Academy of Sciences (GIN RAS). Two sets of seven samples from collections 3807 (Son'e Bay) and 3803 (Dembi Bay), and eight samples from Collection 3804 (Bui Bay) were analyzed by palynological method. Preparations were macerated at the Laboratory of Paleofloristics, GIN RAS, following procedure elaborated by V.P. Grichuk.

RESULTS AND DISCUSSION

Microphytofossils were found in all the seven samples with plant imprints of the Son'e Bay site. Because of a poor preservation, they were identified at the genus or family level. The samples are rich in organic matter and fragments of plant tissues. Abundance rates of spores and pollen are given in Table 1. In general, the spores-and pollen assemblage (SPA) of the Son'e Bay site shows the following distinctive features: (1) Polypodiaceae spores are abundant and dominated by larger forms; (2) among gymnosperms, spores of Pinaceae prevail over common spores of Taxodiaceae; (3) pollen of Betulaceae and Fagaceae dominate among angiosperms, amid which elements of the thermophilic flora are also present; (4) among formal taxa, there is triporate and tricolpoporate pollen of unclear taxonomic affinity. The SPA studied is similar, in general, to the assemblage distinguished earlier in these deposits by V.F. Morozova (see in Akhmet'ev, 1973).

Spore-and-pollen spectra from flora-bearing deposits of the Bui Bay are of diverse composition (Table 2). Their distinctive features are as follows: (1) the prevalence of angiosperm pollen (families Myricaceae, Betulaceae, Juglandaceae, Fagaceae, and Ulmaceae), species diversity of Junglandaceae, and presence of thermophilic pollen species; (2) predominance of Pinaceae among gymnosperms (the most abundant *Pinus* genus is represented by five species), among which Taxodiaceae are less common; (3) constant presence of fine triporate and tricolpoporate pollen grains of uncertain taxonomy.

The SPA distinguished is similar in composition of conifers to that described from these deposits by Morozova (Akhmet'ev, 1974) and Zaporozhets (Akhmet'ev and Manchester, 2000) but has a slightly higher content of gymnosperm pollen.

Two assemblages (SPA-1 and SPA-2) were distinguished in samples from the Dembi Bay site (Table 3). In the SPA-1, the gymnosperm pollen is more abundant than the angiosperm pollen and accessory spores. The *Pinus* genus dominates among gymnosperms. Angiosperms are represented by Ulmaceae, Betulaceae, and Juglandaceae. The SPA-1 is similar to SPA distinguished from the Dembi Bay deposits by Morozova (Akhmet'ev, 1974). In contrast to the latter, the SPA-1 is characterized by a lower content of angiosperm pollen that is depleted in thermophilic elements.

Gymnosperms and angiosperms are almost equally abundant in the SPA-2. Gymnosperm species of abundant Pinaceae mostly belong to the genus *Pinus*. The distinctive feature of the complex is domination of diverse *Fagus* species, whereas other Fagaceae are much less abundant. Percentages of Betulaceae, Juglandaceae, and Ulmaceae pollen are comparable. In order to determine their age, all assemblages were compared with those known from Paleogene–Neogene deposits in southern Far East areas and Sakhalin.

In the taxonomic composition and proportions of Pinaceae, Taxodiaceae, Betulaceae, Fagaceae, and Juglandaceae pollen, the SPA of the Son'e Bay site can be correlated with the SPA-2 from lower coal-bearing beds of the Orekhovskaya depression (Baskakova, 1990), or with assemblage from clayey–silty strata of the Bolotnaya deposit of brick earth (Kundyshev and Petrenko, 1987), the SPA-2 from the lower coal-bearing sequence of the Omogunskaya depression of the Amgun–Gorin region (Baskakova, 1997). All the spore-and-pollen complexes cited above are dated back to the late Eocene. The peculiar taxonomic composition, presence of characteristic Eocene species (*Myrica vera, Quercus gracilis, Ulmoideipites krempii, U. planeraeformis, Ulmipollenites verrucatus*, and others), and results of correlation with pollen assemblages from Paleogene deposits of the southern Far East indicate the late Eocene age of the SPA from the Son'e Bay site.

The SPA from flora-bearing deposits of the Bui Bay, judging from its composition (prevalence of Pinaceae among gymnosperms and diversity of Betulaceae, Juglandaceae, Fagaceae, and Ulmaceae), is similar to the SPA of the Nadezhdinskoe and Ust'-Davydovka formations of the Rechnoi Peninsula (Pavlyutkin and Petrenko, 1993), to the SPA-3 from the tuff–siltstone sequence of the Rakovskaya Depression in the Khanka Massif (Pavlyutkin and Petrenko, 1994a), to the SPA-1 of the Pushkinskaya depression (Pavlyutkin and Petrenko, 1994b), and to the Sivak assemblage of the Amur–Zeya depression (Ziva, 1973). All the assemblages listed above are dated back to the late Eocene–early Oligocene. Their similarity with the early Oligocene SPA-6 of the Amgun'–Gorin region (Baskakova, 1997) and with the Oligocene Mukhinka assemblage of the Amur–Zeya depression (Varnavskii and Mamontova, 1975; Mamontova, 1978) is also estab-

Table 1. General composition of spores and pollen from flora-bearing deposits of the Son'e Bay site (%)

Spores and pollen	Sample number						
	18	114	133	11	119	23	160
Spores (total)	**17.2**	**17.1**	**22.3**	**21**	**24.3**	**23.1**	**20.4**
Cyathea sp.	0.2	–	–	0.2	0.4	–	0.2
Polypodiaceae gen. indet.	11.3	11.3	15.1	15.3	18.2	19.1	15.4
Lygodium sp.	1.6	2.2	1.8	1.3	0.6	1.6	0.8
Osmunda sp.	1.6	1.4	1.4	1.9	1.2	1.6	1.8
Botrychium sp.	0.8	0.6	1.8	0.6	2.1	0.4	0.6
Ceratopteris sp.	–	–	0.2	–	–	–	–
Marsilea sp.	–	–	0.2	–	–	–	–
Lycopodium sp.	1.1	1.4	1.2	1.3	0.4	0.2	0.8
Leiotriletes sp.	0.4	0.2	0.6	0.4	1.4	0.2	0.8
Gymnosperm pollen (total)	**24.5**	**38.1**	**30.9**	**24.7**	**27.2**	**34.7**	**33.5**
Ginkgo sp.	1.6	2	0.2	2.4	1.2	0.4	4.1
Podocarpus sp.	0.2	0.8	0.6	–	0.4	0.2	0.4
Fam. Pinaceae (total)	15.3	22.5	14.9	5.2	12.6	22.9	10.5
Abies sp.	0.2	0.4	0.6	–	–	0.6	–
Cedrus sp.	0.2	1.8	0.4	0.2	1	1.6	1
Picea sp.	1	1.4	1	0.2	0.4	0.4	1.1
Tsuga (total)	2.3	4	1.8	1	1.7	2.6	0.8
Tsuga diversifolia (Max.) Mast.	0.2	0.2	–	0.2	–	–	–
T. torulosa Zakl.	0.2	0.2	–	–	–	–	0.2
Tsuga sp.	1.9	3.8	1.8	0.8	1.7	2.6	0.6
Pinus protocembra Zakl.	–	–	0.2	–	–	0.4	0.2
Pinus sp.	9.1	12.5	9.7	3	7.2	14.5	6.6
Pinaceae gen. indet.	2.5	2.2	1.2	0.8	2.3	2.6	0.8
Fam. Taxodiaceae (total)	4.1	10.6	10.5	12.2	10.3	7.9	11.9
Taxodium sp.	2.5	6	7.5	6.7	5.4	6.5	6.8
Sciadopitys (total)	0.8	0.8	0.4	1	0.8	0.4	0.6
Sciadopitys tuberculata Zakl.	0.2	0.6	–	0.8	0.2	–	0.6
Sciadopitys sp.	0.6	0.2	0.4	0.2	0.6	0.4	–
Glyptostrobus sp.	–	0.2	0.2	0.2	–	0.2	0.2
Cryptomeria sp.	0.4	0.6	0.2	0.8	1.2	0.2	0.6
Sequoia sp.	0.4	1.4	1	1.5	1.7	0.2	1.6
Taxodiaceae gen. indet.	–	1.6	1.2	2	1.2	0.4	2.1
Cupressaceae (total)	0.2	0.2	0.6	0.6	0.6	1	1
Thuja sp.	–	0.2	0.2	0.2	0.2	0.2	0.2
Cupressaceae gen. indet.	0.2	–	0.4	0.4	0.4	0.8	0.8
Taxodiaceae or Cupressaceae	3.1	2	4.1	4.3	2.1	2.3	5.6
Angiosperm pollen (total)	**58.3**	**44.8**	**46.8**	**54.3**	**48.5**	**42.2**	**46.1**
Salix sp.	0.6	0.2	0.4	0.4	–	0.8	0.4
Fam. Myricaceae (total)	1.3	4.6	2.6	4.1	2.1	2.7	0.4
Myrica (total)	1.1	4.4	2	3.9	1.9	2.7	0.2
Myrica vera Sauer	–	–	–	0.6	0.2	–	–
Myrica sp.	1.1	4.4	2	3.3	1.7	2.7	0.2
Comptonia sp.	0.2	0.2	0.6	0.2	0.2	–	0.2
Fam. Betulaceae (total)	24.4	15.8	16.3	13.8	15.1	14.9	8.8
Alnus sp.	4.3	3.2	2.6	3.8	4.4	3.8	3.5
Betula sp.	3.7	5.4	2.8	2.6	1.6	1.8	1
Corylus sp.	7.4	2.8	3.3	1.8	2.1	3.4	1
Carpinus sp.	7.6	3	6	3.5	6	5.3	2.1
Ostrya sp.	0.4	0.6	0.4	0.6	–	–	0.2
Betulaceae gen. indet.	1	0.8	1.2	1.5	1	0.6	1
Fam. Juglandaceae (total)	5.1	3.6	5.1	8.4	8	3.6	7.3
Juglans (total)	0.2	0.8	1	1.1	1.6	0.2	0.8
Juglans polyporata Vojc.	–	0.2	0.2	–	0.2	0.6	–
Juglans sp.	0.6	0.6	0.8	1.1	1.4	0.8	0.8
Carya sp.	2.9	1.6	3.3	5.6	5	1.4	5.9
Platycarya sp.	0.2	0.4	–	0.2	–	–	–
Pterocarya sp.	–	–	0.2	0.2	–	–	–

Table 1. (Contd.)

Spores and pollen	Sample number						
	18	114	133	11	119	23	160
Engelhardtia sp.	1.4	1	0.6	1.3	1.4	0.8	0.6
Fam. Fagaceae (total)	7.4	8.2	9.8	10	7.3	7.8	10.3
Fagus sp.	1.9	1.2	2.4	1.8	0.6	1.2	2.9
Quercus (total)	5.3	6.8	7.2	6.9	6.3	6.4	6.6
Quercus gracilis Boitz.	0.4	0.4	–	1.3	0.4	–	1.9
Q. graciliformis Boitz.	1	1.2	0.6	1.3	1	1	1.4
Q. conferta Boitz.	–	–	0.2	0.4	0.6	0.2	–
Q. williamsonia Trav.	–	–	–	–	0.2	0.2	–
Quercus sp.	3.9	5.2	6.4	3.9	4.1	5	3.3
Castanea sp.	0.2	0.2	0.2	1.3	0.4	0.2	0.8
Fam. Ulmaceae (total)	4.2	3	1.2	0.8	1	1.2	1.9
Ulmus sp.	1.6	1	1	0.2	0.8	0.8	–
Ulmoideipites (total)	2.4	2	0.2	0.6	2	0.4	1.9
Ulmoideipites krempii Anders.	0.2	0.6	–	–	–	–	0.2
U. planeraeformis Anders.	0.6	0.2	–	–	1	–	1.1
Ulmoideipites sp.	1.6	1.2	0.2	0.6	1	0.4	0.6
Ulmipollenites verrucatus Nort.	0.2	–	–	–	–	–	–
Fam. Hamamelidaceae (total)	5.6	1	2	4.4	3.9	2.4	4.4
Hamamelis sp.	1.9	0.4	0.6	1.3	0.8	0.8	1.8
Corylopsis (total)	2.7	0.4	1.2	2.3	2.7	0.2	1.6
Corylopsis princeps Lubom.	0.8	–	–	1.1	0.4	–	0.8
C. compacta Lubom.	–	–	–	0.2	0.2	–	–
C. crassa Lubom.	–	–	–	0.4	–	–	–
Corylopsis sp.	1.9	0.4	1.2	0.6	2.1	0.2	0.8
Fothergilla vera Lubom.	–	–	0.2	–	0.2	0.2	–
Fothergilla sp.	0.6	–	–	0.2	–	0.4	0.2
Liquidambar (total)	0.4	0.2	–	0.4	–	0.6	0.4
Liquidambar orientalis Mill.	0.2	–	–	–	–	–	–
L. styraciflua L.	–	–	–	–	–	–	0.2
Liquidambar sp.	0.2	0.2	–	0.4	–	0.6	0.2
Hamamelidaceae gen. indet.	–	–	–	0.2	0.2	0.2	0.4
Trochodendron sp.	0.2	–	0.2	–	0.2	–	0.2
Cercidiphyllum sp.	–	0.2	0.4	0.2	0.2	0.2	0.4
Magnolia denudatoides Lubom.	0.4	0.2	0.4	0.4	0.2	0.2	0.4
Rhus sp.	–	0.2	–	0.4	0.2	0.2	0.2
Ilex sp.	0.2	0.4	1	0.6	0.8	0.2	0.4
Nyssa sp.	–	–	–	0.2	–	0.2	–
Daphne sp.	–	0.2	–	–	–	–	–
Myrtus sp.	–	–	–	0.2	0.2	–	0.2
Cardiospermum sp.	–	–	–	0.2	–	–	–
Tilia sp.	0.2	–	–	0.4	0.2	0.2	0.2
Acer sp.	0.4	0.2	1.4	1.5	0.6	0.4	1
Sparganium sp.	0.2	0.2	0.2	0.2	–	0.2	0.2
Potamogeton sp.	–	0.2	–	–	–	–	–
Nelumbo sp.	0.2	0.2	0.2	0.4	0.8	0.6	1.1
Moraceae gen. indet.	0.4	0.8	1	0.2	–	0.4	0.2
Proteaceae gen. indet.	0.2	–	–	0.4	–	–	–
Ericaceae gen. indet.	1.3	2.4	0.4	0.6	0.2	0.6	1.1
Leguminosae gen. indet.	0.6	0.2	0.4	1.3	0.8	1.4	1
Triporopollenites plicoides Zakl.	1	0.2	0.2	0.4	0.4	0.6	0.8
Triporopollenites sp.	2.1	1.2	1.2	2.2	1.2	0.8	2.9
Tricolpopollenites sp.	0.4	–	0.2	0.4	0.2	–	0.4
Tricolporopollenites cf. *cingulum* (R. Pot.) Th. et Pfl.	–	0.2	–	–	–	–	0.2
Tricolporopollenites sp.	1.4	0.2	0.4	0.4	0.6	1	0.2
Angiosperm pollen of uncertain taxonomic affiliatio	0.8	1.4	1.8	1.8	2.5	1.6	1.5

Table 2. General composition of spores and pollen from flora-bearing deposits of the Bui Bay site (%)

Spores and pollen	Sample number							
	81	604	117	12	74	209	2	69
Spores (total)	**6.4**	**5.9**	**3**	**7.2**	**3.4**	**5.3**	**4.3**	**5.3**
Polypodiaceae gen. indet.	5.2	4.7	2.8	5.8	3	3.7	3.5	4.3
Lygodium sp.	0.6	0.4	–	–	–	0.2	0.2	–
Osmunda sp.	0.2	0.4	0.2	0.2	0.2	0.6	0.2	0.2
Botrychium sp.	0.2	0.4	–	1	0.2	0.6	0.2	0.4
Marsilea sp.	–	–	–	–	–	–	–	0.2
Lycopodium sp.	0.2	–	–	0.2	–	0.2	0.2	0.2
Gymnosperm pollen (total)	**22.7**	**22.7**	**32.4**	**46.7**	**48.8**	**44.8**	**30.8**	**44.6**
Agathis sp.	–	0.2	0.2	0.4	–	–	–	–
Ginkgo sp.	1.6	1.4	1.4	1.2	0.8	–	0.2	0.6
Podocarpus sp.	0.2	–	0.8	0.4	0.4	0.2	–	0.2
Fam. Pinaceae (total)	6.1	7.4	10.2	22.8	26.8	27.4	17.8	28.5
Abies sp.	–	0.2	0.2	1.4	2.2	3.7	0.6	4.3
Cedrus sp.	0.2	–	0.4	1.4	–	0.6	0.6	–
Picea (total)	–	0.4	0.8	1.2	1	7.2	1.6	3.2
Picea sect. *Eupicea*	–	0.4	0.6	1.2	1	7	1.2	3
Picea cf. *excelsa* Link	–	–	–	–	–	–	0.4	0.2
Picea sect. *Omorica*	–	–	0.2	–	–	0.2	–	–
Tsuga (total)	0.8	0.6	0.6	0.8	2.2	2.2	1.4	2.6
Tsuga canadensis (L.) Carr.	–	–	0.2	0.4	0.6	0.2	0.2	0.6
T. parva Brutm.	–	–	–	–	0.2	0.2	0.2	0.2
Tsuga sp.	0.8	0.6	0.4	0.4	1.4	1.8	1	1.8
Pinus (total)	3.3	5.8	7.4	18	20.6	12.5	13	16.8
Pinus protocembra Zakl.	–	–	–	0.6	0.2	0.4	0.2	0.6
P. strobiformis Zakl.	–	–	0.2	0.8	0.2	–	0.2	0.2
P. silvestris L.	0.8	1.6	2.6	6.6	3.6	3.7	6	4.1
P. banksianaeformis Zakl.	0.2	0.2	–	0.2	0.2	0.2	0.8	0.2
P. minutus Zakl.	0.2	0.4	0.4	0.2	0.6	0.4	1.2	0.4
Pinus sp.	3.3	3.6	4.2	9.6	15.8	7.8	4.6	11.3
Pinaceae gen. indet.	0.6	0.4	0.8	–	0.8	1.2	0.6	1.6
Fam. Taxodiaceae (total)	10.3	10.2	12.2	13.8	12.8	12.3	9.7	10.4
Taxodium (total)	7.1	7.2	8.2	7.8	7	7.9	5.5	6.6
Taxodium distichiformis Zhezh.	1.2	2.7	2.4	2.2	1.8	2.4	1.8	3
Taxodium sp.	5.9	4.5	5.8	5.6	5.2	5.5	3.7	3.6
Sequoia sp.	0.6	0.8	1.2	0.8	0.2	1	0.8	0.2
Sciadopitys (total)	0.2	0.2	0.6	1.8	1.2	1.8	1.4	1.4
Sciadopitys tuberculata Zakl.	0.2	0.2	–	1.2	1.2	1.6	1.2	1.4
S. verticillata Sieb. et Zucc.	–	–	0.2	0.6	–	0.2	0.2	–
Sciadopitys sp.	–	–	0.4	–	–	–	–	–
Glyptostrobus sp.	1.2	1	1	1.4	2	0.8	1.2	0.8
Cryptomeria sp.	–	–	0.2	–	0.2	–	0.2	–
Taxodiaceae gen. indet.	1.2	1	1	2	2.2	0.8	0.6	1.4
Fam. Cupressaceae (total)	1.4	0.6	4	2.2	1	1.4	1	1.8
Juniperus sp.	0.2	0.2	0.8	0.2	0.6	0.8	0.6	0.6
Thuja sp.	0.4	0.2	0.4	0.2	–	0.2	–	0.2
Cupressaceae gen. indet.	0.8	0.2	2.8	1.8	0.4	0.4	0.4	1
Taxodiaceae or Cupressaceae	2.9	2.9	3.6	5.9	7	3.5	1.9	3.1
Ephedra sp.	0.2	–	–	–	–	–	0.2	–
Angiosperm pollen (total)	**70.9**	**71.4**	**64.6**	**46.2**	**47.8**	**49.9**	**64.9**	**50.1**
Salix sp.	0.4	0.2	0.4	0.2	–	–	0.2	0.2
Fam. Myricaceae (total)	2.2	6.9	1.8	2.6	2.4	3.8	4	4
Myryca (total)	1.4	4.7	1.8	1.2	1.4	1.8	2	2.2
Myrica carolinensiformis Gladk.	–	–	–	–	–	–	0.2	–
M. lubomirovae Gladk.	0.4	0.6	–	0.2	–	–	0.6	–
M. pseudogranulata Gladk.	–	0.2	0.2	–	–	–		–
M. galiformis Gladk.	–	0.2	–	–	0.2	0.6	0.2	0.6
M. vera Sauer	–	–	0.2	–	–	–	0.2	–
Myrica sp.	1	3.7	1.4	1	1.2	1.2	0.8	1.6

Table 2. (Contd.)

Spores and pollen	Sample number							
	81	604	117	12	74	209	2	69
Comptonia (total)	0.8	2.2	–	1.4	1	2	2	1.8
Comptonia compacta Gladk.	0.2	0.2	–	0.2	–	0.2	0.8	–
Comptonia sp.	0.6	2	–	1.2	1	1.8	1.2	1.8
Fam. Betulaceae (total)	15.7	20.2	9.8	9.9	8	8.8	15.9	9.3
Alnus sp.	3.5	2.9	3.8	1.8	1.8	2.2	2.1	2
Betula sp.	4.8	3.1	1	1	0.2	0.8	2.7	1
Corylus sp.	2.9	6.5	1	2.2	3.4	2.6	5	2
Carpinus sp.	3.9	7.1	3.2	4.9	2.4	3	5.9	4.3
Ostrya sp.	–	0.2	–	–	0.2	–	–	–
Betulaceae gen. indet.	0.6	0.4	0.8	–	–	0.2	0.2	–
Fam. Juglandaceae (total)	9.4	13.2	11	10	9	6	11.7	8
Juglans (total)	2.2	1	2	3.2	1.4	2.4	1.2	1.8
Juglans hebelata Bolot.	–	–	–	–	–	0.2	0.4	–
J. jondonica Bolot.	–	–	–	–	0.2	0.2	–	0.2
J. manshurica Max.	0.4	0.2	–	0.4	0.2	0.2	0.2	0.2
J. orbiculata Bolot.	0.2	–	–	–	0.4	–	–	–
J. polyporata Vojc.	0.2	0.2	–	–	–	0.2	0.2	0.2
J. sieboldianaformis Vojc.	0.6	0.2	0.2	1.2	–	0.2	0.2	0.2
Juglans sp.	0.8	0.4	1.8	1.6	0.6	1.4	0.2	1
Carya (total)	6.8	9.6	8	6	7.2	3.2	10	5.8
Carya bella Bolot.	–	0.2	0.2	–	–	–	0.4	–
C. communis Bolot.	0.4	–	–	–	0.2	–	1.2	0.4
C. elegans Manyk.	–	0.2	–	–	–	–	0.2	–
C. insignis Bolot.	–	0.6	0.2	0.2	–	–	–	0.2
C. spackmania Trav.	–	0.2	0.4	0.2	0.2	0.4	0.6	–
C. tenuissima Bolot.	–	–	0.2	–	0.2	–	–	–
C. triangulata Bolot.	–	–	–	–	–	0.2	–	–
C. ulmiformis Bolot.	–	–	0.2	–	–	–	0.2	–
Carya sp.	6.4	8.2	6.8	5.6	6.6	2.8	7.3	5.2
Pterocarya singularis Bolot.	–	0.2	–	–	–	–	–	–
P. hupehensiformis Bolot.	–	0.2	–	–	–	–	–	–
Pterocarya sp.	0.2	0.2	–	0.2	–	0.2	–	0.2
Platycarya sp.	–	1	–	0.2	–	–	–	0.2
Engelhardtia (total)	0.6	1	1	0.2	0.4	0.2	0.6	–
Engelhardtia paleogenica Bolot.	–	0.4	–	–	0.2	–	–	–
E. chrysolepiformis Bolot.	0.2	0.2	–	–	0.2	–	–	–
Engelhardtia sp.	0.4	0.4	1	0.2	–	0.2	0.6	–
Juglandaceae gen. indet.	–	–	–	0.2	–	–	–	–
Fam. Fagaceae (total)	20.5	9.2	20.8	6.5	14.2	12.4	14.3	8.6
Fagus (total)	7	4.5	9.8	3.9	7.8	7.5	8.8	4.8
Fagus grandifoliiformis Pan.	0.6	0.4	2.6	–	1	0.2	1.7	0.4
F. japoniciformis Anan.	1	0.4	1.8	1	0.6	0.8	1.9	1.4
F. tenella Pan.	0.2	0.4	0.8	–	0.2	–	0.8	–
Fagus sp.	5.2	3.3	4.6	2.9	6	6.5	4.4	3
Quercus (total)	7.2	3.3	6.8	2.6	5.8	4.7	4.5	3.2
Quercus gracilis Boitz.	0.2	–	–	–	–	–	–	–
Q. graciliformis Boitz.	1.8	0.6	2	0.4	0.6	0.4	0.2	–
Q. conferta Boitz.	0.4	0.2	0.2	–	–	–	–	–
Q. williamsoniana Trav.	–	–	–	–	–	0.4	0.2	–
Quercus cf. *sibirica* Pan.	0.4	–	0.8	0.2	1	0.6	1.6	1.2
Quercus sp.	7.2	2.5	3.8	2	4.2	3.3	2.5	2
Castanea sp.	2.5	0.6	3	–	0.4	0.2	0.8	0.6
Castanopsis sp.	0.8	0.8	1	–	0.2	–	0.2	–
Nothofagus sp.	0.2	–	0.2	–	–	–	–	–
Fam. Ulmaceae (total)	7.3	3.5	5.4	3.9	2	4.1	5.8	4.2
Ulmus inaequaliarcuata Trav.	0.6	0.6	0.8	0.2	–	–	0.4	0.4
U. flexuosa Pan.	–	–	0.2	0.2	–	–	–	–
Ulmus sp.	4.1	2.5	2	3.3	2	3.5	4.4	3.2
Zelkova sp.	0.8	–	0.2	0.2	–	–	0.8	0.4

Table 2. (Contd.)

Spores and pollen	Sample number							
	81	604	117	12	74	209	2	69
Ulmaceae gen. indet.	–	–	0.2	–	–	–	–	–
Ulmoideipites (total)	1.8	0.4	2	–	–	0.6	0.2	0.2
Ulmoideipites krempii And.	0.8	–	0.6	–	–	–	–	0.2
U. planeraeformis And.	–	–	0.6	–	–	0.2	–	–
Ulmoideipites sp.	1	0.4	0.8	–	–	0.4	0.2	–
Fam. Hamamelidaceae (total)	2.4	2.2	2.2	3.6	4.2	3	2.8	4.2
Hamamelis sp.	–	0.2	0.8	1	0.2	0.2	0.2	–
Corylopsis (total)	0.2	0.4	0.4	0.8	1.4	0.8	–	0.4
Corylopsis princeps Lubom.	–	–	0.2	0.2	–	–	–	–
Corylopsis sp.	0.2	0.4	0.2	0.6	1.4	0.8	–	0.4
Fothergilla vera Lubom.	–	–	–	–	–	–	0.2	–
Fothergilla sp.	–	–	–	–	–	–	0.4	–
Liquidambar (total)	2	1.6	0.8	1.8	2.4	1.8	1.6	3.2
Liquidambar formosana Hance	0.2	–	–	0.6	0.4	0.2	0.4	0.8
L. orientalis Mill.	0.2	0.2	0.2	0.4	0.2	0.4	0.4	0.4
L. styraciflua L.	–	–	0.2	–	0.2	0.6	–	0.4
Liquidambar sp.	1.6	1.4	0.4	1.8	1.6	0.6	0.8	1.6
Altingia sp.	–	–	0.2	–	0.2	0.2	0.2	1.6
Hamamelidaceae gen. indet.	0.2	–	–	–	–	–	0.2	–
Magnolia globosiformis Lubom.	–	–	–	0.2	–	0.2	–	–
M. acuminatiformis Lubom.	–	–	–	–	–	–	–	0.2
Magnolia sp.	–	–	–	0.2	–	–	–	–
Laurus sp.	0.4	0.2	–	0.2	0.2	0.2	0.4	–
Rhus sp.	0.8	1.2	0.6	0.4	0.6	1	0.8	0.6
Ilex sp.	0.2	0.4	0.2	0.2	0.2	0.4	0.6	1.2
Sterculia sp.	–	–	–	0.4	–	–	–	–
Diervilla sp.	0.2	–	0.2	0.2	0.2	0.2	–	0.2
Nyssa sp.	0.2	0.2	0.2	0.2	0.2	0.2	0.2	0.2
Cercidiphyllum sp.	1	2.5	0.6	0.4	0.2	1	1	0.2
Trochodendron sp. (?)	0.2	0.2	–	–	–	–	–	–
Vitys sp.	0.2	–	0.2	0.2	0.4	0.2	0.4	1.2
Daphne sp.	–	–	–	–	–	–	0.2	0.2
Berberis sp.	–	–	–	0.2	–	–	–	–
Platanus sp.	–	–	–	–	–	–	0.2	–
Aralia sp.	0.4	0.2	0.2	–	0.2	–	0.2	0.2
Fatsia sp.	–	–	–	0.2	–	–	–	–
Myrtus sp.	0.2	–	–	–	–	–	–	0.2
Loranthus sp.	0.2	–	–	–	–	–	–	–
Tilia pseudinstructa Mai	0.2	0.4	–	–	–	–	0.2	–
T. sulcata Pan.	–	–	–	–	–	–	0.2	0.2
Tilia sp.	0.2	–	0.2	0.2	0.2	0.2	–	–
Acer sp.	1	0.8	0.8	–	0.2	0.2	1.9	0.2
Fraxinus sp.	–	–	0.2	–	–	–	0.2	–
Sparganium sp.	0.2	0.2	0.4	–	0.2	0.2	0.2	0.2
Potamogeton sp.	–	–	–	–	–	0.4	–	–
Nelumbo sp.	–	0.8	–	–	–	1	–	0.2
Nymphaea sp.	–	–	0.2	–	–	–	–	–
Nuphar sp.	–	–	0.2	–	–	–	–	–
Proteaceae gen. indet.	–	–	–	0.2	–	0.2	–	–
Moraceae gen. indet.	0.6	0.6	0.8	0.8	0.2	0.4	0.6	0.6
Rhamnaceae gen. indet.	–	–	0.2	0.2	0.1	–	0.2	–
Leguminosae gen. indet.	2.7	1	1.6	–	0.2	0.4	–	0.2
Ericaceae gen. indet.	–	–	0.2	–	–	0.2	–	0.2
Triporopollenites plicoides Zakl.	–	–	0.2	–	0.2	0.2	–	–
Triporopollenites sp.	0.2	1.8	1	1.6	0.2	0.2	–	0.8
Tricolpopollenites sp.	0.4	0.2	0.2	0.2	0.2	0.2	–	–
Tricolpopollenites sp.	2.7	3.7	2.6	2.2	2.8	2.1	1.9	2.4
Angiosperm pollen of uncertain taxonomic affiliation	1	1.2	2.2	1	1.4	2.3	0.8	2.2

Table 3. General composition of spores and pollen from flora-bearing deposits of the Dembi Bay site (%)

Spores and pollen	Sample number						
	SPA-1			SPA-2			
	592	164	386	804	897	149	864
Spores (total)	**0.8**	**1.8**	**0.4**	**2.6**	**1.8**	**2.2**	**0.4**
Polypodiaceae gen. indet.	0.2	1.6	0.2	2	1.6	1.8	0.2
Osmunda sp.	–	–	–	0.4	–	0.2	0.2
Botrychium sp.	0.4	0.2	–	–	0.2	–	–
Lycopodium sp.	0.2	–	0.2	0.2	–	0.2	–
Gymnosperm pollen (total)	**88.4**	**82.4**	**89.2**	**34.3**	**35.3**	**40.9**	**42.4**
Ginkgo sp.	0.2	0.8	–	0.2	–	0.2	–
Podocarpus sp.	1.2	0.6	0.6	–	0.4	0.2	0.4
Pinaceae (total)	80.4	72.6	79.8	22.1	18.6	27.7	25
Abies sp.	4.7	15.4	11.7	2	3	2.4	3.6
Cedrus sp.	0.2	–	0.2	0.2	–	–	–
Picea (total)	17.1	12.2	12.7	2	2	2	2.6
Picea sect. *Eupicea*	15.1	11.2	11.1	1.8	1.8	2	1.3
Picea media Anan.	–	–	–	–	0.2	–	0.2
Picea sect. *Omorica*	2	1	1.6	0.2	–	0.2	0.4
Tsuga (total)	2.6	2.2	0.8	0.4	1.6	0.2	0.8
T. aculeata Anan.	0.4	–	–	0.2	0.4	–	–
Tsuga sp.	2.2	2.2	0.8	0.2	1.2	0.2	0.8
Pinus (total)	49.1	39.2	50.4	16.5	10.6	21.9	17
Pinus tertiaria (Moreva) Anan.	–	–	–	0.4	0.2	–	1.4
P. miriabilis (Rudolph) Anan.	–	–	–	0.4	–	–	–
P. silvestris L.	–	–	–	–	–	–	0.2
P. banksianaeformis Zakl.	–	–	–	–	0.4	–	–
Pinus sp.	49.1	39.2	50.4	15.7	10	21.9	15.4
Pinaceae gen. indet.	6.7	3.6	4	1	1.4	1.2	1
Taxodiaceae (total)	5.2	4.2	6	9.2	14.5	4.8	14
Taxodium (total)	3	1	3	5.2	7.9	2.2	7.8
Taxodium distichiformis Zhezh.	–	–	–	1.2	0.4	–	–
Taxodium sp.	3	1	3	4	7.5	2.2	7.8
Sequoia sp.	0.4	–	1	0.6	0.8	0.4	1
Sciadopitys (total)	–	1	–	0.6	2.2	0.2	2
Sciadopitys tuberculata Zakl.	–	0.6	–	–	1.2	0.2	0.6
S. verticillata Sieb. et Zucc.	–	–	–	0.4	–	–	0.6
Sciadopitys sp.	–	0.4	–	0.2	1	–	0.8
Glyptostrobus sp.	0.2	0.8	1	1	1.2	0.8	0.8
Cryptomeria sp.	–	–	–	–	0.2	0.2	0.4
Taxodiaceae gen indet.	1.6	1.4	1	1.8	2.2	1	2
Cupressaceae gen. indet.	–	–	0.6	–	0.4	–	–
Taxodiaceae or Cupressaceae	1.4	4.8	2.2	2.8	1.4	8	3
Angiosperm pollen (total)	**10.8**	**15.8**	**10.4**	**63.1**	**62.9**	**56.9**	**56.6**
Salix sp.	–	–	–	–	–	0.2	–
Myrica sp.	–	–	–	0.2	0.2	–	0.2
Fam. Betulaceae (total)	1	3.8	1.8	6.6	6.4	6.2	5.8
Alnus sp.	0.4	0.2	1.2	1.2	1	1.4	0.2
Betula sp.	0.2	0.2	0.2	1.2	0.8	0.2	0.8
Corylus sp.	0.4	1.8	0.4	2.8	2	2.6	1.4
Carpinus sp.	–	1.4	–	1	2.6	2	3.4

Table 3. (Contd.)

Spores and pollen	Sample number						
	SPA-1			SPA-2			
	592	164	386	804	897	149	864
Ostrya sp.	–	0.2	–	–	–	–	–
Betulaceae gen. indet.	–	–	–	0.4	–	–	–
Fam. Juglandaceae (total)	0.6	3.2	2.2	6.4	6.4	3.6	4.4
Juglans (total)	0.6	1.8	1.6	4	3.2	1.4	2
J. manshurica Max.	–	1	0.4	0.6	1	0.2	0.2
J. orbiculata Bolot.	–	–	–	0.2	0.4	–	0.2
J. polyporata Vojc.	0.2	–	0.6	1	0.4	–	–
J. sieboldianaformis Vojc.	–	–	–	–	0.2	–	–
Juglans sp.	0.4	0.8	0.6	2.2	1.2	1.2	1.6
Carya sp.	–	1.4	0.4	1.8	3	1.8	2.4
Pterocarya sp.	–	–	0.2	–	–	0.2	–
Platycarya sp.	–	–	–	0.2	–	–	–
Engelhardtia sp.	–	–	–	0.4	0.2	0.2	–
Fam. Fagaceae (total)	5.2	4.8	3.4	38.9	36.7	38.3	37.4
Fagus (total)	3.6	3.2	1.6	32	29.9	32.9	31.6
Fagus grandifoliiformis Pan.	–	–	–	0.2	0.8	–	0.6
F. tenella Pan.	–	–	–	0.2	0.6	–	0.2
F. japoniciformis Anan.	–	–	–	0.6	0.6	–	0.6
F. silvatica Erdt.	–	–	–	–	–	–	0.4
Fagus sp.	3.6	3.2	1.6	31	27.9	32.9	29.8
Quercus (total)	1.4	1.6	1.6	6.7	5.4	5.2	5.8
Quercus dentatiformis Pan.	–	–	–	0.4	–	–	–
Quercus sp.	1.4	1.6	1.6	6.3	5.4	5.2	5.8
Castanea sp.	0.2	–	0.2	0.2	1.4	0.2	–
Fam. Ulmaceae (total)	2.8	2.8	2	5.2	4.6	4.2	3.2
Ulmus sp.	2.8	2.8	2	5.2	4.6	4.2	3
Zelkova sp.	–	–	–	–	–	–	0.2
Fam. Hamamelidaceae (total)	0.2	–	–	1	2.2	1.2	0.8
Hamamelis sp.	–	–	–	1	0.4	0.8	0.4
Corylopsis sp.	–	–	–	0.6	1.4	0.2	0.4
Liquidambar sp.	–	–	–	–	0.2	0.2	–
Hamamelidaceae gen. indet.	0.2	–	–	–	0.2	–	–
Rhus sp.	–	–	–	0.2	0.2	0.4	–
Ilex sp.	–	–	–	–	0.2	–	–
Tilia sp.	–	–	–	–	0.2	–	–
Acer sp.	0.8	0.2	0.2	1	0.6	0.2	1.6
Sparganium sp.	–	–	–	–	–	–	0.2
Nelumbo sp.	0.2	–	–	1	2.8	0.8	1.6
Nuphar sp.	–	–	–	–	–	–	0.2
Moraceae gen. inet.	–	0.4	0.4	–	–	0.4	0.2
Leguminosae gen. indet.	–	0.2	0.4	0.2	–	0.2	–
Ericaceae gen. indet.	–	0.2	–	0.2	–	–	0.2
Triporopollenites sp.	–	–	–	–	–	–	0.6
Tricolpopollenites sp.	–	–	–	–	0.2	–	–
Tricolporopollenites sp.	–	0.2	–	1.2	1.6	1.2	0.8
Angiosperm pollen of uncertain taxonomic affiliation	–	–	–	0.4	0.6	–	0.8

lished. The SPA of the Bui Bay site is characterized by coexistence of Eocene–Oligocene species (*Quercus gracilis, Q. graciliformis, Q. conferta, Myrica vera, Corylopsis princeps, Fothergilia vera, Ulmoideipites krempii, U. planeraeformis*, and others) and Oligocene–Miocene species (*Tsuga parva, Myrica lubomirovae, M. pseudogranulata, Juglans sieboldianaformis, Carya bella, C. spackmania, Ulmus inaequaliarcuata*, and others). Hence, this taxonomic composition and correlation results within the southern continental part of the Far East suggest that the SPA from flora-bearing deposits of the Bui Bay is transitional between those of the late Eocene and early Oligocene.

The SPA-1 of the Dembi Bay site resembles to some extent the pollen assemblages from the Machigar and the lower part of the Tum' formations from the section of the Shmidt Peninsula of northern Sakhalin (*Ekosistemy kainozoya...*, 1999), from the Gastello and Kholmsk formations, and from lower beds of the Nevel'skoi Formation of the Makarov section in southern Sakhalin (*Opornyi razrez ...*, 1992), which are referred to the *Podocarpus totara–Tsuga parva* palynological zone (upper Oligocene–lower Miocene). The above-mentioned assemblages are characterized by prevalence of conifers and by low content of thermophilic pollen taxa. The difference between the SPA-1 and Sakhalin assemblages is domination of *Tsuga* pollen (up to 22%) among gymnosperms in the former and a high content of spores in Sakhalin deposits. These data imply that the SPA-1 of the Dembi Bay site is of the late Oligocene–early Miocene age.

The SPA-2 of the Dembi Bay is the most similar compositionally to assemblages the so-called "Fagus" Horizon recognized by Kartasheva (1974) in the Yana River section. The characteristic feature of the latter is prevalence of *Fagus* pollen in the angiosperm group, where this genus is represented, as a rule, by several species with an insignificant content or complete absence of other Fagaceae forms. The SPA-2 of the Dembi sequence resembles as well the SPA-6 from the upper coal-bearing member of the Lipovtsy depression of southwestern Primor'e (Baskakova and Gromova, 1989), the SPA of the Khanka beds in Primor'e (Mamontova, 1982), and the SPA-V from the upper coal-bearing subformation of the Verkhnii Due Formation of the Mgachi coal field in western Sakhalin (Bolotnikova, 1989). The SPA-6 of the Lipovtsy depression is referred to the middle Miocene. The SPA of Khanka beds is of the early–middle to, probably, latest middle Miocene in age. According to Bolotnikova, the SPA-V from the Mgachi coal field corresponds to the second middle Miocene climatic optimum. Hence, the peculiar taxonomic composition and correlation with spore-and-pollen assemblages from other regions allow the SPA-2 to be attributed to the middle Miocene.

When studying assemblages of the climatic optimum, Bolotnikova (1989) pointed out that those of latest early–earliest middle Miocene show a high content of Juglandaceae and Fagaceae forms, with oaks and chestnut dominating among the former. Predominance of *Fagus* pollen along with other, very rare representatives of Fagaceae is typical of the second climatic optimum distinguished by Bolotnikova with certain reservations. As mentioned above, 35–40% of plant imprints in the collection from the Dembi Bay are those of oaks. The SPA-2 likely corresponds to the first climatic optimum of the early Miocene but not to its terminal phase. It counts in favor of this inference that oaks could probably develop hybrid forms producing a small amount of pollen, whereas pollen of entomophilous chestnuts was irregularly disseminated in a smaller amount as compared to that of anemophilous plants. The lack of corresponding pollen in spectra not necessarily evidences that these plants were absent, as they could present in minor amounts in the vegetation cover. Hence, the palynological analysis suggests that flora-bearing deposits of the Dembi Bay can be dated back to the late Oligocene–middle Miocene.

The study results by different methods show that ages of flora localities near the Son'e and Bui bays, the late Eocene and early Oligocene, respectively, coincide. Flora-bearing deposits of the Dembi Bay can be referred by virtue of flora imprints to the second half of the early Miocene, whereas data of palynological analysis slightly extend their time range to the late Oligocene–middle Miocene period.

When comparing compositions of spores, pollen, and fossil leaf floras at the generic level (Table 4), one can see that palynological method reveals a greater amount of genera in floras of the Son'e and Bui bays, whereas macrofloral method happened to be more effective in the case of the Dembi Bay flora. In the last case, the established species composition of imprints is much more diverse than that of pollen, and we may suspect that pollen of many plants is inadequately preserved.

Many works are devoted to the problem of compositional correspondence and quantitative distinctions between fossil and subfossil microfloras and coeval vegetation communities. As many genera of Paleogene and Neogene floras are preserved in the current vegetation cover of the Earth, we can use the present-day distribution regularities, though with precaution, for correlation of spore-and-pollen assemblages with fossil leaf floras and for restoration of the vegetation cover peculiarities.

Sporophyte imprints have not been found in all the discussed sites, although spores are present in all palynological assemblages studied. Spores, as a rule, are large, often having a sculptured exine. For this reason, their volatility must be low, and their presence in spectra indicates hence participation of sporophytes in plant communities of the given territory, even though their imprints are missing in the studied samples.

Table 4. Comparison of the generic composition of leaf- and palynoflora from the section of Eocene–Miocene deposits in the Tatar Strait coast between the Son'e and Bui bays

Generic composition	Son'e		Bui		Dembi		
	1	2	1	2	1	2	
						SPA-1	SPA-2
Amount of genera	33	66	21	81	51	34	48
Genera in total	79		88			75	
Pteridospermaphytes							
Cyathea	–	+	–	–	–	–	–
Polypodiaceae gen. indet.*	–	+	–	+	–	+	+
Lygodium	–	+	–	+	–	–	–
Osmunda	–	+	–	+	–	–	+
Botrychium	–	+	–	+	–	+	+
Ceratopteris	–	+	–	–	–	–	–
Marsilea	–	+	–	+	–	–	–
Riccia	–	–	–	+	–	–	–
Lycopods							
Lycopodium	–	+	–	+	–	+	+
Trees and bushes							
Gymnosperms							
Ginkgo	+	+	–	+	–	+	+
Ephedra	–	–	–	+	–	–	–
Taxus	+	–	–	–	–	–	–
Podocarpus	+	+	–	+	–	+	+
Abies	–	+	–	+	+	+	+
Keteleeria	–	–	–	–	+	–	–
Tsuga	–	+	+	+	+	+	+
Picea	–	+	–	+	+	+	+
Cedrus	–	+	–	+	–	+	+
Pseudolarix	–	–	–	–	+	–	–
Larix	–	–	–	–	+	–	–
Pinus	+	+	+	+	+	+	+
Taxodium	+	+	–	+	+	+	+
Sciadopitys	+	+	–	+	+	+	+
Sequoia	–	+	–	+	–	+	+
Metasequoia	+	–	–	–	+	–	–
Glyptostrobus	–	+	–	+	+	+	+
Cryptomeria	+	+	–	+	–	–	+
Cunninghamia	+	–	–	–	–	–	–
Thuja	+	–	+	+	+	–	–
Thujopsis	+	–	–	–	+	–	–
Juniperus	–	–	–	+	–	–	–
Cupressaceae gen. indet.*	–	+	–	+	–	+	+
Agathis	–	–	–	+	–	–	–
Angiosperms							
Salix	–	+	–	+	–	–	+
Populus	–	–	+	–	+	–	–

Table 4. (Contd.)

Generic composition	Son'e		Bui		Dembi		
	1	2	1	2	1	2	
Myrica	+	+	–	+	–	–	+
Comptonia	+	+	–	+	+	–	–
Juglans	–	+	–	+	+	+	+
Carya	–	+	+	+	+	+	+
Pterocarya	–	+	–	+	–	+	+
Platycarya	–	+	–	+	–	–	+
Engelhardtia	–	+	–	+	+	–	+
Alnus	+	+	+	+	–	+	+
Betula	+	+	+	+	–	+	+
Corylus	–	+	–	+	+	+	+
Carpinus	+	+	+	+	+	+	+
Ostrya	+	+	–	+	+	+	–
Fagus	+	+	+	+	+	+	+
Quercus	–	+	+	+	+	+	+
Castanea	+	+	–	+	+	+	+
Castanopsis	–	–	–	+	+	–	–
Nothofagus	–	–	–	+	–	–	–
Fagopsis	–	–	–	–	+	–	–
Ulmus	–	+	–	+	+	+	+
Zelkova	–	–	–	+	+	–	+
Ulmoideipites	–	+	–	+	–	–	–
Ulmiopollenites	–	+	–	–	–	–	–
Hamamelis	–	+	–	+	–	–	+
Corylopsis	–	+	–	+	–	–	+
Fothergilla	–	+	–	+	–	–	–
Liquidambar	–	+	–	+	–	–	+
Altingia	–	–	–	+	–	–	–
Moraceae gen. indet.*	–	+	–	+	–	+	+
Laurus	–	–	–	+	–	–	–
Machilus	–	–	+	–	–	–	–
Pistacia	–	–	–	–	+	–	–
Rhus	–	+	–	+	+	–	+
Astronium	–	–	–	–	+	–	–
Celastrus	–	–	–	–	+	–	–
Aesculus	–	–	–	–	+	–	–
Ilex	–	+	–	+	–	–	+
Magnolia	–	+	–	+	–	–	–
Tilia	–	+	+	+	+	–	+
Sterculia	–	–	–	+	–	–	–
Nyssa	–	+	–	+	+	–	–
Cocculus	+	–	–	–	–	–	–
Cornus	+	–	–	–	–	–	–
Cercidiphyllum	+	+	+	+	+	–	–
Trochodendron	+	+	–	+	–	–	–

Table 4. (Contd.)

Generic composition	Son'e		Bui		Dembi		
	1	2	1	2	1	2	
Myrtus	–	+	–	+	–	–	–
Cardiospermum	–	+	–	–	–	–	–
Loranthus	–	–	–	+	–	–	–
Proteaceae gen. indet.	–	+	–	+	–	–	–
Cercis	–	–	–	–	+	–	–
Leguminosites	+	–	–	–	+	–	–
Leguminosae gen. indet.*	–	+	–	+	–	+	+
Aralia	–	–	–	+	–	–	–
Fatsia	–	–	–	+	–	–	–
Eucommia	–	–	+	–	–	–	–
Zizyphus	+	–	–	–	+	–	–
Rhamnaceae gen. indet.*	–	–	–	+	–	–	–
Vitys	+	–	–	+	+	–	–
Ericaceae gen. indet.*	–	+	–	+	–	+	+
Rosa	–	–	+	–	–	–	–
Sorbus	–	–	–	–	+	–	–
Sorbaria	–	–	–	–	+	–	–
Amelanchier	–	–	–	–	+	–	–
Diervilla	–	–	–	+	–	–	–
Berberis	–	–	+	+	–	–	–
Daphne	–	+	–	+	–	–	–
Platanus	+	–	+	+	–	–	–
Styrax	–	–	–	–	+	–	–
Ligustrum	–	–	–	–	+	–	–
Macaranga	–	–	+	–	–	–	–
Alangium	+	–	+	–	–	–	–
Diospyros	–	–	–	–	+	–	–
Viburnum	+	–	–	–	–	–	–
Acer	+	+	+	+	+	+	+
Fraxinus	–	–	–	+	–	–	–
Herbaceous plants							
Sparganium	–	+	–	+	–	–	+
Potamogeton	–	+	–	+	–	–	–
Nelumbo	–	+	–	+	–	+	+
Nymphaea	–	–	–	+	–	–	–
Nuphar	–	–	–	+	–	–	+
Arundo	–	–	–	–	+	–	–
Cyperites	+	–	–	–	–	–	–
Phragmites	–	–	+	–	–	–	–
Hemitrapa	–	–	–	–	+	–	–

Note: (1) leaf flora; (2) palynoflora; + genus present, – genus absent; * spore and pollen taxons of the family level.

As for the gymnosperm group, it should be pointed out that most of their genera are identified in localities of the Son'e and Bui bays by the palynological method. In the Dembi Bay locality, they are identified among pollen and plant imprints as well. The Pinaceae pollen dominates in all the spore-and-pollen assemblages in

spite of insignificant amount of Pinaceae imprints. First, this could be a result of high pollen productivity by these plants. Second, the Pinaceae pollen (especially that of *Pinus*) is easily transportable by wind owing to its structure. The bisaccate pollen of spruce, fir, and cedar is larger and heavier, and hence transportable for a shorter distance (Fedorova and Vronskii, 1980). In particular, the content of spruce and cedar pollen can be lower in spectra than the actual abundance of these plants in the vegetation cover (Makhova, 1971). Malygina (1950) established that the spruce pollen content exceeding 10% indicates the distribution of spruce forests over the study area. As we suspect, pollen grains of the *Larix* genus are very rare in the studied samples because of a poor preservation and low volatility. In spectra from larch forests, the content of *Larix* pollen is rarely as high as 10% (Makhova, 1971; Stefanovich, 1971; Aleksandrova, 1978). When its content in spectra is 1–6%, this may indicate that more than half of the studied territory was occupied by larch forests (Makhova, 1971). The fossil *Tsuga* pollen is, as a rule, well preserved and easily identifiable at the species level, whereas imprints of corresponding plant remains can be identified at a genus level only. Moreover, cones of some recent *Tsuga* species bear similarities to larch cones, and their identification is difficult.

In all the studied macrofloras, imprints of Taxodiaceae and Cupressaceae remains dominate over those of conifers, whereas both families are less abundant in spore-and-pollen assemblages as compared to Pinaceae. Kvavadze (1988) who studied the preservation of the Taxodiaceae pollen in subfossil and fossil spectra in the Black Sea coast of the Caucasus established that pollen productivity of *Cryptomeria* and *Sciadopitys* is high, while *Metasequoia, Taxodium*, and *Sequoia* produce a moderate amount of pollen. The least pollen productivity is characteristic among Taxodiaceae of the *Cunninghamia* genus. The pollen of the *Cryptomeria, Metasequoia, Cunninghamia*, and *Sciadopitys* is best preserved in deposits, whereas pollen grains of the *Taxodium* and *Sequoia* genera are often deformed. This is characteristic of spore-and-pollen spectra of rocks favorable for pollen preservation (fine humus-rich soils, or lacustrine and alluvial deposits). A partial destruction of upper exine layer and breakage near the pollen aperture are characteristic features of many genera at the early stages of their pollen fossilization under unfavorable conditions. In coarse soils, this takes place during few years after the pollen burial.

Flora-bearing deposits of the studied localities repeatedly appeared under extreme conditions of elevated pressure and temperature that resulted in the destruction of the pollen (a greater or lesser admixture of plant detritus is typical of all spore-and-pollen assemblages). It is likely, that just these unfavorable conditions are responsible for a low content and poor preservation of the Taxodiaceae pollen in spectra.

As to the angiosperm group, it should be pointed out that the anemophilous pollen taxa plants are often present in spore-and-pollen spectra, even if these plants are missing from plant imprints. Pollen of small-leaved *Alnus* and *Betula* is highly volatile. It is found to be more abundant than that of other genera in all spore-and-pollen spectra. Pollen of broad-leaved plants (*Carpinus, Juglans, Fagus, Quercus, Ulmus*, and others) was found practically in all spectra. It is less volatile as compared to alder and birch pollen and can be transported beyond the geographical range boundaries in negligibly small amounts. Its systematic occurrence in the spectra even in a small amount indicates therefore the presence of these genera in phytocoenoses. The total percentage of pollen of broad-leaved plants may be 2–5 times lower than their actual abundance in plant groupings, as is established by Makhova (1971) for the Amur River basin. Pollen of *Populus* and *Fraxinus* genera is easily destructible by fossilization. Accordingly, the *Populus* pollen has not been found in the spectra at all, whereas the *Fraxinus* pollen is encountered but as a single grains.

A great amount of oak imprints in macrofloras of the Son'e and Dembi bays engages the attention, whereas the content of oak pollen in spectra slightly exceeds 2%. It is likely that this is also a reflection of the oaks ability to develop hybrid forms characterized by low pollen productivity.

The content of pollen of entomophilous plants (*Salix, Tilia, Castanea, Sterculia, Nyssa, Alangium, Magnolia, Trochodendron, Cornus, Ilex*, and others) is low in all spectra, where individual grains are registered. This pollen is often missing from the spectra even with the availability of imprints of that plant remains. As is evident from recent and subfossil spectra, the content of *Salix* pollen in spectra is considerably lower than the actual abundance of this taxon in the vegetation cover (Makhova, 1971). It seems to be a consequence of transportation mode and morphology of the *Salix* pollen that is large, as a rule, having a sculptured exine, or small but often agglutinated into pellets. So, even single pollen grains of entomophilous plants indicates their participation in plant groupings.

As is established, pollen of most herbaceous plants is either missing from spore-and-pollen spectra, or present in insignificant amounts. The explanation is that reproduction of many herbaceous plants in forest phytocoenoses is vegetative, whereas the herbaceous horizon in shady woods is poorly developed (Fedorova and Vronskii, 1980).

Hence, qualitative and quantitative distinctions between assemblages of plant imprints and spore-and-pollen spectra characterizing the Son'e, Bui and Dembi localities reflect variable preservation of macro- and microfossils and biological peculiarities of plants (the pollen productivity, pollination mode, pollen morphology, and transportability).

Vegetation in the study area was greatly affected by the intense volcanic activity and related landscape rearrangement. Within the Pribrezhnyi volcanic belt, most of flora localities are confined to alluvial facies, mainly to sediments that accumulated in the ox-bow and small dammed lakes. Flora-bearing deposits of the Son'e, Bui, and Dembi localities accumulated in lakes located within the volcanic field. Such lakes originated in response to damming of small rivers or creeks by lava flows or downfalls. The lakes were likely short-lived as is evident, for instance, from confinement of the Dembi Bay flora to dolomite interlayers intercalated with tuff beds, tuffites, and pillowed basaltic flows (Akhmet'ev, 1988). All palynological specimens comprise colonies of botryoid algae and *Ovoidites* sp., the analogs of modern zygmatacean algae of the genus *Spyrogira* indicative of fresh-water sedimentation environments.

Analyzing taxonomic composition of macro- and palynofloras with due regard to proportions of their constituent taxa and ecological peculiarities of modern analogs, we can get insight into general climatic conditions in the studied region.

Such thermophilic genera as *Ginkgo, Podocarpus, Cryptomeria, Cocculus, Magnolia, Trochodendron,* and others, which are present in the Son'e Bay flora, indicate that the Late Eocene climate in the territory was humid and moderately warm, approaching that of the subtropical zone.

The vegetation cover near the Bui Bay site can be restored mainly on the basis of palynological data. It was characterized by domination of conifer–broad-leaved forests with the prevailing Turgai genera. Accordingly, climate of that time (the late Eocene–early Oligocene) was warm–temperate. The macroflora composition is compatible with this inference.

Judging from flora composition at the Dembi Bay site, one can concede that during its development (late Oligocene–early Miocene) there were coniferous forests with a minor admixture of broad-leaved elements and beech forests (palynological data), where some other broad-leaved species grew. The presence of *Engelhardtia, Cercidiphyllum, Castanopsis, Liquidambar,* and some other taxa indicates that the Dembi Bay flora is comparable with other Far East floras corresponding to the Miocene climatic optimum.

During the Eocene, Oligocene, and Miocene, the climate in the study area changed essentially. It is impossible to trace all changes in fossil plant communities during the entire period in question, but some its intervals can be satisfactory characterized. The data obtained indicate that a warm and temperate climate prevailed during the formation time of all three flora-bearing sequences discussed above.

CONCLUSION

The obtained data on plant imprints and palynological spectra of Eocene–Miocene deposits in the Tatar Strait coast between the Son'e and Dembi bays, as well as the comparative analysis of Cenozoic palynological assemblages of the southern Far East and Sakhalin, lead to the following conclusions.

(1) Flora-bearing deposits of the Son'e Bay and Bui Bay localities each yields one palynological assemblage. Age determinations based on compositions of macro- and microfloras are concordant in both cases, corresponding to the late Eocene in the first locality and to the late Eocene–early Oligocene in the second one. Two palynological assemblages are identified in samples with plant imprints from the Dembi Bay locality. Flora-bearing deposits of this locality are dated back to the second half of the early Miocene by virtue of macroflora composition and to the late Oligocene–middle Miocene according to palynological data.

(2) The established generic compositions of spore-and-pollen spectra and plant imprint assemblages demonstrate reproducibility of results obtained by macrofloristic and palynological methods. Both methods revealed presence of anemophilous plants. Entomophilous plants are mostly recognized among plant imprints, whereas abundance of their taxa in pollen spectra and corresponding macrofloras does not coincide. A poor preservation state is established for fossil pollen of Taxodiaceae and Cupressaceae, for that of *Larix* among Pinaceae, and for *Populus* and *Fraxinus* angiosperm genera.

(3) Mountain forests with various plant associations dominated in the study region in the late Eocene to middle Miocene inclusive. The late Eocene was the initial period of the Turgai flora development in the region. That flora included abundant deciduous angiosperms, mostly broad-leaved species (Akhmet'ev, 1993). The Bui Bay flora most closely resembles the Turgai-type flora.

(4) In the period, when each of the three floras formed, climate was temperate, warm and fairly humid. Palynological data confirm that the Dembi Bay flora developed in the Miocene climatic optimum.

ACKNOWLEDGMENTS

I express my sincere gratitude to M.A. Akhmet'ev (GIN RAS), who suggested the research theme and donated materials for studying. G.M. Bratseva (GIN RAS) and I.A. Basov (IL RAS) are acknowledged for their helpful consultations, N.I. Zaporozhets and G.N. Aleksandrova (GIN RAS) for assistance in technical processing of the materials, and N.G. Tremasova (IL RAS) for drafting the figures. The work was supported by the Russian Foundation for Basic Research, project no. 99-05-65604.

Reviewers M.A. Akhmet'ev and V.A. Krasilov

REFERENCES

Akhmet'ev, M.A., *Miotsenovaya flora Sikhote-Alinya (r. Botchi)* (The Miocene Flora of Sikhote Alin, the Botchi River Area), Moscow: Nauka, 1973a.

Akhmet'ev, M.A., Paleocene and Eocene Floras of Southern Far East of the USSR and Adjacent Countries and Their Stratigraphic Range, *Sov. Geol.*, 1973b, no. 7, pp. 14–29.

Akhmet'ev, M.A., Oligocene and Miocene Floras of Southern Far East of the USSR as Indicators of the Climatic Environment, *Izv. Akad. Nauk SSSR, Ser. Geol.*, 1974, no. 4, pp. 134–143.

Akhmet'ev, M.A., Cenozoic Floras of Eastern Sikhote Alin, *Preprint of Geol. Inst. Russ. Acad. Sci.*, Moscow, 1988.

Akhmet'ev, M.A., *Fitostratigrafiya kontinental'nykh otlozhenii paleogena i miotsena vnetropicheskoi Azii* (Phytostratigraphy of Continental Paleogene and Miocene Deposits in Extratropical Asia), Moscow: Nauka, 1993.

Akhmet'ev, M.A. and Vikulin, S.V., Peltate Leaves *Macaranga* Thouin (Euphorbiaceae) in the Cenozoic of Eastern Sikhote Alin, *Paleontol. Zh.*, 1995, no. 4, pp. 151–156.

Akhmet'ev, M.A. and Manchester, S.R., A New Species *Palaeocarpinus* (Betulaceae) from the Paleogene of Eastern Sikhote Alin, *Paleontol. Zh.*, 2000, no. 4, pp. 107–112.

Aleksandrova, A.N., Spore-and-pollen Spectra of Recent Deposits in Sakhalin, in *Palinologicheskie issledovaniya na Dal'nem Vostoke* (Palynological Studies in the Far East), Grichuk, M.P. and Korotkii, A.M., Eds., Vladivostok: DVO AN SSSR, 1978, pp. 77–82.

Baskakova, L.A., Coal-bearing Deposits in the Orekhov Depression of Primor'e: Lithology and Palynological Age Substantiation, *Tikhookean. Geol.*, 1990, no. 3, pp. 54–61.

Baskakova, L.A., The Palynostratigraphic Subdivision and Correlation of Paleogene–Miocene Deposits in the Amgun'–Gorin Region (Middle Courses of the Amur River), *Stratigr. Geol. Korrelyatsiya*, 1997, vol. 5, no. 6, pp. 51–63.

Baskakova, L.A. and Gromova, N.S., The Pre-Quaternary Cenozoic Section of the Lipovtsy Depression (Lithological and Palynological Characteristics), in *Kainozoi Dal'nego Vostoka* (The Cenozoic of the Far East), Krasilov, V.A. and Klimova, R.S., Eds., Vladivostok: DVO AN SSSR, 1989, pp. 90–100.

Bolotnikova, T.N., Palynological Characteristics of the Mgachi Coal Field (Sakhalin, the Neogene), in *Paleontologo–stratigraficheskie issledovaniya fanerozoya Dal'nego Vostoka* (Paleontological and Stratigraphic Studies of the Phanerozoic in the Far East), Burii, G.I. and Tochilina, S.V., Eds., Vladivostok: DVNTs AN SSSR, 1989, pp. 104–110.

Ekosistemy kainozoya Okhotomorskogo regiona. Opornyi razrez paleogena i neogena Severnogo Sakhalina (p-ov Shmidta): stratigrafiya, paleogeografiya i geologicheskie sobytiya (Cenozoic Ecosystems of the Sea of Okhotsk Region. The Key Section of the Paleogene and Neogene in Northern Sakhalin (Shmidt Peninsula): Stratigraphy, Paleogeography, and Geological Events), Moscow: GEOS, 1999.

Fedorova, R.V. and Vronskii, V.A., Dissemination Regularities of Spores and Pollen in the Air, in *Byul. Komissii po izucheniyu chetvertichnogo perioda* (Bulletin of the Commission on the Study of the Quaternary), Gromov, V.I., Ivanova, I.K., and Tseitlin, S.M., Eds., Moscow: Nauka, 1980, pp. 153–165.

Kartasheva, G.G., The *"Fagus"* Horizon of the Miocene in Northern Yakutia, *Dokl. Akad. Nauk SSSR*, 1974, vol. 219, no. 5, pp. 1206–1208.

Klimova, R.S., The Miocene Flora and Phytostratigraphic Horizons of the Primorskii Krai, in *Paleobotanika i fitostratigrafiya Vostoka SSSR* (Paleobotany and Phytostratigraphy of Eastern USSR), Krasilov, V.A., Ed., Vladivostok: DVNTs AN SSSR, 1983, pp. 65–76.

Kvavadze, E.V., *Pyl'tsa taksodievykh i ee osobennosti* (The Taxodiaceae Pollen and Its Peculiarities), Tbilisi: Metsniereba, 1983.

Kundyshev, A.S. and Petrenko, T.I., On the Age of the Bolotnaya Fossil Flora of Southern Primor'e, in *Palinologiya Vostoka SSSR* (The Palynology of Eastern USSR), Markevich, V.S., Ed., Vladivostok: DVNTs AN SSSR, 1987, pp. 53–59.

Makhova, Yu.A., Spore-and-pollen Spectra from Modern Alluvium in Middle Courses of the Amur River, in *Sporopyl'tsevoi analiz pri geomorfologicheskikh issledovaniyakh* (Spore-and-pollen Analysis by Geomorphological Studies), Voskresenskii, S.S. and Grichuk, M.P., Eds., Moscow: MGU, 1971, pp. 33–47.

Malygina, E.A., Correlation between Pollen and Plants Distribution Areas within the European Part of the USSR, *Tr. Inst. Geogr., USSR Acad. Sci.*, 1950, vol. 46, no. 3, pp. 42–50.

Mamontova, I.B., The Miocene Flora of Khanka Beds in Primor'e (Palynological Data), in *Novye dannye po stratigrafii i paleogeografii Dal'nego Vostoka* (New Data on the Stratigraphy and Paleogeography of the Far East), Ablaev, A.G., Ed., Vladivostok: DVNTs AN SSSR, 1982, pp. 102–105.

Mamontova, I.B., Palynological Criteria for the Subdivision and Correlation of Paleogene and Neogene Deposits in the Amur–Zeya Depression, in *Raschlenenie i korrelyatsiya osadochnykh tolshch* (Subdivision and Correlation of Sedimentary Sequences), Kosygin, Yu.A., Ed., Moscow: Nauka, 1978, pp. 20–60.

Miotsen Mamontovoi Gory (stratigrafiya i iskopaemaya flora) (The Miocene of the Mt. Mamontovaya: Stratigraphy and Fossil Flora), Saks, V.N., Ed., Moscow: Nauka, 1977.

Oleinikov, A.V. and Klimova, R.S., New Data on the Neogene Stratigraphy of Volcanogenic Deposits in the Samarga River Basin, in *Stratigrafiya kainozoiskikh otlozhenii Dal'nego Vostoka* (Stratigraphy of Cenozoic Deposits in the Far East), Kosygin, Yu.A., Ed., Vladivostok: DVNTs AN SSSR, 1977, pp. 76–80.

Opornyi razrez paleogen–neogenovykh otlozhenii yugo-vostochnogo Sakhalina (Makarovskii razrez) (The Reference Paleogene–Neogene Section in Southeastern Sakhalin, the Makarov Site), St. Petersburg: VNIGRI, 1992.

Pavlyutkin, B.I. and Petrenko, T.I., New Materials on Stratigraphy of Tertiary Deposits of the Rechnoi Peninsula (Southern Primor'e), *Tikhookean. Geol.*, 1993, no. 5, pp. 42–50.

Pavlyutkin, B.I. and Petrenko, T.N., Stratigraphy of Tertiary Coal-Bearing Deposits in the Southeastern Flank of the Khanka Massif, *Tikhookean. Geol.*, 1994a, no. 2, pp. 18–29.

Pavlyutkin, B.I. and Petrenko, T.N., Stratigraphy of the Oligocene–Miocene Boundary Beds in Primor'e, *Stratigr. Geol. Korrelyatsiya*, 1994b, vol. 2, no. 6, pp. 119–127.

Plakhotnik, V.G., New Data on the Stratigraphy and Age of the Extrusive Kizi Formation in Northeastern Sikhote Alin, *Sov. Geol.*, 1962, no. 4, pp. 120–122.

Rybalko, V.I., Ovechkin, V.N., and Klimova, R.S., Cenozoic Basaltoids of the Amga Group (Northeastern Primor'je), *Sov. Geol.*, 1980, no. 12, pp. 59–71.

Stefanovich, E.N., The Comparative Analysis of Spore-and-pollen Spectra of Recent Slope Deposits in the Taiga Zone of Transbaikalia, in *Sporo–pyl'tsevoi analiz pri geomorfologicheskikh issledovaniyakh* (Spore-and-pollen Analysis by Geomorphological Studies), Voskresenskii, S.S. and Grichuk, M.P., Eds., Moscow: MGU, 1971, pp. 24–32.

Varnavskii, V.G. and Mamontova, I.B., The Paleogene–Neogene Boundary in the Sedimentary Sequence of the Amur–Zeya Depression, in *Materialy po paleobotanike i stratigrafii kontinental'nykh otlozhenii Sovetskogo Dal'nego Vostoka* (Materials on Paleobotany and Stratigraphy of Continental Deposits in the Soviet Far East), Ablaev, A.G. and Smirnov, A.M., Eds., Vladivostok: DVNTS AN SSSR, 1975, pp. 16–23.

Ziva, M.V., Palynological Characteristic of Paleogene Deposits in the Amur–Zeya Depression, in *Trudy III Mezhdunarodnoi palinologicheskoi konferentsii* (Proceedings of the 3rd International Palynological Conference), Zaklinskaya, E.D., Ed., Moscow: Nauka, 1973, pp. 89–93.

Stratigraphy and Geological Correlation, Vol. 9, No. 4, 2001, pp. 406–418. Translated from Stratigrafiya. Geologicheskaya Korrelyatsiya, Vol. 9, No. 4, 2001, pp. 99–112.
Original Russian Text Copyright © 2001 by Chekhovskaya, Basov, Gorbarenko.
English Translation Copyright © 2001 by MAIK "Nauka/Interperiodica" (Russia).

Late Quaternary Planktonic Foraminifers of the Extreme Northeastern Kuril Basin (Sea of Okhotsk, Station V34-98)

M. P. Chekhovskaya*, I. A. Basov, and S. A. Gorbarenko*****

** Shirshov Institute of Oceanology, Russian Academy of Sciences, Nakhimovskii pr. 36, 117218 Russia*

*** Institute of the Lithosphere of Marginal Seas, Russian Academy of Sciences, Staromonetnyi per. 22, 109180 Russia*

**** Pacific Oceanological Institute, Far East Division, Russian Academy of Sciences, Baltiiskaya ul. 43, 690041 Russia*

Received July 29, 1999

Abstract—The paper presents the results of quantitative and qualitative analyses of planktonic foraminifer distribution in the Upper Pleistocene–Holocene sediments of the northeastern part of the Kuril Basin in the Sea of Okhotsk. Several assemblages different in their taxonomic composition and corresponding to certain stages of the sea hydrological evolution are established. Comparison of defined foraminiferal assemblages with their coeval counterparts from the Akademii Nauk Rise indicates that they are similar in some and different in other features because of dissimilar impact of Pacific waters, which penetrate into the Sea of Okhotsk via straits in the northern Kuril island arc, on two areas.

Key words: planktonic foraminifers, glaciation, deglaciation, post-deglaciation, Kuril Basin, Sea of Okhotsk.

INTRODUCTION

The Sea of Okhotsk located in the northwestern part of the Pacific is a semiclosed marginal sea basin connected with the ocean via many Kuril straits and with the Sea of Japan via the Tatar and Soya straits. In its hydrological structure, the Sea of Okhotsk is a kind of the unique basin. Its characteristic component is the so-called Sea-of-Okhotsk water mass (Moroshkin, 1966) or the subsurface dichothermal layer (Yang and Honjo, 1996). Formation of this layer with the temperatures close to the freezing point is related to the ice regime of the sea.

The highly contrast seasonal fluctuations, distinct stratification of surface waters during the warm season, and active water exchange with the ocean are favorable conditions for the intense development of phyto- and zooplankton and, as a result, for the high rate of organic matter flux to the bottom.

In response to the specific hydrological structure, development of the Sea-of-Okhotsk water mass, and extremely high productivity of surface waters, biocoenosis of planktonic foraminifers in the sea substantially differs from that in the Subarctic Pacific in proportions and dwelling environments of species (Bradshaw, 1959; Be, 1977; Reynolds and Thunell, 1985; Sautter and Thunell, 1989; Alderman, 1996).

The analysis of taxonomic composition and distribution of Late Quaternary planktonic foraminifers in the Sea of Okhotsk (Station V34-90) revealed peculiar features of assemblages enclosed in sediments deposited during the glacial period, deglaciation, and post-deglaciation time. It was established that the productivity of surface waters in the sea was significantly lower during the last glaciation than at present (Chekhovskaya and Basov, 1999).

The specific hydrological structure of the sea and its different evolution, as compared with that in the North Pacific, is also emphasized by differences in development of siliceous planktonic microorganisms in two basins. For instance, the modern diatom community of the Sea of Okhotsk essentially differs in the composition and structure from its counterpart in the northern part of the ocean, being close to the diatom assemblage that was discovered in northern oceanic region from sediments of the last glacial period (Sancetta and Silvestri, 1986). Similar results are also obtained for radiolarian assemblages (Morley and Hays, 1983).

In this work, we consider dynamics of compositional and structural changes in planktonic foraminifer assemblages in the Upper Pleistocene–Holocene sediments at the continental slope foot of the northern Kuril Island arc in the southeastern Sea of Okhotsk, in the area influenced by Pacific waters inflowing via north Kuril straits. The obtained data elucidate hydrological changes for the last 17000 years.

MATERIALS AND METHODS

The studied sediment core was obtained during Leg 34 of the R/V *Vulkanolog* at Station V34-98 near the foot of the underwater slope of Kamchatka in the southeastern Sea of Okhotsk: 50°06.6′ N; 153°12.0′ E; water depth of 1175 m (Fig. 1). The core length is 330 cm.

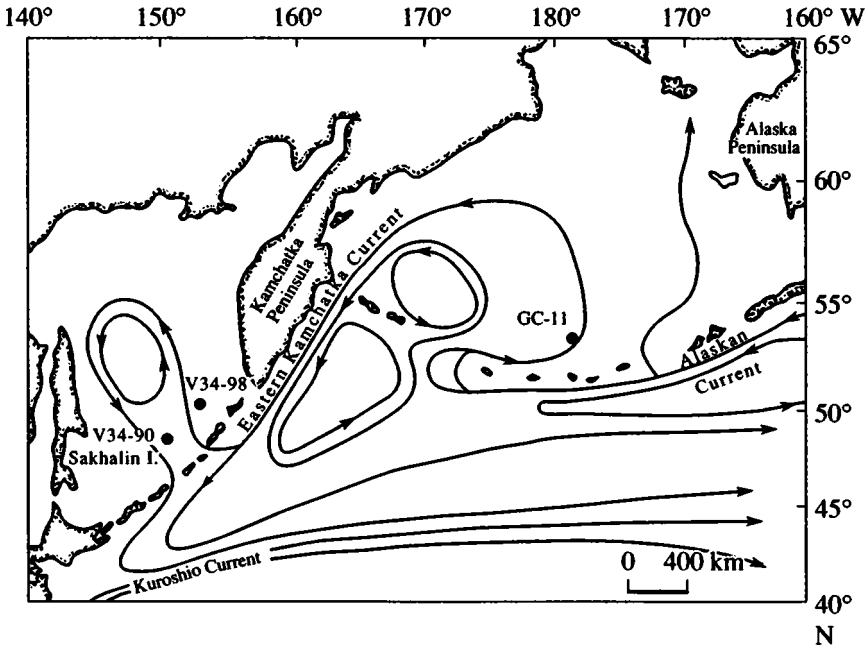

Fig. 1. Surface circulation in the North Pacific, Bering and Okhotsk seas (after Dodimead *et al.*, 1963) and location of cores V34-98 and V34-90.

From the base upward, the core section is composed of gray silt (330–250 cm), greenish gray silty–pelitic mud (250–135 cm), and green diatomaceous ooze (upper 135 cm). The lower part of the section encloses two thin (several centimeters) interbeds of volcanic ash occurring at levels of 195 and 170 cm.

Planktonic foraminifers were examined in 63 samples collected from every 5-cm-long interval. In fractions of >0.05 mm from all sample, abundance and relative content of individual species were counted and calculated per 1 g of dry sediment. Radiocarbon dates obtained for planktonic foraminifer tests from levels of 44, 99, 204, 214, 219, 244, 294, and 325 cm are 2670, 4850, 9440, 9670, 11640, 12280, 15170, and 16130 years, respectively. Age determinations were performed at the Lawrence Livermore National Laboratory (California, USA) using the AMS technique (Gorbarenko *et al.*, in press).The radiocarbon age is reduced for the reservoir-correction factor of surface waters of the Sea of Okhotsk by subtracting 1000 years (Southon *et al.*, 1993). The sediment age between radiocarbon dates is determined using the interpolation method.

MODERN HYDROLOGY

Core V34-98 was obtained in the southeastern part of the sea, in the area located near northern straits in the Kuril island arc, through which an intense flow of Pacific intermediate waters enters the basin.

The vertical structure of surface waters in the Sea of Okhotsk is similar to that characteristic of Subarctic waters in the Pacific (Moroshkin, 1966). It has however a sharper temperature minimum and near-surface halocline hindering the vertical water exchange. In winter, a significant part of the sea is covered by ice, and floating ice is preserved during five months. The southeastern part of the sea, where the core was taken, is free of ice year round owing to the influence of Pacific waters. The vertical surface structure is subjected to sufficiently sharp variations during the year. During the late autumn and winter, water in the surface layer of 100–200 m thick is cooled and uniform owing to mixing. The spring and summer heating affects only the upper layer 20–40 m thick. The surface temperature in August–September is highest in the central part of the sea, where it amounts to 10–14°C. The heated surface layer is underlain at this time by a specific, so-called Sea-of-Okhotsk water mass (Moroshkin, 1966), or by regional dichothermal layer (Yang and Honjo, 1996) that extends throughout the entire sea in the depth interval from 30–40 to 150–200 m and has year round the temperatures close to the freezing point. The hydrological structure of the sea with its distinct stratification during the warm season is determined by sea ice and Amur River fresh water discharge.

In the Station V34-98 area influenced by Pacific waters (Fig. 2), the water temperature at depth of 20–30 m is 0.71–1.24°C in winter and spring (January–June) and 3.86–8.63°C (July–December). In the depth interval of 50–200 m, it varies from about 1 to 1.84°C depending on the season (Levitus, 1982). At a depth of 250 m, the temperature falls down to 1.3°C and then increases to maximum values of 2.59 and 2.55°C at depths of 800 and 900 m, respectively. Downward, it

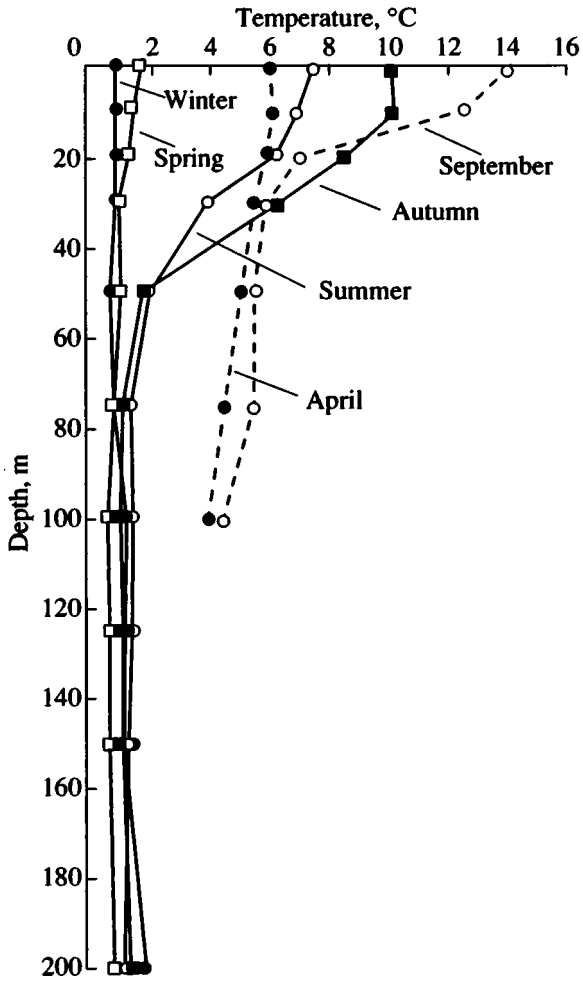

Fig. 2. Seasonal variations of water temperature in the upper 200 m. Solid line designates this parameter in the Station V34-98 area; dashed line, that in the North Pacific (Station PAPA, 50°N, 145°W; Reynolds and Thunell, 1985).

gradually decreases again to reach the value of 2.37°C at a depth of 1000 m.

MODERN PLANKTONIC FORAMINIFER ASSEMBLAGES

First data on taxonomic composition and distribution of planktonic foraminifers in the surface sediment layer of the Sea of Okhotsk can be found in works by Shchedrina (1953), Saidova (1957, 1961), Lipps and Warme (1966). According to these researchers, species of planktonic foraminifers from that layer are *Neogloboquadrina pachyderma* (Ehrenberg), *N. dutertrei* (d'Orbigny), *Globigerina bulloides* d'Orbigny, *G. quinqueloba* Natland, *Globigerinita uvila* (Ehrenberg), *G. glutinata* (Egger), and *Globorotalia scitula* Brady. The foraminiferal assemblage is universally dominated by *N. pachyderma* and *G. bulloides* representing together usually about 95% of total test abundance. A high abundance and maximum diversity of planktonic foraminifers are confined to the southeastern part of the sea, where the inflow of Pacific waters is most intense. In the near-shore areas, they are missing and only *N. pachyderma* and *G. bulloides* are recorded north of 54°N. All above-mentioned species of planktonic foraminifers are also characteristic of their assemblages occurring in waters and bottom sediments of the modern Subarctic Pacific (Bradshaw, 1959; Be, 1977; Reynolds and Thunell, 1985; Thunell and Honjo, 1987; Sautter and Thunell, 1989). In addition, rare specimens of tropical–subtropical species *Globigerinoides ruber* and *G. conglobatus* occur in the extreme southern part of the sea (Shchedrina, 1953).

The sediment trap that was installed in the Sea of Okhotsk at the station with coordinates 53°19′ N and 149°50′ W at the depth of 256 m and operated from August, 1990 to August, 1991, provided data on the modern biocoenosis of planktonic foraminifers and their response to hydrological changes (Alderman, 1996). It was shown that prevalent in the modern planktonic foraminifer assemblage are the polar species *Neogloboquadrina pachyderma* sin. and relatively thermophilic species *Globigerina bulloides*. Such a combination of species is characteristic of their modern Subarctic biocoenosis (the table). Two peaks of foraminifer production, the poorly expressed vernal (the second half of May–June) and sufficiently distinct autumnal (the second half of September–November), were established in the Sea of Okhotsk. The second one is responsible for 74% of annual production of planktonic foraminifers. The average annual composition of the assemblage is shown in the Table. Species *N. pachyderma* sin. is abundant at the end of spring to beginning of summer (May–June) and in autumn (September–November), whereas *G. bulloides* and *G. quinqueloba* form noticeable concentrations only in the autumn season (Alderman, 1996). Large tests (over 0.25 mm) of species *G. bulloides* are dominant in autumn foraminiferal production, whereas its smaller generation is prevalent during the spring production season.

DISTRIBUTION OF PLANKTONIC FORAMINIFERS THROUGH THE SECTION

Changes in the structure of planktonic foraminifer assemblages, oxygen isotope composition in the *Neogloboquadrina pachyderma* sin. tests, and radiocarbon dating allowed us to distinguish glacial, deglacial, and postglacial sediments in Core V34-98 (Fig. 3). Simultaneously, the distinguished intervals differ from each other in preservation of tests and $CaCO_3$ contents in sediments.

The glacial planktonic foraminifer assemblage discovered in the interval of 333–253 cm (16130–12500 years) includes only two species: *Neogloboquadrina pachyderma* and *Globigerina bulloides*. Prevalent is first of them represented by *N. pachyderma* sin. (69–87%) and *N. pachyderma* dex. (less than 1 to 4%) varieties. The share of *G. bulloides* varies from 9 no 32%.

Comparison of planktonic foraminifer composition in modern sediments and sediment traps in the Sea of Okhotsk and North Pacific

Species	Pacific				Sea of Okhotsk
	Bradshaw, 1959	Sautter, Thunell, 1989			Alderman, 1995
	plankton traps	sediment traps September, 1982–August, 1984	sediment traps November, 1984–February, 1986	bottom sediments, depth of 2255 m	sediment rap August, 1990–August, 1991
G. quinqueloba	1–50%	45–75%	50–55%	Not recorded	8%
N. pach. dex.	No data	10–20%	5–10%	3%	1%
N. pach. sin.	1–20%;	5–15%	25–30%	87%	57%
G. glutinata	Single	5–15%	5–7%	<1%	<1%
G. bulloides	1–20%	5%	10%	10%	31%
G. uvula	Over 20%	No data	No data		<1%
G. scitula	Not recorded	<1%	<1%	Not recorded	<1%
O. universa		5%	10%	Not recorded	

Glacial sediments are characterized by low foraminiferal abundance. Against this background, their content in the middle part of the interval (295–260 cm) slightly increases. Throughout the entire glacial section, the assemblage bears signs of tests dissolution. Foraminiferal tests are fragile, frequently broken, with etched walls; small tests (0.1–0.05 mm) are usually missing. Sediments from the intervals of 325–315 cm (fraction 0.25–0.05 mm) and 295–290 cm (fraction 0.1–0.05 mm) are enriched in diatoms, the content of which amounts there to 50–70 and 40%, respectively. In the intervals of 310–300 and 285–260 cm, diatoms are scarce.

Transition from glacial to deglacial sediments was established in the interval from 260 (13200 years) to 250 cm. The boundary between them is arbitrary, because changes in composition and abundance of foraminifers are established in two, relatively long core samples (10 cm) characterizing the transitional interval. In the sample from the interval of 260–270 cm, tests of planktonic foraminifers compose about 5% of fraction 0.25–0.1 mm and are represented by species *Neogloboquadrina pachyderma* sin. (85%) and *Globigerina bulloides* (15%); large tests of the last species (over 0.25 mm) make up less than 1%. In the overlying sediments (interval of 250–260 cm), the proportion of planktonic foraminifers increases to about 50% of fraction 0.25–0.1 mm. Their assemblage consists of *N. pachyderma* sin. (about 68–69%), *G. bulloides* (25%, including 8% of large tests in the uppermost layer of the interval), and Globigerina quinqueloba (6%), all associated with single *Globigerinita uvula* and *G. glutinata* first occurring in the section. Data on oxygen isotope composition in tests of planktonic and benthic foraminifers and radiocarbon dating (Gorbarenko *et al.*, in press) indicate that Termination 1A of the last glacial period corresponding to accelerated glacier melting and sea-level rise (Fairbanks, 1989) is recorded in Core V34-98 at the depth of about 250 m. Chronologically (about 12500 years BP), this level coincides with the global Bolling Alleröd warming event. In sediments of the Sea of Okhotsk, this event is marked by a sharp increase in the carbonate and organic carbon contents.

As is evident from the above characteristic of planktonic foraminifers, their assemblage of the first deglacial phase differs from the glacial one in the higher production rate, higher diversity, and more thermophilic composition. The last point is emphasized by appearance (in addition to the above-mentioned species *Globigerina quinqueloba, Globigerinita uvula*, and *G. glutinata*) of *Globorotalia scitula* representatives at the level of 235 cm. In the bottom sediments of the modern Sea of Okhotsk, the latter species is very scarce, whereas in the North Pacific it is registered only in its eastern part (Bradshaw, 1959). The appearance of species *G. uvula, G. glutinata*, and *G. scitula* at the level of 12280 years is also recorded in Core V34-90 (Gorbarenko *et al.*, 1998; Chekhovskaya and Basov, 1999).

Variations in the content of *Globigerina bulloides* in sediments corresponding to Termination 1A are less sharp as compared with those in glacial sediments, from 18 to 32%. Simultaneously, the content of large (more than 0.25 mm) forms shows significant variations, from 8–21% in the interval of 245–230 cm to 3.6% in the interval of 225–220 cm. The noticeable role in the assemblage belongs to *G. quinqueloba* whose content ranges from 1–2 to 6–14%.

Foraminifers from the interval of 230–245 cm corresponding to the beginning of the Termination 1A episode are mainly represented by well-preserved tests. Fragments are rare, test walls bear no apparent dissolution signs, and the assemblage includes small transparent thin-walled tests, the content of which amounts to 13% at the level of 235 cm. Also present are lobate specimens of *Neogloboquadrina pachyderma* sin. with

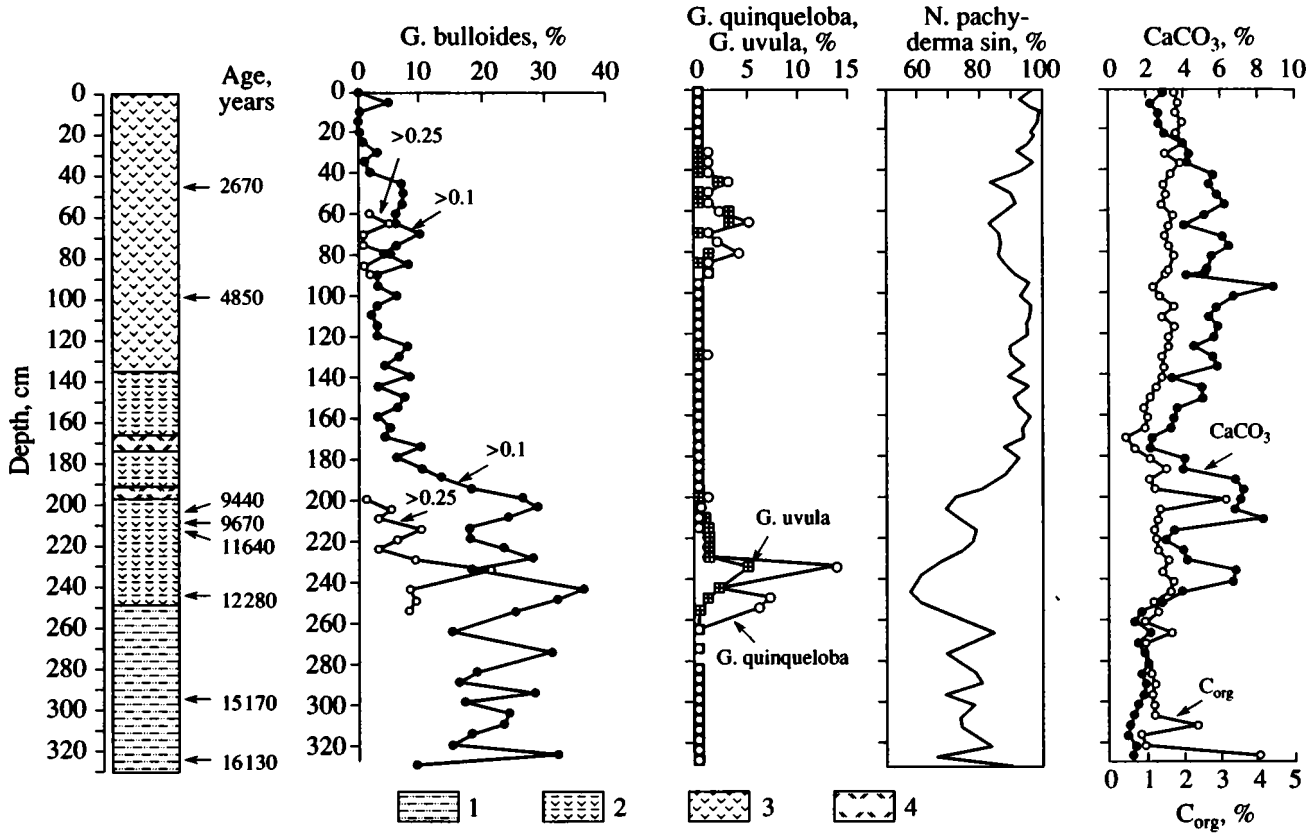

Fig. 3. Lithology, age of sediments, and proportions of some planktonic foraminiferal species (%), and contents of C_{org}, SiO_2, and $CaCO_3$ in sediments of Core V34-98: (1) silty terrigenous mud; (2) silty–pelitic terrigenous–biogenic mud; (3) pelitic biogenic (diatomaceous) ooze; (4) volcanic ash.

five chambers. The end of Termination 1A (interval of 220–225 cm) is marked by the decrease in total abundance and share of small forms. Sediments are enriched in fragments of planktonic foraminifer tests, and test walls become fragile and etched by dissolution. Thus, the initial stage of deglaciation is characterized by the low intensity of dissolution, whereas the later period of the Termination 1A is marked by activation of this process.

Judging from radiocarbon dates and sedimentation rates, the interval of 214–219 cm coincides with a hiatus of about 2000 years long. This is evident from a sharp increase of silty material in sediments at this level.

Sediments from the interval of 214–175 cm corresponding to Termination 1B (from 9700 to about 8000 years BP) yield more abundant planktonic foraminifers than sediments of Termination 1A. Moreover, their tests are frequently fragile, broken, and etched. Abundant are test fragments, which compose 40–50% of fraction 0.1–0.05 mm, whereas the share of well-preserved tests 0.1–0.05 mm in size does not exceed 1%.

The corresponding assemblage of planktonic foraminifers includes *Neogloboquadrina pachyderma* sin. (70–90%), *Globigerina bulloides* (5–35%), rare *G. quinqueloba* and *Globigerinita uvula* (below 1%), single *G. glutinata* and *Globorotalia scitula.*

Foraminifers are most abundant in the interval of 214–195 cm, where their tests compose up to 80–100% of fraction 0.25–0.1 mm. The share of *Globigerina bulloides* amounts to 28–34%, and the content of large tests varies here from 1 to 5–10%. Higher in the section, in the interval of 195–175 cm (the end of Termination 1B), abundance of planktonic foraminifers decreases and their content in fraction 0.25–0.1 mm is reduced up to 40–60%. The share of *G. bulloides* decreases from 18 to 6%; large tests are scarce.

The planktonic foraminifer assemblage from sediments of the upper part of the section (170–0 cm) deposited during the postglacial, or current interglacial period (last 8000 years) differs from earlier ones by even greater prevalence of *Neogloboquadrina pachyderma* sin. (up to 90% and more) and by several-fold abundance decrease of *Globigerina bulloides.* The second half of this period is marked by noticeable development of *G. quinqueloba.* The test appearance and composition of planktonic foraminifers suggest their intense dissolution: tests are fragile, thinned, and small specimens are rare or single.

Against the background of a generally uniform foraminiferal composition, there are intervals slightly different in their total abundance and relative proportion of some species, e.g., of *Globigerina bulloides, G. quinqueloba*, and *Globigerinita uvula*, as well as in the content of $CaCO_3$ and diatom frustules in fraction 0.25–0.1 mm.

The interval of 130–170 cm (8000–6000 years BP) marks a gradual transition from terrigenous to biogenic calcareous–siliceous sedimentation. Fraction 0.25–0.1 mm from this interval largely consists of tests of planktonic foraminifers. The *Globigerina bulloides* content ranges here from 3 to 8%. Present are small forms of *Globigerina quinqueloba* and *Globigerinita uvula.*

In the interval of 90–130 cm (6000–4000 years BP), the share of *G. bulloides* slightly decreases (usually less than 5%). Occasional large tests of *G. quinqueloba* and *G. uvula* occur as well. Fraction 0.25–0.1 mm consists mainly of diatom frustules, although foraminiferal tests still represent a noticeable share. The $CaCO_3$ content up to 9% in these sediments is highest for the entire interglacial period (Fig. 3).

The interval of 45–90 cm (4000–2470 years BP) is distinguished owing to a relative decrease in the content of *Neogloboquadrina pachyderma* sin. (up to 82–85%) and because of the increased role of *Globigerina quinqueloba* (1–5%), *G. bulloides* (4–10%) and *Globigerinita uvula* (1–3%). The last species shows the increased share of specimens more than 0.25 mm in size. Present are large specimens of *N. pachyderma* sin. and *G. bulloides*. Tests of the latter species are lobate, slightly elongated, having additional apertures. The $CaCO_3$ content somewhat decreases, remaining though at a sufficiently high level (about 6%).

The upper 45 cm of sediments (the last 2470 years) show the increased share of *Neogloboquadrina pachyderma* sin. (up to 95–100%) and reduced content of *Globigerina bulloides* (up to 5–7%), *G. quinqueloba*, and *Globigerinita uvula* to complete disappearance of last two species. The $CaCO_3$ content in sediments falls down to 2–4%.

Most significant lithological changes occur in the interval of 135–90 cm (6000–4000 years BP) where terrigenous sediments are completely replaced by biogenic siliceous ones. Simultaneously, planktonic foraminifers also show substantial changes: the role of *Globigerina quinqueloba* and *Globigerinita uvula* increases, common are large forms of *Globigerina bulloides* and abnormal species of *Neogloboquadrina pachyderma* sin. Similar changes in lithology and foraminiferal composition are also noted in the interval of 140–110 cm (about 6000–4000 years BP) at Station V34-90 in the Akademii Nauk Rise area.

DISCUSSION

As is seen from above characteristic of planktonic foraminifers from glacial, deglacial, and interglacial sediments recovered by Core V34-98, their assemblages are generally characterized by poor preservation. Universally, they are dominated by *Neogloboquadrina pachyderma* sin. whose share varies from 60 to 100% of population. The second in importance is *Globigerina bulloides*, whose content amounts to 30–35% in glacial and deglacial sediments. In postglacial sediments (the last 8000 years), its share is several times lower. Accessory species are represented by *N. pachyderma* dex., *Globigerina quinqueloba*, and *Globigerinita uvula.* Their concentration is usually lower than 1%, but the content of latter two species increases (up to 5–15 and 3–5%, respectively) in sediments deposited during periods from 12500 to 12000 years BP and from 4000 to 2500 years BP. First of these periods is also marked by occasional occurrence of *Globorotalia scitula.*

Changes in composition of planktonic foraminifers throughout the section reflect transformation of hydrological conditions in the southeastern Sea of Okhotsk during the last 17000 years covering a terminal stage of the last glaciation, deglaciation, and postglacial (current interglacial) period. The analyzed distribution of planktonic foraminifers in sediments from the southern slope of the Akademii Nauk Rise in the central part of the Sea of Okhotsk (Chekhovskaya and Basov, 1999) revealed similar changes in composition and structure of their assemblages. Comparison between two sites elucidates ecology of different species and offers a possibility to reconstruct hydrological and hydrochemical environments in the study area.

Thanatocoenosis of planktonic foraminifers in last glacial sediments formed at the time of low productivity in surface waters and dissolution of tests at the sea floor. It is not inconceivable that composition of the fossil assemblage in this case does not correspond to that of biocoenosis. The intense dissolution of foraminiferal tests at that time is indicated by low $CaCO_3$ contents in sediments and by habit of tests proper. They are usually fragile, having secondary thinned wall, and frequently fragmented. The absence of *Globigerina quinqueloba* in the glacial foraminiferal assemblage is probably a consequence of dissolution. This species occurs permanently along with *Neogloboquadrina pachyderma* sin. and *Globigerina bulloides* in coeval glacial sediments of the Akademii Nauk Rise in the central Sea of Okhotsk (Station V34-90), where its content makes up 2–4%. Dissimilar to Station V34-98, the foraminiferal assemblage is characterized there by relatively good preservation.

Differences in hydrological regime of two areas can be explained by their different geographic position and, correspondingly, by different influence of Pacific waters. The Station V34-98 located near the northeastern part of the Kuril island arc, within the area of a high

phytoplankton productivity owing to the intense influx of Pacific waters enriched in nutrients (Arzhanova and Zubarevich, 1997). The modern abundance of planktonic foraminifers in this area is also the highest (Lipps and Warme, 1966). It can be confidently assumed that the intense water exchange between the Pacific and Sea of Okhotsk could exist, at least intermittently, also during the glacial period, and this would result in higher productivity of surface waters as compared with other areas of the sea. The diatom-rich sediments from intervals of 295–290 and 325–315 cm were probably deposited precisely during such periods of the intense water exchange between the Pacific Ocean and Sea of Okhotsk. It is established in the North Pacific that the higher phytoplankton (including diatoms) production in surface waters was characteristic of the glacial period (Sancetta, 1992; Gorbarenko, 1996). The relatively high biological productivity of surface waters in this region is supported by higher C_{org} content in glacial sediments, as compared with the Akademii Nauk Rise area (over 1.0% versus 0.6–0.8%). Nevertheless, surface water temperatures were low, probably negative during the winter season (Moore *et al.*, 1980), and ice could cover also the southeastern part of the sea. This should negatively affect community of planktonic foraminifers and its productivity.

The onset of deglaciation (12500 years BP) is marked by significant changes in productivity and composition of planktonic foraminifers. The boundary between glacial and deglacial sediments in the studied section is well manifested and easily recognizable by a sharp increase in abundance of foraminifers. The concentration of foraminiferal tests in deglacial sediments (interval of 253–175 cm) is the highest for the entire section. A sharp abundance increase in these sediments, despite slightly fluctuating sedimentation rates and, correspondingly, low dilution, implies a high production of planktonic foraminifers in surface waters. The $CaCO_3$ content in sediments also increases noticeably during this period.

Thus, one can suggest a substantially higher productivity of surface water during deglaciation as compared with the preceding glacial period. A similar trend is also characteristic of the central part of the Sea of Okhotsk (Gorbarenko, 1996; Gorbarenko *et al.*, 1998; Chekhovskaya and Basov, 1999).

Compositionally, the foraminiferal assemblage of deglaciation time also sharply differs from that buried in glacial sediments, and indicates a warmer state of surface waters. In addition to *Neogloboquadrina pachyderma* and *Globigerina bulloides*, the deglacial assemblage includes *Globigerinita uvula, G. glutiniata, Globorotalia scitula*, and *Globigerina quinqueloba*, which occasionally occur also in younger, including modern, sediments. Most abundant is the last species. Its appearance and abundance increase up to 12% during Termination 1A (12500–11640 years BP) indicates a circulation vigor and water temperature rise. In the Norwegian–Greenland basin, this postglacial species shows concentration peaks in periods of vigorous hydrodynamics (Bauch, 1992). The content of *Globigerina bulloides*, the species second in abundance after *Neogloboquadrina pachyderma* sin., is comparable with that observed in glacial sediments (up to 15–30%). Its share increases up to 40% only at the onset of deglaciation. Simultaneously, the deglacial assemblage shows an increased content of large tests of *Globigerina bulloides*, which are characteristic of its autumn generation in the modern biocoenosis of planktonic foraminifers (Alderman, 1996), in contrast to sinistral variety of *N. pachyderma* whose abundance decreases down to 60% and less. All these characteristics unambiguously indicate vigorous surface circulation and intense inflow of Pacific waters at the time in question. It is noteworthy that the Akademii Nauk Rise area, where similar patterns in distribution of the entire *Globigerina bulloides* population were established, shows no comparable peak in abundance of large specimens of this species.

Bottom waters also experienced significant parametric variations during the first phase of deglaciation (Termination 1A). Waters of this phase were less aggressive with respect to $CaCO_3$ than those of the later phase. This is indicated by better preservation and higher abundance of foraminiferal tests, and by elevated $CaCO_3$ content in sediments (over 6%). The foraminiferal assemblage from sediments corresponding to the end of the early phase of deglaciation (interval of 220–225 cm) bears signs of more intense dissolution. The fall in the $CaCO_3$ content up to 3% is accompanied by the decrease in foraminiferal abundance.

Similar variations are also characteristic of the second deglacial phase (Termination 1B). Its beginning was most likely marked by a high production of planktonic foraminifers, which is reflected in their high abundance and elevated $CaCO_3$ content (up to 8%) in sediments. The relative content of *Globigerina bulloides* in the assemblage of that time was slightly lower than during the first phase, though still rather high (up to 35%). Simultaneously, the share of its large specimens is noticeably lower (up to 10%). In sediments corresponding to the end of the second deglacial phase, the total abundance of foraminifers sharply decreases, and large specimens of *G. bulloides* occur just occasionally. The $CaCO_3$ and C_{org} contents in sediments decrease down to 2 and 0.5%, respectively. All this indicates the lower production of planktonic organisms, including foraminifers, in surface waters as compared with the first deglacial phase. The decreased influx of planktonic foraminifer tests to the floor was accompanied by enhance dissolution and, as a result, by their worse preservation.

The considered deglaciation phases correspond to negative excursions of isotope composition in foraminiferal tests (Terminations 1A and 1B; Gorbarenko, 1996) and to episodes of intense ice melting in the North Atlantic (Duplessy *et al.*, 1991). They are sepa-

rated by the short-term but sharp Younger Dryas cooling event, which likely corresponds to a hiatus in the studied core section.

Composition of planktonic foraminifers and their distribution throughout the section suggest that hydrological conditions in the Sea of Okhotsk during the postglacial period (the last 8000 years) were steadier than in the previous period. The foraminiferal assemblage from relevant sediments is almost entirely represented by *Neogloboquadrina pachyderma* sin. (up to 95%) that associates with subordinate, though permanently occurring *Globigerina bulloides*. Tests of both species bear signs of intense dissolution. Accessory species are *Globigerina quinqueloba, Globigerinita uvula, G. glutinata*, and *Globorotalia scitula*. Despite the relative taxonomic uniformity of all postglacial foraminiferal assemblage, they show certain variations, which, combined with lithology, elucidate changes in their living and burial conditions.

The beginning of the postglacial period (8000–6000 years BP; interval of 135–175 cm) is marked by the relatively low abundance of planktonic foraminifers and by low contents of $CaCO_3$ and C_{org} (2 and below 0.5%, respectively). The foraminiferal assemblage from this level is dominated by *Neogloboquadrina pachyderma* sin. whose proportions range from 89 to 97%. Present are also rare *N. pachyderma* dex. (1–2%) and *Globigerina bulloides* (2–8%). The latter is almost entirely represented by small forms. *Globigerina quinqueloba* and *Globigerinita uvula* occur as single specimens.

Similar changes in foraminiferal assemblages were also noted in the central part of the Sea of Okhotsk (Chekhovskaya and Basov, 1999). The synchronous decrease in production of planktonic foraminifers and concurrent cold-resistant assemblages in both areas of the sea suggest a cooling phase. It is noteworthy that palynological data from Holocene sediments of the Laptev Sea (Naidina, 1998) also indicate cold conditions at that time (8500–6300 years BP).

By the end of this time interval, the $CaCO_3$ and C_{org} contents in sediments increases up to 6 and 1.5%, respectively, which reflects the enhanced productivity of surface waters. This is also confirmed by gradual upward increase in the content of the biogenic siliceous material in sediments. Sediments from the upper part of the considered interval enclose single large specimens of *Globigerina quinqueloba*.

The production of planktonic foraminifers grew also in the period from 6000 to 4000 years BP, when their total abundance and $CaCO_3$ content in sediments were at the maximum (Fig. 3). The proper foraminiferal assemblage includes single large tests of *Globigerina quinqueloba, Globigerinita uvula, G. glutinata*, and *Globorotalia scitula*. Simultaneously, the biogenic material (SiO_2 and $CaCO_3$) becomes a prevalent component in sediments making up 50% and more in total.

In the section V34-90, this period is marked by the maximum abundance of planktonic foraminifers and $CaCO_3$ content in sediments, as well as by a sharp increase in the production of siliceous microorganisms in surface waters that caused accumulation of large volumes of biogenic silica at the sea floor. Like in the study area, sediments of the Akademii Nauk Rise area are characterized by an elevated content of large *Globigerina quinqueloba* specimens and by occasional occurrence of large *Globigerinita glutinata* and *G. uvula* forms. According to oxygen isotope data, this interval in section V34-90 corresponds to the negative $\delta^{18}O$ anomaly (0.5‰), which allowed Gorbarenko *et al.*, (1998) to define the Termination 1C event. A similar anomaly is also characteristic of section V34-98.

All these events correspond to the Holocene climatic optimum that is established by different methods in many areas. In the North Atlantic, that period was characterized by maximum (for the Holocene) summer temperatures of surface waters (Bard *et al.*, 1990; Koc Kapuz and Schrader, 1990; Baumann and Matthiessen, 1992). According to the model of global atmosphere circulation (COHMAP-Members, 1988), summer temperatures around 6000 years BP were higher than now. By virtue of palynological data, significant warming is also registered in the Arctic at that time. Naidina (1998) showed that the second half of the Atlantic period (6200–4800 years BP) is marked in the Laptev Sea by an increased content of arboreal pollen in sediments, which indicates a substantial warming. The palynological data point to a similar warming in the Sea of Okhotsk (Morley *et al.*, 1991) and in Hokkaido Island (Tsukada, 1988).

As was shown above, the composition of planktonic foraminifers in the study area did not change substantially at that time. The water temperature rise is indicated only by a slight increase in the content of large specimens of *Globigerinita glutinata* and by occurrence of large *Globigerinita glutinata* and *G. uvula* forms. The Holocene climatic optimum (from 6000 to 4000 years BP) is manifested here in the increased production of planktonic foraminifers (the increase in foraminiferal abundance and $CaCO_3$ content) and siliceous phytoplankton. Particularly sharp was an increase in production of diatoms, which became main components in sediments since that time.

Such a sudden increase in silica accumulation was probably related to the change of the ice regime in the Sea of Okhotsk and to northward migration of sea ice distribution boundary. Today, the vernal peak (May–June) in biogenic silica production, corresponding to 80% of its total annual volume, coincides with the beginning of water heating and stratification (Arzhanova and Zubarevich, 1997). As was established in the northwestern part of the Pacific (St. RAMA 44-PC; Keigwin *et al.*, 1992), the increase in biogenic opal content in sediments from 10 to 40%, as well as in an abundance of planktonic foraminifers and $CaCO_3$ content (from 1 to 15%) correspond to the onset of deglaciation (Termination 1A). In the Sea of Okhotsk, winter sea-

sons of the glacial and, probably, deglacial periods were longer than now, and therefore the spring bloom of phytoplankton was not pronounced. The ice and hydrological conditions, close to modern ones, were settled here most likely in the period of 6000 to 4000 years BP. It is noteworthy that according to palynological data (Naidina, 1998), climatic conditions of the last 4700 years in the Laptev Sea region were similar to modern ones and experienced only slight variations.

In sediments corresponding to the period of 4000–2700 years BP, the relative content of *Neogloboquadrina pachyderma* sin. tests decreases to 85% and less. Simultaneously, the role of *Globigerina quinqueloba, Globigerinita uvula*, and large *Globigerina bulloides* increases to 5, 3, and 10%, respectively. Such a composition of foraminiferal assemblage indicates probably an intense inflow of Pacific waters.

Bottom waters of the last 2470 years were most aggressive with respect to calcium carbonate, whose content gradually decreases upward the section from 6 to 2%. The foraminiferal assemblage of this period is almost entirely composed of *Neogloboquadrina pachyderma* sin. accompanied by rare *Globigerina bulloides* and *G. quinqueloba*. No tests of *Globigerinita uvula, G. glutinata*, and *Globorotalia scitula*, both permanently occurring in underlying sediments, are recorded in this interval. Sediments of the last 1500 years are also barren of *G. quinqueloba* and *G. bulloides*. Rare tests of the last species are registered only in the interval of 5–10 cm.

Peculiar Features of Globigerinita uvula, Globigerinita glutinata, and Globorotalia scitula Distribution

Species *Globigerinita uvula, G. glutinata*, and *Globorotalia scitula* are most thermophilic forms amid planktonic foraminifers populating the modern Sea of Okhotsk (Lipps and Warme, 1966). This is also evident from their distribution in Upper Pleistocene–Holocene sediments of the central and southeastern parts of the basin. In glacial sediments, these species are not recorded. Although they are usually scarce in the modern ocean and low-resistant to dissolution, their absence in terrigenous sediments of the glacial period can hardly be explained by the influence of dissolution. In the Sea of Okhotsk, they are missing from glacial sediments of the core-section V34-98, where the foraminiferal assemblage bears signs of intense dissolution, and at Station V34-90 in layers with well-preserved foraminiferal tests (Chekhovskaya and Basov, 1999).

All three species live in the modern North Pacific. *Globigerinita uvula* and *G. glutinata* are permanently present in waters of the northwestern Pacific (Reynolds and Thunell, 1985; Sautter and Thunell, 1989). The latter species is particularly abundant near the Kuril Island arc composing more than 20% of foraminiferal population (Bradshaw, 1959). *Globorotalia scitula* is present during warm season (April–October) in foraminiferal biocoenosis of the northeastern Pacific, migrating there from the temperate zone with the beginning of a spring season (Reynolds and Thunell, 1985).

The absence of these species in glacial sediments of the Sea of Okhotsk can be explained if we assume that their distribution areas were located during glaciation southerly, outside the Eastern Kamchatka and Oyashio currents in the northwestern part of the Pacific. According to paleotemperatures reconstructed for the northwestern part of the Pacific, the surface water in this region (including the Sea of Okhotsk) was by 2°C cooler 18000 years ago than at present (Moore *et al.*, 1980, Figs. 6, 8). Such a cooling of surface waters in the high-latitude region represented a factor of a critical importance, particularly during the winter season. As a result, the isotherm 0°C shifted in winter from the Kuril islands and Kamchatka far to the east and south reaching the northern Honshu (Moore *et al.*, 1980; Figs. 5–8). Based on these data, one can assume that low winter temperatures and, probably, sea-ice conditions during the glaciation in northwestern Pacific resulted in a significant reduction of *Globigerinita uvula, G. glutinata*, and *Globorotalia scitula* distribution areas. Today, the seasonal reduction is characteristic of the *Globorotalia scitula* distribution area in the Subarctic Pacific (Reynolds and Thunell, 1985).

In the V34-98 section, *Globigerinita uvula, G. glutinata*, and *Globorotalia scitula* appear simultaneously at the level of 250 cm, which corresponds to Termination 1A (about 12280 years BP). In the Akademii Nauk Rise area (St. V34-90), this level (12180 years BP) is marked by a first occurrence of *Globigerinita uvula* and *Globorotalia scitula*, whereas *Globigerinita glutinata* appears slightly later, at the Termination 1B level. The synchronous appearance of these species in the central and southeastern parts of the sea suggests a rapid and substantial rise of surface water temperature in the considered region, probably in response to the inflow of Pacific waters.

Despite the fact that *Globorotalia scitula* occurs in the modern foraminiferal biocoenosis only in the northeastern Pacific and has never been found in plankton traps in its northwestern part (Bradshow, 1959), we assume that its appearance in the Sea of Okhotsk could be related to the inflowing Pacific waters. The Soya Strait 50 m deep is a passageway for thermophilic species penetrating now from the Sea of Japan into the Sea of Okhotsk (Shchedrina, 1953; Lipps and Warme, 1966), and it was proposed (Belyaeva and Burmistrova, 1997) that *Globorotalia scitula* migrated via this strait at the beginning of the deglacial period. As the sea level was presumably lower by 80–90 m during the Termination 1A (Fairbanks, 1989), the strait was most likely closed. According to our data, occasional specimens of *G. scitula* occur, along with *Globigerinita glutinata* and *G. uvula.* in glacial and younger sediments (22370 years BP; Gorbarenko, 1996) of the eastern part of the Bering Sea (St. GC-11). In deglacial sediments, abun-

dance of the latter two species noticeably increases, whereas *G. scitula* continues to occur as single specimens. It is not inconceivable that these species could migrate in the summer season northward, as they do now, even during the glaciation. One can assume that with the onset of deglaciation and relevant warming, which intensified the anticyclonic circulation, these species could enter the western part of the Bering Sea and penetrate further into the Sea of Okhotsk with the Kamchatka Current. Subsurface waters (at a depth of 30 m) in the northwestern part of the Bering Sea, in the Kamchatka Current, and Sea of Okhotsk are characterized by similar temperatures (Levitus, 1982). All the aforesaid favor our assumption. Nevertheless, *G. scitula* has not been registered as yet in waters and modern sediments of the northwestern Pacific, and its migration from the Sea of Japan, as was proposed by Belyaeva and Burmistrova (1997), cannot be completely ruled out.

Glacial–Deglacial Assemblage and Modern Biocoenosis

The performed study shows that the planktonic foraminifer assemblage occurring in glacial–deglacial sediments (16130–8000 years BP) of the considered area of the Sea of Okhotsk substantially differs from that observed in postglacial sediments. The peculiar feature of foraminifers in sediments of glaciation and deglaciation is a sharp prevalence of sinistral *Neogloboquadrina pachyderma* and *Globigerina bulloides*. The share of the latter species at some levels of the glacial section is over 30%, whereas in deglacial sediments it never exceeds 10% usually making up 3–6%. Similar situation is also characteristic of the central part of the Sea of Okhotsk (Chekhovskaya and Basov, 1999).

In the latter article, we proposed, following Morley *et al.* (1991), that the difference between assemblages of planktonic microorganisms can be related to specific hydrological structure of the basin during the corresponding periods. The data on the planktonic foraminifer biocoenosis of the Sea of Okhotsk obtained recently using the sediment trap indicate that such a relation is not doubtless, and situation could be much more complex. In her dissertation thesis, Alderman (1996) showed that these two species are sharply prevalent in the foraminiferal biocoenosis of the Sea of Okhotsk, where the share of *Globigerina bulloides* amounts to 31%. Thus, with respect to the content of these two species, the glacial and deglacial foraminiferal assemblages appear to be almost identical to the modern one that implies the similarity rather than difference between hydrological conditions during relevant periods.

Through most of the interglacial period, the surface water productivity was substantially higher than during the deglacial and, furthermore, glacial intervals. This is evident from intense development of siliceous phytoplankton and formation of biogenic siliceous sediments (diatom oozes) beginning from about 6000 years BP. Glacial sediments enclose only separate terrigenous diatom-rich interbeds deposited probably during the intermittent phases of Pacific water inflow. The changes in productivity of surface waters, which depends on their chemical properties and structure, are indicators of hydrological evolution.

For its development, phytoplankton needs, in addition to nutrients, a stable stratification of surface waters (Smith and Nelson, 1985; Arzhanova and Zubarevich, 1997). In the modern Sea of Okhotsk, phytoplankton production increases at the end of March, when a stable stratification of surface waters enriched in nutrients after the winter mixing begins to form in response to spring heating and freshening owing to sea ice melting (Arzhanova and Zubarevich, 1997).

As was mentioned, winter and spring surface water temperatures in the Sea of Okhotsk during the last glacial maximum (18000 years BP) were only by 2°C lower than today (Moore *et al.*, 1980), i.e., in August they were 10–12°C. Accordingly, we can assume that seasonal stratification of surface waters could exist also during the glacial (and deglacial) period. Thus, phytoplankton development at that time was probably decelerated by some other factor. Taking into consideration that the maximum phytoplankton production in the modern Sea of Okhotsk is characteristic of the spring–summer periods (Arzhanova and Zubarevich, 1997), the most likely factor was a longer duration of winter seasons. Simultaneously, conditions of the autumn season, which is marked by a peak of the planktonic foraminifer production (Alderman, 1996) and which determines proportions of species in the biocoenosis, were similar to modern ones.

As for coexistence of polar species *Neogloboquadrina pachyderma* dex. (up to 57%) and relatively more thermophilic mid-latitude species *Globigerina bulloides* (up to 31%), the present-day planktonic foraminifer community of the Sea of Okhotsk differs in this respect from that of the Subarctic Pacific despite the common taxonomic composition. The other difference is prevalence of sinistral *N. pachyderma* (98%) in the Sea of Okhotsk over its dextral variety regardless the season and even the high temperature of surface waters (up to 14.8°C). Such a proportion between sinistral and dextral forms is typical of waters with significantly lower temperature. In opinion of Alderman (1996), the peculiar composition of planktonic foraminifer community in the Sea of Okhotsk is related to its distinct seasonal character, strong stratification of surface waters, and high productivity of the latter. According to her data, representatives of *N. pachyderma* sin. and *G. bulloides* build their tests at a depth of 20–40 m under the water temperature of 2–7 and 0.5–5°C, respectively. In the North Atlantic, the inversion from dextral to sinistral coiling of *N. pachyderma* occurs under water temperature of around 8°C (Ostermann *et al.*, 1998). Ear-

lier, it was also noted (Reynolds and Thunell, 1985) that the planktonic foraminifer production, including *G. bulloides*, can be controlled, in addition to temperature conditions, by food availability. High concentrations of *N. pachyderma, G. bulloides*, and *G. quinqueloba* related, as is believed, to well-manifested seasonal changes and high productivity of surface waters of the basin are recorded in the Californian Current area (Ortiz *et al.*, 1995) and in sediments of isotopic Stage 3 (25–50 ka BP) in the North Atlantic (Oppo *et al.*, 1995). At least three of above-mentioned potential factors, which could be responsible for the observed development pattern of *G. bulloides* (stratification, seasonal variations, and low temperatures), were probably characteristic of surface waters of the glacial Sea of Okhotsk.

It is apparent that the oceanographic situation, close to the modern one, exists in the Sea of Okhotsk at least during the last 4000 years. Thus, the planktonic foraminifer assemblage from sediments of the second half of the interglacial period should be close in composition and structure to the modern foraminiferal community. Their difference indicates that many tests of *Globigerina bulloides* were most likely eliminated being dissolved in bottom waters. Despite the fact that dissolution signs are typical of foraminifer tests through the entire studied section, they become most distinct with the onset of deglaciation. Moreover, as was mentioned, foraminiferal tests in sediments corresponding to initial phases of Terminations 1A and 1B are characterized by better preservation than in sediments of terminal deglaciation phases. Precisely in sediments of initial phases, the share of *Globigerina bulloides*, its large tests included, is particularly high. Dissimilar to previously mentioned areas of the Californian Current and North Atlantic, the high productivity of surface waters in the Sea of Okhotsk during the interglacial period most likely influenced negatively the *G. bulloides* abundance, as the high influx of organic matter into sediments and its oxidation intensified dissolution processes at the floor.

CONCLUSION

The quantitative and qualitative analyses of planktonic foraminifers enclosed in Upper Pleistocene–Holocene sediments of the southeastern Sea of Okhotsk revealed several their assemblages different in overall taxonomic composition and structure and corresponding to certain stages in hydrological evolution of the basin.

At the end of the glacial period (16300–12500 years BP), the foraminiferal assemblage included only two species: *Neogloboquadrina pachyderma* sin. and *Globigerina bulloides*. This unusual combination of the polar (first) and relatively thermophilic (second) forms differs their assemblage from all other foraminiferal assemblages of high latitudes and makes it almost identical to the modern community established in sediment traps (Alderman, 1996). This allows an assumption that, despite lower temperatures of surface waters, the hydrological structure of glacial surface waters was similar to the modern one in some parameters (well-developed stratification, seasonal variations, food availability), which are important for these species (Reynolds and Thunell, 1985; Oppo *et al.*, 1995; Ortiz *et al.*, 1995; Alderman, 1996), at least during the summer–autumn season.

The glacial and deglacial foraminiferal assemblages are sharply dominated by the same species. The deglacial assemblage is characterized by a higher diversity owing to occurrence of subordinate *Globigerinita uvula, G. glutinata, Globorotalia scitula*, and *Globigerina quinqueloba*. Simultaneously, it becomes sharply enriched in large forms of *Globigerina bulloides*, which are characteristic of the autumnal production peak in the modern Sea of Okhotsk (Alderman, 1996), and shows the reduced role of the sinistral *Neogloboquadrina pachyderma* form. All this indicates the rise of surface water temperatures probably related to vigorous circulation and intense inflow of Pacific waters.

Distribution of foraminifers in sediments corresponding to deglaciation (12500–8000 years BP) reflects two steps of its development: periods with relatively diverse and thermophilic assemblage of planktonic foraminifers corresponding to isotopic Terminations 1A and 1B events (Gorbarenko, 1996) are separated by the short-term Younger Dryas cooling event marked by the cold-resistant assemblage of foraminifers and their lower production. Hydrologic and climatic changes during deglaciation are reflected in C_{org} and $CaCO_3$ record in sediments. The assemblage of planktonic foraminifers in postglacial (or interglacial) sediments (the last 8000 years) is uniform and largely represented by *Neogloboquadrina pachyderma* sin. (up to 80–90% and more) accompanied by rare or occasional species of relatively thermophilic type (*Globigerina bulloides, Globigerinita quinqueloba, G. uvula, G. glutinata, Globorotalia scitula*). Against this background, there were periods characterized by the increased or decreased contents of these species and corresponding to episodes of relative warming or cooling, respectively. Warmest conditions were probably characteristic of the period of 6000–4000 years BP (Holocene optimum), which is marked, in addition to relatively thermophilic composition of foraminifers (presence of large *Globigerinita quinqueloba, G. uvula, G. glutinata*, and *Globorotalia scitula* specimens), by a rapid increase in production of calcareous and, particularly, siliceous microplankton in surface waters.

The low content of *Globigerina bulloides* in interglacial sediments, whose share in the modern foraminiferal biocoenosis amounts to 30% and more, like in the glacial and deglacial assemblages, indicates most likely an intense dissolution of calcium carbonate in bottom waters of the Sea of Okhotsk.

ACKNOWLEDGMENTS

We express our sincere gratitude to T.A. Khusid and I.G. Yushina for useful discussions during preparation of the manuscript. The work was supported by the Russian Foundation for Basic Research, project nos. 97-05-64924, 99-05-65604, and 99-05-64533.

Reviewers V.A. Krasheninnikov and M.N. Alekseev

REFERENCES

Alderman, S.E., Planktonic Foraminifera in the Sea of Okhotsk: Population and Stable Isotopic Analysis from a Sediment Trap, Massachusetts Institute of Technology. Woods Hole Oceanographic Institution, *Thesis for the degree of Master of Science*, 1996, pp. 1–88.

Arzhanova, N.V. and Zubarevich, V.L., Seasonal Variations in the Nutrient Content in the Sea of Okhotsk as a Basis for Phytoplankton Production Assessment, *Kompleksnye issledovaniya ekosistemy Okhotskogo morya* (Complex Research of the Sea of Okhotsk Ecosystem), Moscow: VNIRO, 1997, pp. 92–97.

Bard, E., Labeyrie, L.D., Pichon, J.-J., *et al.*, The Last Deglaciation in the Southern and Northern Hemispheres: A Comparison Based on Oxygen Isotope, Sea Surface Temperature Estimates, and Accelerator ^{14}C Dating from Deep-sea Sediments, *Geologic History of the Polar Oceans: Arctic versus Antarctic (NATO Advanced Workshops; ASI Ser., 308.)* Bleil, U. and Thiede, J., Eds., Kluwer, Dordrecht, 1990, pp. 405–415.

Bauch, H.A., Test Size Variation of Planktonic Foraminifers as Response to Climate Changes, *Fourth International conference on Paleoceanography*, ICP IV, Kiel, Germany, 1992, p. 56.

Baumann, K.H. and Matthiessen, J., Variations in Surface Water Mass Conditions in the Norwegian Sea: Evidence from Holocene Coccolith and Dinoflagellate Cyst Assemblages, *Marine Micropaleontol.*, 1992, vol. 20, no. 2, pp. 129–146.

Be, A.W.H., Ecological, Zoogeographic and Taxonomic Review of Recent Planktonic Foraminifera, *Oceanic Micropaleontology*, London: Academic Press, 1977, vol. 1, pp. 1–100.

Belyaeva, N.V. and Burmistrova, I.I., Paleohydrology of Sea of Okhotsk during the Last 60 ka, *Okeanologiya*, 1997, vol. 37, no. 3, pp. 377–385.

Bradshaw, J.S., Ecology of Living Planktonic Foraminifera in the North and Equatorial Pacific Ocean, *Contrib. Cush. Found. Foram. Research.*, 1959, vol. 10, pt. 2, pp. 25–64.

Chekhovskaya, M.P. and Basov, I.A., Planktonic Foraminifers in the Sea of Okhotsk Sediments (Core V34-90): the Last 20000 years, *Stratigr. Geol. Korrelyatsiya*, 1999, vol. 7, no. 2, pp. 104–115.

COHMAP-Members, Climatic Changes of the Last 18000 years, *Science*, 1988, no. 241, pp. 1042–1052.

Dodimead, A.J., Favorite, F., and Hirano, T., Salmon of the North Pacific Ocean-II, Review of Oceanography of the Subarctic Pacific Region, *Bull. Int. North Pacific Comm.*, 1963, vol. 13, pp. 1–195.

Duplessy, J.C., Bard, E., Arnold, M., *et al.*, How Fast Did the Ocean-Atmosphere System Run during the Last Deglaciation?, *Earth Planet. Sci. Letters*, 1991, vol. 103, pp. 27–40.

Fairbanks, R.G., A 17000-year Glacio-eustatic Sea-level Record: Influence of Glacial Melting Rates on the Younger Dryas Event and Deep-ocean Circulation, *Nature*, 1989, vol. 342, pp. 637–642.

Gorbarenko, S.A., Stable Isotope and Lithologic Evidence of Late-Glacial and Holocene Oceanography of Northwestern Pacific and Its Marginal Seas, *Quaternary Res.*, 1996, vol. 46, pp. 230–250.

Gorbarenko, S.A., Chekhovskaya, M.P., and Southon, J.R., Paleoenvironments of the Central Sea of Okhotsk during the Last Glacial and Holocene, *Okeanologiya*, 1998, vol. 38, no. 2, pp. 305–308.

Gorbarenko, S.A., Khusid, T.A., Basov, I.A., *et al.*, The Paleoenvironment of the South-Eastern Part of the Okhotsk Sea during Last Glaciation-Holocene: Evidence from Geochemical and Paleontological Data, *Palaeogeogr., Palaeoclimatol., Palaeoecol.* (in press).

Keigwin, L.D., Jones, G.A., and Froelich, P.N., A 15000-year Paleoenvironmental Record from Meiji Seamount, Far Northwestern Pacific, *Earth Planet. Sci. Letters*, 1992, no. 111, pp. 425–440.

Koc Kapuz, N. and Schrader, H., Surface Sediment Diatom Distribution and Holocene Paleotemperature Variations in the Greenland, Iceland and Norwegian Sea, *Paleoceanography*, 1990, no. 5 pp. 557–580.

Levitus, S., Climatological Atlas of the World Ocean, *NOAA Profess. Pap.*, 1982, no. 13, pp. 1–173.

Lipps, J.Y. and Warme, J.E., Planktonic Foraminiferal Biofacies in the Okhotsk Sea, *Contrib. Cush. Found. Foram. Research*, 1966, vol. 17, pt. 4, pp. 125–134.

Moore, C., Jr., Burckle, L.H., Geitzenauer, *et al.*, The Reconstruction of Sea Surface Temperature in the Pacific Ocean of 18000 B.P., *Marine Micropaleontol.*, 1980, no. 5, pp. 215–247.

Morley, J.S. and Hays, J.D., Oceanographic Conditions Associated with High Abundances of Radiolarian *Cycladophora davisiana*, *Earth Planet. Sci. Letters*, 1983, no. 66, pp. 63–72.

Morley, J.J., Heusser, L.E., and Shackleton, N.J., Late Pleistocene/Holocene Radiolarian and Pollen Records from Sediments in the Sea of Okhotsk, *Paleoceanography*, 1991, vol. 6, no. 1, pp. 121–131.

Moroshkin, K.V., *Vodnye massy Okhotskogo morya* (Water Masses of the Sea of Okhotsk), Moscow: Nauka, 1966.

Naidina, O.D., Palynological Evidence of Holocene Climatic Changes in Arctic Siberia, *Paleoenvironmental Changes along the Northeastern Siberia Margin since the Last Glacial Maximum*, AGU Fall Meeting, San Francisco, December 6–10, *EOS Transactions*, 1998, vol. 79, no. 45, p. 500.

Oppo, D.W. and Lehman, S.J., Suborbital Timescale Variability of North Atlantic Deep Water during the Past 200000 years, *Paleoceanography*, 1995, vol. 10, no. 5, pp. 901–910.

Ortiz, J.D., Mix, A.C., and Collier, R.W., Environmental Control of Living Symbiotic Foraminifera of the California Current, *Paleoceanography*, 1995, vol. 10, no. 6, pp. 987–1009.

Ostermann, D.R., Curry, W.B., Olafsson, J. and Honjo, S., Variability of Foraminiferal flux and Isotopic Composition at Sites around Iceland and the Sea of Okhotsk, with a Special Focus on *N. pachyderma* (sinistral and dextral), and *G. quinqueloba*, *6th International Conference on Paleoceanography. 1998. August 24–28. Portugal*, Lisbon, 1998, p. 180.

Reynolds, L.A. and Thunell, R.C., Seasonal Succession of Planktonic Foraminifera in the Subpolar North Pacific, *Journ. Foram. Res.*, 1985, vol. 15, pp. 282–301.

Saidova, Kh.M., Quantitative Distribution of Foraminifers in the Sea of Okhotsk, *Dokl. Akad. Nauk SSSR*, 1957, vol. 114, no. 6, pp. 1302–1305.

Saidova, Kh.M., *Ekologiya i paleogeographiya Dal'nevostochnykh morei i severo-zapadnoi chasti Tikhogo okeana* (Ecology and Paleogeography of the USSR Far East Seas and Northwestern Pacific), Moscow: Akad. Nauk SSSR, 1961.

Sancetta, C., Primary Production in the Glacial North Atlantic and North Pacific, *Nature*, 1992, vol. 360, pp. 249–251.

Sancetta, C. and Silvestri, S., Pliocene-Pleistocene Evolution of the North Pacific Ocean-Atmosphere System, Interpreted from Diatoms, *Paleoceanography*, 1986, vol. 1, no. 2, pp. 163–180.

Sautter, L.R. and Thunell, R.C., Seasonal Succession of Planktonic Foraminifera: Results from a Four-year Timeseries Sediment Trap Experiment in the Northeast Pacific, *Journ. Foram. Res.*, 1989, vol. 19, no. 4, pp. 253–267.

Shchedrina, Z.G., Hew Data on the Foraminiferal Fauna in the Sea of Okhotsk and Its Distribution, *Trudy Zool. Inst. Akad. Nauk SSSR*, 1953, vol. 18, pp. 12–32.

Shiga, K. and Koizumi, I., Latest Quaternary Changes in the Okhotsk Sea Based on Diatom Record, *Marine Micropaleontol.*, 2000, vol. 38, pp. 91–117.

Smith, W.O. and Nelson, D.M., Phytoplankton Bloom Produced by a Receding Ice Edge in the Ross Sea: Spatial Coherence with the Density Field, *Science*, 1985, vol. 227, pp. 163–166.

Southon, J.R., Kashgarian, M., Gorbarenko, S., *et al.*, Calcite Dissolution and the Radiocarbon Age of Pre-bomb Surface Water in North Pacific Coastal Region, *EOC. Transaction. Amer. Geophys. Union*, 1993, p. 198.

Thunell, R.C. and Honjo, S., Seasonal and Interannual Changes in Planktonic Foraminiferal Production in the North Pacific, *Nature*, 1987, vol. 328, pp. 335–337.

Tsukada, M., Japan, *Vegetation History*, Huntley, B. and Webb, T., Eds., Boston: Kluwer, 1988, pp. 459–518.

Yang, J. and Honjo, S., Modeling of the Near-freezing Dichothermal Layer in the Sea of Okhotsk and Its Interannual Variations, *Journ. Geophys. Res.*, 1996, vol. 101, no. 7, pp. 16421–16433.

GEOLOGY OF ORE DEPOSITS

Editor-in-Chief
Nikolai P. Laverov
Professor, Member of the Russian Academy of Sciences

GEOLOGY OF ORE DEPOSITS was founded in 1959. Since 1993 the journal has been published simultaneously in both Russian and English. The journal is one of a few special periodicals devoted to metallic minerals and the conditions of their formation and distribution. Since the advent of glasnost, many restrictions on publication of geological data have been lifted, making available more complete and concrete information on important deposits throughout the former USSR, including such unique ore districts as Noril'sk, Udokan, and Muruntau. Also included are articles submitted by foreign contributors on strategic deposits throughout the world.

Scope:

- *Economic Geology of Metal Ore Deposits*
- *New and Traditional Types of Nonmetallic Minerals*
- *Mineral Composition of Ores*
- *Experimental and Isotope Studies of Ore-Forming Systems*
- *Ore-Forming Processes and Their Physicochemical Parameters*
- *Geochronology of Ore-Forming Processes and Their Evolution*

2001 Volume 43 • ISSN 1075-7015 • Bimonthly
$1068 US/Canada
$1226 Rest of World

Tel: 800-633-4931
205-995-1567 (outside US and Canada)
Fax: 205-995-1588

INTERPERIODICA
Subscription Office
P.O. Box 1831
Birmingham, AL 35201

PETROLOGY

Editor-in-Chief
Vilen A. Zharikov
Member of the Russian Academy of Sciences

PETROLOGY is a journal of magmatic, metamorphic, and experimental petrology, mineralogy, and isotopic geochemistry. The journal offers comprehensive information on all multidisciplinary aspects of theoretical and experimental petrology. By giving special consideration to studies on the petrography of different regions of the former Soviet Union, **PETROLOGY** will provide all readers with a unique opportunity to refine their understanding of the geology of the vast territory of the Eurasian continent.

Scope:

- *Petrology of magmatic, metamorphic, and metasomatic rocks in continental and oceanic environments*
- *Experimental petrology and mineralogy*
- *Geothermobarometry*
- *Physicochemical analysis of mineral assemblages*
- *Isotopic geochemistry and geochronology*

2001 Volume 9 • ISSN 0869-5911 • Bimonthly
$1069 US/Canada
$1226 Rest of World

Tel: 800-633-4931
205-995-1567 (outside US and Canada)
Fax: 205-995-1588

INTERPERIODICA
Subscription Office
P.O. Box 1831
Birmingham, AL 35201

The International Academic Publishing Company "Nauka/Interperiodica"

announces the results of the 2000 competition for the best articles published in its journals. Listed below are the authors who won MAIK "Nauka/Interperiodica" prizes for articles in the Earth Sciences:

1. F.V. Kashin, V.N. Aref'ev, K.N. Visheratin, N.E. Kamenogradskii, V.K. Semenov, V.P. Sinyakov

Results of Experimental Studies of Radiatively Active Atmospheric Constituents in Central Eurasia

☆ ***Izvestiya, Atmospheric and Oceanic Physics***

2. T.I. Moiseenko, M.G. Hublarian

A series of publications: Anthropogenic Impact on Water Bodies and Its Ecological Consequences: Theoretical Background for Determining Critical Loads

☆ ***Water Resources, Geochemistry International, Doklady Earth Sciences, Journal of Ichthyology, Russian Journal of Ecology, Herald of the Russian Academy of Sciences***

1. K.R. Kovalev, I.V. Gas'kov, A.P. Pertseva, E.G. Distanov

A series of publications: Geologic Structure, Isotopic Composition, and Genesis of Base-Metal Sulfide Ores at Deposits in the Asian Part of Russia

☆ ***Geology of Ore Deposits***

2. V.V. Yarmolyuk, V.I. Kovalenko, M.I. Kuz'min, V.G. Ivanov, V.P. Kovach, A.B. Kotov, E.B. Sal'nikova, G.S. Kharin

A series of publications: Mantle Plumes and Their Role in the Genesis of the Lithosphere and Deep-Seated Geodynamics

☆ ***Geotectonics, Petrology***

3. M.B. Gnilovskaya, A.F. Veis, Yu.R. Bekker, V.G. Olovyanishnikov, M.E. Raaben

Pre-Ediacarian Fauna from Timan (Annelidomorphs of the Late Riphean)

☆ ***Stratigraphy and Geological Correlation***

4. V.B. Polyakov, S.D. Mineev

A series of publications: Application of Moessbauer Spectroscopy to Isotopic Geochemistry

☆ ***Geochemistry International, Russian Journal of Physical Chemistry***

5. Yu.P. Neprochnov, Yu.M. Pushcharovsky, G.A. Semenov, A.L. Volokh, B.N. Grin'ko, V.V. Bezverbnaya, Hao Tianyao, O.Yu. Ganzha

A series of publications: Problems of the Inner Structure and Heterogeneity of the Earth Crust and Upper Mantle Beneath Seas of Russia and World Ocean

☆ ***Oceanology, Doklady Earth Sciences***

Subscribe to the journals from the Russian Academy of Sciences

Translated and Published by MAIK "Nauka / Interperiodica"
(International Academic Publishing Company "Nauka / Interperiodica")
Distributed Worldwide by INTERPERIODICA

Copy this form to mail or fax your order today

	TITLE	Volume	ISSN	ISSUES	RATE IN US DOLLARS US/CAN	RATE IN US DOLLARS INTERNATIONAL	YOUR ORDER
❑	Biophysics	46	0006-3509	6	$2825	$2943	$ _____
❑	Computational Mathematics and Mathematical Physics	41	0965-5425	12	$2657	$3232	$ _____
❑	Doklady Earth Sciences	376-381A	1028-334X	9	$3170	$3640	$ _____
❑	Doklady Mathematics	63-64	1064-5624	6	$1520	$1745	$ _____
❑	Entomological Review	81	0013-8738	9 + 2 Suppl.	$2870	$3300	$ _____
❑	Eurasian Soil Science	34	1064-2293	12 + 1 Suppl.	$2390	$2750	$ _____
❑	Geochemistry International	39	0016-7029	12 + 2 Suppl.	$2940	$3378	$ _____
❑	Geology of Ore Deposits	43	1075-7015	6	$1068	$1226	$ _____
❑	Geomagnetism and Aeronomy	41	0016-7932	6	$834	$958	$ _____
❑	Geotectonics	35	0016-8521	6	$650	$706	$ _____
❑	Herald of the Russian Academy of Sciences	71	1019-3316	6	$1622	$2059	$ _____
❑	Izvestiya, Atmospheric and Oceanic Physics	37	0001-4338	6 + 1 Suppl.	$1058	$1137	$ _____
❑	Izvestiya, Physics of the Solid Earth	37	1069-3513	12	$952	$1052	$ _____
❑	Journal of Communications Technology and Electronics	46	1064-2269	12	$3115	$3585	$ _____
❑	Journal of Computer and Systems Sciences International	40	1064-2307	6	$2289	$2638	$ _____
❑	Journal of Ichthyology	41	0032-9452	9 + 2 Suppl.	$2469	$2839	$ _____
❑	Laser Physics	11	1054-660X	12	$1921	$2321	$ _____
❑	Oceanology	41	0001-4370	6	$806	$868	$ _____
❑	Paleontological Journal	35	0031-0301	6 + 3 Suppl.	$2262	$2605	$ _____
❑	Pattern Recognition & Image Analysis	11	1054-6618	4	$763	$872	$ _____
❑	Petroleum Chemistry	41	0965-5441	6	$3095	$3215	$ _____
❑	Petrology	9	0869-5911	6	$1069	$1226	$ _____
❑	The Physics of Metals and Metallography	91-92	0031-918X	12 + 2 Suppl.	$3019	$3477	$ _____
❑	Physics of Particles and Nuclei	32	1063-7796	6 + 1 Suppl.	$2498	$2648	$ _____
❑	Polymer Science. Series A	43	0965-545X	12	$2867	$3300	$ _____
❑	Polymer Science. Series B	43	1560-0904	6	—	—	$ _____
❑	Polymer Science. Series C	43	Pending	2	—	—	$ _____
	Polymer Science. Ser. A+B+C	43	—	20	$3469	$4011	$ _____
❑	Proceedings of the Steklov Institute of Mathematics	232-235	0081-5438	4 + 2 Suppl.	$1530	$1765	$ _____
❑	Russian Journal of Biotechnology	1	Pending	4	$700	$795	$ _____
❑	Russian Journal of Inorganic Chemistry	46	0036-0236	12 + 3 Suppl.	$3711	$4267	$ _____
❑	Russian Journal of Mathematical Physics	8	1061-9208	4	$655	$748	$ _____
❑	Russian Journal of Physical Chemistry	75	0036-0244	12 + 1 Suppl.	$3405	$3915	$ _____
❑	Stratigraphy and Geological Correlation	9	0869-5938	6	$1068	$1226	$ _____
❑	Studies on Russian Economic Development	12	1075-7007	6	$779	$893	$ _____
❑	Thermal Engineering	48	0040-6015	12	$1667	$1918	$ _____
❑	Thermophysics and Aeromechanics (only distribution)	8	0869-8643	4	$715	$858	$ _____
						TOTAL	_____

❶ Name _____
Institution _____
Address _____
_____ State _____
City _____ Country _____
Zip/Postal Code _____
Telephone (_____)

Delivery is not made until payment is received

To order by phone call **1 800 633-4931**
or (205) 995-1567 outside the US and Canada

❷ ❑ My payment for $_____ is enclosed.
OR
❑ Bill me. My library's purchase order number is _____

❸ Send this order and payment to:
INTERPERIODICA
P.O. Box 1831
Birmingham, AL 35201-1831
Or fax this order form to (205) 995-1588

Order now for immediate delivery. All journals will be published in 2001!

MAIK "Nauka/Interperiodica" Publishing

is pleased to present to the international scientific community simultaneous Russian- and English-language publication of the journals of the Russian Academy of Sciences

MAIK "Nauka/Interperiodica" 2001 volumes include the following titles:

- *Biophysics*
- *Computational Mathematics and Mathematical Physics*
- *Doklady Earth Sciences*
- *Doklady Mathematics*
- *Entomological Review*
- *Environmental Geoscience*
- *Eurasian Soil Science*
- *Geochemistry International*
- *Geology of Ore Deposits*
- *Geomagnetism and Aeronomy*
- *Geotectonics*
- *Herald of the Russian Academy of Sciences*
- *Izvestiya, Atmospheric and Oceanic Physics*
- *Izvestiya, Physics of the Solid Earth*
- *Journal of Communications Technology and Electronics*
- *Journal of Computer and Systems Sciences International*
- *Journal of Ichthyology*
- *Laser Physics*
- *Oceanology*
- *Paleontological Journal*
- *Pattern Recognition and Image Analysis*
- *Petroleum Chemistry*
- *Petrology*
- *Polymer Science, Series A*
- *Polymer Science, Series B*
- *Polymer Science, Series C*
- *Physics of Particles and Nuclei*
- *Proceedings of the Steklov Institute of Mathematics*
- *Russian Journal of Biotechnology*
- *Russian Journal of Inorganic Chemistry*
- *Russian Journal of Mathematical Physics*
- *Russian Journal of Physical Chemistry*
- *Stratigraphy and Geological Correlation*
- *Studies on Russian Economic Development*
- *The Physics of Metals and Metallography*
- *Thermal Engineering*
- *Thermophysics and Aeromechanics**

* *Thermophysics and Aeromechanics* is only distributed by MAIK "Nauka/Interperiodica" Publishing

Please direct all inquiries about the above journals to: **INTERPERIODICA**, P.O. Box 1831, Birmingham, AL 35201-1831.
For faster service call toll-free (800) 633-4931 or (205) 995-1567 (outside US and Canada). Fax: (205) 995-1588, E-mail: interperiodica@ebsco.com

- *Applied Biochemistry and Microbiology*
- *Automation and Remote Control*
- *Biochemistry (Moscow)*
- *Biology Bulletin*
- *Colloid Journal*
- *Combustion, Explosion, and Shock Waves**
- *Cosmic Research*
- *Differential Equations*
- *Doklady Biochemistry and Biophysics*
- *Doklady Biological Sciences*
- *Doklady Chemistry*
- *Doklady Physical Chemistry*
- *Fluid Dynamics**
- *Functional Analysis and Its Applications**
- *Glass Physics and Chemistry*
- *High Energy Chemistry*
- *High Temperature*
- *Human Physiology*
- *Inorganic Materials*
- *Instruments and Experimental Techniques*
- *Journal of Analytical Chemistry*
- *Journal of Applied Mechanics and Technical Physics**
- *Journal of Evolutionary Biochemistry and Physiology*
- *Journal of Mining Science**
- *Journal of Structural Chemistry**
- *Kinetics and Catalysis*
- *Lithology and Mineral Resources*
- *Mathematical Notes**
- *Microbiology*
- *Molecular Biology*
- *Problems of Information Transmission*
- *Programming and Computer Software*
- *Protection of Metals*
- *Radiochemistry*
- *Russian Chemical Bulletin**
- *Russian Journal of Applied Chemistry*
- *Russian Journal of Bioorganic Chemistry*
- *Russian Journal of Coordination Chemistry*
- *Russian Journal of Developmental Biology*
- *Russian Journal of Ecology*
- *Russian Journal of Electrochemistry*
- *Russian Journal of General Chemistry*
- *Russian Journal of Genetics*
- *Russian Journal of Marine Biology*
- *Russian Journal of Nondestructive Testing*
- *Russian Journal of Organic Chemistry*
- *Russian Journal of Plant Physiology*
- *Russian Microelectronics*
- *Siberian Mathematical Journal**
- *Solar System Research*
- *Theoretical and Mathematical Physics**
- *Theoretical Foundations of Chemical Engineering*
- *Water Resources*

* *The journal* is produced by MAIK "Nauka/Interperiodica" under contract with Kluwer Academic/Plenum Publishers

Please direct all inquiries about the above journals to: **Kluwer Academic/Plenum Publishers**, P.O. Box 322, 3300 AH Dordrecht, The Netherlands. Phone: (31 78) 639-2392. Fax: (31 78) 654-6474, E-mail: orderdept@wkap.nl

- *Acoustical Physics*
- *Astronomy Letters*
- *Astronomy Reports*
- *Crystallography Reports*
- *Doklady Physics*
- *JETP Letters*
- *Journal of Experimental and Theoretical Physics*
- *Optics and Spectroscopy**
- *Physics of Atomic Nuclei*
- *Physics of the Solid State*
- *Plasma Physics Reports*
- *Semiconductors*
- *Technical Physics*
- *Technical Physics Letters*

* *Optics and Spectroscopy*: Optical Society of America, 2010 Massachusetts Ave., NW, Washington, DC 20036-1023, Attn.: Publications Department. Tel. (202) 223-8130, (800) 582-0416. Fax: (202) 416-6140.

Please direct all inquiries about the above journals to: **American Institute of Physics**, Circulation and Fulfillment Services, Suite 1NO1, 2 Huntington Quadrangle, Melville, NY 11747-4502 USA. Tel. (516) 576-2270, 1-800-344-6902. Fax: (516) 349-9704, E-mail: subs@aip.org

International Academic Publishing Company "Nauka/Interperiodica" (MAIK "Nauka/Interperiodica")
Profsoyuznaya ul., 90, Moscow, 117997, Russia, Phone: 7 (095) 3361600; Fax: 7 (095) 3360666,
E-mail:compmg@maik.ru, http://www.maik.ru